DOCTORAL THESIS DISSERTATION

UNDERSTANDING THE ROLE OF NRG1 SIGNALING UPON BRAIN DAMAGE: NOVEL MODELS OF CORTICAL REGENERATION

UNIVERSITAT POLITÈCNICA DE VALÈNCIA

PhD in Biotechnology

Submitted by

Ana González Manteiga

PhD Supervisor

Dr Pietro Fazzari

UPV Tutor

Dr Máximo Ibo Galindo Orozco

Valencia, September 13th 2023

UNIVERSITAT POLITÈCNICA DE VALÈNCIA

PRINCIPE FELIPE
CENTRO DE INVESTIGACION

PIETRO FAZZARI, PhD in Cell Science and Technology by the Università degli Studi di Torino and MÁXIMO IBO GALINDO OROZCO, PhD in Biology by Universidad de Valencia,

CERTIFY that:

The work titled **"UNDERSTANDING THE ROLE OF NRG1 SIGNALING UPON BRAIN DAMAGE: NOVEL MODELS OF CORTICAL REGENERATION"** has been developed by Ana González Manteiga in Centro de Investigación Príncipe Felipe (CIPF) under the supervision of Dr Pietro Fazzari and the academic tutorship of Dr Máximo Ibo Galindo Orozco as Thesis project to achieve the degree of PhD in Biotechnology at the Universitat Politècnica de València.

Valencia, September 13th 2023

Firmado Electronicamente por Pietro Fazzari en Valencia, España.

Dr Pietro Fazzari

GALINDO OROZCO MAXIMO IBO - 04577807W

Firmado digitalmente por GALINDO OROZCO MAXIMO IBO - 04577807W
Fecha: 2023.09.13 13:20:24 +02'00'

Dr Máximo Ibo Galindo Orozco

七転八起

Seven times fall,
Eight times rise.

Japanese proverb.

AGRADECIMIENTOS

Después de todas las páginas que llevo aquí escritas, pensé que esta sección sería la fácil. Sin embargo, me encuentro con las emociones a flor de piel, ya que este camino se caracteriza por las personas que me han acompañado a hacerlo posible.

Gracias a todas las entidades colaboradoras que han financiado este proyecto: el Ministerio de Economía, Industria y Competitividad de España, la Generalitat Valenciana (ayudas ACIF, PROMETEO) y Fondos FEDERER de la Unión Europea. Si algo hemos aprendido en estos últimos años, es que para ofrecer una sociedad competitiva y a la vanguardia, hace falta una mayor inyección económica en la investigación que ofrezca una ciencia digna y de calidad que nos permita avanzar.

En primer lugar, quiero agradecer a mi director de tesis Pietro Fazzari por la oportunidad que me brindó al aceptarme en el laboratorio, conformando el inicio de este sendero. Esta experiencia me ha labrado a muchos niveles, pero sobre todo me ha hecho ser mejor científica. Tampoco me olvido de todas las personas y Servicios que forjan el Centro de Investigación Príncipe Felipe, que en tantas ocasiones ha sido mi segunda casa en Valencia. No obstante, la Ciencia no sólo la hace quienes se dedican estrictamente a ella, sino también aquellos sectores que hacen posible el funcionamiento del centro: la administración, servicio de compras, vigilancia, limpieza, mantenimiento, y un largo etcétera. En especial, guardo un gran cariño a Jesús Raimundo, que tanto nos ayudó a construir el queridísimo Rotating Pole.

En segundo lugar, la mención más importante se la hago a mis queridos ratones, porque sin ellos este proyecto no existiría. Sólo espero que toda esta experimentación animal haya merecido la pena, ayudando a la sociedad en un futuro. Asímismo, doy gracias al excepcional Servicio de Animalario del CIPF, un grupo de profesionales siempre dispuestos a ayudar, con una integridad digna y velando por las buenas prácticas éticas en el bienestar animal.

Siguiendo con el CIPF, gracias a las primeras mesas enormes en las comidas donde una Ana recién mudada a Valencia y con mucha ansiedad social se sintió completamente arropada: Estefi, Alberto, Mari Paz, Salva, Magda, Ale, Araceli, Gema, Elena y Blanca. Aunque la pandemia hiciera que abandonásemos las mesas de boda, siempre tendré gran recuerdo de aquello. También mención especial a la peñita de Jóvenes CIPF que forjaron un grupo de predocs post-pandemia para apoyarnos entre todas, y sobre todo reavivar la vida social que a veces se nos queda por el camino durante la tesis: Paz, Inés, Doria, Mili, Raúl, Fito, Paula, Diego, Jaime, Irene, Carla... En concreto, gracias a Isa por las conversaciones en el baño y los audios infinitos, por ser de las tías más chulas que he conocido nunca y por apoyarme siempre. Gracias a Rubén y Gersio por pasar de echarnos unas risas a conversaciones extremadamente profundas en un

garito random de Beni un viernes a las 2AM. Gracias a Bea, Eric, Sonia y Mari Mar por acogerme en las comidas en mi última etapa de tesis y por estar siempre disponibles a ayudar. En este sentido, tampoco me puedo olvidar de María que siempre escuchó mis razonamientos y dudas, pero sobre todo me ayudó a sentirme válida y reafirmarme en la ciencia que hago.

Para finalizar con el sector CIPF, tenía que dedicar unas frases a mi gente del I-64. A Héctor, porque, aunque fuese breve, sin duda aprendí mucho de ti, en especial a relativizar y que desde la calma se piensan mejor las cosas. A Carmen, porque a ella le debo el 50% de esta tesis, por ser técnico, postdoc y psicóloga. Por ser una de las personas más válidas y excepcionales que conozco. Aunque ya no nos veamos tanto, espero que esta amistad se quede para siempre. A Yaiza, por estar siempre disponible para echar una mano, por ser nuestra corresponsal especial de TikTok y sus recetas, por las risas flojas en el lab, que hacían de los días grises un poco menos feos. Sigo esperando esa quedada para ver dibujitos mientras comemos chuches, por cierto. A Valentina, por la empatía, la sensibilidad y la amabilidad que desprendes. Eres un ser de luz allá donde vas, no me cansaré de decirlo. Siento muchísimo los sermones que te haya podido echar en tu etapa de TFG. Diría que intentaré cambiarlo, pero tú y yo sabemos que soy un poco chapas por naturaleza. Por último, Angie, mi compañera y amiga desde el máster, por la que gracias a ella llegué a este lugar. Por pensar en mí y recomendarme, por siempre estar dispuesta a echarme un cable, por las críticas constructivas que me han hecho ser mejor en equipo, por tu tiempo en escucharme y secar mis lágrimas, incluso cuando no lo tenías. Siempre te voy a estar agradecida. En general, todas vosotras sois mi equipo, hemos luchado juntas contra viento y marea, y me da pena pensar que quizá nunca encuentre un grupo en el que me sienta tan arropada, acompañada, comprendida y apoyada. Esto no es un adiós, porque allá donde yo esté, tendréis un hogar al que venir.

En 2019 llegué a Valencia sin conocer a nadie y decidí apuntarme a teatro musical (por si la ciencia no era lo mío, pasar a Broadway). No salió del todo bien, la pandemia no lo hizo posible. No obstante, de aquello me llevo a dos personas maravillosas: Carlos y Sonia. Muchas gracias por nuestras tardes de tontunas y las risas, pero también por las conversaciones intensas sobre la vida. En especial, gracias a Carlos por todos los paseos con Neito (aunque no pudiéramos abrazarnos nunca), por estar ahí, apoyándome y haciéndome sentir tan bien. No en Teatro Musical, pero sí de forma inesperada, el reencuentro con Juan y, por consiguiente, conocer a Mónica e Ítala. Gracias por las risas, el apoyo, la comprensión, la complicidad y por todas las maravillosas recetas de nuestro chef favorito. Me habéis hecho sentir en casa estando a 450km de la mía.

Mudarse a otra ciudad puede ser estimulante, pero también da tristeza dejar atrás a tu familia. No obstante, a pesar de la distancia agrandada en pandemia, varias personas me han demostrado que siempre van a estar ahí por mí. Mamá, aún recuerdo cuando te dije de repente

que me venía a Valencia a hacer la tesis, necesitaba poner distancia y encontrarme. Me miraste preocupada y preguntaste "pero si aún no has contemplado otras opciones". Ya me conoces, siempre he sido un poco impulsiva. Aún así, no tardaste ni un poquito en apoyarme, aunque fuese desde el miedo, porque sé que separarnos no ha sido fácil para ninguna de las dos. Por llamarme cada día y, aunque a veces no te cogiera el teléfono porque no quería que notases que estaba mal, sé que tú pensabas en mí y me mandabas toda tu energía. Has velado por mí toda la vida de la forma más bonita que sabes y puedes estar tranquila porque, gracias a ti, estoy donde estoy. Ojalá en algún momento logre agradecerte una ínfima parte de todo lo que has tenido que apostar para darme lo mejor. Miguel, gracias por siempre darme el discurso motivacional y esperazandor que necesito, por ese empujoncito cuando creo que no puedo más. Para mí, tu figura siempre ha sido mi referente, una estela en el cielo que me orienta en la oscuridad. No obstante, ahora siento que ha llegado mi hora de avanzar sin rumbo ni brújula, porque tú me has demonstrado que soy fuerte, que siempre lo he sido. Fue durísimo alejarme y no tenerte cuando volvía a casa triste para que me enseñases los últimos memillos o viéramos un anime, parando el tiempo por un instante. A pesar de que vuele lejos, siempre dejo miguitas de pan por el camino para volver a casa.

No puedo olvidarme de la familia que se elige. Santi, mi fiel confesor y consejero en todos estos años, la persona que más audios ha aguantado, que siempre ha tenido tiempo para hacerme sentir comprendida y despotricar conmigo. Ojalá no perderte nunca y que en un futuro logremos reencontrarnos en el mismo espacio. A María, Paola y Sergio, porque lo que unió la biología aún permanece, y porque siempre habrá un Madrid para reencontrarse. A mi piñita, mis niños: Riki, Bustos, Lobo, More y Muri. Por contrarrestar mi síndrome de la impostora, por las conversaciones para salvar este mundo hostil, los memes, los abrazos, las mañanas de campo y las tardes de juegos de mesa. Me quedo tranquila pensando que en un apocalipsis ya tengo al mejor equipo de rescate. Marta, Clara y Ana, porque dais sentido a la palabra amistad. Gracias por los momentos de terapia, por las risas, las noches de fiesta, los viajes, por todo lo que hemos vivido y nos queda por vivir. Sin duda, quiero que independientemente de la edad que tengamos, estemos juntitas siempre para querernos. Andrea, mi amiga desde los 5 años y confesora, que nos hemos visto en los mejores y peores momentos. Gracias por los paseos por el pueblo y las llamadas telefónicas eternas. Cada vez que digo "no puedo más", tú siempre me respondes "siempre dices lo mismo, y siempre lo consigues". Eso es amor, hermana. Gracias a Elvira por querer colaborar en este proyecto, diseñando la portada de esta tesis doctoral.

No podía dejar atrás a la persona que más me ha apoyado (y sufrido de manera colateral) en esta tesis. Héctor, ya sabes todo lo que pienso y siento, pero nunca podré agradecerte lo suficiente tu presencia en estos años. Dejaste tu estabilidad por apostar por la mía, porque tú crees en mí todo lo que yo no creo. Aún sigo flipando cuando se me ocurre cualquier locura y

te falta tiempo para embarcarte en ella. Gracias por la familia que hemos formado, por saber qué necesito en cada momento, por arroparme, por secarme las lágrimas, por aguantar mi pico de actividad en momentos insólitos, por la paciencia y la tranquilidad que me contagias. Me has hecho ser mejor persona y, sobre todo, me has enseñado a quererme a mí misma. No conozco mejor forma de amar que esa. Mi pequeño Neo, aunque nunca leas estas líneas, sin duda has sido el mejor compañero en las noches de soledad mientras escribía esta tesis, el que secaba mis lágrimas cuando lloraba a escondidas o el que me hacía salir a la calle a relativizar que a veces lo más importante en la vida es seguir a una mariposa que se posa de flor en flor. Os adoro a ambos, y estoy feliz de formar esta familia, llegue a donde llegue.

Por último, me gustaría terminar dedicando unas palabras a la persona que ha hecho posible todo este trabajo, incluso cuando estaba en lo más hondo, cuando no se veía capaz, cuando fallaban las fuerzas. A mí. Porque he sabido apretar los dientes y tirar para adelante, afrontar los retos que ha supuesto y salir lo más airosa posible. Soy consciente de que he aprendido a ser mejor persona conmigo misma y que eso debe ser lo más sagrado a partir de ahora. Eso y saber que, después de todo, siempre hay luz en toda esa oscuridad.

No prometí que fuera a ser breve en estos agradecimientos, quienes me conozcáis sabréis que eso no me caracteriza. Y aun así siento que me dejo personas en el tintero. Así, permitidme la licencia de pedir perdón si alguien se echa en falta, y dar las gracias por última vez. Nos vemos en la siguiente etapa.

ABSTRACT

Brain damage is the leading cause of disability in adults, particularly in the elderly population. Regardless of the cause, different types of brain injury share similar physiopathological events. Most studies to date have focused on the immediate post-injury response, whereas less is known about cortical regeneration and plasticity after brain injury. Neuregulin 1 (Nrg1) is essential for the development of cortical circuits and has been implicated in several psychiatric disorders, such as schizophrenia. In the last decades, several works proposed Nrg1 signaling as an emergent modulator of neuroprotection upon damage. However, most research has focused on the early response of Nrg1 diffusible isoforms mediated by ErbB receptor activation after injury, which does not fully recapitulate the complexity of Nrg1 signaling. In this context, we have previously shown that Nrg1 intracellular signaling is activated under hypoxic conditions and promotes neuronal survival after cortical stroke.

The overall goal of this dissertation is to investigate the role of Nrg1 signaling in cortical regeneration and plasticity after cortical damage. To achieve this goal, we developed novel, refined models to 1) provide new methodological approaches to study axonal regeneration *in vitro* and *in vivo* and 2) specifically target Nrg1 signaling and particularly investigate the role of Nrg1 intracellular pathway upon cortical injury.

First, we developed a novel *in vitro* model of axonal injury in cortical neuron cultures. Specifically, we performed sparse labeling of the cultures by electroporation techniques and induced physical injury by mechanical transection of the axons. In this model, we also performed gain- and loss-of-function approaches to investigate the role of Nrg1 in axonal outgrowth. Our results showed that Nrg1, and specifically the activation of its intracellular signaling, potentiates axonal outgrowth upon injury.

Second, we developed a novel methodology in mice that combines cortico-cortical projection tracing with focal mechanically controlled cortical damage (CCD) to study cortical regeneration. We performed extensive functional characterization of the model and provided meaningful behavioral tasks to detect motor impairment in unilateral focal injuries. Since tissue processing is performed in serial floating sections, we combined different immunolabeling and 3D brain reconstruction to evaluate stereological measurements and analysis of axonal projections and different cell populations. As a biological result, we showed a correlation between perineuronal nets (PNNs) disruption and microglial activation in the perilesional region.

Later, we applied the CCD methodology in novel genetic mouse models to better understand the role of Nrg1 signaling *in vivo* after cortical injury. We induced acute Nrg1 deletion prior to

injury in young and aged mice and observed that Nrg1 deletion promoted neuroinflammatory response and limited axonal preservation and spontaneous motor recovery after cortical injury. Finally, we specifically expressed Nrg1-ICD to provide a mechanistic perspective and observed that activation of this intracellular pathway decreased the neuroinflammatory response. Collectively, our results shed light on Nrg1 signaling, and specifically the activation of its intracellular pathway, as a promising molecular target in neuroprotection, cortical regeneration, and recovery after brain injury.

RESUMEN

El daño cerebral es la mayor causa de discapacidad en la etapa adulta, particularmente afectando a la población anciana. Independientemente de la causa, los diferentes tipos de daño cerebral comparten eventos fisiopatológicos similares. Hasta ahora, la mayoría de los estudios se han enfocado en estudiar las respuestas inmediatas tras la lesión, mientras que los mecanismos que subyacen bajo los procesos de plasticidad y regeneración cortical aún son poco comprendidos. Neuregulina 1 (Nrg1) es una proteína esencial en el desarrollo de los circuitos corticales que se ha asociado a diferentes trastornos psiquiátricos, como la esquizofrenia. En las últimas décadas, varios trabajos proponen a Nrg1 como un factor neuroprotector emergente en el ámbito de lesión. No obstante, la mayoría de las investigaciones se centran en estudiar la respuesta temprana de la forma soluble de Nrg1 tras el daño, mediada por la activación de los receptores ErbB, la cual no recapitula la compleja señalización de Nrg1 en su totalidad. De este modo, nuestro laboratorio ha demostrado previamente que la señalización intracelular de Nrg1 se activa en situaciones de hipoxia, promoviendo la supervivencia neuronal tras ictus.

El principal objetivo de esta tesis es estudiar el papel de la señalización de Nrg1 en la regeneración y plasticidad cortical tras daño cerebral. Para ello, hemos desarrollado novedosos modelos para 1) ofrecer una nueva metodología que permita estudiar la regeneración axonal *in vitro* e *in vivo* y 2) específicamente centrarnos en el papel de la señalización intracelular de Nrg1 en el ámbito de daño cortical.

Primero, hemos desarrollado un nuevo modelo *in vitro* de lesión axonal en cultivos de neuronas corticales. En él, se utilizaron técnicas de electroporación para marcar un número limitado de neuronas, combinado con una posterior lesión física basada en una transección mecánica de los axones. En este modelo, también se realizaron estudios de ganancia y pérdida de función para comprender el papel de Nrg1 en el crecimiento axonal. Nuestros resultados mostraron que Nrg1, y específicamente la activación de su vía intracelular, potencia el crecimiento axonal tras daño.

Posteriormente, hemos diseñado una metodología novedosa en ratones para estudiar la regeneración cortical, combinando técnicas de trazado de conexiones cortico-corticales con una lesión focal y mecánica en la corteza primaria motora. Además, se realizó una extensa caracterización funcional empleando diversas pruebas comportamentales específicas para detectar déficits motores en lesiones unilaterales como la ofrecida en este modelo. Gracias al procesamiento del tejido cerebral en secciones coronales distribuidas en series flotantes, se combinaron diferentes tinciones para realizar reconstrucciones 3D del cerebro y, así, ofrecer un estudio completo incluyendo desde medidas volumétricas hasta un análisis de diferentes poblaciones celulares y estructuras subcelulares. Como ejemplo de la potencia de este método,

se observó la correlación entre la eliminación de redes perineuronales y la activación de células microgliales en la zona adyacente a la lesión.

Esta metodología de lesión cortical *in vivo* ha sido utilizada a lo largo de esta tesis en innovadores modelos genéticos de ratón para entender el papel de Nrg1 tras daño cortical. En este sentido, se eliminó la expresión del gen de Nrg1 en ratonas jóvenes y maduras previamente a la lesión, observando que la ausencia de Nrg1 promueve la respuesta neuroinflamatoria y una preservación axonal limitada, conllevando una menor recuperación motora espontánea tras la lesión.

Finalmente, para ofrecer una visión mecanicista del papel de la señalización intracelular de Nrg1, su dominio intracelular se expresó específicamente en neuronas corticales, observando que la activación de esta vía de señalización reduce la respuesta inflamatoria tras lesión cortical. En conclusión, nuestros resultados señalan que la señalización de Nrg1, y específicamente la activación de su vía intracelular, podría ser una diana molecular prometedora en el contexto de neuroprotección, regeneración y recuperación cortical tras daño cerebral.

RESUM

El dany cerebral és la major causa de discapacitat en l'etapa adulta i particularment afecta a la població anciana. Independentment de la causa, els diferents tipus de dany cerebral comparteixen esdeveniments fisiopatològics similars. Fins ara, la majoria dels estudis s'han enfocat a examinar les respostes immediates després de la lesió, mentre que els mecanismes que subjauen sota els processos de plasticitat i regeneració cortical encara són poc compresos. Neuregulina 1 (Nrg1) és una proteïna essencial en el desenvolupament dels circuits corticals i s'ha associat a diferents trastorns psiquiàtrics, com l'esquizofrènia. En les últimes dècades, diversos treballs proposen a Nrg1 com un factor neuroprotector emergent en l'àmbit de lesió. No obstant això, la majoria de les investigacions es centren en estudiar la resposta primerenca de la forma soluble de Nrg1 després del mal, mediada per l'activació dels receptors ErbB, la qual no recapitula la complexa senyalització de Nrg1 íntegrament. D'aquesta manera, el nostre laboratori ha demostrat prèviament que la senyalització intracel·lular de Nrg1 s'activa en situacions d'hipòxia, promovent la supervivència neuronal després de l'ictus.

El principal objectiu d'aquesta tesi és estudiar el paper de la senyalització de Nrg1 en la regeneració i plasticitat cortical després del dany cerebral. Per a això, hem desenvolupat nous models per a 1) oferir una nova metodologia que permeta estudiar la regeneració axonal *in vitro* i *in vivo* i 2) específicament centrar-nos en el paper de la senyalització intracel·lular de Nrg1 en l'àmbit de dany cortical.

Primer, hem desenvolupat un nou model *in vitro* de lesió axonal en cultius de neurones corticals. En ell, es van utilitzar tècniques de electroporació per a marcar un nombre limitat de neurones, combinat amb una posterior lesió física basada en una secció mecànica dels axons. En aquest model, també es van realitzar estudis de guany i pèrdua de funció per a comprendre el paper de Nrg1 en el creixement axonal. Els nostres resultats van mostrar que Nrg1, i específicament l'activació de la seua via intracel·lular, potència el creixement axonal després del dany.

Posteriorment, hem dissenyat una nova metodologia en ratolins per a estudiar la regeneració cortical, combinant tècniques de traçat de connexions cortico-corticals amb una lesió focal i mecànica en l'escorça primària motora. A més, es va realitzar una extensa caracterització funcional emprant diverses proves comportamentals específiques per a detectar dèficits motors en lesions unilaterals com l'oferida en aquest model. Gràcies al processament del teixit cerebral en seccions coronals distribuïdes en sèries flotants, es van combinar diferents tincions per a realitzar reconstruccions 3D del cervell i, així, oferir un estudi complet incloent des de mesures volumètriques fins a una anàlisi de les diferents poblacions cel·lulars i estructures subcelul·lars. Com a exemple de la potència d'aquest mètode, es va observar la correlació entre l'eliminació de xarxes perineuronals i l'activació de cèl·lules microglials en la zona adjacent a la lesió.

Aquesta metodologia de lesió cortical *in vivo* ha sigut utilitzada al llarg d'aquesta tesi en innovadors models genètics de ratolí per a entendre el paper de Nrg1 després de dany cortical. En aquest sentit, es va eliminar l'expressió del gen de Nrg1 en ratolins joves i madurs prèviament a la lesió, observant que l'absència de Nrg1 promou la resposta neuroinflamatoria i una preservació axonal limitada, el que comporta una menor recuperació motora espontània després de la lesió.

Finalment, per a oferir una visió mecanicista del paper de la senyalització intracel·lular de Nrg1, el seu domini intracel·lular es va expressar específicament en neurones corticals, observant que l'activació d'aquesta via de senyalització redueix la resposta inflamatòria després de la lesió cortical. En conclusió, els nostres resultats assenyalen que la senyalització de Nrg1, i específicament l'activació de la seua via intracel·lular, podria ser una diana molecular prometedora en el context de neuroprotecció, regeneració i recuperació cortical després de dany cerebral.

PUBLICATIONS

Part of the results obtained along this PhD dissertation has been published in the following scientific article:

1. **González-Manteiga, A**., Navarro-González, C., Sebestyén, V., Saborit-Torres, J., Talhada, D., de la Iglesia-Vayá, M., Ruscher, K., Fazzari, P. A novel in vivo model for multiplexed analysis of callosal connections upon cortical damage. *Int J Mol Sci*, 2022; 23(15):8224. doi: 10.3390/ijms23158224.

ABBREVIATIONS AND ACRONYMS

AAVs: adeno-associated viral vectors

ADM17: A disintegrin and metalloprotease 17

ADM19: A disintegrin and metalloprotease 19

ARSB: arylsulfatase B

BACE: beta-site APP cleaving enzyme 1

BBB: blood-brain barrier

BI: brain injury

Ca^{2+}: calcium

CAP-23: cytoskeleton-associated protein

CC: corpus callosum

CCD: controlled cortical damage

CCR5: C-C chemokine receptor 5

chABC: chondroitinase ABC

CNS: central nervous system

CST: corticospinal tract

CRD: cysteine-rich domain

CRD-Nrg1: cysteine-rich domain Nrg1 (=Nrg1 type III)

CREB: cAMP-response-element binding protein

CSPGs: chondroitin sulfate proteoglycans

DRG: dorsal root ganglia

EDTA: ethylenediamine tetraacetic acid

EGF: epidermal growth factor

FDA: Food and Drug Administration

FEDACE: Federación Española de Daño Cerebral

GABA: gamma-Aminobutyric Acid

GAP43: growth associated protein 43

GDF10: growth and differentiation factor 10

GFAP: glial fibrillary acidic protein

GFP: green fluorescence protein

GOF: gain-of function

HA: hyaluronidase

HBSS: hank's Balanced Salt Solution

HEPES: N-2-Hydroxyethylpiperazine-N'-2-Ethanesulfonic Acid

Iba1: Ionized calcium-binding adaptor molecule 1

IgG: Immunoglobulin G

KO: knockout

LH: left hindlimb

LOF: loss-of function

MAPK: mitogen-activated protein kinase

MCAO: middle cerebral artery occlusion

MEM: minimum Essential Medium

MGE: medial ganglionic eminence

NG2: Neural/glial antigen 2

NMDA: N-methyl-D-aspartate

Nrg1: Neuregulin 1

Nrg1-FL: CRD-Nrg1 full-length

Nrg1-ICD: Nrg1 intracellular domain

NSL: narrow-spaced ladder

OGD: oxygen glucose deprivation

PCR: polymerase chain reaction

PFA: paraformaldehyde

PKC: protein kinase C

PL: perilesional

PNNs: perineuronal nets

PNS: peripheral nervous system

PSD95: postsynaptic density protein 95

PT: phototrombosis

PV interneurons: parvalbumin interneurons

RFP: red fluorescence protein

RH: right hindlimb

rNrg1: recombinant human Nrg1

ROI: regions of interest

RPT: rotating pole test

RTL: rotation to the left

RTR: rotation to the right

SCI: spinal cord injury

Sema3a: Semaphorin 3A

TBI: traumatic brain injury

tPA: tissue plasminogen activator

TTC: 2,3,5-Triphenyltetrazolium chloride

WFA: Wisteria Floribunda agglutinin

WSL: wide-spaced ladder

WT: wild type

LIST OF FIGURES AND TABLES

FIGURES:

TABLES:

SUPPLEMENTARY MATERIAL:

INDEX

BRAIN DAMAGE

Brain damage constitutes the leading cause of adult disabilities worldwide. According to the cause, brain damage can be classified into traumatic and not traumatic. In the last category, neural infections, brain tumor, aneurism or stroke are encountered (Najem et al., 2018). Thanks to scientific and clinical research advance in terms of prevention, early detection and therapy, the mortality rate has been reduced in recent decades. However, brain damage leads to physical, cognitive and neurological impairment that compromise patients'quality of life and correspond to a socioeconomical burden (Ma et al., 2014; Najem et al., 2018). Alarmingly, there is emerging evidence that both stroke and TBI are an important risk factors for the development of dementia in later life stages (Jamjoom et al., 2021; Moskowitz et al., 2010). Therefore, brain damage must be addressed in the scientific and clinical fields to develop effective treatments.

Etiology and epidemiology

Describing all the different types of brain injury is beyond the scope of this dissertation. Hence, in the next section we will focus on traumatic brain injury (TBI) and stroke, the most typical causes of brain damage. Consequently, several experimental animal models have been developed in the scientific literature to investigate the mechanisms underlying brain damage and how to promote neuroprotection and regeneration (Fluri et al., 2015; Ma et al., 2019; Sommer, 2017; Xiong et al., 2013).

Stroke

Stroke is the major cause of brain damage and the second leading cause of death worldwide, caused by a sudden interruption of blood supply to a specific brain region, resulting in tissue death. Depending on the insult, there are two main subtypes of stroke: ischemic, which is more common, and hemorrhagic, which is more lethal (Zhao & Willing, 2018).

According to statistics, more than 700.000 cases of stroke occur every year in the United States (US). In Spain, 70.000 new cases of stroke occur every year (Sociedad Española de Neurología, 2019). Although approximately the 80% of the patients survived, half of them suffer from permanent functional disabilities, depending on the size and location of the injury (Benowitz & Carmichael, 2010).

Different risk factors are associated with an increased prevalence of stroke. While some of them are not modifiable, such as familiar antecedents, genetic conditions, aging and sex condition, others can be partially controlled, including hypertension, hyperlipidemia, diabetes, hypercholesterolemia, smoking, poor diet and cardiopathies, which encompass the 60-80% of

stroke risk (Caprio & Sorond, 2019). These factors increase stroke susceptibility by damaging cerebral vascular structure mediated by the uprise in oxidative stress and vascular inflammation. Ultimately, this scenario increases the permeability of the blood-brain barrier (BBB), leading to a positive feedback effect throughout the brain. These cellular and molecular changes compromise an adequate blood perfusion rate in the cerebral tissue. However, while it has been identified different factors that predispose to stroke, little is known about what are the specific signals that ultimately trigger the stroke (Moskowitz et al., 2010).

Notably, stroke is associated with aging, with the elderly population being the most vulnerable and experiencing higher rates of mortality and morbidity. Therefore, they present a limited functional recovery compared to young people. In the case of sex, it has also been described that higher incidence is presented in men, compared to women (Roy-O'Reilly & McCullough, 2018). This fact has been mainly associated with the neuroprotective effect of some estrogens in the female brain. However, the situation is reversed after menopause, in which women showed an increase stroke incidence. Hence, the prevalence is also age-related (Murphy et al., 2004). Remarkably, more women than men are affected nowadays, which is partly explained by the higher life expectancy of women (Chauhan et al., 2017). Therefore, providing a sex and age perspective is a critical step for therapeutic development.

Interestingly, while there are some risk factors that cannot be modified, such as age, sex or genetic conditions, others are largely influenced by the lifestyle, such as high blood pressure, smoking and poor diet. Therefore, from a therapeutic point of view, a valuable approach could be to promote healthy and sustainable habits that can be incorporate in our daily lives to help prevent stroke, calling up for a preventive medicine (Caprio & Sorond, 2019).

Traumatic brain injury

TBI is the second cause of brain injury, caused by an external mechanical force, produced by nonpenetrating insults, including concussion, rapid acceleration or deceleration or blast waves; or penetrating insults, such as projectiles. Currently, the most common causes are traffic accidents, certain sports activities, and falls (Xiong et al., 2013).

In the US, it has been registered that approximately 1,5 million people suffer from TBI within one year (Najem et al., 2018), and in Spain, according to the Spanish Organization of Cerebral Injury (FEDACE in Spanish), nearly 74.000 causes are counted each year. Noteworthy, it is important to mention that this alarming number can be explained by the heterogeneity of situations that produce TBI, compared to stroke disorder. However, this fact should not diminish the impact that TBI has in our society, causing a robust percentage of patients with permanent disabilities and, therefore, a relevant economical and human cost (Caprio & Sorond, 2019).

Conversely to the stroke scenario, TBI is caused by several diverse insults mentioned above, but the young population is much more affected. In fact, it is considered one of the leading causes of nonspecific death and disabilities in young adults under 45 years of age, mainly affected by dangerous sportive practices and traffic accidents. Fortunately, this incidence is recently decreasing due to the increase in safety regulations and government policies in richer countries (Najem et al., 2018). Remarkably, the incidence of TBI is also relevant in the elderly population, mainly due to falls. Even though the severity of TBI is strongly dependent on the insult and the size of the injury, it has also been reported that elderly population has a limited ability to recover after brain damage, as in the stroke scenario (Conde & Siebner, 2020; Dixon, 2017; Heegaard & Biros, 2007).

The development of therapeutic approaches is a challenging task in the field of TBI, partly explained by the heterogeneity in terms of injury causes, patient response, and clinical manifestations, leading to a worst-case paradigm in terms of prevention, diagnosis, and treatment (Najem et al., 2018).

Physiopathological events upon brain damage: the relevance of enhancing the subacute phase

Albeit each type of brain damage undergoes specific cellular events, all of them share similar physiopathological mechanisms which can be classified into four distinct phases, according to the time of onset: hyperacute, acute, subacute, and chronic (**Figure 1**).

Immediately after brain damage, different simultaneously molecular and cellular events are triggered, leading to massive cell death within the first hours. Briefly, the lack of energy supply to the affected neurons impairs the maintenance of the resting potential, resulting in neuronal depolarization. This depolarization promotes glutamate release which, through the N-methyl-D-aspartate (NMDA) receptor, triggers Ca^{2+} internalization which in turn increases glutamate release (Lai et al., 2014). Hence, a positive depolarization feedback is established, reaching neighboring neurons. Of note, intracellular Ca^{2+} also triggers mitochondrial dysfunction, which ultimately leads to a release of reactive oxygen species, promoting oxidative stress. Consequently, this excitotoxic environment activates apoptotic pathways, ending in a massive loss of neurons, the most vulnerable cells in the brain (Carmichael, 2016b).

Subsequently, the acute phase is characterized by the emergence of a neuroinflammatory response within the first week after injury, displayed in two phases: an early response mediated by activation of astrocytes and microglia, followed by a posterior infiltration of peripheral immune cells, due to BBB disruption and the production of attractive chemokines by glial cells (Anrather & Iadecola, 2016). These cell populations are mainly involved in the removal of cellular debris and engulfment of dysfunctional synaptic boutons, releasing different cytokines and free

radicals that eventually signal neuronal repair (Karve et al., 2016; Michinaga & Koyama, 2021). However, an excessive inflammatory response can lead to detrimental processes that contribute to cell death (Anrather & Iadecola, 2016; Moskowitz et al., 2010; Witcher et al., 2021). In addition, reactive astrocytes form a glial scar around the injured area which produces growth inhibitory molecules such as chondroitin sulfate proteoglycans (CSPGs), which restrict axonal sprouting near the injured zone (Carmichael et al., 2005).

Once the inflammatory response has subsided, there follows a subacute phase characterized by the maximum window of plasticity, which lasts up to 1 month in rodents and 3 months in human patients. This endogenous plasticity is prompted by different molecular and cellular mechanisms. For instance, a unique transcriptional gene program is regulated in sprouting neurons, involved in relevant regenerative functions, such as growth factors, cytoskeletal dynamics, and synaptogenesis (Li et al., 2010). Interestingly, this sprouting transcriptome differs between young and aged mice, partially explaining the limited regenerative capacity in aged population. Thus, the activation of these molecular pathways ends in axonal sprouting and dendritic spine turnover, leading to synaptic plasticity (Brown et al., 2009; Carmichael et al., 2001; Jones et al., 1996; Takatsuru et al., 2009). Remarkably, these events are not just restricted to the perilesional (PL) area, but also affect other adjacent and connected brain regions, promoting new cortical remapping events (Brown et al., 2009; Carmichael et al., 2017; Dancause et al., 2005). However, this recovery is generally not sufficient to restore motor functioning, due to the limited regenerative capacity of the central nervous system (CNS) (Curcio & Bradke, 2018), leading to permanent disability in adulthood and, hence, the establishment of the chronic phase (Joy & Carmichael, 2021).

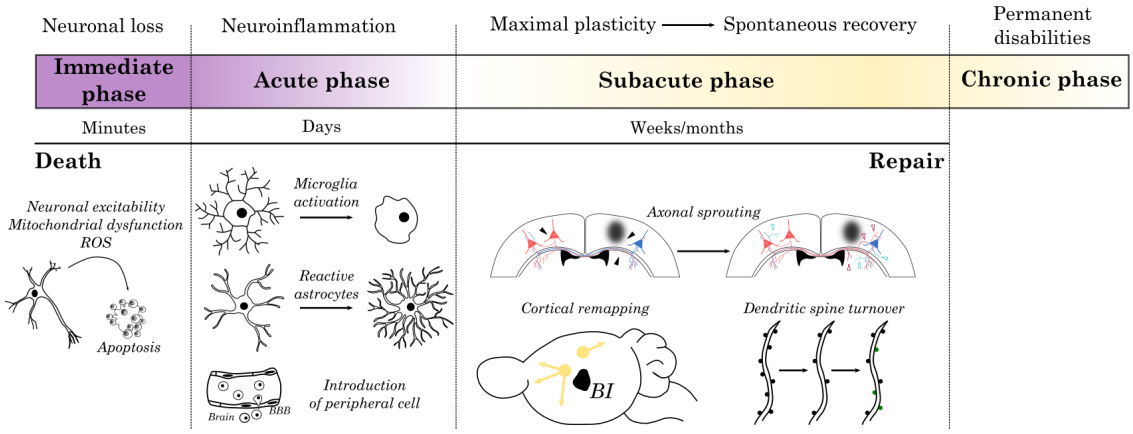

Figure 1. Physiopathological phases upon brain damage. Remarkably, the subacute phase is defined by a maximum period of plasticity, corresponding to an intriguing and wide therapeutic window of response.

The process of axonal sprouting after cortical damage suggests that trigger events are produced in the injured area, where primary neuronal death leads to the activation of secondary injury

cascades that signal to surrounding and connected neural tissue (Carmichael et al., 2017). Thus, there has been a major effort over the past few decades to understand the mechanisms underlying axonal sprouting and, by extension, which triggering factors are enhanced after brain injury.

After cortical damage, an early synchronous neuronal activity is identified in the PL area within the first 3 days, which also synchronizes neuronal activity in other connected cortical regions. Indeed, blocking this rhythmic neuronal activity decreased axonal sprouting (Carmichael & Oise Chesselet, 2002). Complementary, reactive astrocytes restrict gamma-aminobutyric acid (GABA) uptake, thereby increasing extracellular GABA levels. This results in increased GABAergic transmission, preventing neuronal death early in the injury (Deng et al., 2019). However, a sustained inhibitory response in neurons of the PL area can be detrimental to circuit restoration during the recovery period. Indeed, blocking GABAergic transmission several days after damage is beneficial for functional recovery (Clarkson et al., 2010). In this line, recent data using an elegant model to activate or silence the expression of cAMP-response-element binding protein (CREB) in a limited number of neurons in the PL area through chemogenetic strategies showed that promoting neuronal activity *in vivo* also contributes to the formation of novel cortical circuits and promotes motor recovery upon stroke (Caracciolo et al., 2018). Hence, these data suggest that neuronal excitability contributes to promoting axonal sprouting and, ultimately, functional recovery (Joy & Carmichael, 2021).

The establishment of a permissive growth environment is required for axonal regeneration upon injury. In this regard, it has been described that different growth-promoting and growth-inhibitory factors are expressed and finely regulated over time to determine the degree of axonal sprouting in the PL area after stroke (Carmichael et al., 2005).

In short, although some pro-growth molecules such as GAP43, CAP-23 and cJUN are maintained throughout the time course of axonal sprouting, other regenerative factors are highly overexpressed within the first two weeks upon stroke. Conversely, inhibitory factors such as NG2, Sema3a and different proteins of the CSPGs family are overexpressed after this time point (**Figure 2A**). Therefore, there is a specific window of response between 7 and 14 days upon damage in which axonal sprouting is enhanced (Carmichael et al., 2005). Remarkably, this molecular profile was concretely defined in a broader PL region extending medially up to 2mm in the rat cortex. Hence, this specific regenerative zone is not adjacent to the glial scar, where inhibitory growth factors are released (**Figure 2B**).

Therefore, these data reveal an intriguing temporal and spatial window of response, which may help to develop novel therapeutic strategies to effectively enhance axonal sprouting within this period, or novel molecular targets to widen this window. It is noteworthy, however, that

simultaneously enhancing growth factors and restricting inhibitory molecules may result in increased, but abnormal axonal sprouting which ultimately worsens motor abilities (Carmichael et al., 2017; T. H. Murphy & Corbett, 2009).

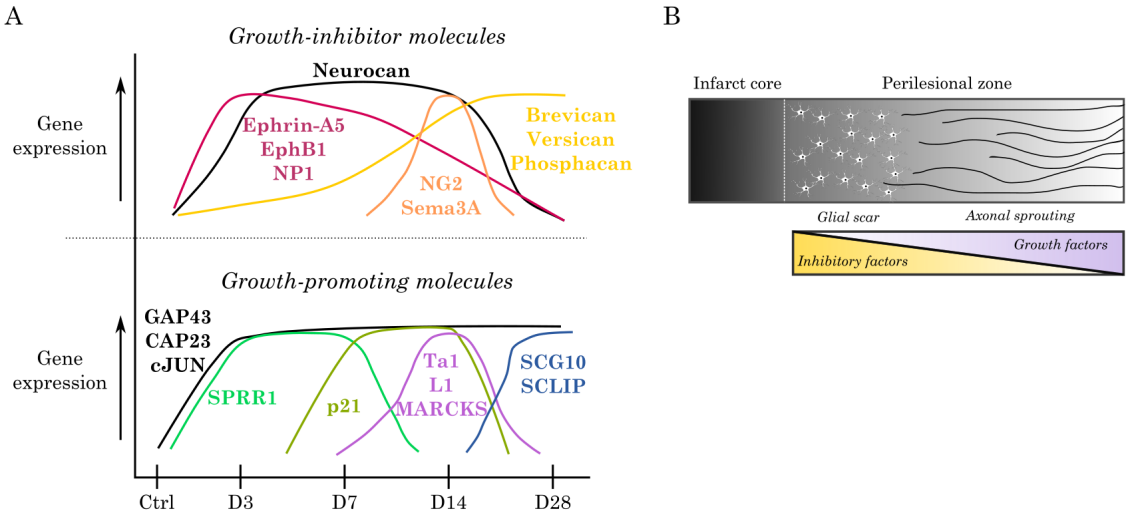

Figure 2. Axonal sprouting is enhanced in the perilesional area. A) Scheme illustrating the time course of expression of growth-associated genes upon stroke. The graph is adapted from Carmichael et al., 2005. B) The cartoon represents the two different PL zones in the rat cortex: a closer one where the glial scar releases inhibitory growth factors; and a broader area where axonal sprouting is enhanced by growth factor expression.

Thus, a critical window of plasticity and axonal sprouting is restored upon damage, sharing some similarities with developmental stages, such as dendritic spine turnover and axonal sprouting. However, regeneration cannot entirely recapitulate development, due to differences in intracellular and extracellular factors between developing and mature brain. As an illustrative example, in the adult brain, some projecting axons are far away from their respective soma, which complicates axonal transport of proteins and molecules required for regeneration upon injury (Hilton & Bradke, 2017). Noteworthy, cortical circuitry is well established in the adult brain, decreasing plasticity to promote neuronal specificity (De León Reyes et al., 2020). In this sense, axonal regeneration can be compromised in order to maintain an adequate neural circuit in adulthood. Therefore, seeking novel molecular targets to enhance plasticity is both an intriguing therapeutic strategy and a clinical challenge.

Current approaches in research and treatment for brain injury: novel insights to promote axonal regeneration and plasticity

In the last decades, considerable scientific advances have been done in understanding the mechanisms underlying the physiopathology of brain damage. However, there has been no significant progress in the development of effective therapeutic strategies to treat brain injury (Moskowitz et al., 2010).

In the field of stroke, most of the strategies are focused on providing therapies to restore blood supply by using thrombolytic agents. In this regard, the only drug approved and available in the clinical scenario is the tissue plasminogen activator (tPA). However, its administration is recommended within the first 3 hours after stroke onset, and it involves an elevated risk of intracerebral hemorrhage, so it can only be applied to a restricted group of patients (Zhao & Willing, 2018).

In the context of TBI, the scenario is even worse. Various neuroprotective agents have been explored in different clinical trials to regulate excitotoxicity, oxidative stress and neuroinflammation (reviewed in Thapa et al., 2021). However, almost all clinical trials failed in phase II/III in the last decades, so there is still no effective treatment to overcome TBI (Xiong et al., 2015).

The scientific challenges underpinning the design of novel therapeutic strategies for brain damage are partly explained by the heterogeneity of the molecular, cellular, and structural events that take place, which are also conditioned by reasons of age and sex (Moskowitz et al., 2010; Zhao & Willing, 2018). Furthermore, most of the proposed therapies have been centered on improving neuroprotection in the early stages after brain damage, which offers a narrow window of response compared to the plasticity period in the subacute phase (Joy & Carmichael, 2021). Hence, novel therapeutic strategies could integrate both cell death and neural plasticity paradigm to offer an effective treatment for brain damage (Carmichael, 2016a).

However, it is noteworthy to mention that the CNS has a limited regenerative ability, defined by a complex combination of intrinsic and extrinsic factors that attempt to modulate axonal regrowth capacity after injury. The intrinsic factors relate to intracellular events, including the gene expression program, growth cone formation, mitochondrial function, and axonal protein transport. Additionally, the extracellular signals are also required to promote a suitable environment for axonal regrowth. In contrast to developmental stages, these events differ upon injury, where the growth-promoting gene expression is decreased, mitochondrial and axonal protein transport is impaired resulting in the formation of retractive bulbs that ultimately fail to regenerate the axons. Furthermore, several inhibitory elements are released after damage, including repulsive axon guidance cues, inhibitory growth factors produced by the glial scar, and myelin-associated molecules, which ultimately contribute to a restrictive regeneration process (BrosiusLutz & Barres, 2014; Curcio & Bradke, 2018; Hilton & Bradke, 2017).

Hence, identifying the different cellular and molecular events underpinning the process of axonal regeneration and sprouting upon brain injury conforms a pivotal step to offer novel therapeutic targets to enhance axonal growth. In this regard, different molecules have been proposed as promising molecular targets to enhance axonal sprouting and, hence, functional recovery.

One promising strategy described is neutralizing the inhibitory growth factors produced in the vicinity of the injured area. To this end, blocking the effect of a neurite growth inhibitory protein named Nogo-A in different chemical and molecular experimental models promotes axonal sprouting and, consequently, motor functional recovery upon stroke. Hence, the usage of antibodies against Nogo-A has been proposed as a feasible and potential clinical treatment upon CNS injury (Huebner et al., 2011; Lindau et al., 2014).

Another intriguing molecular target in this line is the chemical digestion of CSPGs, the second major inhibitory molecule produced by reactive astrocytes in the glial scar. CSPGs are the main component of perineuronal nets (PNNs), a specialized extracellular matrix surrounding neuronal bodies regulating synaptic plasticity. Hence, different compounds, such as chondroitinase ABC (chABC) enzyme, arylsulfatase B (ARSB) and hyaluronidase (HA) inhibition have been proposed as potential treatments, by disrupting PNN integrity to reopen plasticity periods and, ultimately, enhance regenerative states (Katarzyna Greda & Nowicka, 2021; Pearson et al., 2018; Wang & Fawcett, 2012). Remarkably, the combination of anti-Nogo-A and chABC was more effective in improving functional recovery upon spinal cord injury (SCI). Hence, these data provide novel insights into how different treatments with similar molecular mechanisms can provide a synergistic effect (Zhao et al., 2013).

However, the previously described compounds face some difficulties in regulatory approval, and they may have a non-specific effect throughout the organism, not just into the injured brain regions. Hence, another promising alternative which overcomes these limitations is based on epothilones, a drug that promotes polymerization of microtubules into the axon tip, thereby regulating cytoskeletal dynamics, a crucial step for an effective axonal regeneration. In this context, recent data suggest that treatment with epothilone B and epothilone D, already approved by US Food and Drug Administration (FDA), can be a novel therapeutic strategy to promote axonal regeneration in the PL area and reduce glial scar formation, ultimately improving motor recovery upon stroke (Kugler et al., 2020).

Furthermore, several works carried out by the laboratory of Dr Thomas Carmichael have proposed novel intriguing molecular targets to enhance axonal sprouting and, hence, motor recovery upon stroke, including the blockade of EphrinA5 and C-C chemokine receptor 5 (CCR5), and stimulation of growth and differentiation factor 10 (GDF10) (Joy et al., 2019; Li et al., 2015; Overman et al., 2012). Of note, this group also demonstrated that the pharmacological administration of *Maraviroc*, an FDA-approved CCR5 antagonist in human immunodeficiency virus (HIV), promotes neuroprotective effects and axonal sprouting that enhance functional recovery in both stroke and TBI models. These data offered a promising already available therapeutic treatment for future clinical trials related to brain injury (Joy et al., 2019).

Finally, another biological event which can potentiate regeneration outside of axonal sprouting is the process of neurogenesis, which has been identified in the hippocampal dentate gyrus (DG) and subventricular zone (SVZ) in the adult brain (Sawada & Sawamoto, 2013). Intriguingly, it has also been reported that cortical injury can stimulate the formation and migration of neuroblasts from the SVZ to damaged areas. Recent data support that intranasal administration of a plant-derived diterpene (EOF2) stimulates the migration of neuroblasts towards the PL area and their differentiation into mature functional neurons (Domínguez-García et al., 2020). However, it should be mentioned that only a small number of newly generated neurons survived in this scenario, and future studies are required to better ascertain whether newly generated neurons can integrate into the circuit and improve functional recovery. Hence, the relevance of neurogenesis as a potential therapeutic target is still under investigation.

Remarkably, the EOF2 effect was mediated by the activation of protein kinase C (PKC), which facilitates the release of Neuregulin 1 (Nrg1), an important intrinsic growth factor recently proposed as a neuromodulatory factor upon CNS repair. Nrg1 signaling has been extensively studied in this dissertation, so details of its importance in cortical development and neural repair are described below.

THE ROLE OF NEUREGULIN1/ERBB AXIS IN DEVELOPMENT. A NEUROPROTECTIVE FACTOR UPON BRAIN DAMAGE.

Presenting the main characters: Nrg1 and ErbB proteins

Neuregulins (Nrgs) conform an extensive family of growth and differentiation signaling proteins. Even though they are encoded by 6 different genes (NRG1-NRG6), NRG1 is the most well characterized one, involved in essential roles for the development and maintenance of the nervous system (Falls, 2003; Mei & Nave, 2014).

Due to multiple 5' flanking regulatory elements and alternative splicing, the NRG1 gene can produce at least 31 different isoforms, which are classified into six different types. Despite differences in the amino-terminal sequence, they share an extracellular epidermal growth factor (EGF)-like domain, which is crucial for the stimulation of ErbB receptor tyrosine kinases. NRG1 isoforms are generated as transmembrane proteins with the EGF domain exposed to the extracellular side (**Figure 3**). However, they can undergo a process of enzymatic cleavage into the C-terminal region of the EGF domain by ADAM17, BACE and ADAM19 proteases (Mei & Xiong, 2008; Willem, 2016). This leads to the release of the soluble mature form of Nrg1. However, Nrg1 type III (also referred to as CRD-Nrg1) contains a cysteine-rich domain (CRD) in the N-terminal domain, remaining both C and N-termini inside the cell. Hence, while soluble forms of Nrg1 mediate their specific roles in a paracrine manner, Nrg1 type III conforms to a membrane-bound form, acting in a juxtracrine manner (Esper et al., 2006; Falls, 2003). Conversely, Nrg1 types I, II, IV, V contain an immunoglobulin (Ig)-like domain (Falls, 2003).

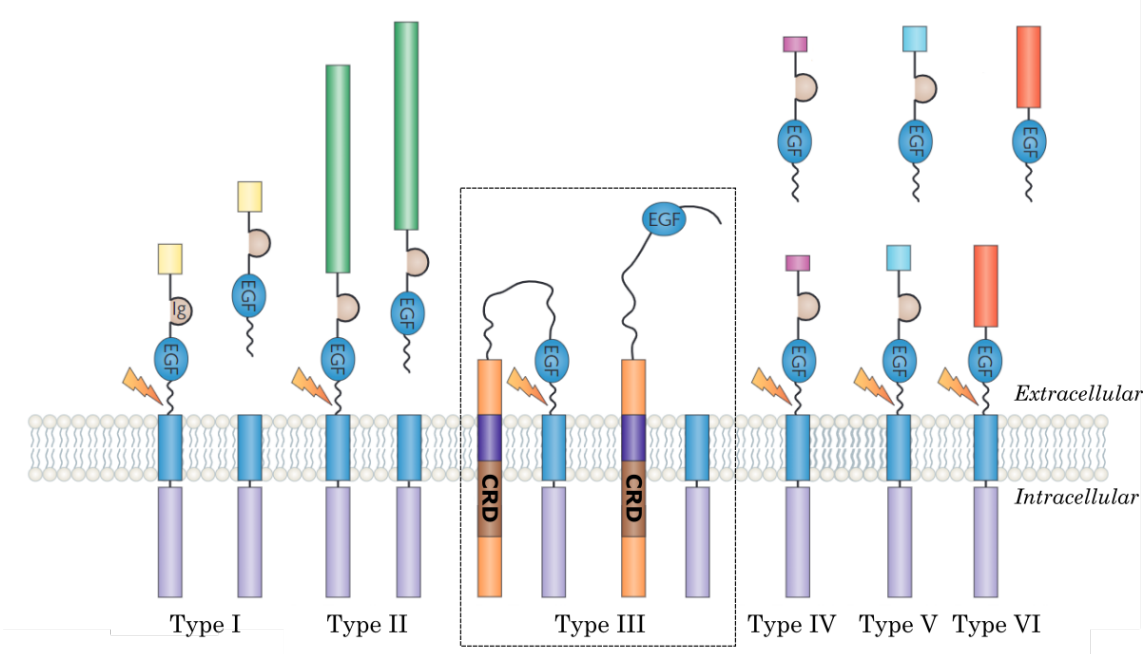

Figure 3. Nrg1 isoforms are classified into six different types, according to their amino-terminal sequences. After enzymatic cleavage, all types of Nrg1 release a soluble form, except transmembrane

Nrg1 type III (boxed), which contains both C- and N-amino terminals inside the cell due to a CRD linked to a transmembrane domain. All Nrg1 isoforms contain an EGF domain which stimulates ErbB receptors. Adapted from Mei & Xiong, 2008.

Nrg1 isoforms are widely expressed in various tissues, including the nervous system. Using mutant mice for specific Nrg1 isoforms, different studies described distinct *in vivo* functions, pointing out that the diverse Nrg1 proteins may have different roles in neuronal development (Falls, 2003). Furthermore, Liu and colleagues performed an extensive genetic profiling to evaluate the expression pattern of Nrg1 isoforms pattern during development and found that Nrg1 type III was the most abundant in both human and rat cortex. Noteworthy, they also demonstrated that Nrg1 isoforms are highly presented in postnatal stages, suggesting that they may play critical roles in neonatal stages. At the cellular level, they also observed that all Nrg1 isoforms were predominantly expressed in excitatory neurons (Liu et al., 2011). Accordingly, recent data using a Nrg1-reporting mouse described a spatial and cellular Nrg1 expression pattern, highly expressed in pyramidal neurons of superficial layers (Ding et al., 2023). Hence, these results strengthen the idea of a versatile function of Nrg1 in the nervous system.

The effect of Nrg1 signaling is mediated by the activation of ErbB receptors, which constitutes a family of single transmembrane tyrosine kinase with four members: ErbB1 (also named epidermal growth factor receptor, EGFR), ErbB2, ErbB3 and ErbB4. Structurally, ErbB receptors are built of an extracellular region including two CRDs, a transmembrane domain and a short intracellular region containing the tyrosine kinase domain (Mei & Xiong, 2008). These transmembrane proteins are widely expressed in different cell types. Briefly, ErbB4 is mainly expressed in parvalbumin (PV) cortical interneurons, whereas ErbB2 and ErbB3 have been observed in Schwann cells, oligodendrocytes, and astrocytes (Esper et al., 2006; Fazzari et al., 2010; Mei & Nave, 2014; Meyer & Birchmeier, 1995).

The ErbB4 receptor is the most well characterized in that is the only autonomous Nrg1-specific ErbB receptor that can both interact with and be stimulated by the ligand to trigger its tyrosine kinase activity. ErbB2, which cannot bind to the ligand, must form heterodimers with other ErbB proteins to exert its catalytic activity. Conversely, ErbB3 can bind to Nrg1, but their homodimers show an impairment in their kinase function. Finally, EGFR does not bind to Nrg1, but can be coupled to the ErbB4 receptor (Bublil & Yarden, 2007). Regarding the intricacy of ErbB receptor complexes, it is worth mentioning that even though ErbB2 cannot bind Nrg1 ligand, it is essential for Nrg1 signaling, so both ErbB2/ErbB3 and ErbB2/ErbB4 mediate the effect of Nrg1 in the early mouse development (Birchmeier, 2009) (**Figure 4**). However, the ErbB4 receptor is the most abundant in the cortex, so we will mainly refer to it along this Thesis.

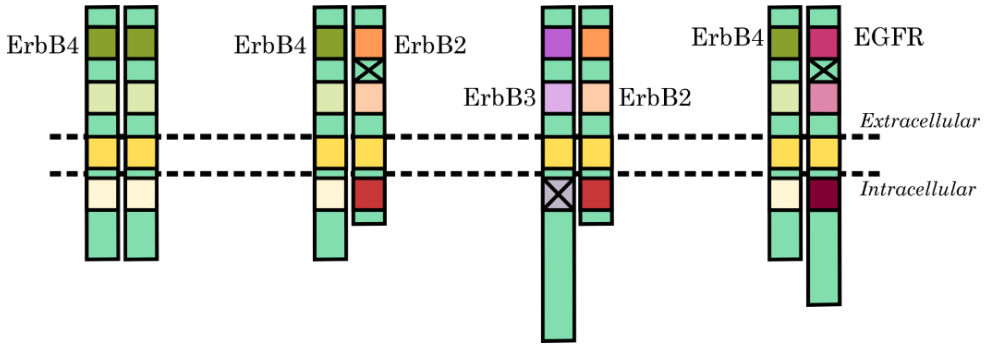

Figure 4. ErbB proteins form dimers complexes to mediate Nrg1 action.

Nrg1/ErbB4: a complex signaling pathway

Nrg1 effect through activation of the ErbB4 receptor can be described in three different pathways (**Figure 5**). In the canonical forward signaling (**Figure 5A**), the EGF domain of both Nrg1 soluble forms and CRD-Nrg1 can interact with the extracellular domain of the ErbB4 receptor, inducing its transition to the ligand-bound conformation. This conformational change leads to ErbB4 dimerization and thus stimulation of its kinase activity by the transphosphorylation of its intracellular domain (Bublil & Yarden, 2007). Different intracellular molecules are recruited to the phosphorylated tyrosine residue, activating diverse signal transduction pathways such as Raf/MEK/ERK and PI3/Akt, and promoting transcriptional modifications involved in cell survival, migration, and proliferation (Birchmeier, 2009; Falls, 2003; Mei & Xiong, 2008).

Even though we have referred to Nrg1 as the ligand of the ErbB4 receptor, the non-canonical signaling and Nrg1 intracellular signaling perfectly illustrate the complexity of Nrg1/ErbB4 signaling, which acts as both ligand and receptor under certain conditions. In the non-canonical signaling (**Figure 5B**), the ErbB4 receptor first undergoes a proteolytic cleavage of its extracellular domain, releasing a soluble form that can bind to Nrg1 (termed ecto-ErbB4). Subsequently, its intracellular domain is cleaved by γ-secretase and translocated to the nucleus for transcriptional regulation (ErbB4-ICD) (Birchmeier, 2009; Falls, 2003; Mei & Xiong, 2008).

Finally, both the diffusible ecto-ErbB4 form and the transmembrane ErbB4 conformation can bind to Nrg1 to initiate its intracellular signaling pathway (**Figure 5C**). As with non-canonical signaling, the intracellular domain of Nrg1 is cleaved by γ-secretase and translocated to the nucleus to promote changes in gene expression (Bao et al., 2003). Remarkably, there are other stimuli that can activate Nrg1 intracellular signaling, such as neuronal activity and, hence, depolarization, which upregulates postsynaptic density protein-95 (PSD95) (Bao et al., 2004). Recently, we have shown that Nrg1 intracellular pathway is stimulated in hypoxic conditions *in vitro* and *in vivo*, promoting neuronal survival (Navarro-González et al., 2019).

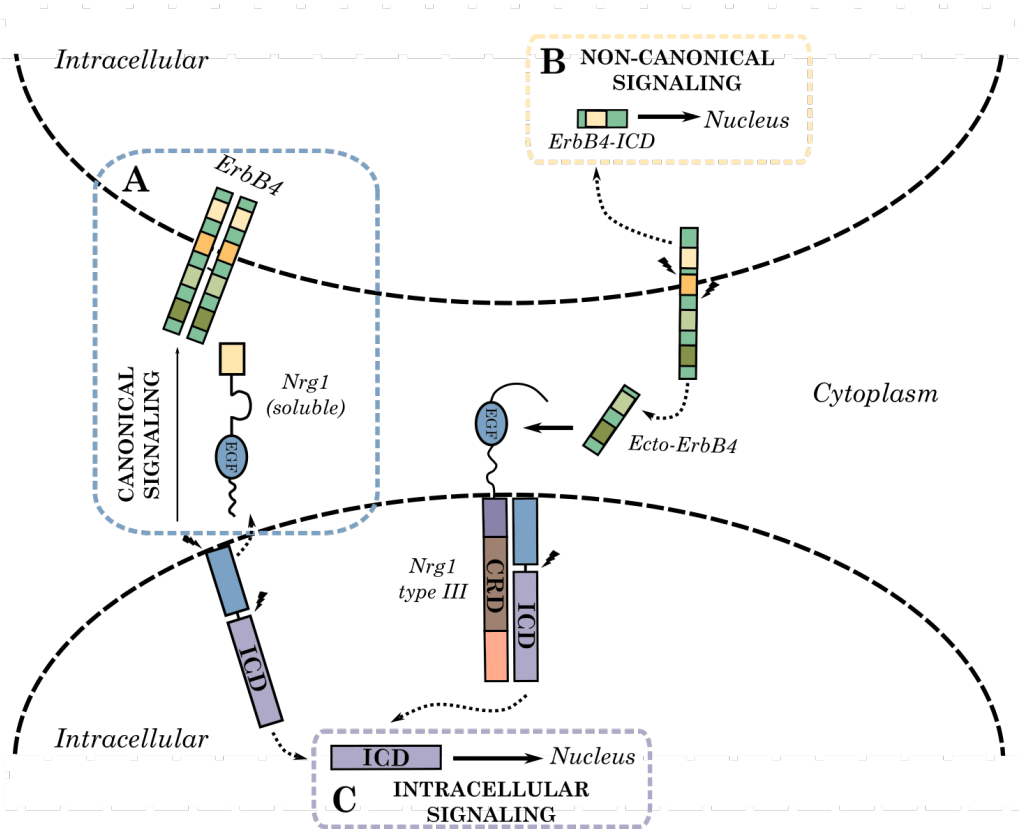

Figure 5. Nrg1/ErbB4 signaling pathways. The scheme represents the effect of Nrg1 mediated by ErbB4, which is the most well characterized receptor in the cerebral cortex. However, Nrg1 can also activate other ErbB heterodimers. Remarkably, the Nrg1 protein can serve as both ligand and receptor, providing a complex signaling pathway. A) The EGF domain of soluble form of Nrg1 or transmembrane Nrg1 type III induced dimerization of ErbB4, activating the ErbB kinase domain and thereby phosphorylating its intracellular domain. B) In the non-canonical signaling, ErbB4 intracellular domain (ErbB4-ICD) is cleaved and translocated to the nucleus for transcriptional regulation. C) ErbB4 extracellular domain (ecto-ErbB4) is released to the cytoplasm, activating pro-Nrg1 and Nrg1 type III. Similarly, the Nrg1 intracellular domain (Nrg1-ICD) is cleaved inside the cell and translocated to the nucleus, regulating gene expression.

The function of Nrg1 signaling in neuronal development

Nrg1 is essential for nervous system development and maintenance (**Figure 6**). Indeed, significant data from a genome-wide association study conducted by Stefansson and colleagues identified Nrg1 as a candidate gene for schizophrenia, a neurodevelopmental psychiatric disorder with a strong genetic component (Stefansson et al., 2002). Accordingly, some Nrg1 isoforms are atypically expressed in patients with schizophrenia (Corfas et al., 2004). Indeed, Nrg1 and ErbB4 transgenic mice exhibited schizophrenia-like behaviors (Olaya et al., 2018; Rico & Marín, 2011; Yin et al., 2013). Hence, multiple studies have been conducted to unravel the functions of Nrg1/ErbB4 signaling in cortical development to better comprehend its involvement in the disease.

Neuronal migration

Nrg1 signaling is necessary in the development of the peripheral nervous system (PNS). For instance, Nrg1, ErbB2 or ErbB3 mutant mice showed similar developmental impairments, affecting the migration and differentiation of neural crest cells into diverse neuronal and glial cells (Birchmeier, 2009; Meyer & Birchmeier, 1995). Particularly, Nrg1 type III has been largely described to regulate the biology of myelinating Schwann cells. Hence, Nrg1 is a pivotal factor in axonal myelination by promoting both Schwann cell proliferation and differentiation (Birchmeier & Bennett, 2016; Lemke, 2006; Mei & Nave, 2014). However, discussing the role of Nrg1 in PNS development will be beyond the scope of this dissertation, so we will primarly focus on Nrg1 function in the CNS.

Furthermore, Nrg1 is involved in neuronal migration in the CNS. In this sense, Nrg1/ErbB2 signaling enhances the formation and elongation of radial cells, necessary for radial migration of excitatory neurons along the cortex (Anton et al., 1997). In addition, different Nrg1 isoforms acts as short- and long-distance attractants to stimulate the tangential migration of ErbB4^{+} interneurons from the medial ganglionic eminence (MGE) to the cortex (Flames et al., 2004).

Neurite outgrowth and axon guidance

Different *in vitro* studies carried out in diverse neuronal populations and cell cultures have tested that recombinant Nrg1 can stimulate neurite outgrowth, suggesting its contribution to axon extension and, ultimately, axon guidance (Bellon, 2007; Fazzari et al., 2010a; Gerecke et al., 2004; Rieff et al., 1999). An elegant study performed by López-Bendito and colleagues using Nrg1 and ErbB4 mutant mice reported that the tangential migration of specific neuronal populations conforms to a permissive corridor that contributes to the axon pathfinding of thalamocortical projections, regulated by both Ig-Nrg1 and CRD-Nrg1 via the ErbB4 receptor activation (López-Bendito et al., 2006).

Additionally, another study reported that CRD-Nrg1 deficient mice were unresponsive to the chemorepellent Sema3A and exhibited an abnormal axon pathfinding in the spinal cord and peripheral projections. Of note, the authors also showed that the activation of Nrg1 intracellular signaling *in vitro* stimulates the expression of the Sema3A receptor neuropilin 1, suggesting CRD-Nrg1 as a regulatory molecule for axon guidance (Hancock et al., 2011). However, most of the studies used heterozygous Nrg1 mutant mice due to the lethal consequences of Nrg1 gene deletion in early embryonic stages. Hence, the precise impact of Nrg1 signaling on axon guidance remains unclear.

Myelination

Myelination is an effective process for isolating neuronal axons and increasing the propagation of electrical impulses. In the CNS, oligodendrocytes constitute the myelinating cells, extending

their processes around the axons and producing diverse myelin proteins (BrosiusLutz & Barres, 2014). Oligodendrocyte dysfunction and impaired myelination have been reported with several psychiatric disorders, such as in patients with schizophrenia (Gouvêa-Junqueira et al., 2020). Hence, the implication of Nrg1/ErbB signaling in CNS myelination has been investigated, although it remains unclear.

Nrg1 enhances the survival and migration of oligodendrocyte precursor cells (OPCs) *in vitro*, suggesting its role in oligodendrocyte development (Fernandez et al., 2000; Mei & Xiong, 2008; Ortega et al., 2012). However, different *in vivo* approaches using transgenic mice for Nrg1 and ErbB receptor showed mild changes in CNS myelination, suggesting that it can be dispensable for initiating myelination, but can modulate its quality (Birchmeier, 2009; Kataria et al., 2019; Mei & Nave, 2014; Roy et al., 2007). In this regard, CRD-Nrg1 heterozygous mice revealed hypomyelination in the forebrain, but not in the optic nerve or spinal cord, suggesting that Nrg1 isoforms mediate different myelination functions along the CNS (Taveggia et al., 2008). Recent data using different Nrg1 specific isoform mutant zebra fish demonstrated that Nrg1 type II is required for normal myelination of spinal cord (Lysko & Talbot, 2022). Interestingly, the authors also observed that Nrg1 type II signals to neighboring interneurons expressing ErbB2, but sheldom to oligodendrocytes, offering a novel paradigm in which both myelinated and unmyelinated neurons may coordinate myelination in the CNS (Lysko & Talbot, 2022).

Overall, Nrg1 signaling entails an intricate effect on CNS myelination due to 1) the differential expression of Nrg1 and ErbB receptor in different cell types and 2) the extensive number of Nrg1 isoforms that may play different roles. Hence, future research will be required to unravel the real significance of Nrg1/ErbB signaling in CNS myelination.

Cortical circuit development: synapse formation

Different genetic studies using ErbB4 and Nrg1 transgenic mice present synaptic impairment, reflected in schizophrenia-like behaviors (reviewed in Rico & Marín, 2011). These data suggest that Nrg1/ErbB4 signaling plays a pivotal role in the synapse formation and, hence, correct functioning of cortical circuits. Nrg1 is highly expressed in excitatory pyramidal interneurons, whereas the ErbB4 receptor is mainly expressed in PV^+ cortical interneurons (Fazzari et al., 2010). Therefore, Nrg1 signaling has been described as modulator of both neuronal type populations (Mei & Nave, 2014; Mei & Xiong, 2008; Rico & Marín, 2011).

Nrg1/ErbB signaling pathway has been involved in dendritic spine maturation, which is essential for an adequate synaptic transmission and thus the establishment of cortical circuits. ErbB2/ErbB4 deficient mice showed a disruption of the NMDA/PSD95 interaction, leading to a subsequent impairment of dendritic spine maturation in hippocampal pyramidal neurons (Barros et al., 2009). However, another study demonstrated that ErbB4 deletion did not modulate

pyramidal neuron spine formation, but it restricted dendritic spines formation in PV^+ interneurons (Yin et al., 2013). Noteworthy, since ErbB4 expression is mainly found in PV^+ interneurons (Fazzari et al., 2010), the effect may be mediated via Nrg1/ErbB2 signaling in pyramidal neurons.

Relevant data have shown that ErbB4 has a cell-autonomous effect in the formation of GABAergic circuits, mediated via Nrg1. In this regard, ErbB4 transgenic mice showed a disruption of inhibitory and excitatory synapses in hippocampal pyramidal and inhibitory neurons, respectively (Fazzari et al., 2010) This synaptic dysfunction potentiates cortical excitability and neuronal synchronous activity across cortical regions, causing schizophrenia-like behavioral phenotypes (del Pino et al., 2013). Mechanistically, *in vitro* data reported that Nrg1 treatment increases the expression of a multifunctional scaffolding protein, named Disrupted in Schizophrenia 1 (DISC1), which can physically bind to the ErbB4 receptor and promote dendrite formation and excitatory synapses to cortical interneurons (Unda et al., 2016).

Noteworthy, most of the studies have used ErbB4 null mutant mice to understand the effect of Nrg1/ErbB4 signaling on cortical circuitry (del Pino et al., 2013; Fazzari et al., 2010; Lu et al., 2014; Rico & Marín, 2011; Tan et al., 2018). However, this experimental approach presents several limitations. First, ErbB4 expression is mainly found in PV^+ cortical interneurons, which constitute the major type of inhibitory neurons, but it is a restricted fraction of the total number of neurons in the cortex (Fazzari et al., 2010; Lim et al., 2018). Second, Nrg1 can act as both a ligand and a receptor, modulating not only the biology of PV interneurons, but also in the excitatory pyramidal neurons themselves (Mei & Nave, 2014; Mei & Xiong, 2008). Lastly, ErbB4 can serve as a ligand for Nrg3, which is also expressed in the cerebral cortex (Bartolini et al., 2017). Hence, ErbB4 null mouse models do not entirely recapitulate the complexity of Nrg1 signaling (**Figure 5**). Therefore, specific animal models that directly target the Nrg1 gene are needed to better comprehend the relevance of Nrg1 in cortical circuit formation. In this sense, we recently offered an extensive molecular, histological, and functional characterization of a newly generated Nrg1 heterozygous mouse model ($Nrg1^{tm1Lex}$, Lexicon genetics). Our data reveal a loss of glutamatergic buttons on PV interneurons and a decreased frequency of spontaneous inhibitory postsynaptic currents, impairing inhibitory cortical circuitry (Navarro-Gonzalez et al., 2021).

Moreover, Nrg1 type III regulates dendritic development in cortical neurons *in vivo* via Nrg1 intracellular signaling (Chen et al., 2010). Nevertheless, this study focused on developmental stages, whereas the role of this signaling pathway in adulthood remains to be elucidated. Accordingly, a loss of dendritic spine was identified in $Aph1bc^{-/-}$ mice, in which the intracellular proteolytic processing of Nrg1 is impaired. Interestingly, this phenotype was rescued by expressing Nrg1-ICD *in vitro* and *in vivo*, providing a novel Nrg1 cell-autonomous mechanism to

modulate cortical circuitry (Fazzari, Snellinx, Sabanov, et al., 2014). However, the γ-secretase activity ablated in Aph1bc$^{-/-}$ mice is not exclusively for Nrg1 proteolytic processing, but also for diverse type I membrane proteins, such as APP or Notch (reviewed in Zhang et al., 2014). Additionally, it has been also reported that Nrg1-ICD formed a complex with a zinc-finger transcription factor (Eos) in the mouse cochlea. This complex can translocate to the nucleus, upregulating PSD-95 expression through a signaling pathway mainly independent of γ-secretase activity (Bao et al., 2004).

Thus, these studies provide intriguing insights in the complexity of Nrg1 signaling in cortical circuit formation, highlighting that it can be also mediated intracellularly in other neuronal types, and not only through ErbB4 activation in PV^{+} interneurons. However, novel models specifically targeting Nrg1-ICD are required to elucidate the molecular mechanisms underlying this intracellular pathway in cortical development and synaptic plasticity.

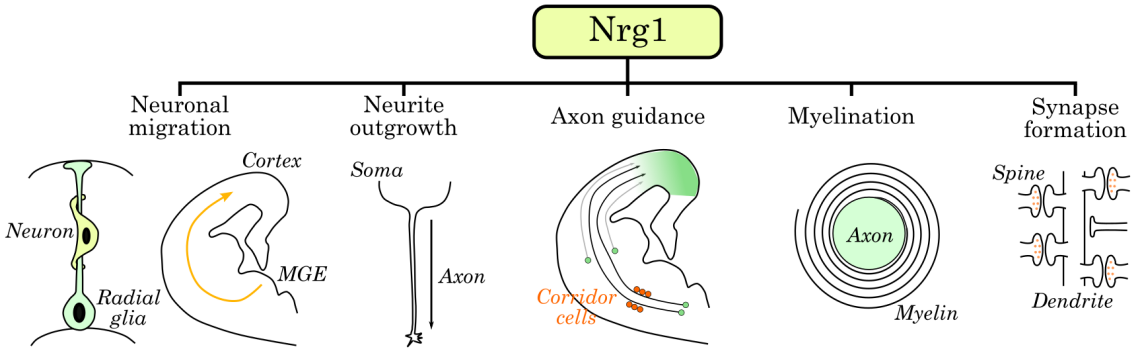

Figure 6. Nrg1 is involved in several functions essential for neural development.

Nrg1: an emerging neuromodulator of CNS repair

Nrg1/ErbB4 has been mainly associated with several neurodevelopmental psychiatric disorders, such as schizophrenia (Buonanno, 2010; Stefansson et al., 2002). However, during the last decades emerging data has shown the potential neuromodulatory effect of Nrg1 signaling on CNS repair (reviewed in Kataria et al., 2019).

Regarding the neurotrophic properties of Nrg1 in the development of the nervous system, it is likely to think that this protein can play a pivotal function upon injury. It has been described that the expression of Nrg1 and ErbB receptors is increased after cortical injury (Parker et al., 2002; Tokita et al., 2001; Xu & Ford, 2005), suggesting that they may carry out attempts at repair and regeneration (Esper et al., 2006).

In this context, several groups observed that Nrg1 treatment promotes functional recovery upon SCI and different cortical damage models (Deng et al., 2019; Gu et al., 2017; Iaci et al., 2016; Ryu et al., 2019; Shyu et al., 2004). Mechanistically, some of the results showed that Nrg1 administration stimulated neuronal survival upon injury in both *in vitro* and *in vivo* approaches,

which may be partly related to an increase in GABAergic transmission (Deng et al., 2019; Guan et al., 2015). Consequently, several groups reported that Nrg1 treated mice presented reduced injury size, using the traditional histologic staining 2,3,5-triphenyltetrazolium chloride (TTC) to superficially check the impact of injury in thick slices (Guan et al., 2015; Guo et al., 2006; Li et al., 2007; Xu et al., 2004; Zhang et al., 2018).

Moreover, administration of the soluble form of Nrg1 has also been observed to regulate glial response, promoting the release of anti-inflammatory cytokines, and decreasing pro-inflammatory cytokines in SCI and stroke models (Alizadeh et al., 2017; Simmons et al., 2016; Surles-Zeigler et al., 2019; Xu et al., 2005). Interestingly, the deletion of ErbB4 in cortical PV^+ interneurons boosted the number of astrocytes and microglia/macrophages in the perilesional area upon TBI, suggesting that the astrocytic and microglial/macrophagic response can be mediated in part by Nrg1-ErbB4 signaling (Deng et al., 2019). For more information on the role of Nrg1 in neuroprotection and inflammatory response upon brain damage, see the chapter 3 of this dissertation.

Most of the studies have been focused on investigating the effect of Nrg1/ErbB signaling in the early stages of brain damage in terms of neuronal survival and inflammatory response. However, whether Nrg1 signaling contributes to axonal regeneration and plasticity upon cortical injury remains poorly understood. Nrg1 treatment can stimulate neurite outgrowth in multiple neuronal cultures (Bellon, 2007; Fazzari et al., 2010; Gerecke et al., 2004; Rahman-Enyart et al., 2020; Rieff et al., 1999). In the context of injury, it has been described that Nrg1 can regulate some signaling pathways associated to axonal outgrowth, such as PI3K/Akt and Rhoa/Cofilin (Guo et al., 2010; Hao et al., 2020; Mòdol-Caballero et al., 2018; Zhang et al., 2016). Hence, it is interesting to investigate in depth the molecular and cellular mechanisms underpinning the effect of Nrg1 in axonal regeneration upon injury. Nevertheless, it is worth noting that axonal regeneration is a limited event in the adult CNS, compared to the PNS (BrosiusLutz & Barres, 2014; Curcio & Bradke, 2018). Further details on the role of Nrg1 in axonal regeneration can be found in the introductory sections of chapter 1 and chapter 4 of this dissertation.

Demyelination is a key pathological marker following injury, in which remyelination is an important regenerative process to enhance functional recovery. While the importance of Nrg1 signaling in the biology of Schwann cells and thus myelination in the PNS has been reported by several groups (Birchmeier & Bennett, 2016; Fricker et al., 2011; Mancuso et al., 2016), its role in CNS repair is still under research.

Nrg1 appears to play a role in the development of the oligodendrocyte cell lineage in the CNS (Mei & Xiong, 2008). However, not much is known about the role of the Nrg1/ErbBs pathway in oligodendrocyte biology and myelination upon CNS injury. In this context, a notable loss of

oligodendrocytes has been described after damage, and the remaining viable oligodendrocytes appear to have a limited effect on CNS repair (BrosiusLutz & Barres, 2014). Hence, promoting oligodendrocyte formation and differentiation is a promising strategy to boost remyelination. Ding and colleagues recently reported that Nrg1 administration promoted transdifferentiation of reactive astrocytes into oligodendrocyte lineage cells via the ErbB receptor upon SCI, potentiating remyelination, axonal preservation and thus functional recovery (Ding et al., 2021). Furthermore, recent data showed that Nrg1 treatment promotes oligodendrocyte proliferation and remyelination upon ischemic stroke (Cui et al., 2023).

However, the effects of Nrg1 entail a complex molecular machinery in which different isoform may exert different effects. For example, in an elegant study using conditional transgenic mice to specifically ablate different Nrg1 isoforms, data revealed that Nrg1 type III controls an endogenous mechanism to promote axon myelination by switching central precursor cells to PNS-like Schwann cell after SCI, thereby enhancing functional recovery and spontaneous tissue repair (Bartus et al., 2016). Overall, future research is needed to better elucidate the relevance of Nrg1 signaling in remyelination upon CNS injury and the molecular and cellular mechanisms implicated.

Similar to the research on Nrg1 signaling in cortical circuit formation under physiological conditions, there are several caveats to the literature. To begin with, these studies mainly investigated the role of exogenous Nrg1 by administering recombinant human Nrg1 (rhNrg1), which is mainly mediated by ErbB4 activation. However, ErbB4 is predominantly expressed in PV^+ cortical interneurons, which represent only one specific group of neuronal types in the adult cortex (Fazzari et al., 2010). In this regard, these models may not represent the intricacy of Nrg1 signaling, which can also modulate the biology of other neuronal types, such as pyramidal neurons, where Nrg1 is largely expressed (Liu et al., 2011; Mei & Nave, 2014; Mei & Xiong, 2008). Hence, it is not unreasonable to propose that such a relevant neuroprotective effect could be mediated by other cell types in the cortex, and not only by PV^+ interneurons.

It is also important to emphasize that Nrg1 possesses multiple different isoforms that plays diverse function in the physiological and injured nervous system (reviewed in Kataria et al., 2019). Additionally, Nrg1 signaling involves complex signaling pathways, acting as both a ligand and a receptor (Mei & Xiong, 2008). In this regard, prior data from our lab suggested that Nrg1 intracellular signaling is an intriguing molecular target to enhance neuroprotection in hemorraghic stroke. In this research, we demonstrated that Nrg1-ICD is stimulated under hypoxic conditions. Furthermore, we induced Nrg1-ICD expression in both *in vitro* and *in vivo* models, resulting in an increased of neuronal survival after injury. As a mechanistic output, we carried out a gene expression characterization, observing that Nrg1 intracellular singaling regulate pro-apoptotic gene, speculating that this signaling pathway may promote a less

vulnerable state of neuronal cells (Navarro-González et al., 2019). These data provide novel insights into Nrg1 intracellular signaling as a promising target for cortical stroke treatment.

Herein, we investigated the role of Nrg1 in neuroprotection and cortical regeneration upon brain damage. To overcome the technical limitations offered by previous studies, we developed novel *in vitro* and *in vivo* approaches to express or delete Nrg1 expression. As a novelty, we offered a refined animal model in which Nrg1 expression is acutely deleted prior to cortical injury. From a mechanistic perspective, we also expressed Nrg1-ICD in a selective number of neuronal cells *in vivo* to better elucidate the role of Nrg1 intracellular signaling upon cortical regeneration upon injury. Taken together, our results obtained in this thesis highlight the relevance of Nrg1 signaling, and its intracellular pathway, as an interesting molecular target for the brain damage scenario.

HYPOTHESIS AND OBJECTIVES

The aim of this thesis was to understand the role of Nrg1 signaling in cortical regeneration after brain injury by developing novel *in vitro* and *in vivo* models to specifically target Nrg1 signaling. The specific objectives referring to each chapter are:

1. To provide a novel *in vitro* model of axonal injury to study the role of Nrg1 signaling in axonal outgrowth, using electroporation techniques to perform gain- and loss-of-function approaches.
2. To develop a novel *in vivo* model for multiplexed analysis of callosal connections after cortical damage to study cortical regeneration and axonal sprouting.
3. To investigate the role of Nrg1 signaling in neuroprotection and functional motor recovery after cortical damage using two different refined transgenic murine models to 1) acutely ablate Nrg1 expression prior to injury induction and 2) specifically express Nrg1-ICD in targeted cortical neurons *in vivo*.
4. To study the effect of Nrg1 in cortico-cortical axonal wiring after cortical injury in both refined transgenic murine models exposed in the previous objective.

MATERIAL AND METHODS

Animals

For *in vitro* studies, we used CD1 (*wild-type* phenotype) and C57BL/6J Nrg1^{tm3Cbm}floxed (named Nrg1 floxed) from Birchmeier lab (http://www.informatics.jax.org/allele/MGI:2447761) mouse embryos at E14.5-15.5 *post-coitum* for gain and loss-of function approaches, respectively. For the Controlled Cortical Damage (CCD) characterization and to study the role of Nrg1 signaling upon CCD, we used young (3-4-month-old) and aged (9-13-month-old) female mice from different littermates of two different mice lines: C57BL/6 (purchased from Charles Rivers Laboratories) and tamoxifen inducible transgenic mice to induce a ubiquitous deletion of Nrg1 (Nrg1-UBC-CreERT2) for gain- and loss-of function approaches, respectively. Of note, the mutation in Nrg1 gene is found in the exon 7, 8, and 9 of the EGF C-terminal, deleting all Nrg1 isoforms (Meyer & Birchmeier, 1995; Yang et al., 2001).

All the animal experiments developed in this thesis were supervised by the bioethical committee of Centro de Investigación Príncipe Felipe (Valencia, Spain), according to the European and Spanish bioethical regulations in terms of Animal Welfare. The animals were group-housed with food and water *ad libitum* in standard housing conditions within a specific pathogen-free animal facility in the institute.

In collaboration with Professor Ruscher, we used a Thy1-GCaMP6 transgenic mice line (Dana et al., 2014) with a C57BL/6J background to perform a pilot study to investigate Nrg1 expression upon cortical focal stroke (phototrombosis) in aged male mice (9-11 months). To this aim, all the animals were bred, kept, and genotyped at the conventional facility of the Biomedical Centre (BMC, Lund, Sweden), in accordance with the international guidelines on experimental animal research, with the approval of the Malmö-Lund Ethical Committee (ethical permit no. 10993/18 BMC-m).

Nrg1 construct and adenoassociated viral vectors

To study the role of Nrg1 signaling upon CCD *in vivo*, we labeled cortico-cortical projections using adeno-associated viral vectors (AAVs). The virus construct, production and validation were previously described (Fazzari et al., 2014; Navarro-González et al., 2019). Briefly, the constructs were subcloned into the pAAV-hSyn-hChR2(H134R)-mCherry vector deposited by Karl Diesseroth into the Addgene repository (https://www.addgene.org/26976). Then, two different AAVs were produced to express Nrg1 intracellular domain (Nrg1-ICD) or GFP under human Synapsin promoter. The vector for GFP expression was deposited by Bryan Roth into the Addgene repository (https://www.addgene.org/50465). To enable visualization, the C-terminal of Nrg1 was fused to GFP, although we combined both GFP and Nrg1-ICD AAVs to

improve fluorescent signal in GOF experiments *in vivo* in 1:4 and 3:4 proportion, respectively. The adeno-associated viral particles (serotype 1) were produced and purchased by the Viral Vector Production Unit (UPV) of the Universitat Autónoma de Barcelona (Spain), following standard protocols.

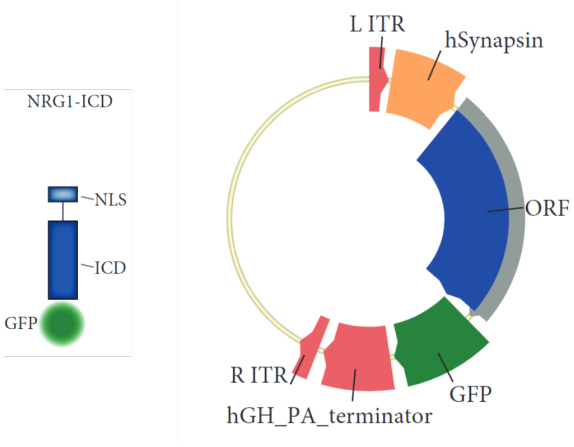

Figure 7. Viral vector used for expressing Nrg1-ICD *in vivo*. The cartoon reflects the construct for the expression of Nrg1-ICD (including the nuclear localization signal (NLS)) under human Synapsin promoter fused to GFP. Adapted from Navarro-González et al., 2019.

Primary neuronal cultures

Primary cortical neuron cultures were prepared from CD1 or C57BL/6J embryonic mice (E14.5-15.5), as previously described (Fazzari et al., 2010c; Fazzari, Snellinx, Ahmed, et al., 2014; Rodríguez-Prieto et al., 2021a). Briefly, a pregnant female mouse was sacrificed using cervical dislocation without sedation to obtain the embryos. Embryonic cortices were dissected, and meninges removed. The tissue was placed into ice-cold sterilized HBSS (7mM HEPES and 0.45% glucose) and disaggregated in trypsin-EDTA buffer at 37˚C for 12 minutes, mixing by tilting. Cortices were washed with HBSS and gently homogenized using a P1000 pipette for maximum 8-12 repetitions in 1.5ml of plating medium (Minimum Essential Medium (MEM) supplemented with 10% horse serum (Invitrogen), 0.6% glucose and antibiotics (penicillin, 10000 U/ml; streptomycin, 10 mg/ml)). To remove cell aggregates and debris, cell solution was filtered through a cell strainer (70µm) and up to 10ml of plating solution was added. Cell concentration was calculated by counting in a Neubauer chamber. To increase the survival of the culture, 110000 cells were plated in 12 well-plates, in which coverslips were previously coated with poly-L-lysine (0.1mg/ml, Sigma-Aldrich).

For neuronal electroporation, the system NEPA21 (Nepa gene) was selected, an open system which offers great possibility of customization. Briefly, an adequate volume of the previous cell suspension was centrifuged at 250g for 5 minutes in electroporation medium (Gibco Opti-MEM, 11524456, ThermoFisher Scientific). To increase cell survival during electroporation pulse, the pellet was resuspended in electroporation medium and mixed with the desired amount of DNA

(see **Table 1**) to obtain a concentration of 10^6 cells/ml in each electroporation cuvettes. After the electroporation, 45000-50000 cells per treated group were plated in 12-well plates. To reduce variability, we combined both control and treated groups in the same well as follows: for GOF studies, control cells were electroporated with pCMV-GFP-ires-Cre (GFP) and pAAV-hSyn-RFP (RFP) plasmids, while treated cells were electroporated with GFP and Nrg1-ICD or Nrg1-FL, according to each condition. For LOF assays, WT cells were electroporated with pLL3.7, while KO cells were obtained using a GFP plasmid expressing Cre and co-electroporated with RFP (**Table 1**). Of note, the plasmids were obtained from transformed bacteria using a commercial kit (MB051, NZYMaxiprep). Remarkably, CRD-Nrg1 full length tagged with GFP was kindly provided by Prof. Bao Jianxin and cloned into pcDNA3.1 TOPO (Invitrogen). Nrg1-ICD was subcloned from pcDNA3.1 TOPO (Invitrogen) to pCAGEN (11160; addgene) (Bao et al., 2003; Fazzari et al., 2014).

Neuronal cultures were stored in a humidified incubator containing 95% air and 5% CO_2. The plating medium was replaced 3 hours later with equilibrated neurobasal medium supplemented with B27, GlutaMAX (Gibco; Life Technologies Co.) and antibiotics (penicillin, 10000 U/ml; streptomycin, 10 mg/ml). To maintain the cells for longer studies, an additional ml of neurobasal medium was added to each well one week later and the medium was refreshed every two days until 14 days *in vitro*. For further details in the composition of the culture media, please check Supplementary material S1.

Name of the plasmid	Promoter	Amount of DNA	References
pAAV-hSyn-RFP	hSyn	3µg	22907 (addgene)
pCMV-GFP-ires-Cre	pCMV	3µg	Described in Fazzari et al., 2010
CRD-Nrg1_FL	CAG	24µg	Described in Fazzari et al., 2014
Nrg1_ICD	CAG	24µg	Described in Fazzari et al., 2014
pLL3.7 (empty)	CMV	5µg	11795 (addgene)

Table 1. Name and amount of plasmid DNA used to electroporate neuronal cultures for GOF and LOF *in vitro* studies.

Electroporation conditions: Poring Pulse					
Length (ms)	**Voltage (V)**	**Interval**	**N pulse**	**Decay rate**	**Polarity**
2	175	50	2	10	+
Electroporation conditions: Transfer Pulse					
Length (ms)	**Voltage (V)**	**Interval**	**N pulse**	**Decay rate**	**Polarity**
50	20	50	5	40	+/-

Table 2. Electroporation settings for NEPA21.

Experimental *in vitro* model of axonal injury

To study axonal regeneration upon injury *in vitro*, we developed a protocol of physical injury *in vitro*, consisting of a mechanical severing of the axons. Briefly, to reduce variability from injury protocol, we perform a sparse labeling of the neurons and plated intrinsic control in each well, as described above. 4 days *in vitro*, we provoked the physical insult by scratching the middle line of the coverslip using a mechanical pencil (0.5mm) in sterilized conditions. 72 hours and 10 days after the scratch, the cells were fixed and immunolabeled to strength the fluorescence. Pictures were taken with a Zeiss Axio Observer Z1 microscope, equipped with a Zeiss AxioCam MRm camera and an illumination system (Colibri) consisting on different excitation LED's (385 for DAPI, 475 for 488, 567 for 555 and 630 for 647 fluorophores) and using the following emission filters: 90 HE D/G/C3/C5 for DAPI and far red (647 fluorophore), 38 HE GFP for GFP staining (488 fluorophore) and 43 HE DsRed for red (555 fluorophore). The pictures were obtained using 20x NA 0.5 dry objective.

Experimental *in vivo* model of CCD

All this procedure was done as previously described (González-Manteiga et al., 2022). Briefly, 100µl of morphine (1.5mg/ml) was administered to mice 30 minutes before the surgery and 100µl of buprenorphine (0.03mg/ml) 6h later and the next morning. To assess fair ethical practices, weight loss was monitored along the experiment as an early humane endpoint parameter. Thus, animals that presented a body weight loss above 20% would be sacrificed and excluded from the study (3 out of 68).

Stereotactic injection of AAVs for the expression of GFP or Nrg1-ICD was performed to trace axonal projection of the corpus callosum as previously described (Navarro-González et al., 2019). Briefly, mice were placed in a stereotactic frame, under isoflurane anesthesia with the skull exposed. To target the primary motor cortex, the selected coordinates (mm) relative to the bregma were as follows: anteroposterior, 0.2; lateromedial, 1.5; and dorsoventral, −0.5. Then, the Hamilton syringe containing the virus was introduced 1mm into the cortex to produce a pocket. Two minutes later, the syringe was risen 0.5mm and 1µL of the virus (diluted 1:4) was

injected at a flow rate of 0.1µl/min. After the injection, the needle was left up to 3 minutes for an appropriate virus diffusion.

For BDA injection (Dextran biotin 3000 MW, Fisher Scientific, Hampton, NH, USA), the stereotactic injection was as previously described with some modifications. Briefly, we diluted 100µg/µl in PBS and injected 1µL at a flow rate of 0.1µl/min. In this case, we trace ipsilateral neurons of the prefrontal cortex to observe other brain areas projections. The coordinates (mm) relative to bregma were as follows: anteroposterior, 1.6; lateromedial, −1.6; and dorsoventral, −0.5.

For LOF studies, one dose of 8mg of tamoxifen (T5648-1G, Merck Life Science, S.L.) diluted in corn oil (C8267-500ML, Merck Life Science, S.L.) was administered to the UBC-Cre line mice 7 days before the injury induction for Nrg1 deletion, independently of their genotyping. Of note, in the LOF experiments with aged female mice, to maintain an adequate number of animals in control group, half of the group was administered with tamoxifen (genotype: nff ucww) while the other half was treated with corn oil to avoid Nrg1 deletion (genotype: nff uc+w).

To perform the controlled cortical damage (CCD), a 2.1mm diameter drill tip was introduced in the right primary motor cortex at a constant speed of 0.5mm/s, using a motorized stereotactic instrument to reduce injury variation (Stoelting, 51730M). Considering the size of the drill, the coordinates relative to bregma (mm) suffer a slight antero-posterior modification, compared to the ones used for AAV injection: anteroposterior, 0; lateromedial, −1.5; and dorsoventral, −2.5. The drill was introduced into the brain 3 times, waiting 2min with the drill inside after the first immersion.

Phototrombosis

Focal ischemic stroke was induced by phototrombosis (PT), as previously described (Häggman Henrikson et al., 2020; Madinier et al., 2014c; Michalettos et al., 2021; Talhada et al., 2019c; H. L. Walter et al., 2015). Briefly, aged (9-11 months) male mice from Thy-GCamps6 transgenic line with a C57BL/6 genetic background were anesthetized and monitored during the surgery, as previously described. Once the head was fixed to the stereotactic structure, 100µl of analgesia (bupivacaine) were subcutaneously injected and disinfected to expose the skull. The area of light exposure will correspond to the right primary motor cortex affecting the left hindlimb (coordinates relative to bregma (mm): anteroposterior, 0; lateromedial, −1.5). To delimit this area, black tape was sticked to the skull during the light exposition. 100µl of Rose Bengal (10mg/mL, Sigma Aldrich, Taufkirchen, Germany) were injected via intraperitoneal and waited for 5 minutes so the compound was well distributed. After that, the arm of the lamp was properly fixed and closed to the delimited area and the skull was illuminated for 20 minutes (Schott KL

1500 LCD, intensity: 3000 K/4D). The same procedure was done to sham group, injecting saline solution instead of Rose Bengal.

Tamoxifen-inducible transgenic mice characterization

To maintain the colony and select the animals for the experimental groups, mice genotype was doubled-check performing PCRs according to manufacturer's protocol (Supreme NZYTaq II 2x Green Master Mix (MB36001-MB36003), NZYTech) and running the product in a 2.5% agarose gel to confirm Nrg1 flox gene mutation and Cre expression (**Table 3**).

Gene	Primer name	Sequences
Cre locus	UBCCre_25285_Trans_F	GACGTCACCCGTTCTGTTG
	UBCCre_oIMR7338_Intern_F	CTAGGCCACAGAATTGAAAGATCT
	UBCCre_oIMR7339_Intern_R	GTAGGTGGAAATTCTAGCATCATCC
	UBCCre_oIMR9074_Trans_R	AGGCAAATTTTGGTGTACGG
Nrg1 floxed	Nco1-s	TCCTTTTGTGTGTGTTCAGCACCGG
	M7-As	GCACCAAGTGGTTGCGATTGTTGCT

Table 3. Primer sequence used to confirm the genotype of tamoxifen-inducible transgenic mouse line.

To check Nrg1 deletion induced by tamoxifen administration, 1 tamoxifen dose of 8mg was administered to 5 Nrg1-UBC-CreERT2 adult mice (3 months old) using gastric gavage. 11 days after, mice were perfused with ice-cold PBS solution and the cortices were dissected and cryopreserved with liquid N_2 to validate Nrg1 deletion using qPCR, explained below. To verify that tamoxifen was not detrimental to functional motor outcome, we also assessed behavioral characterization using the WSL and RPT before and after tamoxifen administration (**Figure 8**).

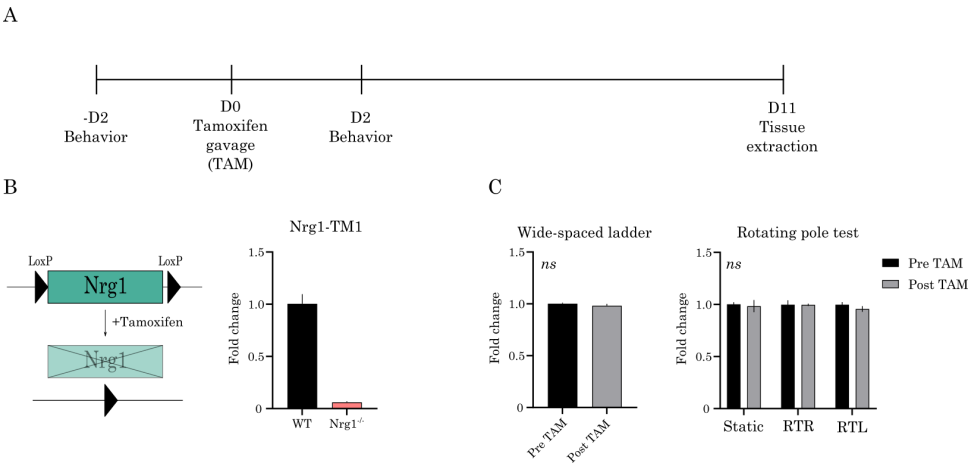

Figure 8. Validation of Nrg1 deletion using tamoxifen-inducible transgenic mouse line. A) The scheme shows the timeline of the mice model characterization. B) On the left, the cartoon represents the Cre-LoxP system to induce Nrg1 deletion through tamoxifen administration. On the right, the graph shows the deletion of Nrg1 measured Nrg1-TM1 gene expression. Mean ± SEM, N= 2 (WT)

and 3 ($Nrg1^{-/-}$) young mice. C) Behavioral test characterization in WSL and RPT. Tamoxifen administration did not induce any functional motor impairment in $Nrg1^{-/-}$ mice prior to injury. Mean ± SEM, N= 7 $Nrg1^{-/-}$ young mice. Statistical analysis: two-way ANOVA and Sídák's multiple comparison test.

RNA extraction and qPCR

Animals were perfused with ice-cold PBS and the brains were removed and cryopreserved. For characterization of the transgenic line, just one hemicortex was used for the study. For analyzing Nrg1 expression upon PT model, the cortex was dissected obtaining the infarct core and the perilesional area of both ipsi- and contralateral hemispheres (**Figure 24A'**).

RNA from one hemicortex was extracted using TRIzol reagent, accordingly to manufacturer's instructions (Invitrogen). RNA quality and concentration was checked using a NanoDrop ND-100 (Thermo Fisher Scientific Inc.). Through reverse transcriptase reaction, 0.5µg of RNA was converted into cDNA using a High capacity reverse transcription kit (Applied biosystems). 50ng of synthesized cDNA were used for Quantitative Real-Time Polymerase Chain Reaction (RT-qPCR) using PrimeScript RT Master Mix (RR036A, Takara). The primers pairs for the RT-qPCR were described in **Table 4**, which were validated by PrimerBank as previously published (Navarro-González et al., 2019; Navarro-Gonzalez et al., 2021). All the values were normalized to the housekeeping gene Gapdh.

Gene target	Sequences	
Nrg1-EGF	Forward	CATCTACATCCACGACTGG
	Reverse	TGAGGGGTTTGACAGGTC
Nrg1-TM1	Forward	AGTGCCCAAATGAGTTTACTGG
	Reverse	AGTTCCTCCGCTTCCATAAATTC
Nrg1-TM2	Forward	TGGCCTACTGCAAAACCAAG
	Reverse	AGGGCCATTCGCTATGTTC
ErbB4	Forward	GGACCCACAGAAAATCACTGCCAG
	Reverse	TCCATAGCACCTGCCATCACATTG
Gapdh	Forward	TCCCACTCTTCCACCTTCG
	Reverse	CATACCAGGAAATGAGCTTGACAA

Table 4. Primer sequence used to characterize Nrg1 and ErbB4 expression upon PT.

Motor behavior analysis

Motor functional outcome was tested using a battery of different behavioral motor test. Considering the increased difficulty in the rotating pole and wide-spaced ladder, mice were trained 3 consecutive days before recording. To ensure that the motor deficits were linked to cortical damage, mice performed the test a couple of days before the CCD surgery.

Since the model proposed involved a unilateral lesion in the right motor cortex, we previously checked whether animals showed side preference before the lesion induction. We evaluated the left and right hindlimb data obtained in the rotating pole test (RPT) before the injury. The comparison between both paws was tested in rotation to the right and to the left modes (two-way ANOVA with Šídák's multiple comparisons test, adjusted $p = 0.809$ and adjusted $p = 0.644$, respectively). The data did not reveal statistical differences, so we discarded hindlimb dominance effect in our experimental groups. All the tests were done 2 and 7 days after the surgery to observe an asymmetrical motor deficit due to a unilateral CCD model.

Rotating pole test

The rotating pole test is a widely used test to assess motor dysfunction in unilateral cortical injuries, providing an effective and sensitive way to detect neurological motor deficits after CCD. The protocol used was previously described (Talhada et al., 2019). Briefly, mice walked through a wooden pole elevated 1m height from the table. The pole can display 3 different modes: 1 static mode, in which it remains stopped, and 2 rotation modes to the right or left at 3rpm speed. It is important to always maintain the same order of performance, from the easier mode (static) to the most challenging one (rotation to the left), considering that the CCD is done on the right primary motor cortex, so the left hindlimb will be the most affected.

Mice were recorded during the task performance to assess functional motor outcome, using a 0 to 6 scoring method (**Table 5**), based on the walking ability and the number of slips per paw, as previously described (Talhada et al., 2019).

Rotating pole test	
Score	**Criteria**
0	Animal falls off immediately upon entry onto the pole
1	Animal remains embraced to the pole unable to cross and eventually falls off the pole
2	Animal falls off during crossing or if the hind limbs do not contribute to forward movement
3	Animal crosses the pole while continuously slipping with the fore- or hind limbs
4	Animal crosses pole with more than 3ft slips
5	Animal traverses the pole with 1–3-foot slips
6	Animal crosses the pole without any foot slips.

Table 5. Score system used in the rotating pole test (RPT) to evaluate motor dysfunction upon CCD (from Talhada et al., 2019).

Catwalk XT

The Catwalk XT system (Version 10.6, Noldus, Wageningen, The Netherlands) consists of an enclosed walkway on a glass surface, illuminated with specific light combination. Hence, once mice walk through the structure, each footprint is perfectly detected. After the recording, the software assesses a semi-automatic analysis to study a huge range of parameters, including paw position, walking pattern, and other run statistics (Catwalk XT 10.6 Reference Manual).

The settings were previously customized for mice, as well as the number of animals and time-point groups. The experimental and detection settings used to perform the experiments are shown in **Table 6**. Three compliant runs were automatically analyzed by the software, using the "auto-classify" option. Note that it is important to establish a proper intensity threshold that should be maintained for all the runs in the experiment. The result statistics are automatically assessed by the software, offering the mean and SEM in the desired selected parameters. In this case, we focused on those which offer a greater phenotype: max contact area (mm^2), print area (mm^2), swing speed (cm/s), and body speed (cm/s). All the data presented refer to the left hindlimb (LH), which should be the most affected according to the CCD coordinates.

- *Max contact area* (mm^2): refers to the maximum area of a paw touching the glass.
- *Print area* (mm^2): the surface of the complete paw print.
- *Swing speed* (cm/s): the velocity of the paw during the swing, which refers to the part of the step cycle in which the paw is not touching the glass.
- *Body speed* (cm/s): the velocity of a paw during the step cycle, which refers to the time travelled since the first contact with the glass until the next contact with the same paw.

Detection settings	
Camera gain (dB)	7,4
Green Intensity Threshold	0,12
Red Ceiling Light (V)	17,7
Green Walkway Light (V)	16
Run criteria	
Minimun run duration (s)	0,55
Maximun run duration (s)	4
Minimun number of compliant runs to acquire	10
Use maximum allowed speed variation (%)	60

Table 6. Experimental options of Catwalk XT software to adjust detection settings for an appropriate animal recording and run criteria to filter valid runs for automatic analysis.

Narrow and Wide-Spaced Ladder

Another way of analyzing motor impairment is skilled ladder walking for detection of paw symmetry and the number of mistakes per paw. To assess this aim, we take advantage of the MotoRater structure, which consists of an enclosed transparent walkway with two mirrors in the upper part to observe the animal from 3 sides simultaneously. In the bottom part, a high-quality camera is installed to record the runs (MotoRater TSE systems). Briefly, mice walked 3 times over two ladders, which differed in bar spaced distance (1 or 3 cm, respectively) to increase the task difficulty, offering a higher sensitivity to motor deficits detection. The videos were analyzed using a 0 to 5 scoring system, considering number of mistakes and walking symmetry. This last parameter is since mice place the hindlimb in the same position where the front limb was previously placed (**Table 7**).

Narrow/Wide-spaced ladder	
Score	**Criteria**
1	Impossible to walk
2	Asymmetric walking pattern, more than 7 mistakes
3	Asymmetric walking pattern, more than 4 mistakes
4	Slightly asymmetric walking pattern, 2-4 mistakes
5	Perfect walking

Table 7. Score system used in the narrow/wide-spaced ladder to evaluate motor dysfunction.

Treadmill

Using the treadmill test, mice are motivated to run to avoid touching the electrified grid located at the back of the lane. Briefly, mice were placed in the lane for a quick training of 30s at 15cm/s (not evaluated). Later, the lane speed was changed to 20cm/s for 1min and to 25cm/s for 2min. These two different slow and fast modes are evaluated on the recorded videos, producing a highly challenging task to the animal. In contrast to the analysis of the previous test, in this case only 1 run per mouse was analyzed using a 1 to 5 scoring criteria (**Table 8**).

Treadmill	
Score	**Criteria**
1	Impossible to walk
2	Difficulties in coordination, clearly unbalanced
3	Obviously impaired and unbalanced
4	Slightly impaired and unbalanced
5	Perfect walking

Table 8. Score system used in the treadmill to evaluate motor dysfunction upon CCD.

Immunofluorescence

Immunostaining was performed using a standard protocol as previously described (Fazzari et al., 2014; Navarro-González et al., 2019). Briefly, cells were fixed with 4% PFA for 10 minutes, permeabilized with PBS + 0.1% Triton solution for 10 minutes and blocked with 2% PBS-BSA for 30 minutes at room temperature. Carefully, the coverslips were removed from the plate and placed them upside up into a humid chamber in which an 80µl-drop of antibody mix was added. Primary antibody was incubated overnight at 4˚C, while the secondary was left for 1h at room temperature. Primary and secondary antibodies were diluted in blocking solution as follows: GFP (1:500), RFP (1:1000), anti-chicken488 and anti-rabbit555, which were both diluted 1:500. Please, check Supplementary material S2 for further antibody information. The coverslips were mounted with mowiol into a slide and images were captured using a Zeiss Axio Observer Z1 microscope with a 10x NA 0.25 and 20x NA 0.5 dry objective with the same characteristics previously described (seen in *Experimental in vitro model of axonal injury*).

Histology

Eight days after CCD, mouse brains were processed as previously described (González-Manteiga et al., 2022; Navarro-González et al., 2019). Briefly, mice were transcardially perfused with 4% PFA to collect the brain, following a 2h postfixation and cryoprotected in 30% sucrose for 72h. The brains were sectioned with a cryostat at 40µm (Cryostat Microm HM550, ThermoFisher Scientific), distributing the slices in 8 different anteroposterior ordered series for 3D reconstruction analysis.

Primary and secondary antibodies used were diluted in PBS with 0.25% Triton and 4% BSA. Incubation with the primary lasted for 48h, while the secondary antibodies were left overnight at 4°C in agitation conditions. The antibodies and dilution used were as follows: anti-GFP (1:1000), anti-Iba1 (1:500), anti-parvalbumin (1:250), anti-WFA biotinylated (1:1000); anti-chicken 488, anti-mouse 555, anti-guinea pig 647, anti-rabbit 555, streptavidin 555 and streptavidin CyTM5. All the secondary antibodies were diluted 1:500. Please, check Supplementary Material S2 for further antibody information.

Fluorescence imaging of the whole slides was performed using a Leica Aperio Versa at 10× NA 0.32 Plan Apo, equipped with a camera model Andor Zyla and the following excitation/emission filters: AT350/50x ET460/50m T400LP for DAPI, ET495/25x ET537/29m T515LP for 488, ET546/22x ET590/33m T565LPXR for 555 and ET640/30x ET690/50m T660LPXR for 647 fluorophores.

Bioinformatic image processing

To obtain a 3D reconstruction and a multilabeling approach, we developed an image processing workflow as previously described (González-Manteiga et al., 2022). Briefly, the pictures obtained in the Leica Aperio Versa are organized into a stack, separating each fluorescence channel into a specific one to facilitate the following workflow.

To sort the images, firstly it was necessary to create a binary mask in Fiji where the complete slice area was selected on the DAPI stack. Next, a Gaussian blur filter (sigma = 3) was selected to homogenize the slice surface. Later, the mask was fixed manually, establishing a threshold that covers all the slice area (**Figure 20B**). The mask was applied to the whole stack and saved on the same folder with the remaining channel stacks. It is important to note that, for code's sake, all the stack should be organized in the same folder per brain and named as follows: Experiment name_**Brain number**_ **Channel name**_mask (if necessary), highlighting in bold words the information required for a correct code running.

The theoretical statement of the code is based on sorting the sample considering that along the anteroposterior axes the slice areas increase following a logarithm curve. Hence, the code calculates the area of the DAPI mask by profiling and contouring the slice borders (shown in **Figure 20B**). Considering that the CCD generally produces a hole on the tissue, it is crucial that the contour processing goes above the injury, so the sorting is not affected by the absence of tissue. Once the area was calculated, the code automatically transfers this information to sort the rest of the channels. It is worthy to mention that in our experiments the selected region of interest expands from 2.5 mm to −1 mm relative to bregma coordinates (see Paxinos mouse brain atlas as a reference), where this theoretical principle applies. If the area of interest belongs to posterior samples, then the code should be optimized. The rate of sorting efficiency with this tool was 95% accurate. Nevertheless, additional checking is suggested in case of broken slices or other artefacts related to tissue manipulation that could change slice dimensions. For further details in the code script and requirements, see below in Supplementary Material S3.

Lastly, the samples are finally aligned, using an adaptation of a previously published Fiji plugin named "Align image by line". This tool allows the alignment of all the slices from the same stack, after providing the midline of each sample and selecting the line of reference to align the rest. This step was also automatized using a macro, which is shown in Supplementary Material S4. As a previous requirement, the macro should be customized considering the number of slices that contain each brain stack.

Image analysis

Quantification of axonal outgrowth *in vitro*

Images were analyzed using a sholl analysis, by counting the number of axons crossing the empty space (72h post-scratch: axons counted at 80, 160 and 240µm far from the border; 10 days post-scratch: axons counted at 160, 240 and 320µm far from the border). These raw data were normalized using the following criterion. First, considering that the injury line is not perfectly placed in the center of the coverslip, we found differences in line length between images. So, the number of axons crossing each line was transformed to axons/mm to overcome this limitation. Second, although we electroporated 2 plasmids in both experimental conditions, we noticed that there was some variability in the number of electroporated cells between groups, which could give a biased data under the premise of one soma, one axon. To solve this question, the data was normalized by the number of neurons counted per condition in different fields along the coverslip (Al-Ali et al., 2017). Lastly, this value was normalized to the quantification obtained in the control condition in the proximal line, which was assumed to be the baseline for axonal outgrowth.

Stereological measurements

From sorted and aligned stacks, the quantification of injury volume, inflammation, and tissue damage impact was done. The methodology used was as previously described (Navarro-Gonzalez et al., 2021). Briefly, the injury area was measured manually and the volume of the injury was lately calculated by the integration of its polynomial fit equation, according to the formula: $V = \int_a^b A(x)dx$ in which A is the cross-sectional area and x represents the width of the interval [a,b].

To estimate inflammation and tissue integrity, Iba1 and IgG staining pictures were used. Briefly, Gaussian blur filter (sigma = 5) was set to facilitate the homogenization and detection of inflammated area. After that, a threshold was manually set, selecting the value that better fit in the whole samples, according to the contralateral hemisphere. The image was converted into a binary mask in which the region of interest per slices was automatically identified using the function named "Analyze particles" (size = 1000-infinity). The area was calculated on the region of interest detected by this tool. From these values, the volume of each parameter was calculated by integration of the polynomial fit equation, as previously described.

Cortical profile and axonal preservation

We used GFP immunostained coronal slices from 2 different series to measure GFP intensity distribution using Image J. To limit the variability in cortical wiring measurements related to the tracing techniques, we used several strategies. First, we discarded samples in which the virus

intensity was not properly detectable, or the injection site was not in the desired bregma coordinates (AP 0.2, LM 1.5). Remarkably, although the injection coordinates were intended to specifically target callosal neurons of the primary motor cortex corresponding to the hindlimb, the virus diffused anteroposteriorly and dorsoventrally along the cortex, leaving some margin for error. According to this criterion, we selected comparable slices relative to the bregma position between 0.86 and 0 mm, using the Paxinos mouse brain atlas as a reference. Second, the regions of interest (ROI) were placed in the right primary motor cortex, close to the lesion in injured samples, so we searched for the equivalent homotopic cortical area in not injured brains to make an adequate comparison between groups. Finally, we selected slices in which the cortical injury was parallel to the injection site, an important consideration given the limited and focal effect of the CCD. Notably, this feature was intentional to allow the study of axonal sprouting in PL regions.

To analyze cortical profile, vertical rectangles were selected in the right primary motor cortex to quantify the distribution along the cortex of the signal intensity using ImageJ. Additionally, the GFP intensity was also quantified in the upper and lower areas of the injection site to study the remodeling process in the contralesional cortex after injury in LOF approaches (**Figure 9A**). Of note, this measurement was also used in the GOF samples as a possible normalizer value for not injured samples.

To analyze axonal preservation within layers upon injury, horizontal rectangles placed in the injury border were selected to quantify GFP signal distribution in layers II/III, IV and V (**Figure 9B**). We provided two different analyses: GFP intensity distribution and the intensity fold change along the cortical layer. To calculate this ratio, we divided the ROI in two halves, distinguishing far from closer pixels to the injury. In each half, mean intensity value was calculated to obtain the ratio close/far, under the premise that axonal sprouting is lost nearby the injury border. Using this approach, we could compare axonal preservation between layers using a two-way ANOVA statistical test.

For both cortical profile and axonal preservation analysis, the data was normalized to the total sum intensity of each rectangle to reduce variability between slices. Of note, to check whether the virus injection affected the quantification in the GOF control samples, raw data was also normalized to the injection site signal intensity, divided in upper and lower half of the cortex.

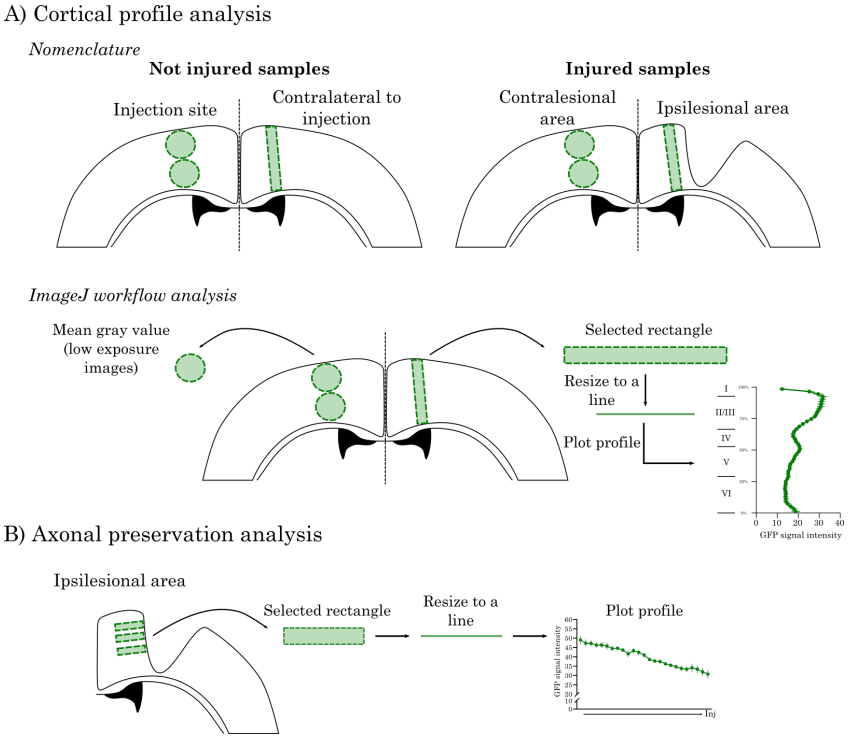

Figure 9. Nomenclature and workflow used in the axonal sprouting analysis. A) In the upper row, the cartoon represents the nomenclature used referring to the cortical areas analyzed in not injured and injured samples. In the lower row, the ImageJ workflow performed to analyze both left and right cortex for cortical profile analysis. B) The cartoon show the ROI selected and the workflow pipeline carried out in ImageJ to analyze axonal preservation within layers in the ipsilesional area of injured mice.

PNNs integrity analysis

To analyze the cell-to-cell interaction between microglia and PNN upon CCD, the number and intensity of WFA$^+$ cells was analyzed in the PL, determined by Iba1$^+$ labeling. Briefly, rectangles in both Iba1$^+$ and Iba1$^-$ (somatosensory cortex) were selected as regions of interest (ROI) in the ipsilateral and contralateral cortex. To delimit the number of WFA$^+$ cells, the same threshold was established on both ROIs in the Iba1$^+$ or Iba1− area, according to contralateral staining which conforms the intrinsic control in each sample. Once the threshold was selected, we automatically detected the contour of the WFA$^+$ cells, using the tool “Analyze particles” (size = 200-infinity) of ImageJ. The ROIs of each cell were saved, and the intensity was measured in the raw images.

Data from ipsilesional regions was normalized to the respective contralateral ROIs for each sample for CCD characterization and LOF ipsilesional regions, while data was normalized to WT group in the contralesional areas of LOF approaches. Of note, the results in GOF approaches were normalized to their respective not injured condition, whereas the comparison between GFP and Nrg1-ICD injured groups were normalized to GFP injured samples. Data represent the fold change in the graph (mean ± SEM).

Statistical analysis and figure design

Statistical analysis and graph preparations of all the figures were done using Graph Pad Prism 9 software. The data is represented as mean ± SEM. The significance is indicated with an asterisk in each figure legend, considering $p \leq 0.05$ as significant. The statistical test used for each analysis is also mentioned in each figure legend. Normality distribution of the samples was assessed using D'Agostino-Pearson and Shapiro-Wilk test to select the most accurate statistical test.

For the quantification of axonal regeneration *in vitro*, a two-way ANOVA with repeated measurements and Sidàk's multiple comparison tests were used to compare between the different groups. All the data was normalized to the number of electroporated cells per group and to control condition.

For the behavioral test assays described in Chapter 2, a two-way ANOVA with repeated measurements and Sídák's multiple comparison tests were used for narrow and wide-spaced ladder and treadmill to compare both control (Ctrl) and injured (CCD) groups along and within the different time-points (pre-tamoxifen:pre-tam; pre-injury: pre-inj; D2 after CCD: D2; and D7 after CCD: D7). For the RPT data, we used a two-way ANOVA with repeated measurements and Dunnett's multiple comparison tests to compare how the CCD group performed the task in the two different models (rotation to the right and rotation to the left) along the different time-points. For the four parameters obtained through the Catwalk XT, a one-way ANOVA with Holm-Sidàk multiple comparison tests were used. The behavioral data analysis of Chapter 3 was assessed using a two-way ANOVA with repeated measurements and Sídák's multiple comparison tests to compare Ctrl and $Nrg1^{-/-}$ within different time points in both RPT and WSL. Noteworthy, the data was normalized to the pre-injury data for the column bar graphs in the RPT test.

To analyze the Nrg1 role in injury impact and neuroinflammatory response *in vivo*, we used an unpaired t-test to compare the volume values between groups. To analyze perineuronal nets upon CCD, we compared the relative fold change of cell number and cell intensity described in Chapter 2 and 3, using different t-test according to statistical needs. Of note, the slices were considered as the N, according to the variability of the WFA expression pattern along the brain. Briefly, we used paired t-test analysis in the PNNs analysis described in Chapter 2, comparing the cell number fold change related to each contralesional area. For the LOF studies assessed in Chapter 3, we calculated the fold change of WFA^+ cell number decrease in the ipsilesional area relative to the contralesional area within each slice and compared both phenotypes using Mann-Whitney t test. For the contralesional region, we compared both WFA^+ cell number and intensity fold change (relative to WT) between groups using a Mann-Whitney t test. For the GOF studies explained in Chapter 3, we evaluated the WFA^+ cell number fold change of GFP and Nrg1-ICD

samples (relative to not injured samples) in both ipsi- and contralesional areas using a two-way ANOVA and Sidàk's multiple comparison tests. Additionally, we also compared WFA^+ cell number fold change in GFP and Nrg1-ICD not injured samples in the injection site and contralateral to the injection site using an unpaired t-test.

Finally, to assess signal intensity measurements described in Chapter 4, two-way ANOVA with repeated measurements and Sídák's multiple comparison tests were performed to compare cortical profile distribution between groups and fold change of intensity increase for axonal preservation within layers. To analyze average intensity per layers, unpaired t-test for Gaussian variables or Mann Whitney analysis for non-gaussian population. Of note, slices were considered as the N and ROUT method (Q=1%) was performed for data curation to identify outliers, revising manually whether the detected slice should be definetely removed.

To show the results, all the figures were designed using a free and open-source vector graphics editor, named InkScape.

CHAPTER 1: NRG1 SIGNALING PROMOTES AXONAL OUTGROWTH IN A NOVEL *IN VITRO* MODEL OF AXONAL INJURY.

GRAPHICAL ABSTRACT

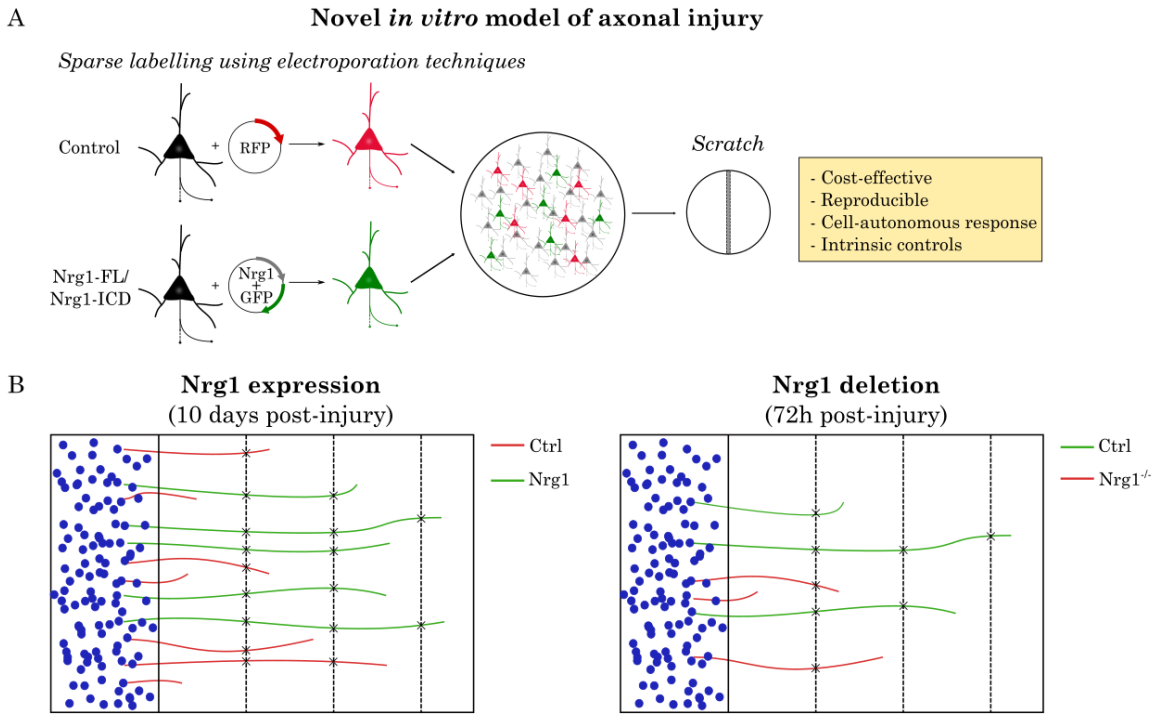

Highlights:

- We developed a novel and reproducible *in vitro* model of axonal injury that allows cell-autonomous readout to study the role of Nrg1 signaling.
- Nrg1 signaling, and specifically the activation of its intracellular pathway, promotes axonal sprouting 10 days after the scratch.
- $Nrg1^{-/-}$ neurons showed a tendency to decrease axonal sprouting 72 hours after the scratch.

INTRODUCTION

Nrg1 is an essential protein in cortical development, involved in diverse functions such as excitatory and inhibitory synapse formation, neuronal migration, oligodendrocyte development, axon myelination and ensheathment (Mei & Nave, 2014; Mei & Xiong, 2008).

Particularly, the role of Nrg1 signaling in neurite outgrowth and elongation has been reported *in vitro* using different cell types, such as PC12 pheochromocytoma cells, cerebellar granule, hippocampal and cortical neurons (Bellon, 2007; Fazzari et al., 2010; Gerecke et al., 2004; Rahman-Enyart et al., 2020; Rieff et al., 1999). In most of these studies, recombinant Nrg1-β was added to the culture medium, observing an increase in both neurite length and number. Furthermore, a reduction in neurite length has been reported using Nrg1 deficient mouse models, confirming the relevance of Nrg1 signaling in axonal elongation (Zhang et al., 2016, 2017).

Recently, Nrg1 has been proposed as a neuroprotective factor upon brain damage by decreasing inflammatory response and promoting neuronal survival *in vitro* and *in vivo* (Deng et al., 2019; Guan et al., 2015; Kataria et al., 2019; Navarro-González et al., 2019; Noll et al., 2019; Xu et al., 2004, 2005). Furthermore, Nrg1 has been also described to promote neurite outgrowth upon injury *in vitro* in retinal cell cultures, spinal cord organotypic cultures and dorsal root ganglia (DRG) explants (Hao et al., 2020; Mòdol-Caballero et al., 2018). Although future research is required to elucidate the molecular and biochemical mechanisms underlying Nrg1 effect in neurite outgrowth after damage, several works demonstrate that Nrg1 can regulate signaling pathways involved in axonal regeneration and neuronal survival, such as PI3K/Akt or RhoA/cofilin (Flores et al., 2008; Guo et al., 2010; Hao et al., 2020; Mòdol-Caballero et al., 2018; Zhang et al., 2016).

Although the molecular and biochemical mechanisms are still unclear, several studies point out that Nrg1 signaling promotes neurite outgrowth through the activation of the ErbB4 receptors, and different pathways involved in axonal elongation, such as mitogen-activated protein kinase (MAPK), protein kinase (PKC) or p42/44 ERK (Bellon, 2007; Gerecke et al., 2004; Rieff et al., 1999). However, ErbB4 is mainly expressed in PV^+ cortical interneurons, which represent a subset of the neuronal subtypes in the cortex (Fazzari, et al. 2010). Furthermore, Nrg1 expression is highly found in pyramidal neurons (Liu et al., 2011), in which other signaling pathways regulate their biology, independently of ErbB4 activation.

Interestingly, Nrg1 intracellular signaling has been reported as a potential modulator of neurite development and excitatory synapsis formation. Using Nrg1 mutant neuromodulatory where its intracellular signaling is impaired, changes in dendrite formation and axonal elaboration have been described (Chen et al., 2010; Fazzari, Snellinx, Sabanov, et al., 2014). Although the

molecular implication of Nrg1-ICD remains widely unaddressed, ICD can be translocated to the nucleus, regulating the gene expression program (Bao et al., 2003; Mei & Nave, 2014; Navarro-González et al., 2019). Noteworthy, we have previously identified that Nrg1 intracellular signaling is stimulated in hypoxic conditions, promoting neuronal survival and, hence, neuroprotection upon stroke (Navarro-González, et al. 2019). Regarding this information, it is a critical step to consider the role of Nrg1 signaling not only on cortical interneurons via ErbB4 stimulation, but also in pyramidal neurons themselves by the regulation of concrete transcriptomical genetic programs.

During developmental stages, neurons effectively connect with their targets by extending specialized cellular processes named axons, sensing guidance cues and forming specific synapses in an activity-dependent manner. However, in the adult stages, the capacity of regenerate is restricted. Although this limitation remains poorly understood, some hypotheses suggest that it could be a defensive respond to avoid ectopic axonal outgrowth and, hence, aberrant synaptic connectivity. Other work suggests that protein transportation required for axonal regeneration upon injury is a complex process in a well-established system, where long-distance connections, such as the cortico-spinal tract (CST), have already been formed. Thus, the regenerative gene program activated in the context of injury is partially different from that active during developmental stages (Hilton & Bradke, 2017; S. Li et al., 2010; Sekine et al., 2018).

Particularly, axonal regeneration is limited in the adult mammalian CNS, conversely to the PNS where the capacity to regenerate after nerve damage has been widely reported (Curcio & Bradke, 2018). Such a relevant disparity can be explained by differences in the intrinsic properties of CNS injured neurons compared to PNS neurons, and the release of extrinsic inhibitory growth molecules that create a non-permissive environment for regrowth in the CNS (BrosiusLutz & Barres, 2014). Hence, understanding 1) the regenerative gene program and environmental factors in developmental periods compared to adulthood periods and 2) the differences between PNS and CNS regenerative ability becomes a crucial step to further comprehend how to promote axonal regeneration in the CNS upon injury.

Much progress has been made in the field of regeneration to unravel molecular, cellular, and systems-level approaches to axonal sprouting. Unfortunately, success has not yet been achieved, due to the complexity and multifactorial nature of brain damage (Tuszynski & Steward, 2012). To investigate the mechanisms underlying brain damage, different *in vitro* approaches permit a high-throughput approach to understanding biochemical and cellular responses. Although they are reductionist models in which 3D architecture is lost, *in vitro* models are a cost-effective strategy where experimental conditions can be controlled and simplified to establish preliminary knowledge in a shorter period and with fewer ethical concerns, compared to *in vivo* assays (Al-Ali et al., 2017; Holloway & Gavins, 2016; Kumaria, 2017).

In the field of stroke, ischemic conditions can be induced either by oxygen/glucose deprivation or by metabolic inhibition using chemical or enzymatic approach such as rotenone, antimycin or sodium azide. Additionally, another way to induce damage *in vitro* is to promote an excitotoxic environment by activating glutamate receptors using NMDA agonists or glutamate, which typically occurs after brain injury (Holloway & Gavins, 2016).

In this context, the Oxygen and Glucose Deprivation (OGD) model is the most common to investigate the role of specific proteins and pharmacological treatment in neuronal survival under hypoxic conditions *in vitro* (Navarro-González et al., 2019; Rodríguez-Prieto et al., 2021; Tasca et al., 2014). This protocol is generally used in primary cultures, which allow the observation of individual cells and thus the study of specific biochemical processes in isolated cells. However, it can be also applied to both organotypic cultures and acute slices, preserving functional connections and interactions between different cell types as an intermediate step between *in vitro* and *in vivo* assays (Tasca et al., 2014). However, some protocols described in the literature tend to expose cell cultures to higher concentrations of glucose and oxygen prior the hypoxic stimulus, which can suppose a resistant response from the culture, perturbing the results. Hence, it is worth emphasizing that physiological conditions should be maintained *in vitro* as much as possible to avoid biased data (Holloway & Gavins, 2016).

On TBI paradigm, different mechanical stimuli can be used to induce damage *in vitro*. A common strategy is the cell stretch assay, widely used to investigate regeneration in PNS, in which cells are cultured on flexible silastic membranes and subjected to controlled stretch inputs. However, it requires specific devices and prior expertise in the technique and does not entirely recapitulating real-world conditions in which nerve injury can be produced by both stretching and twisting forces (Salvador et al., 2018). Another approach is the compression-induced injury models to reproduce compressive neuropathies, consisting of exposing the cell culture to a weight-drop input. Nonetheless, the main drawback is the technical limitations related to the lack of reproducibility in terms of location and load application (Abu-Rub et al., 2010; Kumaria, 2017; Varier et al., 2022).

Overall, although the models described above can reliably reproduce the clinical manifestation, they do not seem to be effective for the specific analysis of axonal outgrowth. To investigate neurite growth and axonal guidance, diverse types of assays have been developed using low-density cell preparations to observe individual neurons. These models consist of plating the cells on a coated surface to which different growth stimulators or inhibitors are added to measure axonal outgrowth (Al-Ali et al., 2017). However, these assays have mainly been used to investigate neurite outgrowth from a developmental perspective, which does not necessarily recapitulate the mechanistic events activated in axonal regeneration upon injury.

Therefore, the specific induction of axonal injury is crucial to recapitulate the molecular and biochemical pathways implicated in this scenario. In this sense, transection models, also named "acute axotomy models", are simple but effective approaches to evaluate axonal regeneration in response to mechanical injury. Of note, sophisticated methods such as laser-induced transection are also used to perform axotomy in single axons to address the intricacy of neurite injuries with single-cell resolution (Varier et al., 2022; Yilmaz et al., 2020; Zhang et al., 2020).

In the last decades, the development of microfluidic chambers has been widely used to provide a specific platform to study axonal growth and regeneration after injury (Abu-Rub et al., 2010; Huang & Sheng, 2022; Kim et al., 2009; Taylor et al., 2005). In 1977, the "Campenot chamber" pioneered the field by offering the first three-chamber culture system to explore neurite growing using sympathetic neurons (Campenot, 1977). Since then, highly refined, and sophisticated devices have been built, consisting of different compartments that are fluidically isolated, but physically connected by microgrooves. Neurons are cultured in one of the chambers, where the soma and dendrites are restricted, while their axonal projections can grow into the other chamber, depending on to the chemical agents supplied (**Figure 10**). Therefore, these specialized devices permit isolation of the axon from the cell body and a precise control of the cellular microenvironment to test axonal growth. However, this experimental setup requires specific and expensive devices that offers an artificial environment in which neurons are forced to grow in a determined direction and specific organization. In this respect, this paradigm does not fully reflect the complexity of *in vivo* conditions, where different cell populations coexist and where neuronal projections do not extend in a straight line. Morevover, another technical limitation is that microfluidic chambers are prone to fluid leakage, compromising reproducibility of future experiments (Al-Ali et al., 2017; Varier et al., 2022).

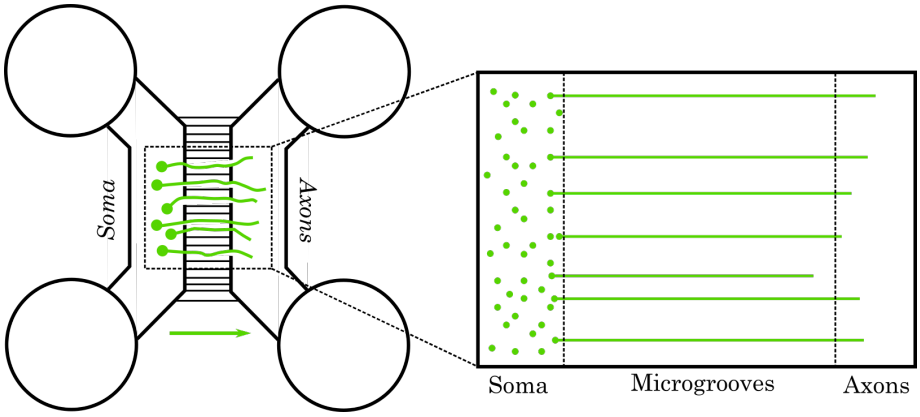

Figure 10. Scheme of a classical microfluidic chamber to investigate axonal outgrowth.

To overcome the technical and biological limitations of the microfluidic chambers exposed above, the scratch model is a powerful tool to induce axonal injury by a mechanical dissecting of the axons in a high-density cell culture. Inspired by the *in vitro* assays typically used to study

cell migration and proliferation in the cancer field (Jonkman et al., 2014), this experimental setup offers an affordable and reproducible method to quantify axonal regeneration upon damage, with minimal technical requirements, which can closely resemble the *in vivo* axonal elongation paradigm, compared to microfluidic chamber approaches.

Here, we developed a novel *in vitro* model of axonal injury that combines a sparse labeling of neurons using electroporation techniques with scratch assays to analyze axonal outgrowth upon damage. This experimental paradigm takes advantage of the affordability and reproducibility of the injury model but offering the visualization of individual and labeled axons to give a cell-autonomous readout. Furthermore, this methodology was used to study the role of Nrg1 signaling upon axonal injury, performing gain- and loss-of function approaches using electroporation techniques.

RESULTS

Characterization of a novel *in vitro* model of axonal injury.

To evaluate the role of Nrg1 signaling in the context of axonal outgrowth upon injury, we developed a novel model of axonal injury (**Figure 11A**). To this aim, we used primary cortical neuronal culture from embryonic mice (E14.5-E15.5). This part of the protocol is largely described in a previous publication from our lab (Rodríguez-Prieto et al., 2021). Briefly, we used the electroporation system NEPA21 to perform a sparse labeling of the neurons combined with co-expression or deletion of Nrg1 to study the working hypothesis. This technology allows us to merge control and treated neurons in the same well, reducing biological variability associated with the injury procedure (**Figure 11B**).

At 4 days *in vitro* (D4), we induced the injury to the cultures by mechanically severing of the axons. Using the fluorescence of electroporated neurons, we monitored the motility of individual axons during the first 20 hours post-scratch, recorded in live time-lapse videos. The images revealed that the axons presented high motility but were unable to cross the empty space left by the scratch during the first hours and moved backwards to the border (**Figure 11C**). Neuronal cultures are very sensitive to external factors such as CO_2 and temperature. Hence, most of the neurons died during the overnight time-lapse experiments, and we failed to obtain further information on axon dynamics in real time.

Considering this result, we planned to evaluate axonal outgrowth 72 hours and 10 days post-scratch in fixed and immunolabeled cultures to improve the fluorescence signal. The analysis consists of counting the number of axons crossing arbitrary lines drawn in the empty space (**Figure 11B**). This corresponds to an effective and affordable quantification thanks to an adequate density of electroporated neurons which permits to see isolated labeled neurons, giving insight into a cell-autonomous response, compared to other models such as viral infection, where the whole culture is treated.

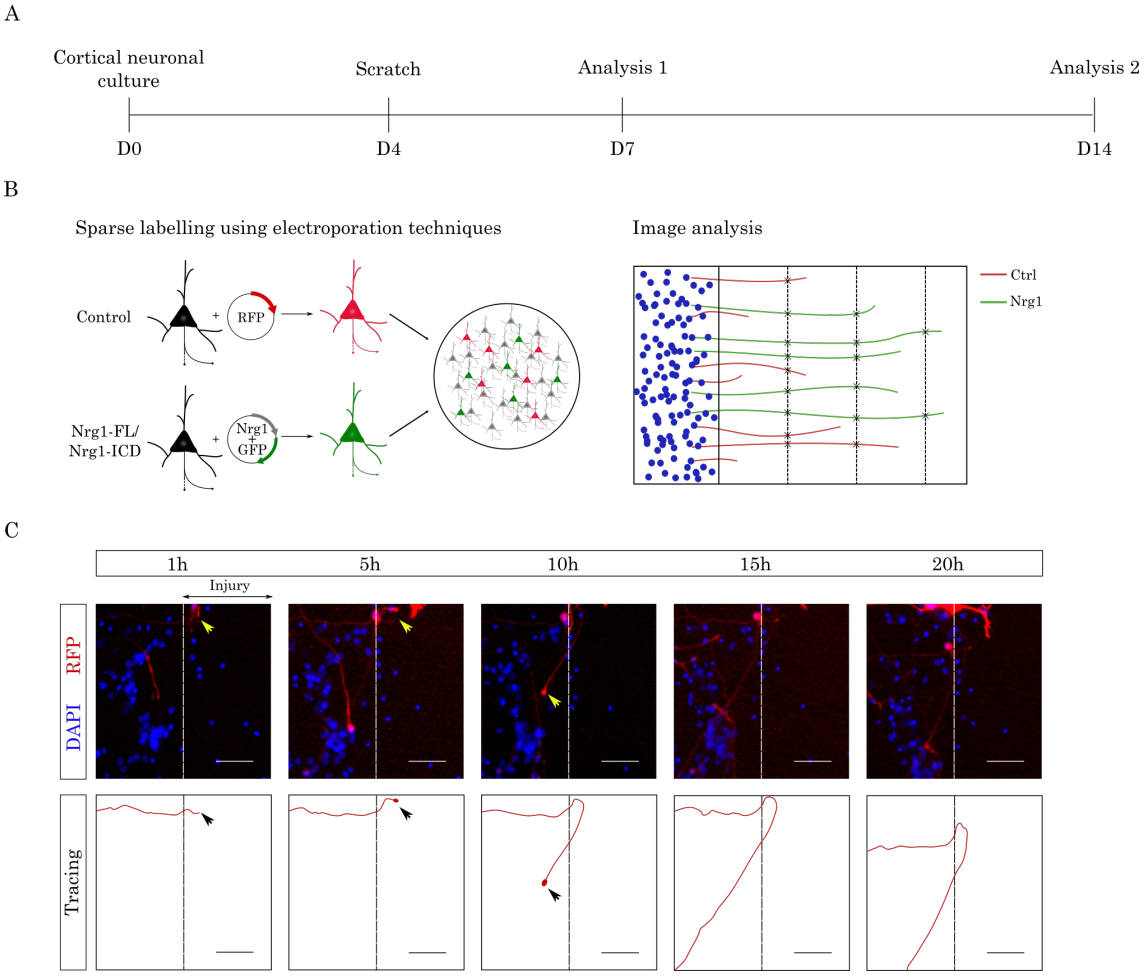

Figure 11. Characterization of the *in vitro* model of axonal injury. A) The scheme represents the timeline of the experimental methodology followed for *in vitro* model design. Cortical neuronal cultures of embryonic mice (E14.5-15.5) were established to induce a mechanical transection of axons at 4 days *in vitro* (D4). Axonal regeneration was analyzed 72 hours (analysis 1) and 10 days post-scratch (analysis 2) in LOF and GOF approaches, respectively. B) On the left, the cartoon illustrates the sparse labeling of the neurons using electroporation techniques to combine both control (labeled in red) and Nrg1-treated (labeled in green) neurons, allowing a cell-autonomous readout. On the right, the cartoon shows image analysis strategy. Due to the sparse labeling, it is possible to quantify axonal regeneration by counting the number of labeled axons crossing the empty spaced after axonal injury. C) The panel shows images (upper row) from a live time-lapse video to illustrate the motility of the axons (labeled with RFP) upon injury along the first 20 hours after the scratch. Note that the neurons exhibit some motility but are unable to cross the empty space during the first few hours after injury. The tracing facilitates the visualization of the axon (bottom row, labeled in red). Scale bar: 50μm.

Nrg1-ICD expression promotes axonal outgrowth upon injury *in vitro*.

Once the *in vitro* model of axonal injury was established, we tested whether Nrg1 expression promotes axonal outgrowth upon injury. To achieve this goal, we first performed gain-of function (GOF) approaches to express the full form of Nrg1 (Nrg1-FL) or specifically its intracellular domain (Nrg1-ICD).

As previously described, we induced the scratch D4 *in vitro* and we analyzed axonal outgrowth 10 days post-scratch (**Figure 12A**). Using immunolabeled culture images, we quantified the number of axons crossing the empty space at different distances: proximal (P, 160µm), medial (M, 240µm) and distal (D, 320µm) to the injury (**Figure 12B**).

To this aim, we used electroporation techniques to combine both GFP labeling and the co-expression of Nrg1-FL and Nrg1-ICD (labeled in green), co-cultured with control neurons (Ctrl) which were electroporated with GFP and RFP plasmids (labeled in red) (**Figure 12B**). For more information on electroporation settings, please refer to the corresponding section in Materials and Methods (*Primary neuronal cultures*). The axonal outgrowth was quantified by counting the number of axons crossing arbitrary lines drawn in the empty space. For more details on data analysis and normalization criterion, please refer to the corresponding section in Material and Methods (*Quantification of axonal outgrowth in vitro*).

The data showed that the number of Nrg1-FL and Nrg1-ICD axons was significantly higher and they were able to grow further along the injured space 10 days post-strach, compared to the control condition (**Figure 12C**). This result suggests that Nrg1, and specifically the activation of its intracellular signaling, promotes axonal outgrowth upon injury *in vitro*. Therefore, this study provides a robust foundation to further investigate the cell-autonomous response specifically driven by Nrg1 intracellular signaling upon injury.

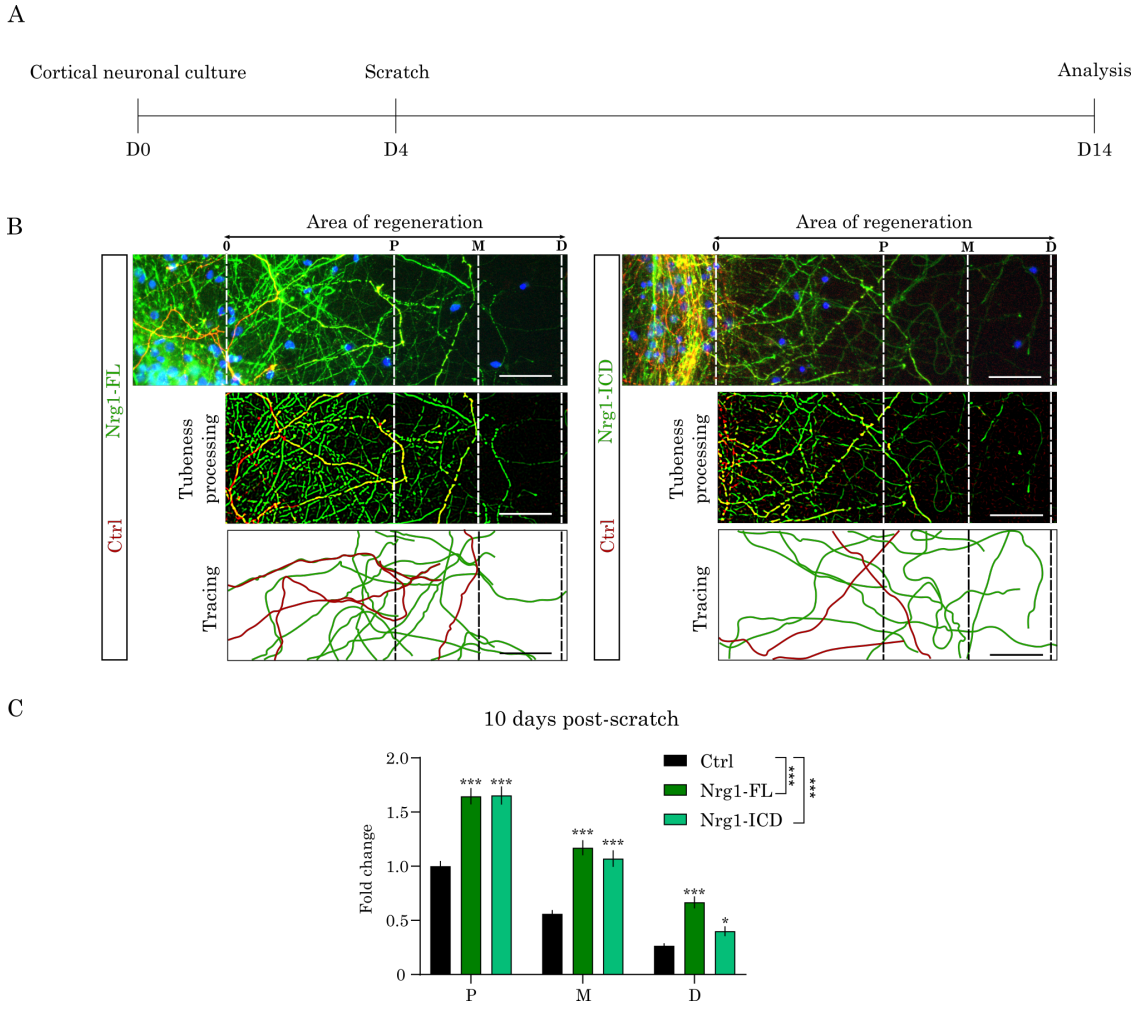

Figure 12. Nrg1-ICD expression specifically promoted axonal outgrowth upon axonal injury *in vitro*. A) The scheme shows the pipeline of the experimental approach followed in the GOF paradigm, in which axonal regeneration was analyzed 10 days after the scratch. B) Representative images to evaluate Nrg1-FL (left) and Nrg1-ICD expression (right) in axonal outgrowth. Control neurons were electroporated with both GFP and RFP plasmids (labeled in red), while Nrg1 treated neurons were electroporated with both GFP and Nrg1-FL or Nrg1-ICD plasmids, depending on the condition (labeled in green). Of note, a manual tracing cartoon of the regenerated area has been included to facilitate the visualization. Scale bar: 50μm. C) The graph shows the data of axonal regeneration 10 days post-scratch obtained in the proximal (160μm, P), medial (240μm, M) and distal (320μm, D) lines placed in the scratched zone. Results were normalized to the control data in the proximal line. Mean ± SEM (N= 270 (Ctrl), 90 (Nrg1-FL and Nrg1-ICD) pictures from 3 independent experiments). Statistical test: Two-way ANOVA with repeated measurements and Sídák's multiple comparison test * $p \leq 0.05$, *** $p \leq 0.001$.

Nrg1 deletion limited axonal outgrowth upon injury *in vitro*.

Given the results from the GOF approaches, the next question was whether the absence of Nrg1 impairs axonal outgrowth following axonal injury *in vitro*. To achieve this goal, we used primary cortical neuronal cultures from Nrg1 floxed mice. In this Cre-driver mouse line, the gene of interest is flanked by repeated *loxP* sites, which are directly identified by Cre recombinase, excising, and inactivating the gene. Based on this principle, we took advantage of the electroporation strategy to induce Nrg1 deletion prior to axonal injury in a limited number of neurons to obtain single axons from both *wild-type* and *knockout* neurons. In this sense, we co-expressed both RFP and GFP-Cre recombinase to obtain $Nrg1^{-/-}$ neurons (labeled in red), while control neurons were electroporated with a GFP which did not contain Cre expression. For more information on electroporation settings, please refer to the corresponding section in Materials and Methods (*Primary neuronal cultures*).

As previously described, we induced the axonal injury D4 *in vitro* and axonal outgrowth was analyzed 72h post-scratch (**Figure 13A**). Considering the timing and axonal length, the arbitrary lines to quantify the number of axons crossing the empty space were closer to the injury border: proximal (P, 80µm), medial (M, 160µm) and distal (D, 240µm) (**Figure 13B**). To avoid misleading results, the normalization criterion was the same as described in the GOF studies section.

In this experimental paradigm, the data reveal that $Nrg1^{-/-}$ axons tend to have a outgrowth rate upon axonal injury ($p=0.058$, **Figure 13C**), suggesting the potential of Nrg1 signaling in the process of axonal sprouting upon injury *in vitro*. We also attempted some experiments at 10 days post-scratch, but we did not obtain consistent results due to technical limitations (*data not shown*).

Overall, although further studies are required to confirm this phenotype, these data suggest that Nrg1 signaling may be necessary for axonal outgrowth upon injury *in vitro* in consonance to the result obtained using GOF approaches.

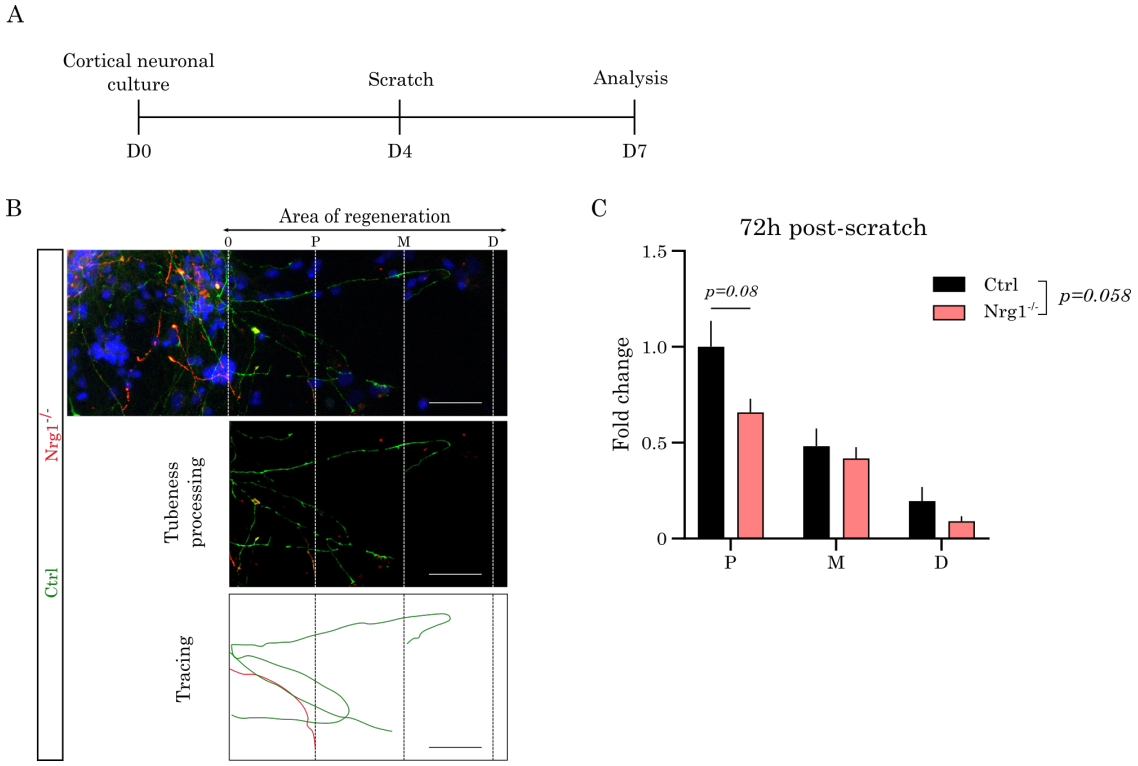

Figure 13. Nrg1 deficient neurons presented a limited axonal outgrowth upon axonal injury *in vitro*. A) The scheme shows the pipeline of the experimental approach followed in the LOF paradigm, where axonal outgrowth was analyzed 72h after the scratch. Of note, we used a Nrg1 floxed mice line to generate $Nrg1^{-/-}$ neurons by electroporation techniques *in vitro*. B) Representative images examining axonal outgrowth in control (labeled in green) and Nrg1 deficient (labeled in red) neurons. Conversely to GOF approaches, control neurons were electroporated with a GFP plasmid, while a co-electroporation of RFP and GFP-expressing Cre plasmids was used to obtain $Nrg1^{-/-}$ neurons. The cartoon illustrates axonal regeneration in the scratched area for better visualization. Scale bar: 50µm. C) The graph shows the data of axonal outgrowth 72h post-scratch obtained in the proximal (80µm, P), medial (160µm, M) and distal (240µm, D) lines placed in the scratched zone. Results were normalized to the control data in the proximal line. Mean ± SEM (N= 56 pictures per group from 3 independent experiments). Statistical test: Two-way ANOVA with repeated measurements and Sídák's multiple comparison test.

DISCUSSION

Axonal regeneration is limited in the adult CNS, resulting in permanent disability upon injury (Benowitz & Carmichael, 2010; Curcio & Bradke, 2018; Joy & Carmichael, 2021). Nrg1 is essential for cortical development, involved in different processes such as, neurite outgrowth, axon guidance, synaptogenesis, axon myelination and ensheathment (Fazzari et al., 2010, 2014; Mei & Xiong, 2008; Rahman-Enyart et al., 2020). Recently, it has also been described as an emergent modulator of the CNS after damage. However, little is known about its role in axonal regeneration upon injury. Particularly, the role of Nrg1 intracellular signaling, whose neuroprotective role we previously demonstrated in stroke, remains unclear (Navarro-González et al., 2019). Here, we developed a novel *in vitro* model of axonal injury to comprehend the role of Nrg1 signaling in the process of axonal outgrowth upon injury.

Most of the studies use the PNS as a model to study axonal regeneration because of its greater regenerative capacity, compared to the CNS (Fricker et al., 2011; R. Li et al., 2020; K. Liu et al., 2011; Varier et al., 2022). Lesions in primary sensory neurons of the DRG are commonly used by presenting a better regenerative ability in the CNS (Tuszynski & Steward, 2012). Unfortunately, these models do not entirely recapitulate the specific intrinsic and extrinsic conditions that limit regeneration in other CNS systems, such as the cortex.

There are distinct cell-based models available in the literature to study axonal regeneration *in vitro*. In our model, we used electroporation techniques to perform a sparse labeling of neurons mixed with naïve cells, which offers several advantages. Using a high-density preparation offers robustness and better viability, compared to low-density approaches. Moreover, although high-density cultures do not allow to study morphological parameters of individual cells, we overcome this limitation by the sparse labeling, thus customizing the number of labeled cells required to study axonal regeneration. Noteworthy, we used the NEPA21 device (Nepa Gene Co), an open system that allows customization of experimental conditions with low operational cost, compared to other devices that require specific kits and equipment.

Various models are available in the literature to perform neuronal injury, such as OGD, excitotoxicity, glutamate-induced excitotoxicity, or chemical/enzymatic inhibition of the electron transport chain (Holloway & Gavins, 2016). However, these models are not effective for observing axonal regeneration per se. Hence, to specifically induce axonal injury *in vitro*, we proposed the conventional scratch assay, originally used in the cancer field to study cell migration and proliferation (Jonkman et al., 2014). This model consists of a mechanical severing of the axons and quantification of the colonization of the axons in the empty space. This protocol is reproducible, affordable, cost-effective and does not require specific expertise, compared to other protocols, such as the microfluidic chambers.

Translated to *in vivo* approaches, the use of primary neuronal cultures supposes a good compromise between cost effectiveness and reliability. In this sense, axons can move freely in the empty space without compromising measurements, compared to the use of organoids or explants. Although these types of preparations could be a middle ground between cell cultures and *in vivo* studies, they are notably laborious and time-consuming where tissue architecture hampers the analysis of neurite outgrowth (Al-Ali et al., 2017; Seo et al., 2022).

Overall, we provided a novel model of axonal injury *in vitro* to investigate axonal regeneration in isolated neurons, allowing cell-autonomous readout thanks to the electroporation strategy (Rodríguez-Prieto et al., 2021a). Nevertheless, we are aware of some of the limitations of this model. For example, it is difficult to isolate electroporated injured neurons from the culture in order to give a further molecular perspective to elucidate specific mechanisms of axonal regeneration using proteomic or transcriptomic strategies. For these studies, it is preferable to use a different experimental paradigm, such as the one proposed by the laboratory of Dr. Strittmatter, based on shRNA lentiviral infection, permitting a functional genome-wide characterization after axonal injury (Sekine et al., 2018).

Complementarily, our model offers the possibility to study specific genes of interest in isolated neurons by electroporating concrete DNA plasmids. In this case, we perform GOF and LOF assays to study the role of Nrg1 signaling, and the activation of its intracellular pathway upon axonal injury. In this sense, our GOF data suggest that Nrg1, and specifically the activation of its intracellular signaling, promote axonal outgrowth *in vitro* 10 days post-scratch. Noteworthy, future experiments are required to confirm the results obtained in LOF approaches. In this sense, we should use a different experimental strategy to induce a complete Nrg1 deletion in all the neurons where the phenotype can be easily detected, such as viral infection expressing GFP-Cre or cultures of Nrg1-Nestin-Cre lines, available in the lab.

In both *in vitro* and *in vivo* approaches, Nrg1 signaling has been shown to promote neurite outgrowth in different neuronal populations (Fazzari et al., 2010b; Mei & Nave, 2014; Mei & Xiong, 2008; Rahman-Enyart et al., 2020). Moreover, several works also pointed out the relevance of Nrg1 in regeneration upon injury. However, most of the studies used the *in vitro* administration of rhNrg1 or ErbB4-deficient mice, which do not specifically recapitulate Nrg1 signaling (Bartus et al., 2016; Fricker et al., 2011; Kataria et al., 2019; Mancuso et al., 2016; Mòdol-Caballero et al., 2018; Zhang et al., 2016). In this sense, we expressed Nrg1-FL and Nrg1-ICD in cortical neurons, giving a novel insight into axonal outgrowth upon injury, which can be partly mediated independently of ErbB4 signaling.

In the last decades, some groups demonstrated that Nrg1 is implicated in the activation of PI3K/Akt pathway, promoting neuronal survival, neurite outgrowth and myelination upon injury

(Cui et al., 2023; Guo et al., 2010; Mòdol-Caballero et al., 2018). A recent publication has also proposed that Nrg1 expression regulates the RhoA/cofilin/F-actin pathway upon optic nerve injury, suppressing retinal cell apoptosis and enhancing axonal growth (Hao et al., 2020). Among other functions, these signaling pathways are implicated in cytoskeletal dynamics and protein translation, which are essential for the formation of the new growth cone and thus the elongation of the regenerated axon (Curcio & Bradke, 2018; K. Liu et al., 2011). Therefore, we can hypothesize that Nrg1 may regulate key signaling pathways implicated in axonal regeneration.

Specifically, Nrg1 intracellular signaling promotes neuronal survival and dendritic spine formation, which could be crucial processes for brain recovery upon injury (Bao et al., 2003; Fazzari, Snellinx, Sabanov, et al., 2014). We previously published that the nuclear translocation of Nrg1-ICD is promoted under hypoxic conditions *in vitro*, thereby activating a genetic program that promotes neuronal survival (Navarro-gonzález et al., 2019). Nevertheless, the direct molecular modulators of Nrg1 intracellular signaling remain poorly understood. In this sense, to further understand the mechanistic basis of Nrg1 intracellular signaling upon axonal regeneration, we should determine if this mechanical stimulation is enough to uprise Nrg1-ICD expression and ascertain which gene program and signaling pathways are regulated using follow-up molecular approaches.

In conclusion, our work brought to the spotlight the relevance of Nrg1 signaling in axonal regeneration and specifically of its intracellular signaling as a promising target for brain damage. We hope that future research in this field will further investigate the signaling pathways modulated by Nrg1 intracellular signaling in the paradigm of axonal injury.

CHAPTER 2: CHARACTERIZATION OF A NOVEL *IN VIVO* MODEL FOR MULTIPLEXED ANALYSIS OF CALLOSAL CONNECTIONS UPON CORTICAL DAMAGE.

GRAPHICAL ABSTRACT

A Biological paradigm

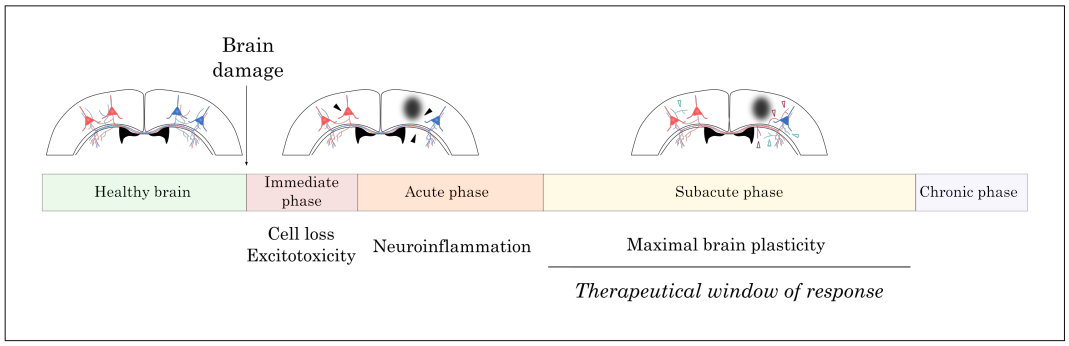

B Methodology used for multiplexed analysis upon brain damage

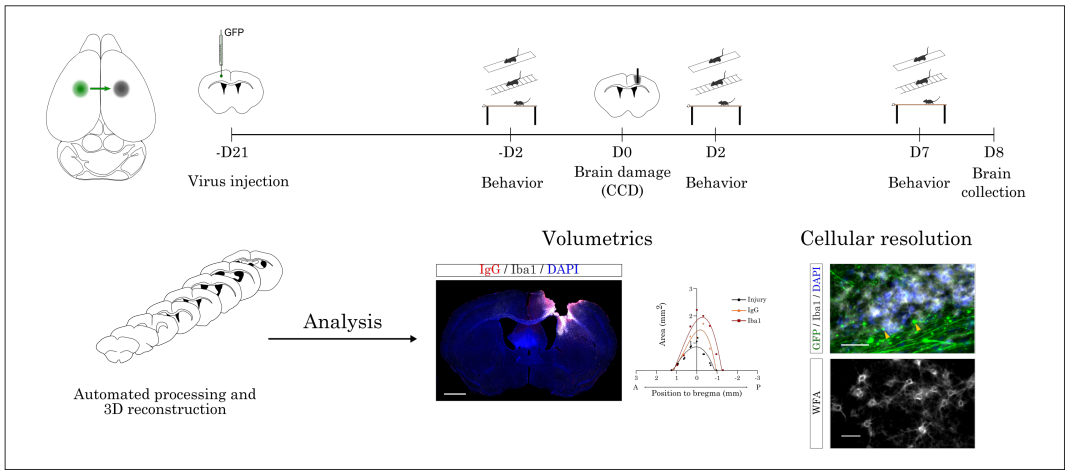

Highlights:

- We developed a novel *in vivo* model of cortical regeneration that combines the tracing of cortico-cortical projections and a controlled cortical damage (CCD).
- The CCD allows the detection of functional motor impairments using various behavioral tests, of which the RPT and WSL were the most sensible.
- We provided a semi-automated workflow that combines 3D reconstruction with different immunolabeling, allowing multiplex analysis of cellular and subcellular changes after CCD.
- There is a correlation between the integrity of the PNNs and the microglial response in the perilesional area.

The results explained in this chapter have been recapitulated in the scientific article "A novel *in vivo* model for multiplexed analysis of callosal connections upon cortical damage", published in the International Journal of Molecular Science in 2022. Part of the experimental research developed in this publication has been carried out in collaboration with Dr. Daniela Talhada and Dr. Karsten Ruscher from the Laboratory of Experimental Brain Research (BMC, Lund University, Sweden), who have been very helpful in providing expertise and technical support in the behavioral test to detect motor impairment in the focal injury model. Furthermore, we developed the semi-automated workflow for image analysis in collaboration with José Manuel Saborit from Biomedical Imaging Department CIPF-FISABIO (Valencia, Spain).

For this publication, I performed the stereotactic surgeries to induce the cortical damage, as well as the behavioral motor testing, acquisition, and processing of the samples for image analysis. I also contributed to this publication in the conceptualization, formal analysis, data curation, visualization, and writing of the original manuscript.

INTRODUCTION

Brain injury (BI) is the leading cause of adult disabilities. The most typical sources of BI are stroke, either hemorrhagic or ischemic, and traumatic brain injury (TBI), either concussive or penetrating. Although the specific mechanisms underlying this complex and heterogeneous disorder remain poorly understood, different brain injuries share similar key pathological events (Galgano et al., 2017; Joy & Carmichael, 2021).

Immediately after brain injury, excitotoxicity and the activation of apoptotic pathways result in into a massive neuronal loss within the first hours, defined as the hyperacute phase. According to this timing, the temporal window of response is highly limited to a few hours, in which a rapid intervention should be required. Subsequently, an inflammatory response led by microglial cells, astrocytes, and the infiltration of peripheral immune cells takes place during the acute phase to remove damaged tissue and repair neuronal circuits. Remarkably, excessive inflammation can also potentiate neuronal loss by increasing oxidative free radicals or releasing matrix metalloproteinases (MMPs) (Anrather and Iadecola 2016; Moskowitz, Lo, and Iadecola 2010).

In the subacute phase, the inflammatory response is reduced, leading to a process of synaptic plasticity and axonal sprouting that promotes spontaneous recovery after injury. In rodent models, this phase can last up to one month, while in humans it has been described to last up to 3 months after injury. In this context, neurons activate a growth transcriptional program to enhance neuronal regeneration, axonal outgrowth and, ultimately, plasticity. In particular, a permissive environment for axonal sprouting, dendritic spine turnover and sensorimotor map plasticity is restricted to the perilesional area (PL), near the core of the damage and these events are linked to motor recovery (Carmichael 2016; Carmichael et al. 2017; Joy et al. 2019; Joy and Carmichael 2021; Kugler et al. 2020). However, the regenerative capacity in the CNS is limited, compared to the PNS paradigm, due to a partial activation of developmental growth programs and the release of extrinsic inhibitory growth molecules from the glial scar and cellular debris upon injury (Curcio & Bradke, 2018). Anatomically, the injury core is defined by a massive neuronal loss and tissue disruption, which is clearly evident in histological preparations. In contrast, most of the studies define the PL as the region proximal to the core, which is not that trivial to establish a boundary (Alia et al. 2016; Michalettos et al. 2021; Talhada et al. 2019). Therefore, understanding how to promote the intrinsic regenerative capacity in the PL region is an important mechanism for neuronal circuit restoration and plasticity after injury, and represents a potential therapeutic window of response.

After this window of plasticity is reduced, the chronic phase is defined by a limited functional and structural recovery of the neuronal circuitry. Therefore, although the mortality rate of BI has

been reduced, there are no specific treatments available to improve this functional recovery, resulting in permanent disabilities that limit the quality of life of the patients.

Prior to clinical trials, there are different animal models of BI, which may have advantages or limitations, depending on the research goal. The most well characterized model in the field of stroke is the intraluminal suture middle cerebral artery occlusion (MCAO) (**Figure 14**). In this protocol, the experimental animal undergoes a complex surgery in which a monofilament is inserted into the internal carotid artery to occlude the MCA, producing an ischemic stroke. Depending on the suturing, the protocol can produce a permanent or transient damage with reperfusion (McBride & Zhang, 2017). Interestingly, most of the thromboembolic infarcts in humans take places in the MCA zone, this model closely resembles to clinical manifestation. Nevertheless, this model provokes larger ischemic lesions reaching other brain regions such as thalamus, hippocampus, or substantia nigra, which is unlikely in human pathology. In addition, it is difficult to perform axonal regeneration and cortical rewiring analysis in such an injury dimension, so the model is generally adequate to study neuronal death, injury volume, glial activation, or blood-brain barrier in ischemic stroke (Canazza et al. 2014; Fluri, Schuhmann, and Kleinschnitz 2015).

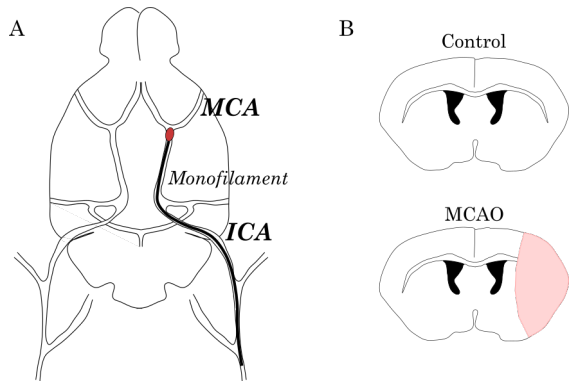

Figure 14. Illustration of the MCAO model. A) The cartoon shows the surgical procedure followed to induce ischemic stroke by introducing a monofilament through the internal carotid artery (ICA) to occlude the middle cerebral artery (MCA). B) Graphical representation of infarct size in the MCAO protocol (labeled in red), affecting both cortical and subcortical regions. It is noteworthy that depending on the timing of MCA occlusion and the procedure, the size of the injury can be regulated to some extent, although large infarcts are generally produced.

In the field of TBI, the first models used were based on concussion as the cause of the injury, in which biomechanical properties were mainly recapitulated. Nowadays, newer strategies have been developed to better understand the molecular mechanisms involved in the trauma. In this context, the most popular methods are the fluid percussion injury (FPI), controlled cortical impact injury (CCI), weight-drop impact acceleration injury (WDIA) and blast injury (Galgano et al. 2017; Joy et al. 2019; Nichols et al. 2018; Ozen et al. 2020). Each one has specific peculiarities, but all require specific equipment to induce the damage, with a limited biomechanical control of

the insult (**Figure 15**). Hence, these methods can be effective in simulating various insults that produce TBI and recapitulate clinical features in humans, such as contusion, intracranial hemorrhage, brain swelling, motor impairment and neurodegeneration. However, they generally produce large brain damage with high variability and mortality rate, where it is not possible to study axonal regeneration and plasticity (Xiong, Mahmood, and Chopp 2013).

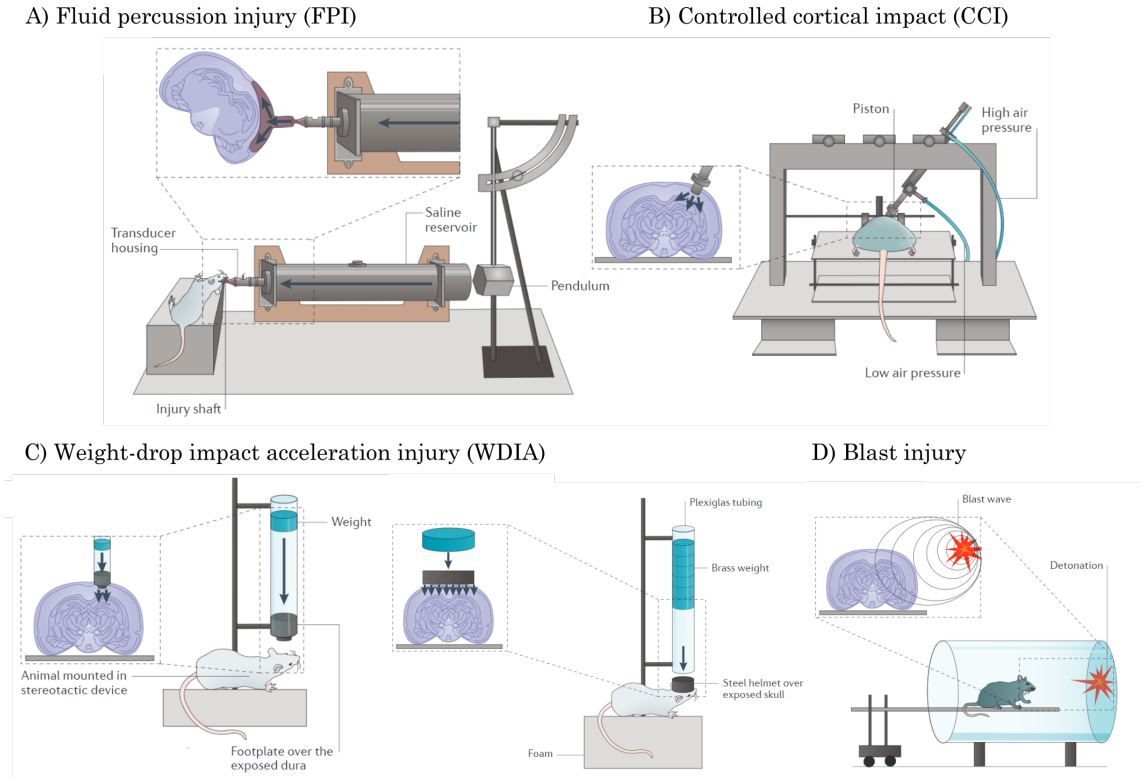

Figure 15. Animal TBI model technical setups. a) The FPI devices inflict the damage by rapidly injecting a fluid pulse into the brain after a craniotomy. b) The CCI uses air-operated piston to hit the brain, controlling the distance and speed. c) In the WDIA models, a free object is delivered directly to the exposed brain of the animal. It can be customized to affect a larger or smaller cortical region. d) Blast injury models consist of exposing the animal to a blast wave produced by a denotation, that closely mimics TBI injuries suffered by military personnel. Modified from Xiong, Mahmood, and Chopp 2013.

There are several ways to induce focal damage. In 1985, Watson and colleagues described an innovative way of inducing ischemic stroke, called phototrombosis, based on the injection of a photosensible dye which remains largely in the brain vasculature, with minimal cell penetration. After illumination, it induced a local oxidative response, platelet aggregation, occlusion of blood vessels and, thus, interruption of cerebral blood supply (Watson et al., 1985). Other methods are based on the stereotactic injection of different compound. To mimic an ischemic insult, endotelin-I is widely used, which is a potent and long-acting vasoconstrictive peptide which can be applied directly to the MCA or to the cortical surface to induce cortical damage. To produce a hemorrhagic stroke, injecting autologous blood from the animal's superficial vessels or bacterial collagenase to disrupt the extracellular matrix in the basal lamina of blood vessels are

commonly used (Barratt, Lanman, and Carmichael 2014; Fluri, Schuhmann, and Kleinschnitz 2015; Sommer 2017; Yan, Chopp, and Chen 2015). Although these strategies provide focal lesions with less invasive protocols compared to MCAO or TBI models, it is difficult to control the duration of the insult and the agent may diffuse to different brain regions, resulting in multiple lesions. Hence, these models may more closely recapitulate clinical hallmarks associated with stroke but, in our experience, they give some variability between them. Of note, in TBI research, the CCI and WDIA can be customized to obtain focal injuries by controlling the air pressure and weight, respectively, which is not so trivial and adds technical variability. However, tissue deformation, edema or apnea in the experimental animals associated with the methodology can compromised future analysis in terms of axonal regeneration and plasticity (Ma et al., 2019).

To overcome these technical variability and complexity, our main goal was to develop a protocol to create a focal injury that should fulfilled two different purposes: 1) to provide a detectable motor behavioral outcome and 2) to allow a multiplex analysis to study cortical recovery after damage. To this end, our work was inspired by the stab wound model developed by Professor Götz (Buffo et al., 2008; Mattugini et al., 2019) and the cortical tracing technique performed by Professor Carmichael's lab as crucial points to build our methodology (Joy et al. 2019; S.Li et al. 2010; Overman et al. 2012).

Briefly, we targeted callosal neurons in the left primary motor cortex, based on the rationale that the corpus callosum is the largest interhemispheric connection in the brain and we can observe both the soma and the projecting axons in the same coronal section (de León Reyes et al., 2020; Fenlon & Richards, 2015). 3 weeks later, we perform the mechanical injury in the right motor cortex, relative to the hindlimb functional area. To offer a functional characterization, we performed a battery of behavioral tests sensible enough to detect motor impairment. Finally, we developed a multiplex histological approach, using immunolabeled serial coronal sections. In this sense, we created a bioinformatics workflow to perform semi-automated 3D brain reconstruction to provide a stereological analysis, such as injury volumetrics or neuroinflammatory response. As an example of the versatility and power of this tool, we investigate the integrity of PNNs after injury. In this context, by combining different immunolabels from adjacent series, we were able to delineate the PL region using Iba1 as a molecular marker, observing an inverse correlation between $Iba1^+$ regions and the number of PNNs upon CCD (González-Manteiga et al., 2022).

RESULTS

Tracing of cortico-cortical connections in young mice.

Although the aged population is the most susceptible to brain damage, we first used young female mice (3-4 months old) to establish both the injections and the injury conditions before performing the research in aged mice.

To trace callosal projection, we performed stereotactic injections using AAV expressing GFP under the Synapsin promoter into the left (contralesional) primary motor cortex of the hindlimb (bregma 0.2; medio-lateral (ML) 1.5, dorso-ventral (DV) 0.5) (Navarro-González et al., 2019). Because the callosal connections run parallel to the coronal sections at this anterior-posterior (AP) level, we were able to observe the injection site (**Figure 16A**, top panels) and the cortico-cortical projections through the corpus callosum to the contralateral target site (**Figure 16A**, bottom panels) in a single section, using different exposure settings to obtain the images. Labeling of GFP-expressing axons provided sufficient resolution to identify axons individually (**Figure 16A**, inset). Incidentally, the use of AAV as tracers gives the opportunity to perform gain- and loss of function assays by expressing or depleting specific genes of interest. This approach allows the soma and axon of the same neurons to be examined separately in the same sections and could be useful to study the role of a particular gene of interest in these specific compartments, such as Nrg1 signaling, which will be described in detail in Chapter 4 of this dissertation.

To target different cortical projections, we showed that the labeling could be combined with different tracers such as biotin dextran amine (BDA). Specifically, we labeled with BDA the ipsilateral connections from the right forelimb (bregma 1.60; ML 1.60; DV 0.5) to the right hindlimb (**Figure 16B**). As observed with AAV injection, this labeling provided a cellular resolution to study individual axons. Overall, the combination of different tracers in diverse brain structures is a useful tool to a better understand of plasticity and connectivity in different neuronal projections in the same sample.

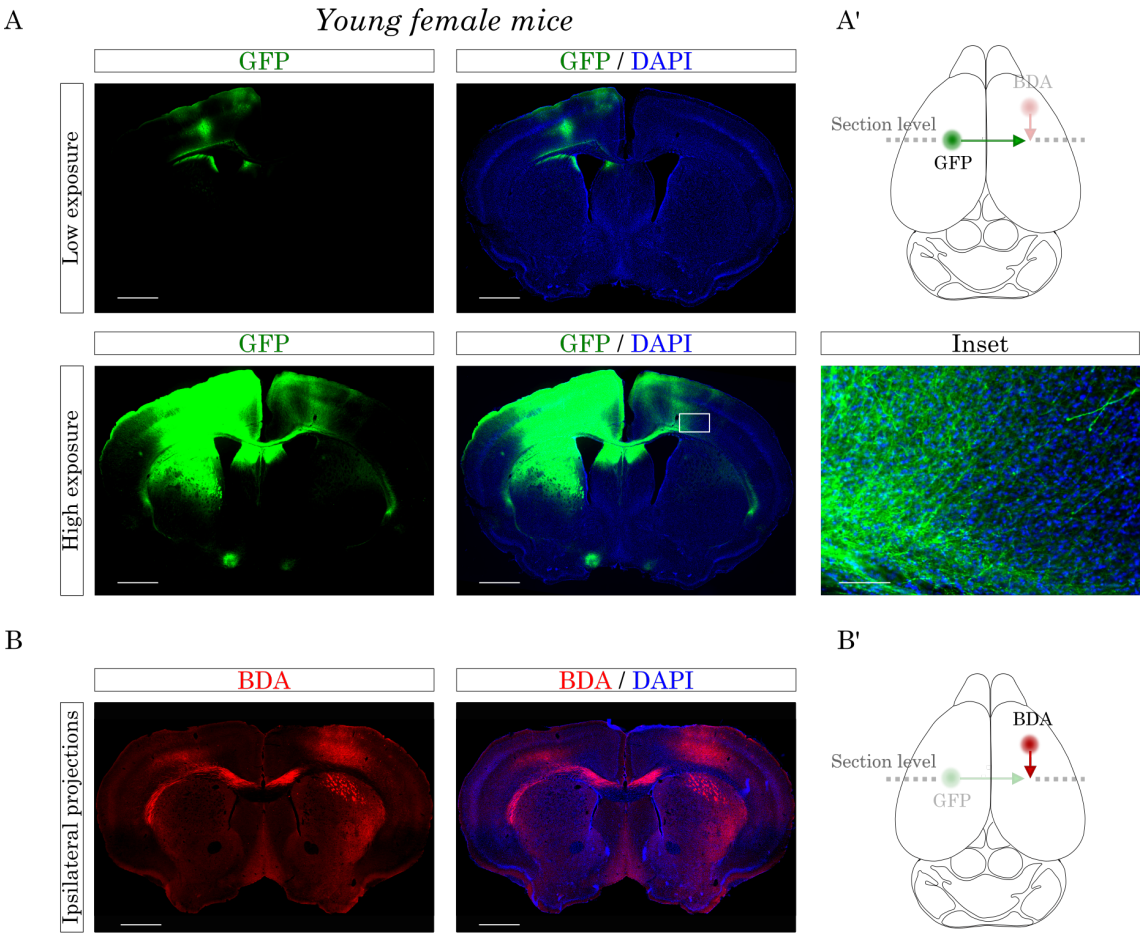

Figure 16. Tracing of cortico-cortical connections. A) The images show the tracing of cortico-cortical projections from the left to right hindlimb motor cortex (bregma: AP 0.2, LM 1.5, DV -0.5). The top row shows low-exposure images to see the virus injection site. The bottom row shows high-exposure images to see the axonal sprouting in the contralateral cortex. The boxed area is magnified in the inset. A') The cartoon shows the schematic location of the contralateral callosal projections (green). In transparency (pink), the ipsilateral connections shown in (B) are labeled. The dashed line indicates the rostrocaudal level of the section. B) Another tracing techniques using BDA is shown here. The injection coordinate was in the ipsilateral prefrontal cortex to target axonal sprouting from the right forelimb to the right hindlimb motor cortex (bregma: AP 1.6, LM 1.6, DV -0.5). B') The cartoon shows the location of the ipsilateral cortico-cortical connections (red). In transparency (green), the contralateral connections shown in (A) are labeled. The dashed line indicates the rostrocaudal level of the section. Scale bar in (A, B), 1mm; scale bar in the inset in (A), 100μm.

Cortical controlled damage in young mice.

To induce the CCD, we performed a mechanical injury targeting the left hindlimb region. Briefly, using a motorized stereotactic apparatus, we performed a craniotomy, and we introduced a metal rod into the right primary motor cortex, traversing the cortex (**Figure 17**). This mechanical procedure was fast, simple, and with a minimal mortality rate (0 of 11 mice). One week after CCD, the brains were collected and processed into floating coronal sections, equidistantly distributed in the series. This sample distribution allows a 3D reconstruction of the brain, a refine tool to identify the location of the injury along the AP axis (**Figure 17B**). Using DAPI labeling, we could easily quantify the injury volume by measuring the injury area of affected slices of only one serie (**Figure 17A**), which greatly simplifies the analysis and reduces the sample size to obtain a robust result, compared to typical TTC staining used for this purpose (Li et al., 2020; Wu et al., 2021; Zhang et al., 2019). For further details on the stereological measurements, please refer to the Materials and Methods sections of this dissertation (*Stereological measurements*).

In young mice, the average volume of the CCD was 1.26 ± 0.13 mm^3 (**Figure 17C**). Overall, the CCD model procedure did not require extensive training, it was cost-effective and provoked a focal and highly reproducible lesion compared to other models. Having obtained satisfactory results in young mice, we next-tested the consistency of this model in aged animals.

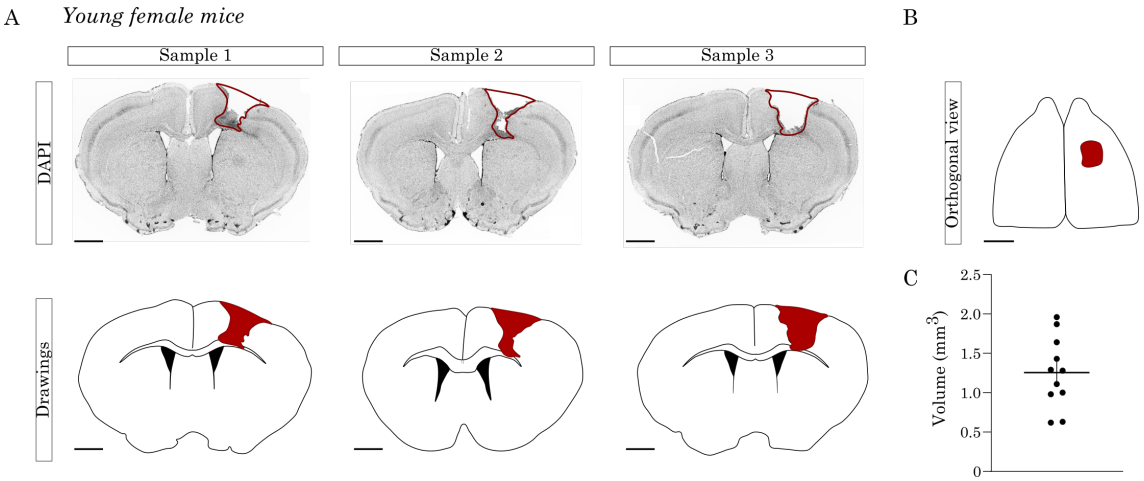

Figure 17. CCD in young mice. A) In the top row, representative images of the CCD injury in three different animals. In the bottom row, the drawings represent the same slices presented above. The area of the lesion is highlighted as a red line above and as a red area below. Scale bar, 1 mm. B) The serial organization of the slices allows to provide an orthogonal view of the injury. Scale bar, 1 mm. C) Graph shows quantification of injury volume in young mice. Graph shows mean ± SEM; n=11 mice.

Tracing cortico-cortical projections and inducing cortical controlled damage in aged mice.

Brain damage is the leading cause of permanent disability, particularly relevant to the elderly (Canazza et al., 2014; Fluri et al., 2015; Joy et al., 2019; Ma et al., 2014). Because plasticity is reduced over time and limited in aged populations, it is critical to understand histologic changes following brain damage in the elderly population. To address this objective, we characterized our CCD model in aged mice (9-13 months).

The scheme of the experimental design is shown in **Figure 18A**. Briefly, 3 weeks prior to injury we performed the tracing of callosal projections in the left (contralesional) primary motor cortex injecting an AAV vector expressing GFP under the human Synapsin promoter to specifically target neuronal cells. Mechanical injury was then induced in the right primary motor cortex as described above. Of note, it is critical to perform the injury in parallel with the viral injection, especially for the analysis of cortical rewiring. To study functional motor outcome after CCD, we performed a battery of behavioral tests 2 days before, 2 and 7 days after the lesion. Finally, the brains were collected and processed in serial sections for further histologic processing.

The quantification showed that the volume and the consistency of the CCD technique were similar to those obtained in young mice (**Figure 18B-C**). Again, the data show that the CCD lesion is highly reproducible compared to other BI models (Fluri et al., 2015; Joy & Carmichael, 2020; Xiong et al., 2013). Notably, we did not observe any mortality in this experimental batch despite the age of the mice (0 deaths out of 11 mice). Overall, the proposed methodology combining tracing and CCD provides an effective tool to investigate cortico-cortical connectivity upon brain damage.

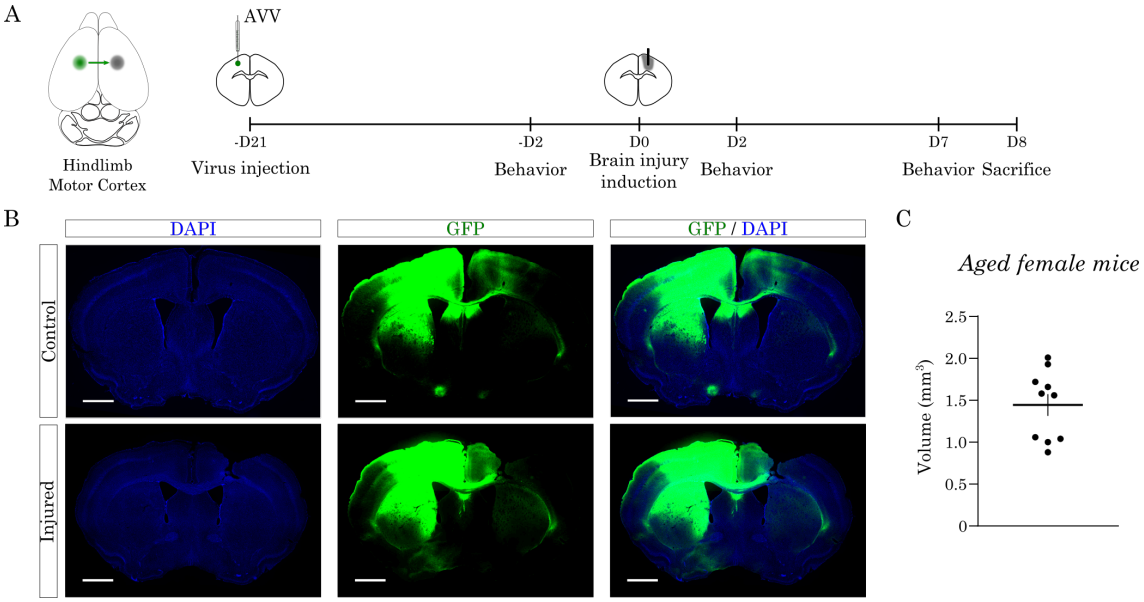

Figure 18. Tracing contralateral cortical projections and CCD in aged mice. A) On the right, the cartoon shows the GFP tracing in shown green while the location of the injury is shown in gray. The scheme shows the pipeline of the experimental approach used to characterize of CCD model in aged animals. B) Representative images of control and injured brains, combined with the GFP tracing. Scale bar, 1mm. C) Graph shows injury volume quantification in aged mice. Mean ± SEM. n=10.

Functional characterization: CCD model produces motor impairment in aged mice.

Another challenge in developing the CCD model was to provide measurable motor deficits in injured mice. Considering the small and focal impact of the injury, the mice did not exhibit significant motor impairments upon CCD in standard housing conditions, as observed in other injury models. Therefore, we performed a battery of behavioral tests to determine which tasks could provide a simple, sensitive, and reproducible functional readout. Regarding injury size and localization, we predicted that the CCD would provoke a subtle motor dysfunction, primarily in the left hindlimb of affected mice.

First, we analyzed the behavioral test 2 days before CCD, to define the basal state of the mice. Considering that the abrupt motor impairment is detected along the first week after injury (Joy et al., 2019; Nudo, 2013; Talhada et al., 2019), we performed a battery of tests 2 days (D2) and 7 days (D7) after CCD. In the treadmill test, mice are forced to run on a moving strip and filmed for a couple of minutes. This assay gives a general readout in terms of body symmetry and coordination. We found a slight imbalance at D2 in the injured group. This deficit was recovered by D7 (**Figure 19A**).

Next, we assessed motor dysfunction upon CCD in the ladder test. We used narrow- and wide-spaced horizontal ladders to further challenge the animals' walking ability. On the narrow-spaced ladder, the mice walk at a normal pace. The wide-spaced ladder forces the mice to

stretch their stride to reach the next step of the ladder. The narrow-spaced ladder showed that injured mice performed worst at D2 but recovered to pre-injury levels by D7 (**Figure 19B**). Conversely, in the wide-spaced ladder, the mice with CCD showed obvious deficits both D2 and D7 (**Figure 19C**). Overall, both ladder tests were simple and reproducible. Increasing the spacing of the ladder was sufficient to improve the sensitivity of the test and reveal the deficits related to the focal injury of CCD.

To gain expertise in functional motor characterization of focal cortical damage, I carried out a short stay at the Laboratory of Experimental Brain Research (BMC, Lund University, Sweden) under the supervision of Dr Karsten Ruscher. During this period, I learned different behavioral tests and analyses to detect motor impairment after phototrombosis, an experimental model of focal ischemic stroke which induced an injury dimension likely to that obtained by CCD, but with higher variability. After testing different behavioral tasks, the rotating pole test (RPT) was the most sensible and suitable one for our objective. Since the CCD model provokes an asymmetric lesion on the right motor cortex, the RPT is an effective asymmetric assay used in the sensorimotor characterization of stroke models (Talhada et al., 2019). Changing the direction and speed of the rotation allows specific motor characterization in unilateral lesions. Due to these advantages, we manually designed and fabricated our homemade rotating pole device with the help and support of Jesús Raimundo, from the Maintenance Department in CIPF.

Therefore, we used the RPT to test the behavioral motor impairment in injured animals. We used a fixed speed of 3 revolutions per minute (rpm), which was already challenging for aged mice. This assay was precise enough to show motor dysfunction at both D2 and D7 upon CCD (**Figure 19D**). As expected, the mice performed better when the pole rotated to the right (counterclockwise), as the dysfunction of the affected left hindlimb (LH) is being compensated by the rotation. Altogether, the RPT was a particularly useful tool to study functional motor outcome in the CCD both in terms of sensitivity and simplicity.

Finally, we used the Catwalk XT technology, which is largely used to test motor phenotypes in different animal models (Bärmann et al., 2021; Walter et al., 2020). This technology offers an automated gait analysis system that extracts multiple parameters related to paw placement or dynamics. For simplicity, here we provide data from four parameters where we found relevant motor impairment induced by CCD (**Figure 19E**). The results show that the max contact and print area of the LH decrease at D2 and D7 upon CCD induction. Furthermore, the swing and body speed decreased at D2. Nevertheless, the animals recovered from this impairment at D7 (**Figure 19E**).

In conclusion, focal CCD provoked a subtle motor deficit that did not overtly affect basic motor functions such as body coordination or normal walking ability. Nonetheless, the CCD impaired

the motor performance, particularly of the LH, in more demanding and sensitive experimental paradigms such as the wide-spaced ladder, RPT, and paw print area analysis.

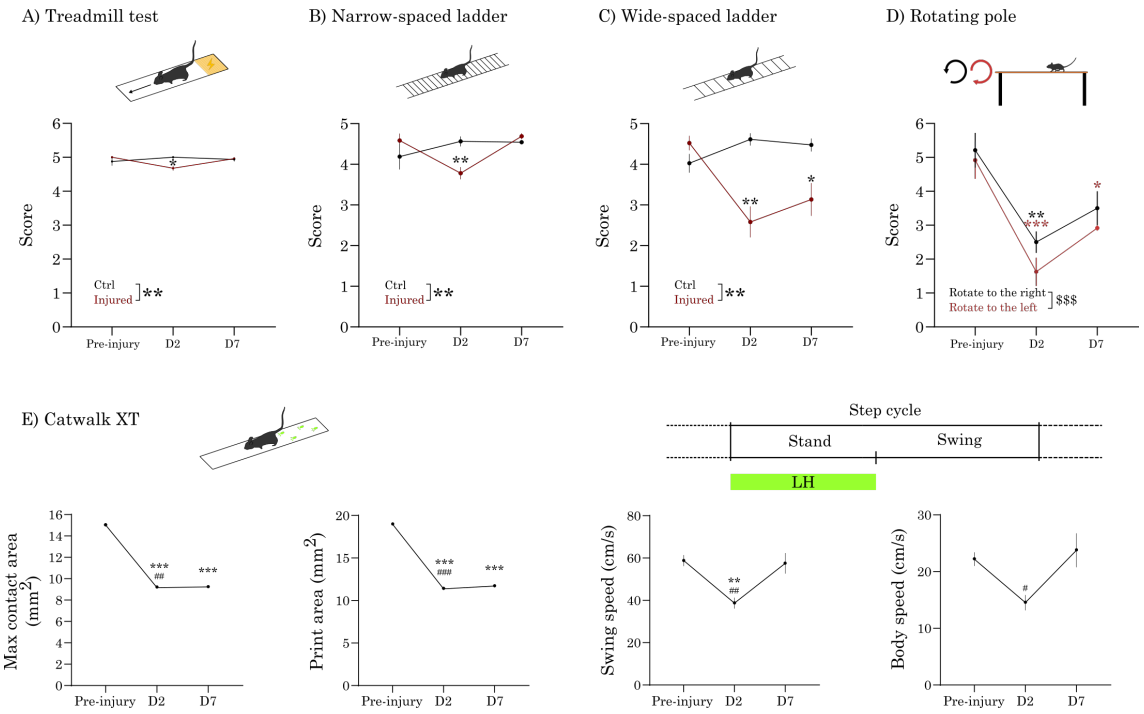

Figure 19. Motor characterization of CCD model in aged mice. A-C) The graphs show the scores of control and injured animals in the multiple assays. The motor tests were performed at three different time points: pre-injury (D-2), at 2 days (D2) and at 7 days (7D) after injury. (A) Treadmill test (B) Narrow-spaced (C) and wide-spaced horizontal ladder. Control, n=4; injured, n=7 mice. Mean ± SEM. *p ≤ 0.05, **p ≤ 0.01, two-way ANOVA with repeated measurements and Sídák's multiple comparison test. Note that the meaning of the * symbol in the lower part of the graphs refers to a statistical interaction between time point and group variables. (D) The graph shows the score of control and CCD mice in the rotating pole test (RPT), using two different rotation modes: rotation to the right (counterclockwise, black line) and to the left (clockwise, red line). n=4 mice. Mean ± SEM. *p ≤ 0.05, **p ≤ 0.01, ***p ≤ 0.001, relative to pre-njury. Two-way ANOVA with repeated measurements and Dunnett's multiple comparison test. Note that the meaning of *$* symbol in the lower part of the graph refers to a statistical difference within the time-point variable in both rotation modes. (E) The graphs show the results of the analysis of the left hindlimb (LH) in four parameters measured in the Catwalk XT software: max contact area and print area (mm^2), swing speed and body speed (cm/s). n=4 mice. Mean ± SEM. **p ≤ 0.01, ***p ≤ 0.001 relative to pre-injury; #p ≤ 0.05, ##p ≤ 0.01, ###p ≤ 0.001 relative to D7. One-way ANOVA and Holm-Sídák's multiple comparison test.

Bioinformatic pipeline of tissue processing and stereological analysis.

To perform the stereological analysis, we developed a bioinformatics workflow to semi-automatically perform tissue reconstruction with a multiplex approach combining different immunostaining from the same mice in different series (**Figure 20**).

Briefly, the brains were cut in series and processed in floating sections. All sections within a series are equidistant from each other to facilitate three-dimensional reconstruction. The

mounted sections were scanned with the Aperio Versa scanner to obtain a complete image of the slide. The images were opened in ImageJ to create the preliminary stacks (**Figure 20A**). To process the stacks, we designed a semi-automated workflow that is divided into two different steps: sorting and alignment.

First, in collaboration with José Saborit from the Biomedical Imaging department in CIPF-FISABIO, we developed an automatic algorithm in Python to sort the sections along the anteroposterior axis. In short, we manually thresholded the images in the DAPI channel. Next, the algorithm processes the images and calculates the area of the contour of the sections. Note that the contour step is important to compensate for the lack of tissue in the damaged area. Finally, the sections are automatically sorted in the stack under the assumption that the area of the contour increases along the anterior-posterior axis (**Figure 20B**; *Supplementary Material S3*). Incidentally, this assumption is valid up to bregma -2.0. It follows that this algorithm worked nicely (~95% accuracy) in our region of interest, which extends from bregma 2.5 mm to -1 mm, but it would not be effective for regions more caudal than bregma -2.0.

Our next challenge was to automatically register/align the sections. Different algorithms have been previously developed for this purpose such as the ImageJ plugin bUnwarpJ or AMaSiNe (Song et al., 2020) which rely on elastic deformation of the images. In our experience, elastic image deformation worked very well for intact brain sections. However, the elastic transformation of injured brain sections often resulted in unsound artefacts that undermined the effectiveness of these approaches for our purposes (*not shown*).

Therefore, we wrote an algorithm in IJ1 macro ImageJ code which is based on "Align image by line ROI" plugin written by Johannes Schindelin (https://imagej.net/plugins/align-image-by-line-roi). This algorithm improves the usability of the original plugin, and it requires only minimal manual assistance to draw a reference line in each slice. It then takes advantage of a quadratic transformation to register the sections (**Figure 20C**; original code in *Supplementary Material S4*).

Overall, this semi-automated workflow is an effective tool for correctly sorting and aligning brain sections for stereological quantification. Once the series are registered, multiple series and immunolabeling can be combined for multiplexed analysis of the callosal connections and of the brain injury, as we show in **Figure 21** and **Figure 22**.

A typical experimental paradigm may entail cutting up to 8 series of sections (e.g., 40 µm thick) from one brain. Since the DAPI channel is always used as a reference for the registration, we can theoretically combine up to 3 different labelings per series in a standard microscope with green, red and far-red channels available. Notably, this approach allows reducing the number of animals utilized by combining different immunolabelings from the same brains.

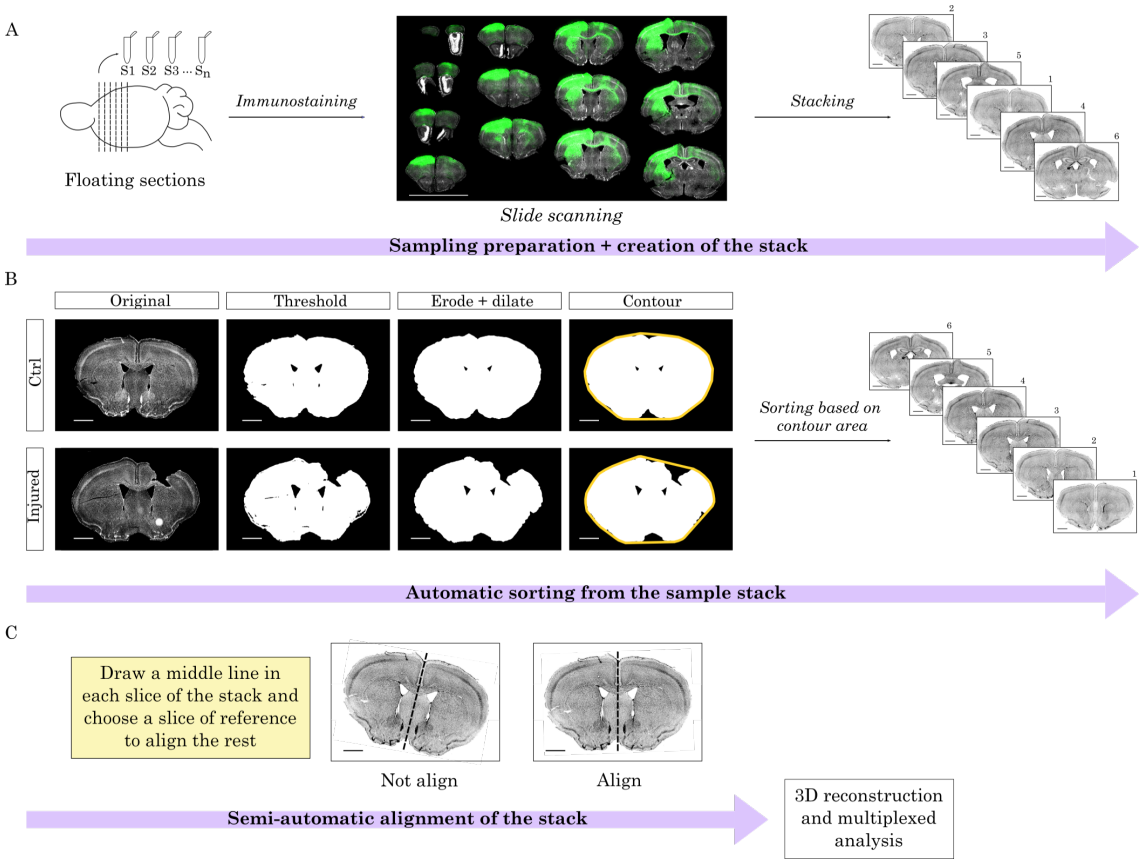

Figure 20. Bioinformatic pipeline of tissue processing and stereological analysis. A) Steps of the workflow from tissue processing to image stacking. Briefly, the brains are processed in serial floating sections. The pictures of the immuno-labeled slides are taken with an automated slide scanner. Using ImageJ, the images of separated slices are grouped into a stack. B) Sample sorting and registration procedure using a code developed in Python. From DAPI staining images, a threshold is manually established to cover all the slice area. Then, the algorithm smooths tissue edges and calculates the contour area of each slice (yellow line). The area value determines the sorting along the anteroposterior axis for each section. C) Tracing manually a reference line in all the slices of the stack and automatic alignment of the stack by ImageJ macro.

Tissue damage and inflammatory response in aged mice.

As a first application of this workflow, we combined the volumetric quantification of the CCD injury with the analysis of the inflammation in the PL. Brain damage results in an inflammatory response that entails the activation of microglia and macrophages infiltrated due to blood barrier disruption. Iba1 is commonly used as a marker to label active microglia in the inflammatory environment. Microglia/macrophages contribute to debris clearance in brain injury (Anrather & Iadecola, 2016; Taylor & Sansing, 2013; Xiong et al., 2013). Furthermore, brain injury and blood-brain barrier leakage induce neuronal tissue permeability, which can be observed using IgG staining as a proxy (Ekmark-Lewén et al., 2013; Hoshino et al., 1996; Nogami et al., 1999). Here, we combined IgG and Iba1 staining to evaluate tissue damage upon CCD.

As expected, the injured samples showed a greater intensity in both markers compared to the control group in the PL. To visualize the distribution of tissue damage and neuroinflammation in

injured brains, IgG and Iba1^{+} areas were measured in each slice and plotted in a Cartesian coordinate system (**Figure 21C**). The curve shows that tissue damage and microglia/macrophage population are localized near the injured area upon CCD, without spreading along the anteroposterior axis. The volume of each staining was calculated by integrating each polynomial fitting equation of the areas calculated in the sections (**Figure 21D**, see Material and methods section: *Stereological measurements*).

Interestingly, the patterns of Iba1 and IgG-positive regions were similar but not completely overlapping (**Figure 21A, B, C**). For instance, we often found more intense Iba1 labeling near areas where we observed the presence of retracting bulbs of injured callosal neurons (labeled with yellow arrows in **Figure 21B**). We speculate that this may suggest that microglial cells may be involved in clearing cell debris upon axonal degeneration in these areas.

Altogether, this analysis indicates that CCD results in a focal and localized injury, causing tissue damage and inflammatory response that is relatively confined to the core region.

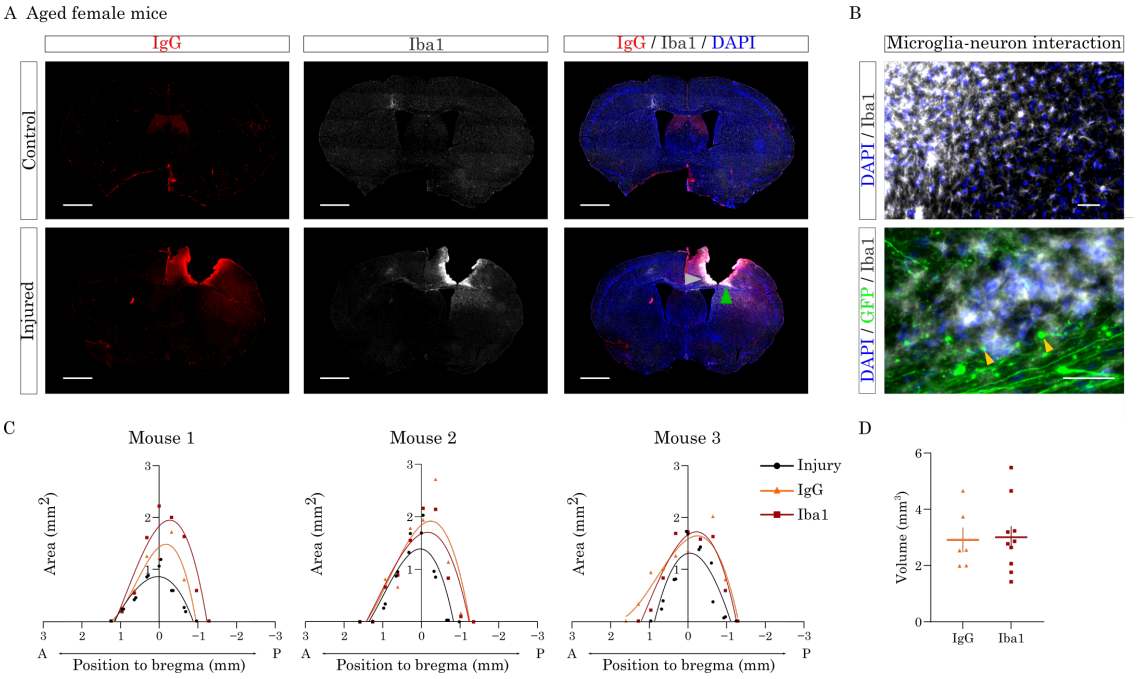

Figure 21. Tissue damage and neuroinflammation in aged mice upon CCD. A) Representative images of control and injured animals labeled for IgG and Iba1 markers after CCD. Gray arrowhead, upper panel in (B). Green arrowhead, lower panel in (B). Scale bar, 1mm. B) Magnified areas from an injured sample are represented to show Iba1 and GFP staining in detail (indicated in merged slice with grey and green arrows). Scale bar, 50µm. C) Cartesian plots represent data of injury (black), IgG (orange) and Iba1 (red) staining areas from three different animals, positioned relative to bregma coordinates. D) Graph shows the volume quantification of IgG and Iba1 labeling in the injured mice. IgG, n=6 animals; Iba1, n=10 animals. Mean ± SEM.

Perineuronal nets are affected in the perilesional area upon CCD.

To further characterize the cellular alterations provoked by CCD in the perilesion, we investigated the remodeling of the PNNs. PNNs are a specialized form of extracellular matrix that specifically enwraps PV interneurons (**Figure 22**). It has been shown previously that, upon CNS injury, PNNs are decreased in the areas surrounding the lesion. This decrease appeared to be variable depending on the model and the methods used for quantification (Alia et al., 2016; Hsieh et al., 2017; Kim et al., 2017; Madinier et al., 2014; Quattromani et al., 2018; Sammali et al., 2017). It is noteworthy that most of these studies simply define the PL as the area physically close to the injury and do not take advantage of other markers to define the PLs more precisely. In addition, macrophages have been previously implicated in extracellular matrix degradation in a different cellular context such as tumor and wound healing (Kim & Nair, 2019; Murray & Wynn, 2011).

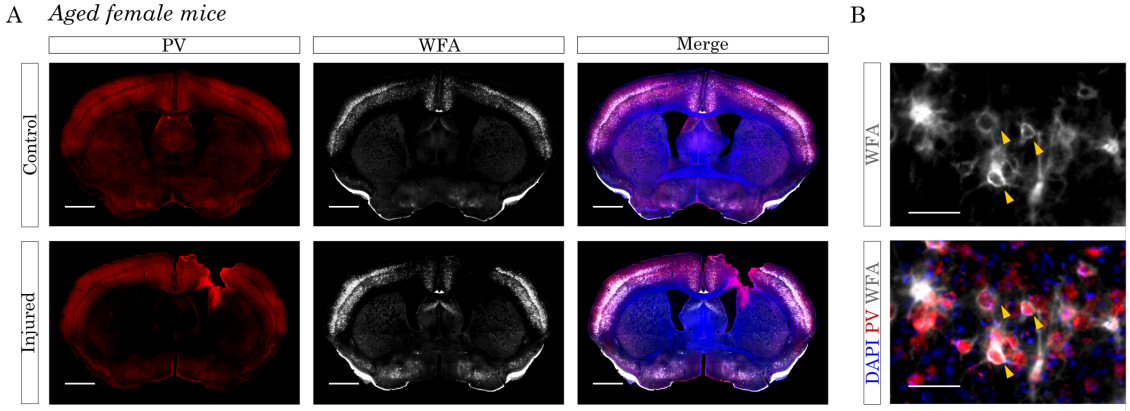

Figure 22. WFA$^+$ PNNs surrounded PV$^+$ interneurons. A) Representative images of PV and WFA staining in control and injured mice. Scale bar, 1mm. B) Magnified areas from an injured sample are represented to show PV and WFA staining in detail. Yellow arrows indicate the co-localization of PV$^+$ interneurons and WFA$^+$ PNNs. Scale bar, 50µm.

To study the plasticity of PNNs upon CCD, we performed labeling with the PNNs marker using Wisteria Floribunda Agglutinin (WFA) staining in control and injured mice (**Figure 23A**). As expected, we observed a reduction in WFA labeling upon CCD in the PL. Interestingly, we serendipitously noticed that this reduction in WFA staining mostly overlapped with regions of activated microglia in the series labeled for Iba1. Therefore, to quantify the WFA decrease in the PL we combined the information from the two series. We took advantage of the Iba1-labeled series (**Figure 21**) to define Iba1-positive (Iba1$^+$) and Iba1-negative (Iba1$^-$) regions in the PLs (**Figure 23B**). Next, we quantified the number of WFA positive cells (WFA$^+$) in Iba1$^+$ and Iba1$^-$ PLs in the WFA-labeled series. Because WFA staining is dependent on the specific cortical region, we used the contralateral (not injured) mirror regions of the cortex as an internal control to quantify the decrease in the number of WFA$^+$ cells in Iba1$^+$ and Iba1$^-$ PLs (**Figure 23C**).

Taken together, this analysis further supports the evidence that PNNs in the PL are remodeled upon injury. In addition, it suggests that Iba1^{+} cells may be involved in the degradation of PNNs.

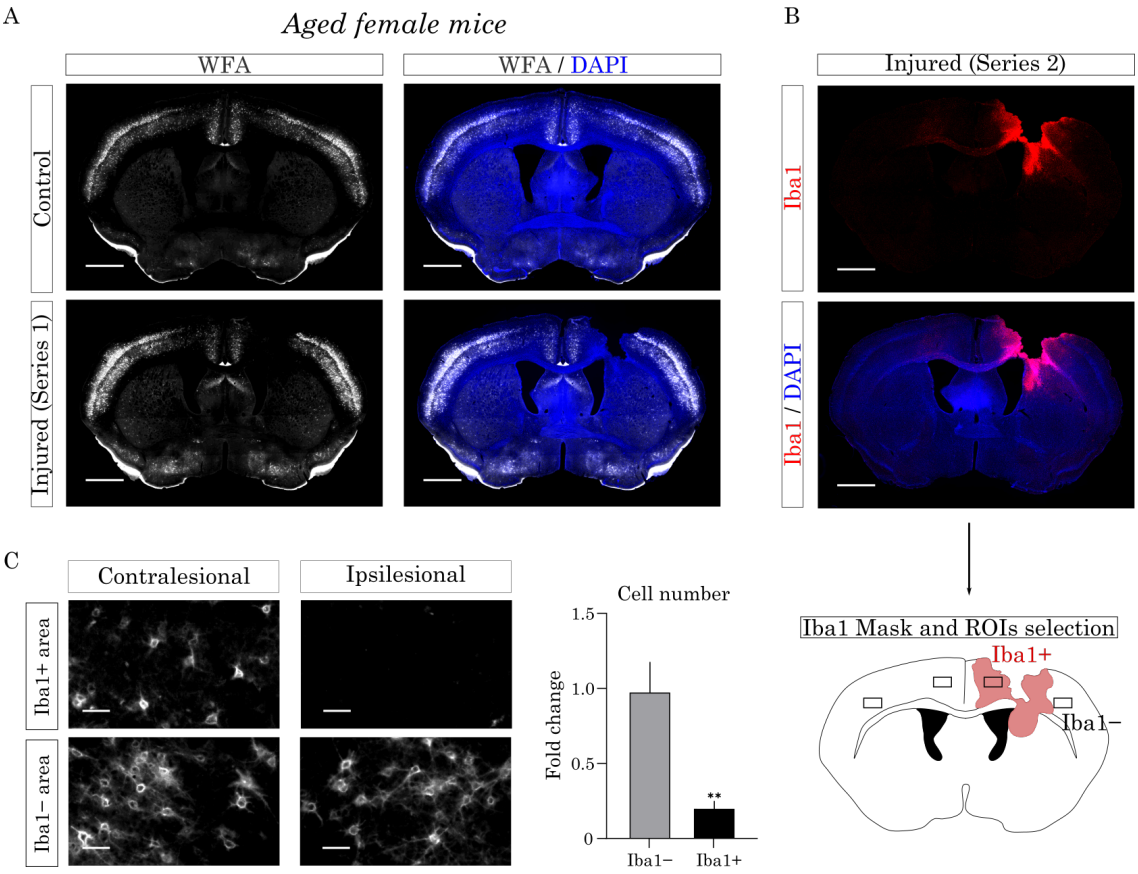

Figure 23. PNNs were affected in the PL area in aged mice upon CCD. A) Representative images of WFA staining in control and injured mice. B) Representative images of the Iba1 staining from another series of the same injured animal presented in (A). C) Representative images of the ROIs corresponding to the boxed areas in the cartoon showing the reduction of WFA labeling in the perilesional area. The graph shows the fold change in cell number in both Iba1^{+} and Iba1^{-} perilesions compared to contralesional area. n=12 slices. Mean ± SEM. ** $p \leq 0.01$. Paired t-test.

DISCUSSION

Although great progress has been made in understading the pathological events upon brain damage, effective treatment is still lacking. Since brain damage is a heterogeneous disorder in humans, so different animal models have been proposed to recapitulate different physiopathological events, mainly focusing on promoting neuronal survival upon damage. However, there are not many effective animal models available in the literature to explore axonal regeneration and cortical rewiring. Here, we offered a novel *in vivo* model which combines tracing techniques with the induction of a focal cortical injury, allowing a multiplex analysis of callosal projections upon brain damage.

Depending on the research goal, choosing a specific animal model can offer advantages and limitations (Mergenthaler & Meisel, 2012). The most well characterized model in the field of stroke is the MCAO, which recapitulates ischemic conditions and lack of blood supply to the brain (Fluri et al., 2015; Shyu et al., 2004; Zhang et al., 2018). However, it requires complex surgical procedures that result in large injuries affecting different brain regions and increase biological variability and animal mortality rate. Furthermore, the injury volume provided by this model complicates the study of plasticity or cortical rewiring events after damage. Several models have been proposed to mimic traumatic brain injury, such as blast waves, crush, or penetration by a projectile. However, the scene is likely to what has been discussed previously, where specific devices are required, provoking big injuries that are difficult to reproduce and higher animal mortality rate (Xiong et al., 2013).

In the search for a focal injury model, there are different possibilities to induce stroke, such as stereotactic injections of collagenase or phototrombosis, offering a more precise protocol to specifically target local cortical regions (Sommer, 2017; Uzdensky, 2018). Nevertheless, in our experience, these strategies also can offer relatively variability. This fact is directly translated into an increase in the number of animals required, which is both time-consuming and contrary to emerging ethical trends in animal welfare.

Our long-term goal was to offer an *in vivo* model to elucidate molecular and structural mechanisms underlying cortical regeneration upon brain injury. As part of this work, we strived to induce a focal and restricted injury in the right motor cortex, while still causing a motor impairment detectable in the injured animals. Inspired by the stab wound lesion protocol proposed by Professor Götz's Lab (Buffo et al., 2008; Mattugini et al., 2019), we reasoned to perform a mechanical injury guided by stereotactic techniques because it will become a simple, reproducible, and cost-effective protocol to selectively target the brain region of interest. Furthermore, the use of a motorized stereotactic devices significantly increases the reproducibility between samples and produces a minimal mortality rate (0 out of 22 mice).

Overall, we obtained an injury protocol that affects a restricted cortical region to enable stereological quantifications to analyze the impact of the injury and inflammatory response, collated a functional motor outcome read out.

The second challenge we faced in developing of the model was the behavioral characterization of the motor deficits provoked by the CCD in the hindlimb motor cortex. Unlike other injury models, focal injuries produce small deficits that are undetectable under standard housing conditions, likely to the case here. We therefore performed a battery of behavioral assays of varying difficulty. We failed to observe any major alterations using the treadmill test or the narrow-spaced ladder, confirming that the impact of the injury is relatively minor. However, more sensitive tests such as the wide-spaced ladder, the Catwalk and the rotating pole offer a functional read out in the CCD model. Specially, we noticed that both the wide-spaced ladder and the rotative pole test constitute the most effective test. Accordingly, we have chosen them for future functional characterization to study the role of Nrg1 upon CCD in the next chapters of this dissertation.

Noteworthy, the rotating pole test is ideal for unilateral focal injuries, as the one we performed for the CCD model (González-Manteiga et al., 2022; Talhada et al., 2019). In detail, this test can be used in both static and rotational modes, allowing asymmetric testing of locomotion and somatosensory balance by reversing the rotation of the pole. Compared to other motor platforms, such as the Catwalk, the equipment needed to build the rotating pole is affordable and the analysis is not very time consuming. Therefore, we concluded that the CCD model offers the possibility of obtaining a small cortical damage that provokes detectable motor impairments in the animals.

Importantly, while focal injury models are more realistic to the clinical manifestations in injured patients, the procedure used to induce mechanical injury in the CCD model does not mimic a common cause of brain damage from a clinical perspective. In this sense, the model does not necessarily display some molecular and cellular clinical hallmarks, such as cerebral edema, ischemia or hemorrhage, or tissue deformation due to the impact of external mechanical force (Xiong, Mahmood, and Chopp 2013). This limitation is seen in most of the experimental models of brain damage, where the complexity and heterogeneity of this disorder in human patients also depends on biological variables such as sex, age, or associated comorbidities (Mergenthaler & Meisel, 2012; Sommer, 2017). In our case, we were fully aware of this weakness in order to provide a simple but robust and reproducible preclinical protocol of focal cortical injury to better study cellular and structural changes in the PL area.

Another important aspect of the methodology was to develop a flexible workflow to obtain as much information as possible from the same samples. Therefore, we selected the strategy of

serial sections combined with a semi-automated bioinformatics pipeline to sort and align the brain samples. Using this approach, we addressed stereological measurements to quantify injury volume, neuroinflammatory response using Iba1 staining as a marker for microglia and macrophages, and tissue permeability using IgG labeling as a proxy (Hoshino et al., 1996; Nogami et al., 1999). Concurrently, the same serial sections were also labeled for GFP to detect callosal projections and for WFA to study PNNs integrity upon CCD. As an example, we have shown some representative images in which the retracting bulbs in the PL area of the targeted callosal projections are clearly visible. For future studies, it is interesting to explore the restoration of cortical plasticity upon CCD by using different synaptic markers in this novel protocol. Overall, this evidence suggest that the methodology proposed offer a multiplex analysis to investigate different histological changes using the same samples, contributing to the 3Rs statement of experimental animal welfare practices.

Lastly, we examined the integrity of PNNs in the PL upon CCD. PNNs are a specialized extracellular matrix that envelop specific subtypes of cortical interneurons, such as PV^+ inhibitory neurons. However, the role of PNNs is poorly understood. Different studies have shown that the formation of PNNs in cortical interneuron counter-correlated with neuronal plasticity during development (Devienne et al., 2021; Wang & Fawcett, 2012). Interestingly, enzymatic degradation of PNNs reactivates plasticity in mature neurons and could enhance functional recovery in some CNS injury models. Moreover, the loss of PNNs in the PL upon brain damage has been previously described using different methodologies, with a variability of between 25% and 60% of decrease compared to control conditions (Alia et al., 2016; Hsieh et al., 2017; Kim et al., 2017; Madinier et al., 2014; Quattromani et al., 2018; Sammali et al., 2017). Notably, to the best of our knowledge, most of the studies delineated the PL as the area closer to the core of the lesion.

Here, we analyzed the presence of PNNs in different serial sections using WFA labeling. Since PNNs generally surround PV^+ interneurons, the specificity of the staining was also confirmed by colabeling with PV staining shown in **Figure 22**. To bound the PL area, we reused the same series for the inflammatory response analysis to define the Iba1 positive and negative regions. Interestingly, we found that WFA staining was robustly reduced in $Iba1^+$ PL (~80% reduction as compared to the control). Of note, the WFA labeling was barely detectable in $Iba1^+$ areas in some samples. Conversely, WFA labeling was scarcely affected in $Iba1^-$ PL areas. We speculate that this counter-correlation between Iba1 and WFA may indicate that activated microglia may directly contribute to the degradation of the PNNs. Indeed, it has been shown in other cellular contexts that innate immune cells such as monocytes and macrophages produce enzymes that degrade the extracellular matrix including MMP9 (Fani Maleki & Rivest, 2019; Gong et al., 2008).

In conclusion, our results show that PNNs are particularly affected in the PL areas, suggesting a remodeling of PNNs by microglial activation upon CCD.

Overall, our CCD model provides a powerful and effective methodology to further elucidate plasticity and tissue repair in the context of brain damage. This workflow allows to carry out 3D reconstruction and combination of different immunolabeling to investigate different cellular and subcellular mechanisms underlying the process of regeneration and plasticity in the perilesional area. We hope this protocol can be exploited in future studies to address the complexity of brain damage and the interaction of different cell types in this paradigm.

CHAPTER 3: NRG1 SIGNALING IS NEUROPROTECTIVE UPON BRAIN DAMAGE

GRAPHICAL ABSTRACT

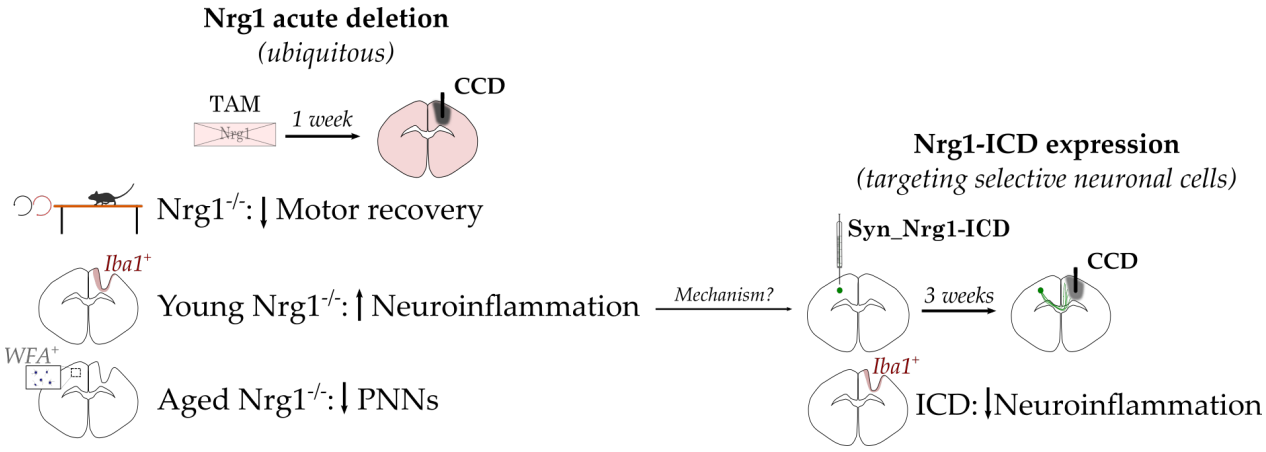

Highlights:

- Nrg1 deletion reduced functional motor recovery in young and aged female mice.
- Nrg1 deletion produced a subtle increase in the inflammatory response in young female mice.
- Activation of Nrg1 intracellular signaling decreased microglia/macrophage response.
- Nrg1 deletion prompted remodeling of PNNs in the contralesional cortex of aged female mice.

INTRODUCTION

Brain damage is considered the principal cause of adult disabilities, becoming a socioeconomic burden that affects patients' quality of life. During brain damage, diverse molecular, cellular, and functional events take place that constitute a complex and heterogeneous disorder. To highlight some important events, this process is characterized by an immediate increase in excitotoxicity and neuronal loss, followed by the release of inflammatory and oxidative stress insults, that hamper neuronal integrity and thus impair brain rewiring (Galgano et al., 2017; Joy & Carmichael, 2021; Moskowitz et al., 2010). Thus, relentless efforts have been conducted to find molecular targets that enhance neuroprotection upon injury. However, an effective therapeutic treatment is not yet available.

Nrg1 is the best characterized member of an extensive family of growth factors, involved in crucial functions for cortical development, such as neuronal migration, neurite outgrowth, axon myelination and ensheathment and formation of excitatory and inhibitory synapses, among others (Mei & Nave, 2014; Mei & Xiong, 2008). It has been mainly implicated in different psychiatric disorders, such as schizophrenia, autism, or depression. However, in the last decades, it has been also proposed as an emerging neuroprotective factor in CNS injury (Kataria et al., 2019; LWu et al., 2015).

To investigate the neuroprotective role of Nrg1/ErbB4 signaling in CNS damage, several works have been performed in rodent models by administering rhNrg1 after injury. In this sense, Nrg1 treatment enhanced functional motor recovery in MCAO and TBI models (Deng et al., 2019a; Gu et al., 2017; Iaci et al., 2016; Shyu et al., 2004). Using TTC staining, which is commonly used to easily assess tissue integrity, it has been widely described that Nrg1 treatment reduces injury volume, suggesting that Nrg1/ErbB signaling promotes tissue preservation (Guo et al., 2006; Li et al., 2007; Noll et al., 2019; Shyu et al., 2004; Zhang et al., 2018). Additionally, a body of work has also reported that Nrg1 prevents from neuronal death in *in vitro* and *in vivo* by regulating GABAergic transmission (Deng et al., 2019; Guan et al., 2015) and various signaling pathways involved in cell survival, including ERK5-dependent MAPK, PI3K/Akt and Bcl-2/Bax pathways (Gu et al., 2017; Guo et al., 2010).

Another important aspect of preventing neuronal loss is the regulation of an adequate inflammatory response. Reactive astrocytes, microglia and the infiltration of peripheral immune cells trigger a complex cellular response to remove cellular debris and damaged tissue, thereby restoring circuit rewiring. However, an exacerbated inflammatory response may lead to a greater neuronal loss and a massive release of inhibitory compounds, impairing axonal regeneration and thus cortical rewiring (Anrather & Iadecola, 2016). In this context, Nrg1 may possibly modulate the expression of inflammatory agents by reducing pro-inflammatory

cytokines and stimulating anti-inflammatory ones (Alizadeh et al., 2017; Kataria et al., 2019; Xu et al., 2005). This evidence has been reported in different *in vitro* models, using primary cultures of astrocytes and microglia, the N9 microglial cell line and U937 monocytic cultures, where Nrg1 exposure modulates their inflammatory response (Alizadeh et al., 2017; Simmons et al., 2016; Xu et al., 2005). Furthermore, histological preparations of brain and spinal cord damaged tissue also show that Nrg1/ErbB4 signaling reduces the presence of astrocytes and microglia/macrophages in the perilesioned area, as well as the release of inflammatory insults (Alizadeh et al., 2017; Deng et al., 2019; Xu et al., 2004).

To the best of our knowledge, most of the studies recapitulate the effect of exogenous Nrg1 via ErbB signaling, by injecting Nrg1 soluble form or developing ErbB4 null animals. However, Nrg1 presents different signaling pathways that not necessarily involucrate ErbB receptors activation, such as the Nrg1 intracellular signaling, involved in gene expression modulation (Bao et al., 2003; Mei & Nave, 2014). The molecular and cellular mechanisms underlying the implication of Nrg1 intracellular signaling in neuroprotection are still unaddressed. Recent data from our lab demonstrated that hypoxic conditions stimulate the nuclear translocation of Nrg1-ICD and promotes neuronal survival both *in vitro* and *in vivo*, which can be partly mediated by the regulation of pro-apoptotic gene expression. Thus, this work suggests Nrg1 intracellular signaling as a promising molecular target in brain damage scenario (Navarro-González et al., 2019). Overall, offering novel and refined models to specifically target Nrg1 signaling is a pivotal step to better comprehend the implication of Nrg1 signaling upon brain damage.

PNNs are specialized extracellular matrix structures, made of a linear non-sulfated hyaluronic acid (HA) polymer to which different proteins adhere, such as CSPGs and lectican proteins, including aggrecan, versican, neurocan and brevican. These specific structures have been mainly implicated in limiting critical periods of plasticity and contributing to synaptic maturation. This idea is supported by several studies in which PNN digestion using chABC can reopen plasticity (Fawcett et al., 2022; Wang & Fawcett, 2012; Wen et al., 2018).

PNNs also play an intriguing role in pathological conditions, where proteolytic processing of these structures may have an impact. In the scenario of brain damage, it has been reported that the PNN integrity is compromised upon injury, which may be required for the induction of plasticity. This idea has been supported by work data in which the administration of chABC or HA inhibitors can enhance functional recovery upon SCI (Katarzyna Greda & Nowicka, 2021; R. R. Zhao et al., 2013). However, other piece of evidence suggests that PNN could be a protective matrix against oxidants and attract bioactive molecules, such as cytokines and growth factors (Bozzelli et al., 2018). Remarkably, PNNs are mainly found enwrapping fast-spiking PV interneurons, whose biological function is highly regulated by Nrg1/ErbB4 signaling (Fazzari et al., 2010; Lu et al., 2014; Mei & Nave, 2014; Navarro-Gonzalez et al., 2021).

Following brain damage, a state of cortical excitability arises, in part due to the loss of PV^+ interneurons, which are crucial regulators of excitatory/inhibitory balance (Ferguson & Gao, 2018). In a model of TBI induced in postnatal mice (P22), PV^+ interneurons were reported to be more vulnerable to the damage, compared to other subtypes of interneurons (Nichols et al., 2018). Furthermore, another study conducted in near-term fetal sheep observed a reduction in interneurons and disruption of the PNNs under hypoxic conditions (Fowke et al., 2018). Similarly, Hsieh and colleagues performed a temporal tracking of inhibitory connections after TBI, observing a transient decrease in PNN prior to the loss of PV^+ cells (Hsieh et al., 2017). So, although the role of PNN in protecting PV interneurons upon injury remains unclear, maintaining the integrity of PNN may also be necessary to regulate GABAergic cell function upon injury.

Herein, we applied a novel *in vivo* mouse model to study the role of Nrg1 signaling in neuroprotection upon CCD (González-Manteiga et al., 2022). Using a novel conditional transgenic mouse model to acutely delete Nrg1 expression prior to injury induction, we observed that Nrg1-deficient mice exhibited a subtle motor impairment and a slightly increase in the inflammatory response. As a mechanistic output, we expressed Nrg1-ICD in a selective number of cortical neruons to better ascertain whether Nrg1 intracellular singaling is involved in neuroprotection and found that Nrg1-ICD treated animals present a trend to reduce the inflammatory response. Finally, although we did not detect differences in PNNs integrity in the PL area, we observed a reduction in WFA^+ cells in $Nrg1^{-/-}$ aged mice, highlighting the relevant remodeling process that takes place in other interconnected brain regions. Taken together, our data highlight the role of Nrg1, and specifically of its intracellular pathway, as a neuroprotective factor after cortical injury, using novel mouse models that particularly target Nrg1 signaling, conversely to the experimental paradigms previously used in the literature to date.

RESULTS

Nrg1-TM1 expression is increased upon phototrombosis in aged mice.

As mentioned above, Nrg1 has been proposed as a neuroprotective factor upon brain damage in stroke and TBI models in the last decades (Deng et al., 2019; Noll et al., 2019; Xu et al., 2004, 2005). Of note, Nrg1 signaling, and specifically its intracellular pathway, has been described to be stimulated under hypoxic conditions (Navarro-González et al., 2019; Parker et al., 2002).

To gain further experience in focal experimental injury models, I did a short stay at the Laboratory for Experimental Brain Research in BMC Biomedical Center of Lund University, under the supervision of Dr Karsten Ruscher. During this internship, I learned a protocol to perform an experimental model of ischemic stroke, named phototrombosis. The principle of the model is to inject a photosensitive dye (e.g., Rose Bengal), capable of crossing the BBB, followed by exposure of the intact skull of the mice to a cold light. The light activates the compound, resulting in the formation of singlet oxygen and superoxide, which provokes endothelial damage, platelet aggregation, blood vessels occlusion, and an ischemic response in the exposed brain area (Sommer, 2017; Uzdensky, 2018).

Once I acquired sufficient experience in this procedure, we conducted a pilot study in collaboration with Dr. Ruscher to investigate Nrg1 expression after PT in aged male mice. The timeline of the experiment is showed in **Figure 24A**. Briefly, we injected 100µl of Rose Bengal intraperitoneally and waited for 5 minutes for a proper distribution of the compound. Next, we illuminated the right primary motor cortex for 20 minutes (bregma 0; medio-lateral (ML) -1.5) to simulate the experiments we were performing for the CCD characterization. For the sham group, we repeated the same surgical procedure, but injected saline solution instead of the dye. For more information on the protocol, please refer to the corresponding section in Material and Methods (*Phototrombosis*).

To study the early and mid-response upon stroke, we harvested the brain 24 hours and 7 days after the PT induction. To investigate Nrg1 expression, we dissected two different brain regions of interest: the perilesional area (ipsilesional) and the corresponding area in the contralateral cortex to the injury (contralesional) (**Figure 24A'**).

To study the expression of Nrg1 mRNA by qPCR, we focused on the primer pair Nrg1-TM1, an effective way to detect the transmembrane domain of all the different Nrg1 isoforms. We also proposed ErbB4 as another gene of interest in the study, regarding that 1) the ErbB4 receptor is the main Nrg1-specific receptor of the ErbB family and 2) Nrg1/ErbB4 canonical signaling pathway has been implicated in the neuroprotective role of Nrg1 upon injury (Guan et al., 2015; Liu et al., 2011; Mei & Xiong, 2008; Yan et al., 2017).

The data obtained from this preliminary study showed an increase in Nrg1-TM1 expression as an early and mid-response to PT, particularly detected in the contralesional cortex at D7 after the stroke (**Figure 24B**). For ErbB4 expression, there is a slight increase in the injured group (p-value=0.07), especially in the ipsilesional cortex 24 hours after the stroke induction (p-value=0.08) (**Figure 24C**).

Overall, this pilot study suggests that Nrg1 signaling may be stimulated in the focal PT model, which correlates with previous data described in other brain damage models, such as MCAO (Parker et al., 2002). Surprisingly, these data insinuate an increase in Nrg1-TM1 expression not only in the PL area, but also in the contralesional cortex. In this sense, the result could highlight the importance of studying not only the areas directly affected by the injury, but also other cortico-cortical connected regions that could contribute to this process, even in focal injuries (Chovsepian et al., 2023; Empl et al., 2022). Noteworthy, these data are very preliminary due to the small N of each experimental group (sham, N=2; PT, N=4) and further experiments are required to confirm this result.

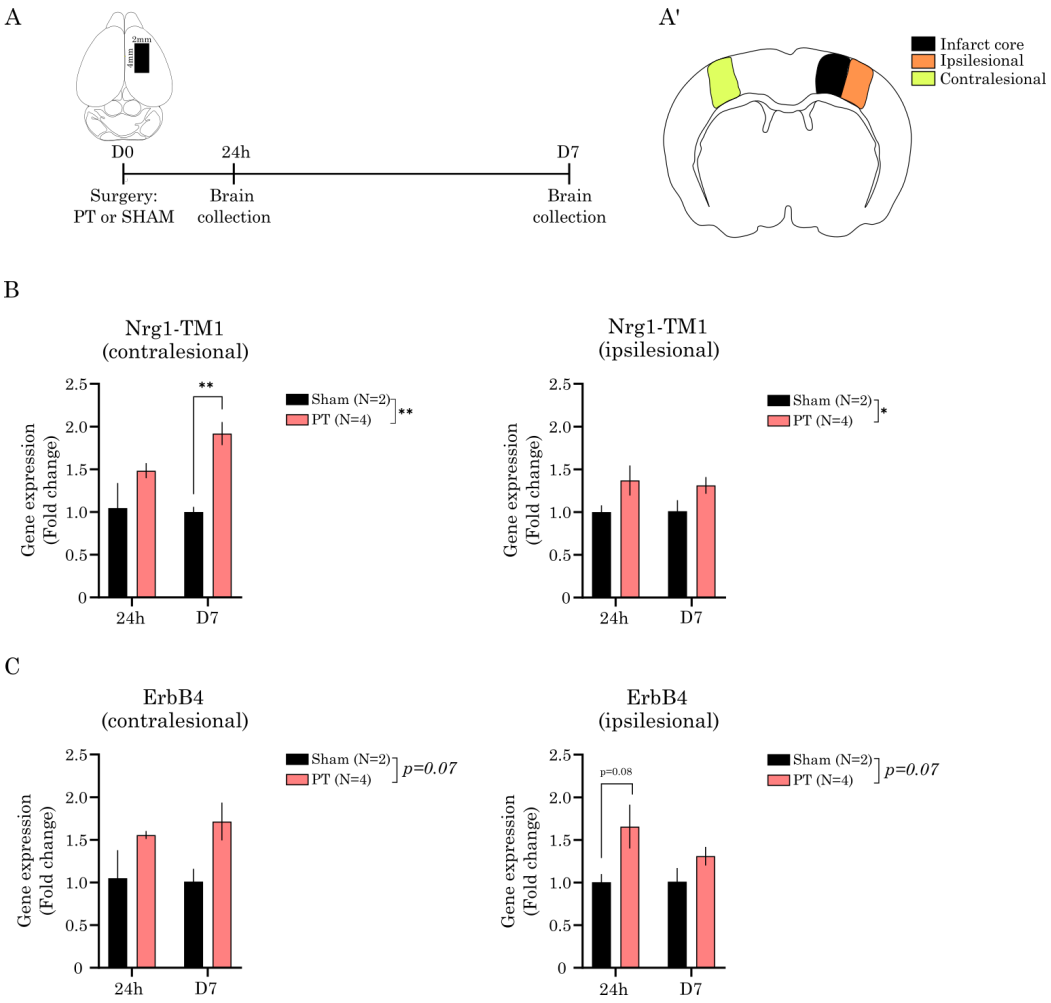

Figure 24. Evaluation of Nrg1-TM1 and ErbB4 expression in aged male mice upon PT model. A) Timeline of the experimental approach followed to analyze Nrg1 expression upon PT. Phototrombic

stroke was induced in the right primary motor cortex of male aged mice (12 months old). Brains were harvested 24 hours and 7 days after the stroke to evaluate the immediate and mid-response to cortical ischemia. A') The cartoon illustrates the selected regions of interest. Briefly, the region adjacent to the infarct core was dissected to evaluate gene expression in the ipsilesional area, while the homotopic region in the contralesional cortex was used for the analysis. B) Nrg1-TM1 expression was analyzed in the contralesional (left graph) and ipsilesional areas (right graph). Of note, Nrg1-TM1 expression is increased upon PT in both regions, but particularly 7 days post-PT in the contralesional region. C) ErbB4 expression was also analyzed, showing a tendency to increase in both ipsi- and contralesional areas of injured mice (p=0.07). Mean ± SEM. Data are normalized to sham control values. (Sham N=2 animals; PT N=4 animals). Statistical test: Mixed-effect model and Sídák's multiple comparison test. * $p \leq 0.05$, ** $p \leq 0.01$.

Nrg1 deletion deteriorated motor recovery upon CCD.

To investigate whether Nrg1 promotes functional recovery upon brain damage, we evaluated motor behavior in Nrg1 deficient young and aged mice. To this aim, we used a tamoxifen-inducible conditional transgenic mouse to generate Nrg1 knockout mice (**Figure 8**). Remarkably, in this model mice development is entirely normal because Nrg1 depletion is induced in adulthood stages, just one-week prior CCD. Compared to the models used in the literature, based on the administration of Nrg1 soluble form or ErbB4 deficient animals, this novel approach conforms an effective way to specifically study Nrg1 signaling upon brain damage.

To assess motor impairment in these animals, we chose the RPT and the WSL assays from the battery of tests described in Chapter 2 because they were the most sensible tasks to detect motor impairment (González-Manteiga et al., 2022). Of note, the animals did not present any alterations in the motor behavior before and after tamoxifen administration prior to injury induction (**Figure 8**). Therefore, the results are completely due to the functional motor recovery upon injury.

As in the description of the CCD model, we evaluated motor behavior analysis before, D2 and D7 post-injury in young and aged female mice. Although we detected a clear motor impairment using the RPT and WSL, we were unable to distinguish differences regardless of the phenotype in the wide-spaced ladder (**Figure 25C-D**). Therefore, we focused on the RPT analysis.

As expected, we detected motor impairments D2 and D7 post-injury in both young and aged groups. To further elaborate, RPT results in the young group revealed that although there were no differences between wild-type and $Nrg1^{-/-}$ mice D2 post-injury, the absence of Nrg1 induced a greater motor impairment D7 post-injury. This may suggest that both groups are equally affected after the injury, but Nrg1 depletion may impair spontaneous motor recovery as seen at D7 post-injury (**Figure 25A**).

In aged animals, the motor impairment was detected at D2 and D7 post-injury in $Nrg1^{-/-}$ mice, compared to wild-type injured animals (**Figure 25B**). Surprisingly, this motor deterioration was

strongly perceived in the static mode. Of note, although mice were trained days before the experiment and the static mode is usually the easiest task, the pre-injury scores were surprisingly under the maximum score in the aged group. This fact could be partly explained because animals started with the static mode on the day of the experiment, which supposed an additional training for the next two rotation modes. In any case, to resolve these misleading data, results are normalized to the pre-injury value for each respective mode in the column bar graphs.

Therefore, these results suggest that the absence of Nrg1 provokes motor impairment upon CCD, especially in aged animals at early stages after injury induction (D2), followed by a limited functional recovery D7 post-injury, compared to wild-type injured animals.

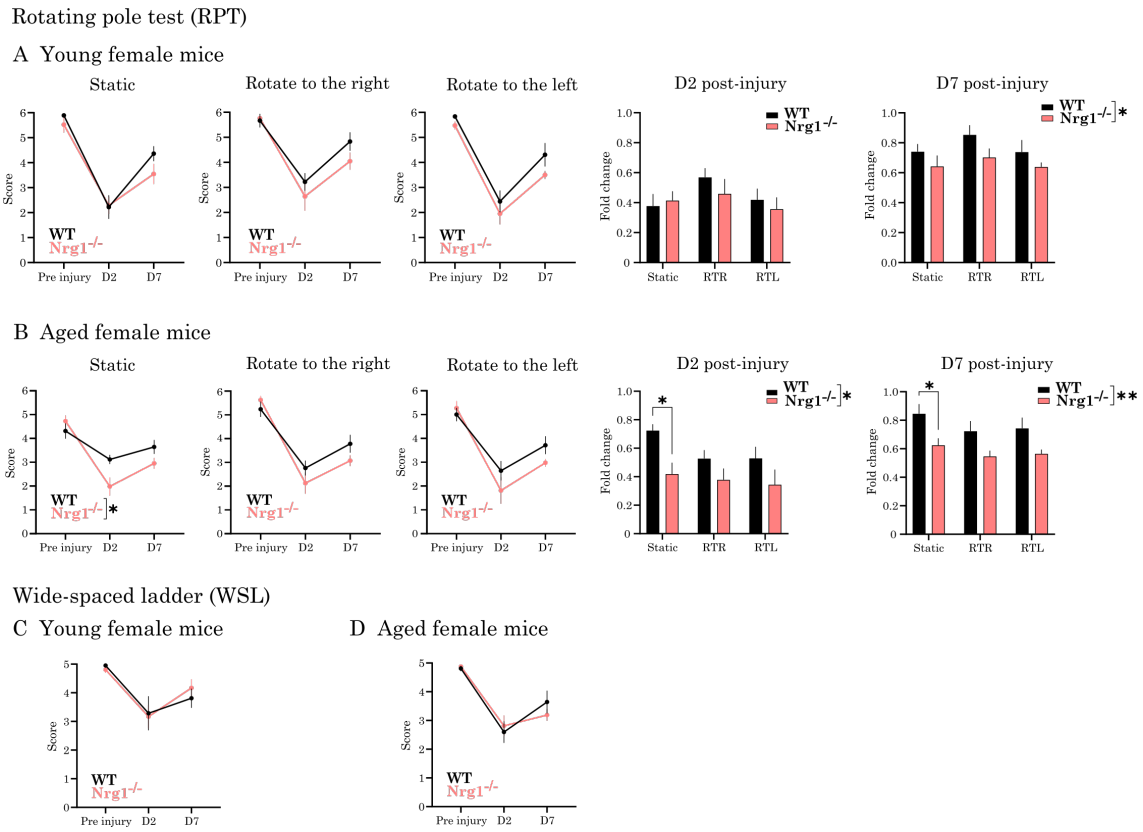

Figure 25. Functional motor characterization in young (3-4 months) and aged (11-13 months) female mice upon CCD model. A-B) Rotating pole test analysis. On the left, the graphs show the performance of wild-type (WT) and Nrg1$^{-/-}$ young (A) and aged (B) mice using three different modes of RPT: static, rotation to the right (counterclockwise, RTR) and to the left (clockwise, RTL). On the right, column bar graphs show the fold change normalized to preinjury data for each RPT mode at D2 or D7 postinjury. Mean ± SEM, N= 6 (WT) and 7 (Nrg1$^{-/-}$) young mice; N = 7 (WT) and 8 (Nrg1$^{-/-}$) aged mice. Statistical analysis: two-way ANOVA with repeated measurements and Sídák's multiple comparison test (time point analysis) or two-way ANOVA and Sídák's multiple comparison test (column bar graphs). C-D) Widespread ladder analysis. The graph shows the score of WT and Nrg1$^{-/-}$ young (C) and aged (D) in the WSL test, where no motor differences between phenotypes were detected. Mean ± SEM, N= 6 (WT) and 7 (Nrg1$^{-/-}$) young mice; N = 7 (WT) and 8 (Nrg1$^{-/-}$) aged mice. Statistical analysis: two-way ANOVA with repeated measurements and Sídák's multiple comparison test * $p \leq 0.05$, ** $p \leq 0.01$.

Nrg1 ablation produces a subtle increase in the neuroinflammatory response upon CCD.

In brain damage paradigm, the neuroprotective role of Nrg1 has been mostly demonstrated by promoting anti-inflammatory response, as well as reducing injury impact in other injury models that perform bigger damage, such as MCAO and experimental TBI (Guan et al., 2015; Noll et al., 2019; Xu et al., 2004, 2005; Zhang et al., 2018). Most studies focus on the exogenous effect of Nrg1 through ErbB receptor, which does not entirely recapitulate the complexity of Nrg1 signaling.

Here, we made use of the tamoxifen-inducible conditional transgenic mice line for Nrg1 available in the lab. The timeline of the experiment is shown in **Figure 26A**. Of note, we traced cortico-cortical callosal projections using viral vector under human Synapsin promoter to express GFP, used for cortical rewiring analysis (assessed in *Chapter 4*). One week prior to CCD induction, we administered tamoxifen by oral gavage to the mice to delete Nrg1 expression immediately before the injury, so the results are directly linked to the injury effect and not an aberrant development, as shown in conventional transgenic mice lines for the study of Nrg1 signaling (Fazzari et al., 2010; Navarro-Gonzalez et al., 2021). Brains were harvested D8 post-injury and processed into floating sections for histologic analysis.

To compare differences in aging, we carried out *in vivo* experiments in young (3-4 months) and aged (9-11 months) female mice using the same methodological protocol. Firstly, we measured injury volume, observing not significant differences between WT and Nrg1 deficient mice, meaning that the results are directly caused by Nrg1 depletion and not by injury variability (**Figure 26B'**). Next, we analyzed neuroinflammation led by macrophague/microglial activation using Iba1 marker staining (**Figure 26B-C**), observing a slight trend of increase in $Nrg1^{-/-}$ young mice (p-value=0.14) (**Figure 26B'**). Using this approach, we did not observe this increased neuroinflammatory response after injury in aged mice, possibly because the inflammation was higher in control mice as well (**Figure 26C'**). In this regard, future experiments using confocal microscopy to analyze microglial morphology in depth are required to better comprehend whether Nrg1 plays an anti-inflammatory role in elderly population upon cortical damage. Taken together, our data indicate that Nrg1 deletion can enhance an inflammatory response, which correlates with previous results obtained in different animal models where Nrg1 soluble form was administered in ErbB4 null models.

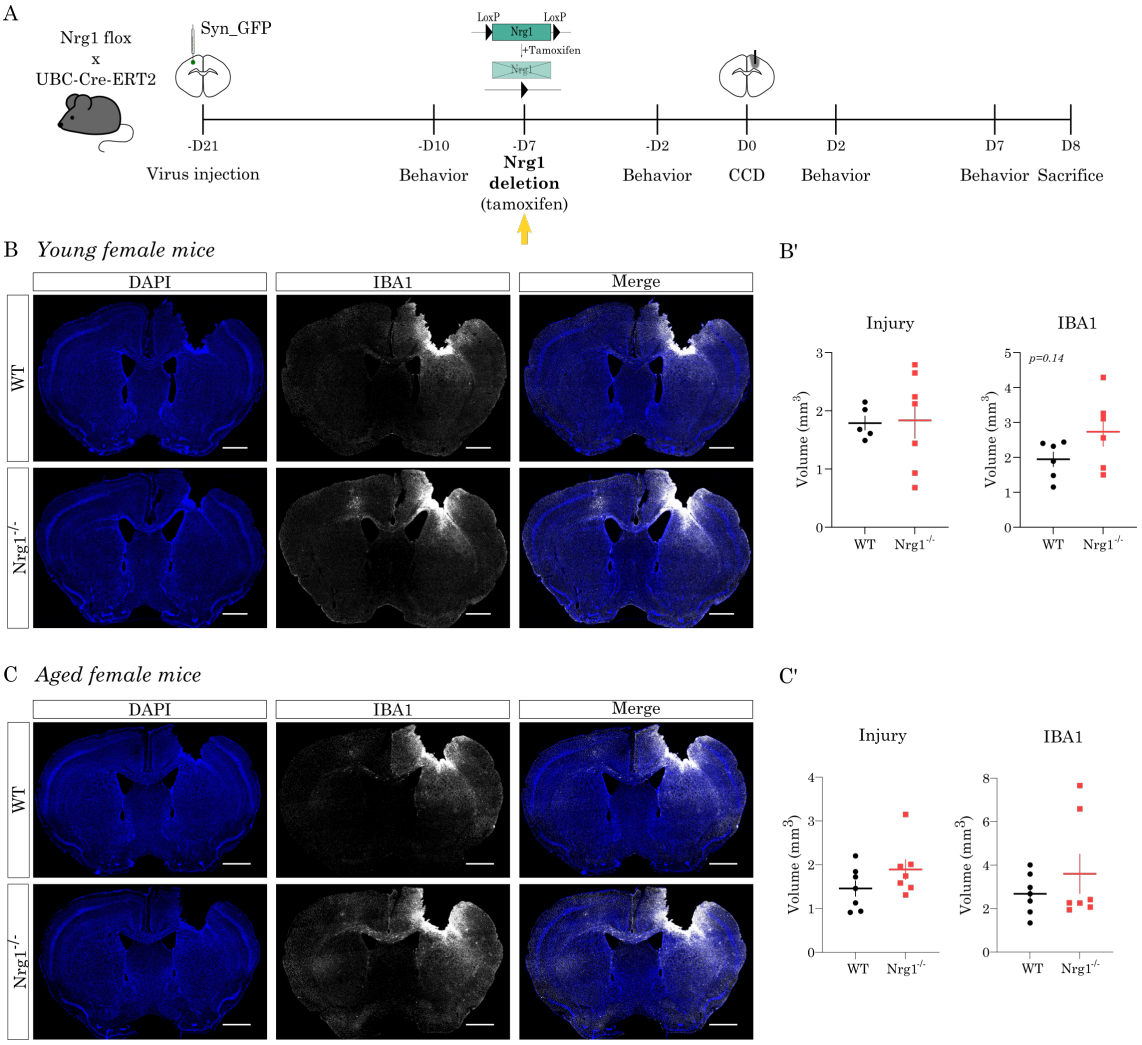

Figure 26. Nrg1 deletion produced a subtle increase in the volume of Iba1 staining in young female mice (3-4 months) upon CCD. A) Timeline of the experimental set up followed for the LOF approaches in young and aged mice. The yellow arrow highlights the time point in which Nrg1 deletion was induced by tamoxifen administration. B) Representative images of young wild-type (WT) and Nrg1$^{-/-}$ samples, labeled for Iba1 marker (white) upon CCD. Scale bar: 1mm. B') Graphs show the volume quantification of the injury (left) and Iba1 marker (right) for both experimental groups. Injury volume (N = 5 WT animals, 7 Nrg1$^{-/-}$ animals), Iba1 marker (N = 6 WT animals, 6 Nrg1$^{-/-}$ animals). C) Representative images of aged (11-13 months) wild-type (WT) and Nrg1$^{-/-}$ samples, labeled for Iba1 marker (white) upon CCD. Scale bar: 1mm. C') Graphs show the volume quantification of the injury (left) and Iba1 marker (right) for both experimental groups. N = 7 animals/group. Mean ± SEM. Statistical analysis: Unpaired t-test with Welch's correction.

Nrg1-ICD expression reduced neuroinflammatory response upon CCD.

To provide novel insights in the molecular mechanism underlying the role of Nrg1 as a neuroprotective factor upon injury, we investigated whether Nrg1 intracellular signaling promotes an anti-inflammatory response in light of previous data from our lab in which the activation of this intracellular pathway was neuroprotective in hemorrhagic stroke *in vivo* (Navarro-González et al., 2019). To this aim, we specifically traced cortico-cortical projections

through the corpus callosum and selectively induced Nrg1-ICD expression in this neuronal population (**Figure 27A**).

The timeline of the experiment is shown in **Figure 27A**. Briefly, we traced cortico-cortical projections by viral injection in the left primary motor cortex of young female mice 3 weeks prior injury. CCD induction was performed in the right primary motor cortex, parallel to the injection site. In this case, we obtained two different groups: animals injected just with GFP-expressing virus (named GFP group) and animals injected with Nrg1-ICD-expressing virus (named Nrg1-ICD group). Remarkably, both viral vectors were under the Synapsin promoter and thus specifically infecting neuronal cells. For more information on viral constructs, please refer to the corresponding section in Materials and Methods (*Nrg1 construct and adenoassociated viral vectors*).

Of note, we also characterized the motor behavior in this model, but we did not detect further differences between GFP or Nrg1-ICD injured animals, as expected considering the reduced number of neurons targeted (*data not shown*).

Brains were harvested at D8 after CCD induction and processed into floating sections for further histologic analysis (**Figure 27B**). First, we measured the injury volume, which did not differ between GFP and Nrg1-ICD groups. Next, we quantified the neuroinflammatory response of macrophages/microglial cells upon injury, labeled with Iba1 staining. Interestingly, the data revealed a trend of reduced Iba1 volume in Nrg1-ICD injured group (p-value =0.06, **Figure 27C**), which correlates with previous data obtained by the administration of Nrg1 soluble form (Guo et al., 2010; Noll et al., 2019; Shyu et al., 2004). In this regard, further investigations are required to confirm these data by analyzing microglial morphology or production of certain cytokines to better understand the cellular and molecular basis of Nrg1 intracellular signaling in the regulation of neuroinflammatory response upon injury.

Overall, this result suggests that the stimulation of Nrg1 intracellular signaling can play an anti-inflammatory role in cortical damage, which may ultimately contribute to the neuroprotective effect previously described by our lab in a hemorrhagic stroke model (Navarro-González et al., 2019).

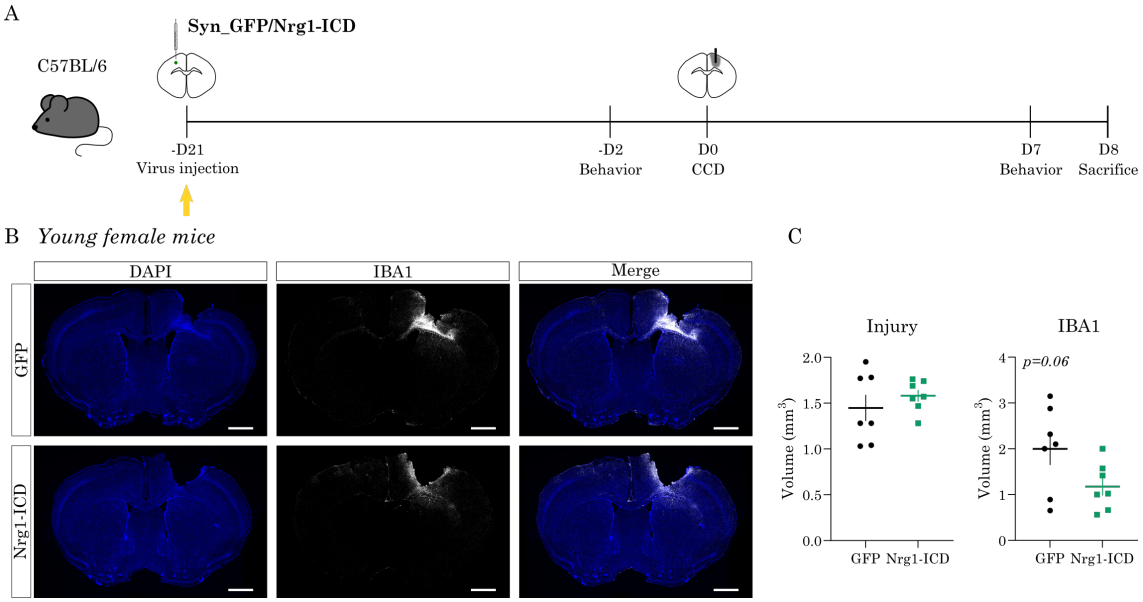

Figure 27. Nrg1-ICD expression was anti-inflammatory in young female mice (3-4 months) upon CCD. A) Timeline of the experimental set up followed for the GOF approaches in young mice. The yellow arrow highlights the time point in which Nrg1-ICD was expressed in the labeled neurons. B) Representative images of GFP and Nrg1-ICD treated brains labeled for Iba1 marker (white) upon CCD. Scale bar: 1mm. C) Graphs show the volume quantification of the injury (left) and Iba1 marker (right) for both experimental groups. N = 7 animals /group. Mean ± SEM Statistical analysis: Unpaired t-test.

Nrg1 deletion compromised PNNs integrity upon CCD in the contralesional cortex of aged mice.

Perineuronal nets (PNNs) are a specialized extracellular matrix formed by different types of proteoglycans, involved in the maturation and stabilization of synaptic circuitry during CNS development (Devienne et al., 2021; Quattromani et al., 2018; Wang & Fawcett, 2012). Notably, PNNs specifically encapsulate fast-spiking PV interneurons, whose biology is highly modulated by Nrg1/ErbB4 signaling (del Pino et al., 2013; Fazzari et al., 2010; Mei & Nave, 2014; Navarro-Gonzalez et al., 2021). Although the role of PNNs in CNS injury context remains unclear, it is largely described that there is a decrease of PNNs in PL areas (Alia et al., 2016; González-Manteiga et al., 2022; Hsieh et al., 2017; Quattromani et al., 2018; Zeiler et al., 2013). Therefore, our next step was to investigate whether Nrg1 signaling could modulate PNNs integrity upon CCD.

As previously described, we used WFA staining as a classical marker to label PNNs (Devienne et al., 2021; González-Manteiga et al., 2022; Hsieh et al., 2017), and we quantified the number of WFA^+ cells in both contralesional and $Iba1^+$ ipsilesional regions of WT and $Nrg1^{-/-}$ injured samples (**Figure 28A**).

To evaluate ipsilesional regions, data were normalized to the respective contralateral equivalent region, as previously described (González-Manteiga et al., 2022). As expected, the results

showed a strong degradation of WFA^+ cells in both young and aged mice. However, we did not detect differences between WT and $Nrg1^{-/-}$ mice in both age groups (**Figure 28B'-C'**). Therefore, these data suggest that Nrg1 signaling does not promote PNNs stability in the PL region upon CCD.

Conversely to ipsilesional areas, the presence of WFA^+ cells was significantly higher in the contralesional regions. Therefore, to properly detect differences in the number and intensity of WFA^+ cells between WT and $Nrg1^{-/-}$ young and aged mice, in this case the data was directly normalized to the WT mean value. Although we did not perceived differences in WFA^+ cell number and intensity between groups in young mice (**Figure 28B-B'**), the data revealed a 30% of reduction in the number of WFA^+ in $Nrg1^{-/-}$ aged mice compared to wild-type animals (**Figure 28C-C'**). Consistent with the previous result, the intensity in WFA^+ cells were slightly lower in $Nrg1^{-/-}$ aged mice (**Figure 28C'**).

Overall, this preliminary study might suggest that, although the CCD model conforms a focal damage which severely impact PNNs integrity in the PL regions, a PNNs remodeling process may take place in the contralesional cortex of $Nrg1^{-/-}$ aged mice upon injury. Nevertheless, further experiments are required to better understand 1) the relevance of PNNs in the cortical circuit remodelling event upon injury and 2) the contribution of the contralateral cortex in plasticity following unilateral cortical injury.

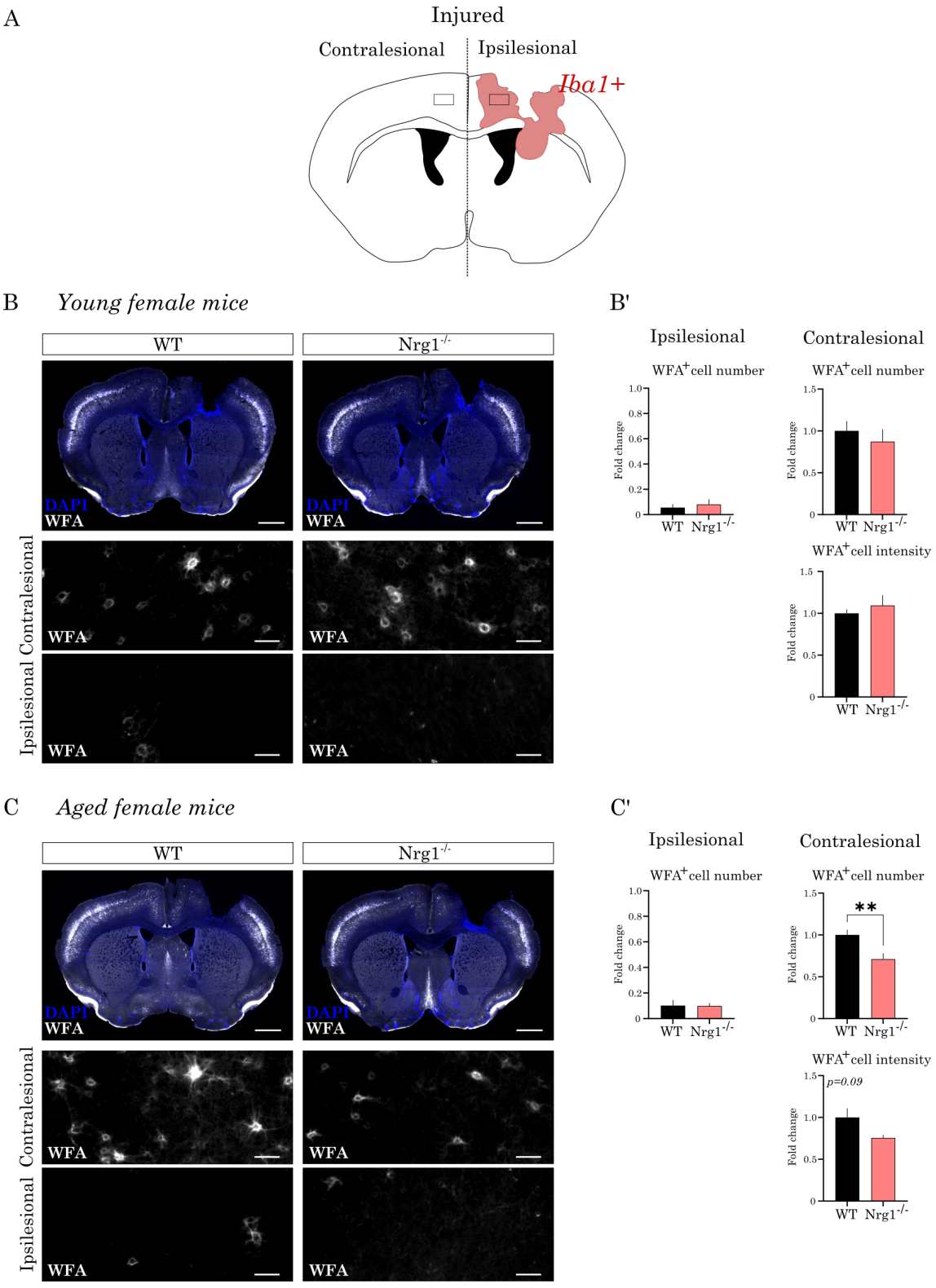

Figure 28. Nrg1 deletion reduced WFA⁺ cell number in the contralesional area in aged female mice upon CCD. A) The cartoon illustrates the ROI selected to perform quantification of PNNs in injured samples. B) In the upper row, representative images of injured brains of WT and Nrg1$^{-/-}$ young mice (3-4 months), labeled with WFA as a specific marker of PNNs (white). Scale bar: 1mm. In the lower rows, the representative images are the ROIs corresponding to the box areas showed in the cartoon (A), showing the reduction of WFA⁺ cell in the ipsilesional area. Scale bar: 50µm. B') Graphs represent the fold change of WFA⁺ cell number and intensity in the contralesional area (left) and the WFA⁺ cell

number in the ipsilesional region (right). Mean ± SEM N= 8 slices per group. C) In the upper row, representative images of injured brains of WT and $Nrg1^{-/-}$ aged mice (3-4 months), labeled with WFA as a specific marker of PNNs (white). Scale bar: 1mm. In the lower rows, the representative images are the ROIs corresponding to the box areas showed in the cartoon (A), showing the reduction of WFA^+ cell in the ipsilesional area. Scale bar: 50µm. C') Graphs represent the fold change of WFA^+ cell number and intensity in the contralesional area (left) and the WFA^+ cell number in the ipsilesional region (right). Mean ± SEM N= 8 slices per group. Statistical analysis: Mann Whitney t-test.

Nrg1-ICD expression did not overtly modulate PNNs integrity upon CCD.

To examine whether Nrg1 intracellular signaling can modulate the integrity of PNNs upon cortical damage, we specifically expressed Nrg1-ICD in a selective number of neurons in the contralesional cortex of young female mice. Again, we quantified the number of WFA^+ cells as a common marker of PNNs.

To verify whether Nrg1-ICD expression could promote an alteration in PNNs integrity prior injury induction, we also measured WFA^+ cell in the injection site cortex and its respective contralateral area of equivalent bregma slices (**Figure 29A**). Surprisingly, we detected a trend toward a slight increase in the number and intensity of WFA^+ cells in the injection site region of Nrg1-ICD not injured samples (**Figure 29D**). Regarding these data, we compared injured samples with their respective not injured group to avoid biased results by viral injection.

The analysis showed that WFA^+ cells were strongly reduced in the $Iba1^+$ ipsilesional areas in injured samples compared to not injured ones (**Figure 29B**), in agreement with previous publication (González-Manteiga et al., 2022). Nonetheless, we did not detect differences between GFP or Nrg1-ICD groups in injured conditions, which can be explained by the limited number of neurons expressing Nrg1-ICD (**Figure 29C**).

Therefore, our results show that the expression of Nrg1-ICD in a certain number of neurons in the contralesional cortex did not affect PNNs integrity upon injury. Nevertheless, future experiments are required to better comprehend the impact of Nrg1 intracellular signaling in PNNs integrity after cortical damage, such as inducing Nrg1-ICD expression directly in the ipsilesional cortex, which is the most vulnerable area.

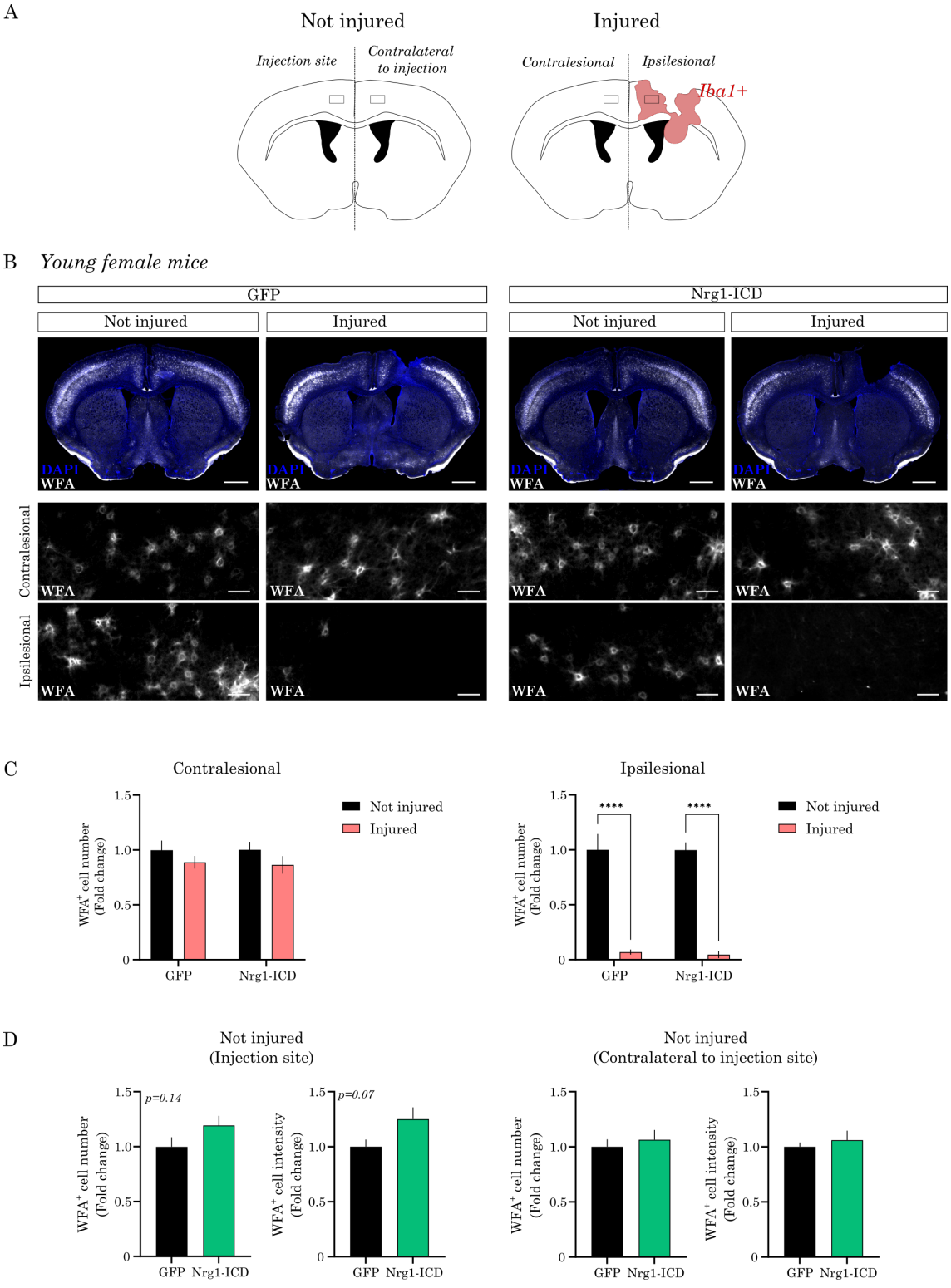

Figure 29. Nrg1-ICD expression did not promote PNNs integrity in the ipsilesional cortex in young female mice upon CCD. A) The cartoons represent the ROI selected to perform the quantification of PNNs in not injured and injured samples. B) Representative images of control (injected with GFP) and Nrg1-ICD slices (upper row, scale: 1mm), labeled with WFA as a specific marker of PNNs. In the lower rows, the representative images are the ROIs corresponding to the boxed areas showed in the cartoons, showing the reduction of WFA^+ cells in the ipsilesional area in injured samples (scale bar: 50μm). C) Graphs represent the fold change of WFA^+ cell number in the contralesional (left) and ipsilesional (right) areas, relative to each respective not injured group. Mean ± SEM. N = 7 slices per

group. Statistical analysis: two-way ANOVA and Sídák's multiple comparison test D) Graphs show the fold change WFA^+ cell number and intensity in the injection site (left) and contralateral to injection site (right) of not injured samples. The data is normalized to GFP group as basal conditions. Mean ± SEM N = 7 slices per group. Statistical analysis: Unpaired t-test.

DISCUSSION

Over the past decades, Nrg1/ErbB signaling has been proposed as a potential modulator in PNS and CNS repair (Birchmeier & Bennett, 2016; Kataria et al., 2019; Mei & Nave, 2014; Mei & Xiong, 2008). Several studies reported an increase of Nrg1 and ErbB receptor upon brain damage (Parker et al., 2002; Ryu et al., 2019; Tokita et al., 2001; Xu & Ford, 2005). Interestingly, a recent study detected an increase in Nrg1 levels in the serum plasma of human patients with TBI and post-traumatic developing epilepsy, suggesting its neuroprotective role upon post-traumatic changes in the brain (Gazaryan et al., 2019).

Similarly, we observed an increase in Nrg1-TM1 and ErbB4 gene expression in the ipsilesional regions upon an experimental focal stroke model in aged male mice, which was even greater in the contralesional cortex. This preliminary data could suggest that Nrg1 is overexpressed not only in the PL areas, but also in other brain-connected regions, speculating a process of remodeling and response to injury. However, future experiments are needed to confirm this result, regarding the reduced number of animals used in this study. We hope that these data provide an intriguing starting point to elucidate whether the raising of endogenous Nrg1 levels could be a pivotal factor to promote neuroprotection not only in the PL area, but also in adjacent connected regions upon brain injury.

Previous studies suggested that Nrg1 promotes neuroprotection and improves functional recovery upon brain damage. However, most of the studies used methods that induce larger brain injuries, affecting different cortical and subcortical regions involved in locomotion (Guan et al., 2015; Guo et al., 2006; Li et al., 2007; Xu et al., 2004, 2005; Zhang et al., 2018). This experimental injury paradigm may complicate the examination of the specific molecular effect of Nrg1 signaling in neuroprotection.

In this sense, we proposed a refined brain injury model to produce focal cortical damage restricted to the primary motor cortex, with a considerable reduced volume. Using this methodological approach, we analyzed motor impairment in a novel conditional Nrg1 transgenic mouse line in young and aged populations. This model conforms a sophisticated and refined way to understand Nrg1 deletion immediately before the injury, avoiding biased data relative to an altered formation of the cortical circuitry as in other transgenic mouse lines (Chen et al., 2010; Fazzari et al., 2010; Navarro-Gonzalez et al., 2021). Of note, this conditional transgenic line disrupts all Nrg1 isoforms and, hence, completely ablates Nrg1 signaling specifically. Thus, this genetic strategy overcomes the limitations of other animal models that only evaluate the exogenous effect of Nrg1 mediated via ErbB4 activation, without recapitulating the entire complexity of Nrg1 signaling.

As expected, using specific and sensible motor behavioral tasks such as the RPT and WSL, we observed motor impairments in injured animals. Regarding the phenotype, we detected that $Nrg1^{-/-}$ exhibited a subtle motor impairment in the RPT, suggesting that Nrg1 deletion worsens spontaneous recovery in both young and aged mice. In conclusion, our data support previous studies in which Nrg1 signaling promotes functional motor recovery upon injury but were newly investigated in a novel *in vivo* model of acute Nrg1 deletion in adult mice.

Several works showed that the administration of Nrg1 soluble form has anti-inflammatory properties upon injury. However, there are some caveats in this literature. In terms of technical procedure, different types of Nrg1 soluble forms are used, such as Nrg1-α or Nrg1-β3, which are administered intravenously through the tail vein or directly into the brain, which may lead to some biological variability between works (Iaci et al., 2016; Y. Li et al., 2007; Shyu et al., 2004; Xu et al., 2004). Moreover, the administration of Nrg-1β may largely affect different cell types in the organism, leading to misinterpretation of data in such a complex paradigm. Recently, Deng and colleagues used an ErbB4 null mutant mouse model, specifically targeting PV^{+} interneurons to investigate Nrg1/ErbB4 signaling after TBI and observed an increased in microglial response in ErbB4 deficient mice (Deng et al., 2019). Although the exogenous effect of Nrg1 is mainly mediated by ErbB4, which is predominantly expressed in PV^{+} cortical interneurons (Fazzari, et al. 2010), this neuronal subpopulation represents a limited fraction of the total neuronal subtypes present in the cortex. Hence, it is ambitious to think that such a strong neuroprotective role is mediated by only a reduced percentage of neurons. Of note, ErbB4 serves as a receptor for Nrg3, a low affinity ligand also expressed in the cortex, which may confound data interpretation.

Thus, providing novel and specific genetic animal models in which Nrg1 signaling is finely targeted is a pivotal step to better comprehend the neuroprotective effect of Nrg1 signaling effect on cortical damage. Herein, we developed two refined and clean animal models to investigate the effect of Nrg1 signaling in neuroinflammation upon CCD. Firstly, we used a tamoxifen-inducible transgenic mice line to acutely delete Nrg1 expression upon injury, in which we observed a subtle increased in Iba1 staining volume in $Nrg1^{-/-}$ injured young mice. Next, to further understand the molecular mechanism underlying Nrg1 signaling in modulating neuroinflammation, we specifically investigated the activation of Nrg1 intracellular signaling in inflammatory response, prompted by previous data reporting the neuroprotective role of Nrg1-ICD in a *in vivo* model of hemorrhagic stroke (Navarro-González et al., 2019). Noteworthy, in this model we took advantage of the viral vector strategy to label and expressed Nrg1-ICD in a restricted number of neurons, which allows an exclusively cell-autonomous readout of the targeted neuron.

We observed a subtle trend of increased Iba1 volume staining in Nrg1 deficient young mice, whereas we did not see differences in the neuroinflammatory response in aged mice. A possible

explanation would be that generally elderly population already presents higher basal inflammatory state (Franceschi et al., 2000), which could unmask subtle differences between WT and $Nrg1^{-/-}$ animals, especially in focal injury models such as CCD. Surprisingly, we detected a trend towards a reduced neuroinflammatory response in injured young mice expressing Nrg1-ICD (p-value=0.06), using Iba1 staining as a canonical marker of microglia/macrophages. Remarkably, we did not observe differences in injury volume in both gain- and loss-of function approaches, conversely to previously studies using bigger injury models of TBI and stroke (Deng et al., 2019; Guan et al., 2015; Guo et al., 2006; Li et al., 2007; Shyu et al., 2004; Xu et al., 2004, 2005; Zhang et al., 2018). This result highlights a major strength of the CCD model, in which the variability of injury is greatly reduced, thus ensuring biological reproducibility within samples. In this regard, the changes detected in the inflammatory response are purely due to Nrg1 signaling and not relative to injury volume disparity, overcoming biased interpretations.

The mechanisms underlying the effect of Nrg1 in neuroprotection upon damage are still unclear. Several studies carried out by the lab of Dr. Byron D. Ford to unveil genetic and transcriptomic changes upon stroke suggest that Nrg1 treatment regulates different gene programs involved in diverse functions crucial for tissue repair such as cell death, response to stress, inflammation, cell migration, synaptic transmission, and others (Simmons et al., 2016; Surles-Zeigler et al., 2019; Xu et al., 2005). Recently, they identified ETS-1 as a potential transcription factor regulated by Nrg1 treatment upon stroke, which was previously associated with neuronal death and inflammation in a rat model of stroke (Surles-Zeigler et al., 2019).

Particularly, diverse groups have also pointed out that the presence of microglia/macrophages and astrocytes in the PL area is reduced due to Nrg1 signaling in models of BI and SCI (Alizadeh et al., 2017; Deng et al., 2019; Kataria et al., 2019). In this sense, some evidence suggest that Nrg1 can restrict the expression of chemokines, necessary to promote the recruitment of microglia and peripheral immune cells to exacerbate inflammatory response upon injury. Furthermore, it has been also described that Nrg1 treatment reduces the production of pro-inflammatory cytokines, such as IL-1, TNF-α, IL-6, while stimulate the release of anti-inflammatory cytokines, such as arginase-1 and IL-10 (Alizadeh et al., 2017; Deng et al., 2019; Kataria et al., 2019; Shahriary et al., 2019; Xu et al., 2005). Mechanistically, this effect appears to be partly mediated by preventing nuclear translocation of the NF-κB p65 subunit, required for upregulation of inflammatory cytokines (Simmons et al., 2016). Consistent with these data, a recent study using the BV2 mouse microglial cell line stimulated with Nrg-1β *in vitro* speculates a potential role for Nrg1 in switching immune cells activity to a M2 profile, commonly associated with a protective function in tissue repair (Ma et al., 2022). Nevertheless, restricting the complexity of the immune cell response to a strict and polarized M1/M2 categorization do not entirely reflects the reality *in vivo* (Ransohoff, 2016). Hence, future research based on novel

technological approaches and molecular markers is needed to elucidate the specific molecular and cellular mechanisms of the inflammatory response and how it is regulated by Nrg1 signaling.

In the studies cited above, Nrg1 soluble form is administered *in vitro* and *in vivo* to analyze its impact in neuroprotection upon brain injury, which mainly refers to the canonical signaling pathway mediated through the activation of the ErbB4 receptors, predominantly expressed in PV^+ cortical interneurons. However, in our novel *in vivo* approach we specifically expressed Nrg1-ICD, observing for the first time a potential role of this intracellular signaling in reducing the microglial/macrophages response. However, we did not address the concrete mechanisms by which Nrg1 intracellular signaling modulates inflammatory response upon injury. We previously reported that Nrg1-ICD expression can downregulate pro-apoptotic gene expression *in vitro* and speculated that the activation of Nrg1 intracellular signaling could promote neuroprotection by reducing neuronal susceptibility to apoptosis (Navarro-González et al., 2019). Therefore, future experiments focusing on cellular and molecular events are required, including the genetic and transcriptomical program regulated by Nrg1 intracellular signaling to modulate immune and glial cell response upon injury.

Finally, we investigated the role of Nrg1 signaling in the remodeling process of PNNs upon CCD. As previously described, we again detected an abrupt reduction of WFA^+ cells in the $Iba1^+$ ipsilesional regions, opposite to the situation in the $Iba1^-$ contralesional region (Bozzelli et al., 2018; González-Manteiga et al., 2022; Quattromani et al., 2018; Wen et al., 2018). Thus, these data again reinforce the correlation between microglial activation and PNNs degradation. However, we did not detect an effect of Nrg1 signaling over PNNs integrity upon CCD in both GOF and LOF approaches. Interestingly, we observed a decrease of WFA^+ cells in the contralesional cortex of $Nrg1^{-/-}$ aged animals upon CCD, suggesting that Nrg1 is involved in the remodeling process of interconnected brain regions in response to injury.

PNNs are specialized extracellular matrix in the CNS, highly associated with plasticity and maturation of synaptic circuitry, specifically enveloping PV^+ interneurons in the cortex (Devienne et al., 2021; Wang & Fawcett, 2012). However, the contribution of PNNs to tissue repair in the CNS remains poorly unaddressed.

On the one hand, previous data indicate an early reduction of PNNs in the PL area, which correlates with an increase in axonal growth-promoting gene expression (Carmichael et al., 2005). Complementarily, some studies suggest that a disruption of hyaluronic acid (HA) and chondroitin sulfate proteoglycans (CSPGs), the main components of PNNs, enhances functional recovery upon stroke and SCI (Katarzyna Greda & Nowicka, 2021; Pearson et al., 2018; Zhao et al., 2013). However, CSPGs are not exclusively found in PNNs, but conform to generic extracellular matrix molecules. In this sense, they are also produced by reactive astrocytes in

the glial scar several days after damage, restricting axonal regeneration into damaged tissue (BrosiusLutz & Barres, 2014). Therefore, even though the therapeutic treatment provides a promising strategy to enhance functional recovery, these results should be interpreted with the caveat that the use of these inhibitory treatments may affect other cellular structures, and not only PNNs.

On the other hand, some studies showed a disruption of PNNs and a loss of PV^+ cells in stroke, suggesting that PNN may be neuroprotective for PV^+ cells in cortical damage (Fowke et al., 2018; Hsieh et al., 2017). Remarkably, the biology of PV^+ interneurons is highly influenced by Nrg1/ErbB4 receptor (Fazzari et al., 2010; Mei & Nave, 2014; Mei & Xiong, 2008). In this context, two recent works also highlights the relevance of the PNN maturation in plasticity during adolescence and Alzheimer disease. Interestingly, both studies show that Nrg1/ErbB4 signaling is required for the proper functioning of the hippocampal subfield CA2 and thus for the restoration of social memory (Domínguez et al., 2019; Rey et al., 2022).

Noteworthy, PNNs are complex structures composed of several key elements, including diverse lectican protein such as aggrecan, neurocan, versican or brevican. Therefore, different markers, such as WFA, AB1031 or Cat-315 are used to label PNNs, resulting in differences in the methodology (Carmichael et al., 2005; Devienne et al., 2021; González-Manteiga et al., 2022; Madinier et al., 2014; Quattromani et al., 2018; Ueno et al., 2019; Wang & Fawcett, 2012; Wen et al., 2018). Hence, future research using a variety of PNN-specific markers and a temporal perspective is needed to further elucidate the dynamic remodeling process of PNNs in CNS recovery upon damage and whether Nrg1 signaling can modulate their biology.

In conclusion, our data support the role of Nrg1 as a neuroprotective factor upon brain injury, using for the first time new refined models to specifically target Nrg1 signaling. As a novelty, this research pointed out that this effect may be mediated not only by the activation of the ErbB4 receptor, but by regulation of neuronal gene expression program via activation of Nrg1 intracellular signaling which may ultimately modulate microglia/macrophage activity. Therefore, we hope that these data can assess the foundations to better understand the molecular and biochemical mechanisms underlying Nrg1 intracellular signaling to identify novel molecular targets to promote cortical repair upon injury.

CHAPTER 4: NRG1 SIGNALING MODULATES CORTICAL CONNECTIVITY UPON BRAIN DAMAGE

GRAPHICAL ABSTRACT

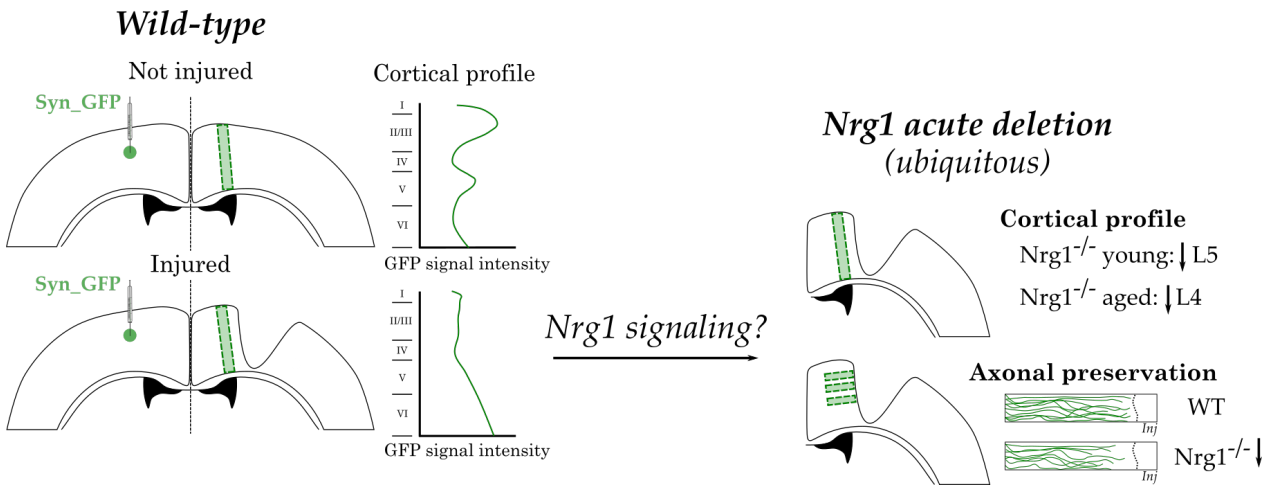

Highlights:

- In wild-type animals, the contralateral cortical profile is altered upon CCD, increased in lower cortical layers.
- Nrg1 deletion modulated the contralateral cortical profile upon CCD in young and aged female mice.
- Nrg1 deletion reduced axonal preservation upon CCD in young and aged female mice.
- Activation of Nrg1 intracellular signaling may shape the contralateral cortical profile prior to injury induction.

INTRODUCTION

The cortex is the outer layer enveloping the cerebral hemisphere, considered the major level of organization in the CNS (Haley & Maffei, 2018; Snell, 2007). The development of the cerebral cortex is generated by three dynamic steps which occurs simultaneously: neuronal proliferation and differentiation through successive symmetric and asymmetric divisions; neuronal migration of neuronal precursors along the cortical plate through radial or tangential movements; and cortical organization into six layers in an inside-out patterning that eventually undergoes a process of synaptogenesis and apoptosis (Agirman et al., 2017).

Cortical layers are mainly composed of two classical neuronal types that are highly interconnected and form cortical circuits: excitatory (pyramidal) and inhibitory (interneuron) neurons. Despite their heterogeneity in morphology, identity and localization, there are some critical features that define their function. Pyramidal neurons have a stereotypical shape based on an apical dendrite that crosses along the cortical layers, and basal dendrites which can span laterally within the cortical layer where the soma is located. Remarkably, their axons can extend either within cortical layers or to different brain regions, promoting excitatory neurotransmission. Conversely, interneurons are restricted to local circuits due to the limited extension of their axonal projections (Haley & Maffei, 2018; Snell, 2007). By targeting excitatory and other inhibitory neurons within the layer, they are considered crucial regulators of the excitatory/inhibitory (E/I) balance, which is essential for maintaining an adequate cortical information processing (Ferguson & Gao, 2018).

Although neurons are non-mytotic cells, cortical circuits can be extensively sculpted and refined by internal and external stimuli, giving rise to cortical plasticity. However, this plasticity is mainly found in the embryonic and postnatal stages and becomes limited in adulthood. Therefore, it is crucial to determine and understand the molecular and cellular mechanisms underpinning critical periods of plasticity (Haley & Maffei, 2018).

Even though limited spontaneous recovery after cortical injury leads to permanent disability in adults, diverse processes of cortical rewiring and plasticity take place in the injured brain to enhance functional recovery. Therefore, unraveling the molecular, cellular, and structural mechanisms underlying this spontaneous regeneration has become a critical step to ultimately offer novel molecular and pharmacological treatments to promote an effective and complete recovery upon injury.

Stroke induces a specific genetic program that is orchestrated in successive waves of gene expression changes within the first month after injury. Between 7 and 14 days upon damage, an increase in growth-promoting factor enhances axonal sprouting in the PL area. After this period,

the glial scar is formed, in which growth-inhibitory factors, such as CSPGs, accumulate (Carmichael et al., 2005). Noteworthy, the production of inhibitory molecules can control unbounded axonal sprouting and thus abnormal circuit rewiring which may be detrimental for functional recovery (Carmichael et al., 2017; Joy & Carmichael, 2021; Li et al., 2010; Murphy & Corbett, 2009). Additionally, it has also been described that there are differences in the post-stroke transcriptomic program regulated in young or aged animals, which can explain the limited recovery response in the aged population. Hence, a unique post-injury machinery is regulated, which does not necessarily recapitulate developmental stages (Carmichael et al., 2017; Li et al., 2010).

However, axonal sprouting is not only restricted to the PL area, but also involves an important remapping of cortical connectivity to adjacent brain regions occurs. In these studies, injury to the motor cortex resulted in novel cortical rewiring to the adjacent ipsilateral somatosensory cortex and other functionally related connected regions, contributing to functional recovery upon cortical injury (Benowitz & Carmichael, 2010; Brown et al., 2009; Dancause et al., 2005; Murphy & Corbett, 2009). Moreover, the activation of the contralesional hemisphere has also been reported in animal experimental models and stroke patients (Brown et al., 2009; Murphy & Corbett, 2009; Takatsuru et al., 2009) which may undergo a process of structural remodeling. In this sense, a dynamic event of dendritic spine turnover has been observed in the contralateral cortex within the first two weeks after cortical injury, which is involved in functional recovery (Empl et al., 2022; Jones et al., 1996; Takatsuru et al., 2009).

Several works used tracing techniques near the injured area for mapping cortical connections in tangential slices, analyzing differences in the location of cortical projections with polar statistics (Carmichael et al., 2017; Joy et al., 2019; Li et al., 2010). Additionally, other groups have used *in vivo* imaging to provide a temporal and spatial monitoring of neuronal activity changes throughout the brain after injury (Brown et al., 2009; Latifi et al., 2020; Takatsuru et al., 2009). These approaches provided an effective tool to obtain a panoramic view of cortical rewiring in ipsi- and contralesional areas after injury.

However, little is known about how new connectivity patterns are specifically shifted within the highly interconnected cortical layers that receive and send information to different CNS areas. To address this question, we proposed the corpus callosum (CC) as an elegant model to study cortical rewiring upon damage. Noteworthy, the CC is the largest axonal tract in the mammalian brain, conforming the main pathway for information transfer between hemispheres (reviewed in De León Reyes et al., 2020). Hence, it offers an ingenious experimental approach to analyze the distribution of axonal projections into the ipsilesional cortical layers, separate from the soma, in the same coronal slice. In addition, existing data describe anatomical and functional changes in

the contralateral hemisphere after cortical damage (Brown et al., 2009; Empl et al., 2022; Jones et al., 1996; Murphy & Corbett, 2009; Takatsuru et al., 2009).

Nrg1 is essential for cortical development. Indeed, mutations in Nrg1 and the ErbB4 receptor have been associated with several neuropsychiatric disorders such as schizophrenia. During development, Nrg1/ErbB4 signaling plays an essential role in the assembly of neuronal circuitry, such as neuronal migration, axonal elongation and myelination, or synapse formation (Fazzari et al., 2010; Flames et al., 2004; López-Bendito et al., 2006; Mei & Nave, 2014; Mei & Xiong, 2008). However, whether Nrg1 signaling remodels cortical circuits in the adult brain upon injury remains poorly understood.

Several groups have explored the relevance of Nrg1/ErbB signaling for myelination in the context of nerve repair and SCI (reviewed in Birchmeier & Bennett, 2016; Kataria et al., 2019), which corresponds to an important regenerative process to enhance functional recovery (Bartus et al., 2016; Joung et al., 2010; Mancuso et al., 2016; Tao et al., 2009). Furthermore, recent data suggested that overexpression of Nrg1 increased retinal thickness and ameliorated optic nerve injury via the inhibition of the RhoA/cofilin pathway (Hao et al., 2020). In addition, the administration of Nrg1-1β3 upregulated the expression of GAP43 and synaptophysin in both ipsi- and contralateral hemispheres 3 weeks after MCAO, suggesting that Nrg1 can promote axonal sprouting and neuroplasticity upon injury (Iaci et al., 2016). However, these studies use classical histologic markers of neurofilaments and synapse-associated proteins, or electron micrographs to quantify myelinated axons, which do not clearly demonstrate axonal sprouting, regarding protein half-life, axonal transport, or other aspects related to immunohistochemical limitations. Complementary, they do not provide spatial information about the origin and target of connections, which is necessary to better understand circuit reorganization after injury (Carmichael et al., 2017). Furthermore, the effect of Nrg1 soluble form mediated through the activation of ErbB4 in the cortex does not entirely recapitulates the complexity that Nrg1 signaling entails in the cortex. It is noteworthy that the ErbB4 receptors are mainly, if not exclusively, expressed in the PV^+ cortical interneuron subtype, the major category of inhibitory cells, but only correspond to the 10% of neuronal cells in the adult cortex (Fazzari et al., 2010; Lim et al., 2018).

To overcome this technical limitation, herein we traced contralateral cortical projections using viral vectors in an inducible transgenic mouse line to acutely ablate Nrg1 expression prior to injury in young and aged female mice, disrupting all Nrg1 isoforms. Mechanistically, we also expressed Nrg1-ICD to investigate the role of Nrg1 intracellular signaling in cortical rewiring. Overall, we provided an effective experimental paradigm to better ascertain the impact of contralateral connectivity in ipsilesional cortical layers, and specifically investigate the role of Nrg1 in cortical rewiring upon damage.

RESULTS

Contralateral cortical wiring was affected upon CCD.

The CC is the largest interhemispheric structure in the brain, playing an important role in processes of functional recovery after CNS injury (Chovsepian et al., 2023; Empl et al., 2022; Wu et al., 2022). Therefore, to better understand the reorganization of cortical circuits after damage, we chose the CC as a model to investigate axonal sprouting upon CCD. Briefly, we performed stereotactical injection in layer II/III to trace cortico-cortical callosal projections, using a GFP viral vector under human Synapsin promoter to specifically label neuronal cells. To analyze contralateral axonal sprouting upon CCD, we quantified GFP intensity along the right motor cortex in not injured and injured samples (**Figure 30A**).

Targeting cortical connections using stereotactic viral injections is a refined and precise approach compared to *in utero* electroporation. However, it may still introduce some technical variability due to anatomical differences between the animals' cranial bones. To limit this variability in the measurements, we discarded inconsistent samples from the analysis. For more information on sample selection, please refer to the corresponding section in Material and Methods (*Cortical profile and axonal preservation*).

After brain damage, previous data described that brain circuitry undergoes a process of reorganization that can induce distinct axonal sprouting patterns depending on the cortical injury process (Brown et al., 2009; Carmichael et al., 2001; Carmichael & Oise Chesselet, 2002; Dancause et al., 2005). Before testing the role of Nrg1 signaling in cortical connectivity remodeling upon brain injury, we first examined the axonal sprouting response in the ipsilesional cortex upon CCD, compared to not injured samples. The ROI selected for this study and the analysis workflow are described in **Figure 30A**. Briefly, we compared equivalent rectangles in the right motor cortex of both not injured and injured samples. We measured the GFP intensity along the selected region, which corresponds to the axonal distribution along the cortical layers (referred to as the cortical profile). To reduce the variability associated with GFP intensity between slices, the data were normalized to the total intensity of each layer.

In not injured samples, the data reflected that GFP intensity was highly increased in layer V and layer II/III, while decreased in layer IV, representing a normal distribution of callosal projections, consistent with previous publications (Fame et al., 2011) (**Figure 30B-C**, labeled in black on the graph). However, data from injured brains revealed a significantly different cortical profile compared to not injured samples, where the GFP intensity appeared to be homogeneously distributed along the cortical layers compared to not injured conditions (**Figure 30B-C**, labeled in red on the graph). Particularly, we noticed an increase in GFP intensity in layer VI and a decrease in layer II/III upon CCD, compared to the control condition (**Figure 30D**).

Overall, this result shows that contralateral sprouting is altered D8 after CCD, suggesting 1) a particular vulnerability in layer II/III, a region preferentially targeted by callosal projection neurons, and 2) an enhancement in layer VI, which normally targets subcortical structures (**Figure 30B-B'**).

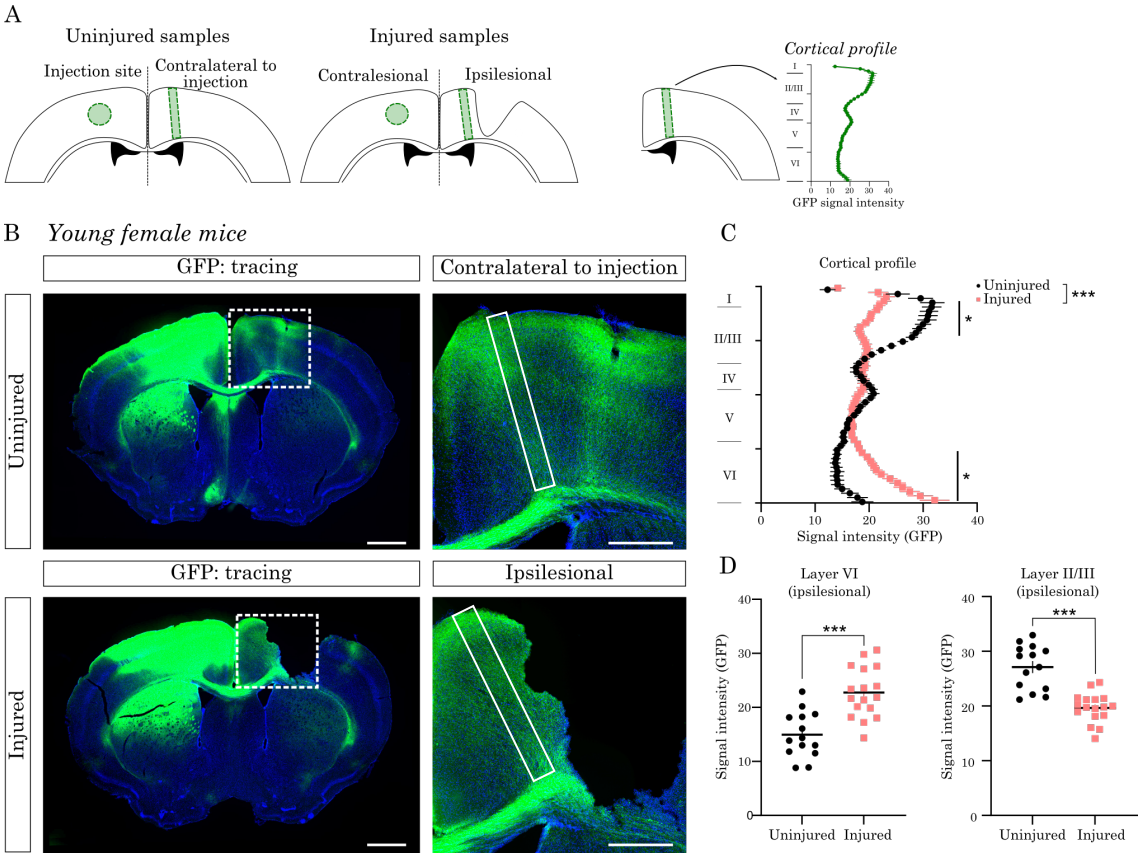

Figure 30. Contralateral cortical wiring was affected in young female mice upon CCD. A) The cartoon represents the methodology used to study the cortical profile in not injured and injured samples by analyzing GFP intensity along the cortex in the right hemisphere. B) Representative images illustrating GFP tracing in not injured and injured samples (left). On the right, the boxed area is isolated to show contralateral sprouting in detail. C) The graph presents the normalized GFP intensity distribution along the cortex, giving the cortical profile of not injured (labeled in black) and injured samples (labeled in red) in the selected rectangle as shown in the cartoon (A). Mean ± SEM, N = 14 (not injured) 17 (injured) slices. Statistical analysis: two-way ANOVA with repeated measurements and Sídák's multiple comparison test. D) The graphs show the normalized GFP intensity in layer VI (left) and layer II/III (right) in the contralateral to the injection cortex of not injured (labeled in black) and the ipsilesional cortex in injured samples (labeled in red). Mean ± SEM. Statistical analysis: Unpaired t-test.

Nrg1 deletion altered contralateral cortical wiring upon CCD.

To ascertain the role of Nrg1 in cortical remodeling upon injury, we used the tamoxifen inducible-transgenic line in young and aged mice to induce an ubiquitary Nrg1 acute ablation before the injury, deleting all Nrg1 isoforms. For more information on this transgenic line, please

refer to the corresponding section in Material and Methods (*Tamoxifen-inducible transgenic mice characterization*).

Again, we traced callosal projections through viral vectors expressing GFP under human Synapsin promoter to specifically label neurons in the left primary motor cortex. Next, we induce Nrg1 deletion one-week prior CCD by tamoxifen administration. Brains were collected 8 days after CCD to study the histology of injured mice (see timeline of the experiment in **Figure 26A**).

As previously described, we measured GFP intensity distribution in the PL area to analyze the contralateral wiring distribution (**Figure 31A**). Similar to the results shown in **Figure 30**, the cortical profile analysis revealed an GFP intensity increase in lower layers, followed by a decrease in upper ones in both young and aged mice. Although we did not detect evident differences in cortical profile between WT and $Nrg1^{-/-}$ (**Figure 31B-C**), we observed a slightly reduction of GFP intensity in cortical layers V and IV in young (**Figure 31B'**) and aged $Nrg1^{-/-}$ mice (**Figure 31C'**), respectively. Of note, we did not observe evident differences in cortical profile distribution in WT and $Nrg1^{-/-}$ not injured samples, suggesting that Nrg1 acute deletion might not modify contralateral cortical wiring prior to the injury (*data not shown*).

As an advantage of using callosal projection as a model, we next investigated the contralesional area to investigate the process of circuitry remodeling in connected cortical regions upon CCD. To this aim, we measured the GFP intensity in upper and lower cortical layers, as shown in **Figure 32A**. We were not able to detect individual neuronal somas, or the scar left by the needle to determine whether the phetoype is biased by stereotactic procedure. However, the virus diffused widely dorsoventrally and lateromedially within the samples, so the GFP intensity was comparable within the selected slices used in the analysis.

Interestingly, the data showed a decline of GFP intensity in the upper layers of $Nrg1^{-/-}$ mice (**Figure 32B-C**), statistically significant in the young population (**Figure 32B'**). Future experiments will be needed to better ascertain whether Nrg1 deletion enhances a remodeling process in connected cortical regions after injury, by quantifying neuronal somas or dendritic spines in confocal images at higher magnification.

Altogether, our results suggest that the acute deletion of Nrg1 expression affected contralateral cortical wiring after cortical damage in cortical layer V and IV in both young and aged mice, respectively. Furthermore, this remodeling process was also detectable in the contralesional cortex, pointing out that Nrg1 signaling can be a promising molecular target to modulate the rewiring process of cortico-cortical projection upon CCD in the adult brain. Nevertheless, future experiments are required to further elucidate the molecular and functional principles beyond the effect of Nrg1 signaling in circuitry refinement and plasticity upon cortical damage.

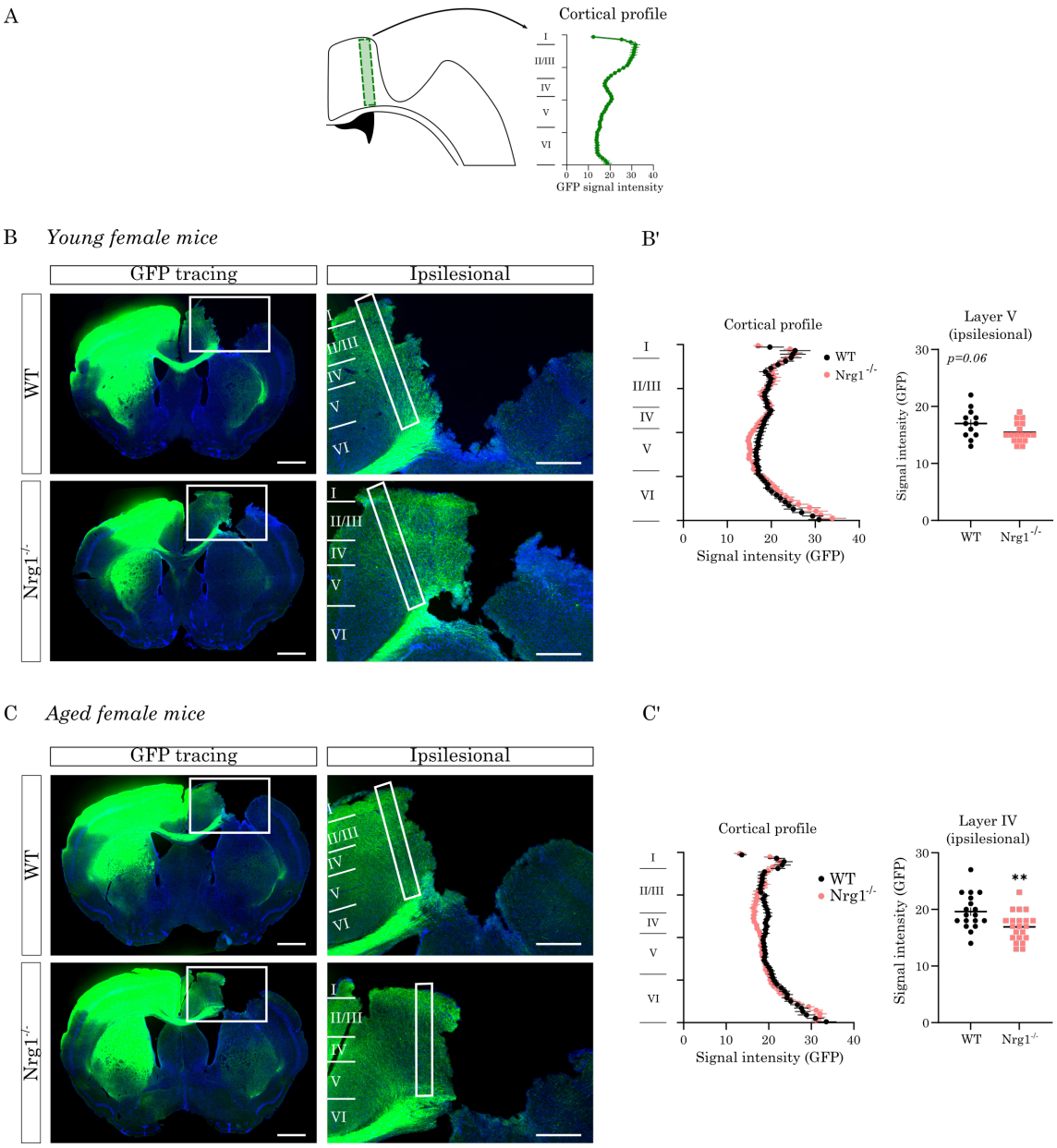

Figure 31. Nrg1 deletion altered contralateral cortical wiring in young and aged female mice upon CCD. A) The cartoon represent the ROI selected to analyze contralateral sprouting in the ipsilesional cortex. B) Representative images of WT and Nrg1$^{-/-}$ injured young mice (3-4 months). Magnified pictures of the boxed area are shown in the right. Scale bar: 1mm, boxed area 500µm. B') On the left, the graph shows the distribution of the normalized GFP intensity along the cortex in WT (black) and Nrg1$^{-/-}$ (red) aged mice. N = 12 (WT) and 17 (Nrg1$^{-/-}$) slices, statistical analysis: two-way ANOVA with repeated measurements and Sídák's multiple comparison test. On the right, the graph represents mean normalized GFP intensity value in layer V (right) in WT (black) and Nrg1$^{-/-}$ (red) young mice. Statistical analysis: Unpaired t-test. C) Representative images of WT and Nrg1$^{-/-}$ injured aged mice (11-13 months). Magnified pictures of the boxed area are shown in the right. Scale bar: 1mm. C') On the left, the graph shows the distribution of the normalized GFP intensity along the cortex in WT (black) and Nrg1$^{-/-}$ (red) aged mice. N = 18 (WT) and 21 (Nrg1$^{-/-}$) from two different series. Statistical analysis: two-way ANOVA with repeated measurements and Sídák's multiple comparison test. On the right, the graph represents mean normalized GFP intensity value in layer V (right) in WT (black) and Nrg1$^{-/-}$ (red) aged mice. Statistical analysis: Unpaired t-test.

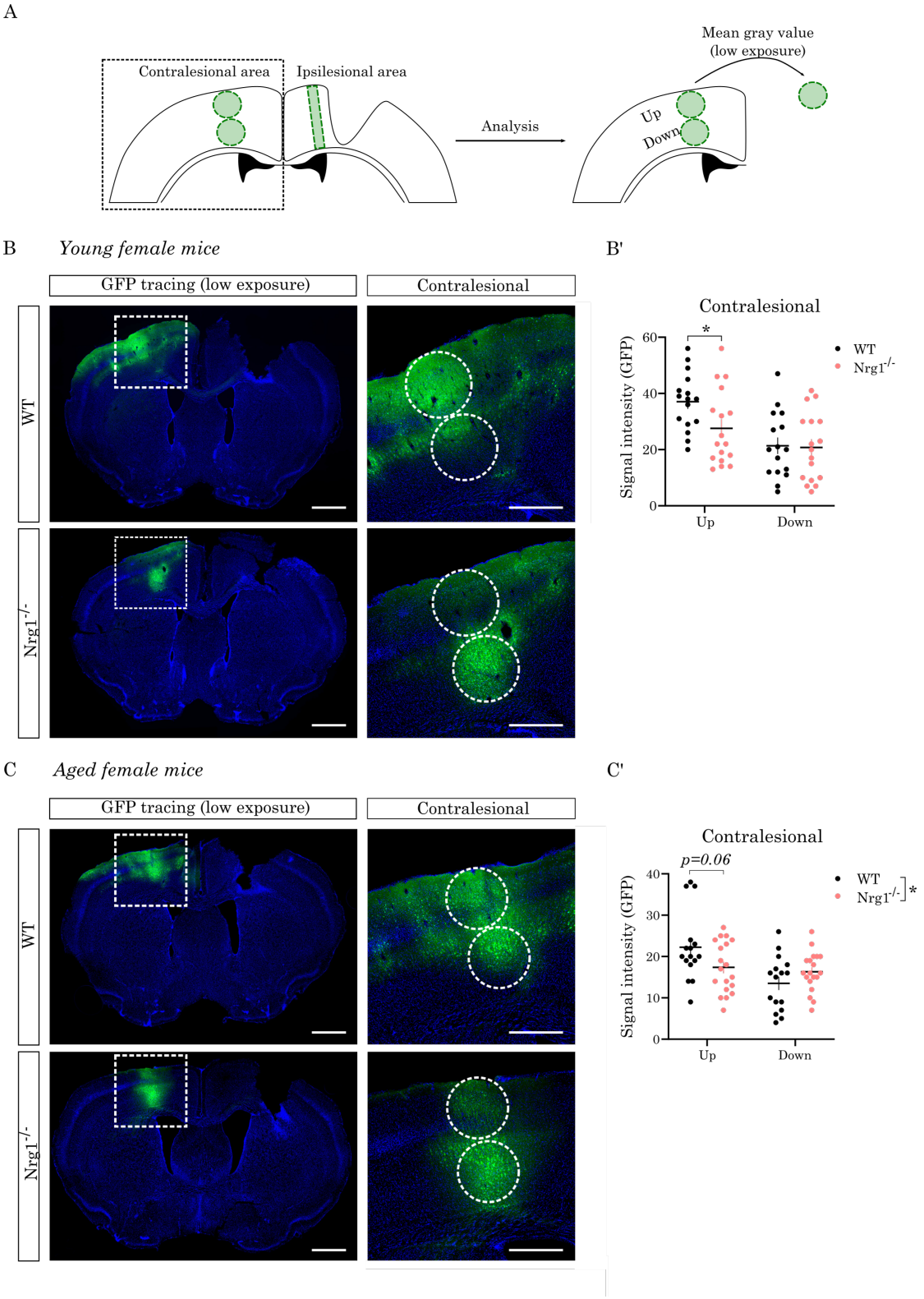

Figure 32. Analysis of the contralesional area in WT and Nrg1$^{-/-}$ young (B) and aged (C) female mice upon CCD. A) The cartoon illustrates the ROI selected to analyze the GFP intensity in the contralesional area, equivalent to the injection site. B-C) Representative images of WT and Nrg1$^{-/-}$ injured young (B) and aged (C) mice. On the right, magnified pictures are selected to show GFP intensity in the contralesional area in detail. 1mm, boxed area 500µm. B'-C') The graph represents the mean GFP intensity values of WT (black) and Nrg1$^{-/-}$ (red) injured young (B') and aged (C') mice,

quantified in the circles as shown in the cartoon (A). Statistical analysis: two-way ANOVA with repeated measurements and Sídák's multiple comparison test.

Nrg1 deletion reduced axonal preservation within cortical layers upon CCD.

The data described in *Chapter 1* revealed Nrg1 signaling as a promising factor to enhance axonal outgrowth upon axonal injury *in vitro*. Hence, we evaluated axonal preservation upon CCD in both young and aged mice, using the Nrg1 transgenic mouse line again (**Figure 8**). For more information on this transgenic line, please refer to the corresponding section in Material and Methods (*Tamoxifen-inducible transgenic mice characterization*).

To achieve this goal, we selected horizontal ROIs closer to the injury border to quantify GFP intensity within cortical layers, under the rationale that axons are more vulnerable near the injury border, translating in a lower GFP intensity. We used the DAPI staining as a reference to determine both injury limit and cortical layer position (**Figure 33A**). GFP intensity was analyzed in cortical layer II/III, IV and V in both young and aged mice (**Figure 33B-C**). The data revealed that the GFP intensity distribution was different between WT and $Nrg1^{-/-}$ young mice within layers IV and V, whereas in $Nrg1^{-/-}$ aged mice was detected in all the layers, observing a reduction of GFP signal nearby the injury (**Figure 33B-C**). As an additional quantification, we calculated the intensity fold change along each cortical layer (named ratio in the graphs of **Figure 33B'-C'**), finding out that axonal preservation was limited in both $Nrg1^{-/-}$ young and aged mice. For more information on axonal preservation analysis, please refer to the corresponding section in Material and Methods (*Cortical profile and axonal preservation*).

Altogether, the result showed that acute Nrg1 deletion prior to the injury was enough to impair axonal preservation 8 days after CCD induction in the adult brain. Hence, these data highlight the relevance of Nrg1 signaling in axonal preservation upon cortical damage, consistent with our preliminar *in vitro* results. Therefore, future experiments focused on synaptic markers, functional read out and different time-point will be required to further elucidate the effect of Nrg1 modulation in axonal regeneration and plasticity upon injury.

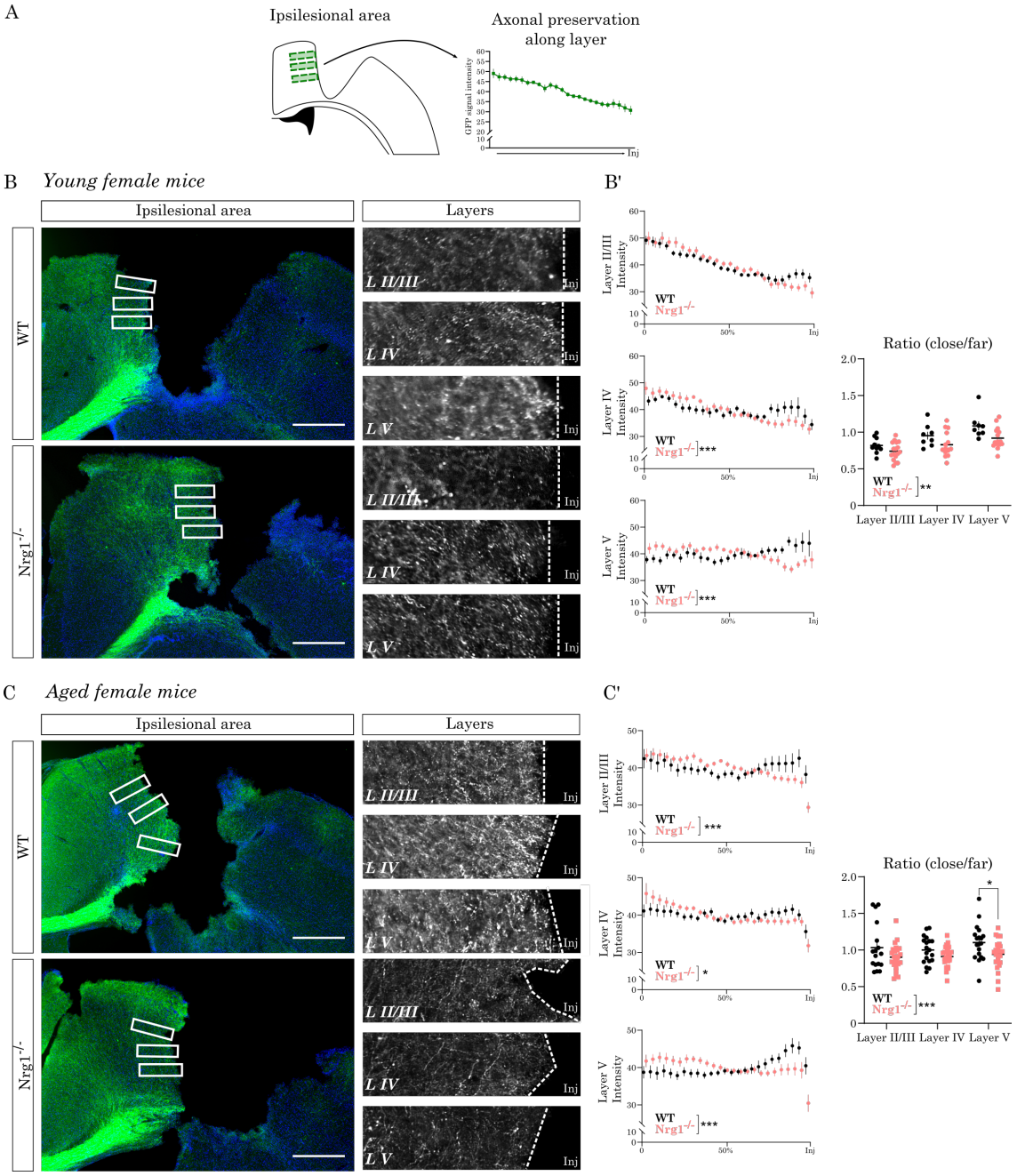

Figure 33. Nrg1 deletion reduced axonal preservation within cortical layers in young and aged female mice upon CCD. A) The cartoon illustrates the horizontal ROI selected to analyze GFP intensity in layer II/III, IV and V in the ipsilesional cortex. B-C) Representative images of young (B) and aged (C) mice to show axonal preservation in the PL region. The boxed areas are magnified on the right to facilitate the visualization. Scale bar: 500µm. B') Data from injured young mice is shown. On the left, graphs represent normalized GFP intensity distribution through each layer, getting closer to the injury border. N=10 (WT) and 17 (Nrg1$^{-/-}$). Statistical analysis: two-way ANOVA with repeated measurements and Sídák's multiple comparison test. On the right, the ratio between close/far is presented as a different analysis to show axonal preservation. Statistical analysis: two-way ANOVA with repeated measurements and Sídák's multiple comparison test. C') Data from injured young mice is shown. On the left, the graphs represent normalized GFP intensity distribution through each layer, getting closer to the injury border. N= 17-19 (WT) and 25 (Nrg1$^{-/-}$) slices. Statistical analysis: two-way ANOVA with repeated measurements and Sídák's multiple comparison test. On the right, the

ratio between close/far is presented as a different analysis to show axonal preservation. Statistical analysis: two-way ANOVA with repeated measurements and Sídák's multiple comparison test.

Nrg1-ICD expression could modulate axonal sprouting in not injured samples.

Most of the studies investigated the role of Nrg1 in cortical neuroprotection mediated via ErbB4 activation, which is mainly expressed in PV^+ cortical interneurons (Fazzari, et al. 2010). However, this signaling pathway does not entirely recapitulate the complexity of Nrg1 signaling and would only consider the communication between pyramidal and PV^+ interneurons. In this regard, we have previously identified that Nrg1 intracellular signaling is a promising molecular target upon stroke, promoting neuronal survival by regulating pro-apoptotic gene expression (Navarro-González, et al. 2019). Nevertheless, its effect in axonal regeneration upon injury is still unaddressed. Therefore, we next investigated whether Nrg1-ICD expression can modify cortico-cortical projections prior CCD.

To achieve this objective, we traced cortico-cortical projections using GFP or Nrg1-ICD-expressing viral vector in young female mice (4 months), where a selective number of neuronal cells are just targeted. For more information on viral construct and dilution used, please refer to the corresponding section in Material and Methods (*Nrg1 construct and adenoassociated viral vectors*).

To evaluate whether Nrg1-ICD expression modifies cortico-cortical sprouting prior to injury, we analyzed cortical profile in the right motor cortex (contralateral to the injection site) in GFP and Nrg1-ICD not injured groups (**Figure 34A-B**). Surprisingly, the data showed differences in cortical profile distribution 1 month after Nrg1-ICD expression (**Figure 34C**). Particularly, GFP intensity was increased in layer VI while decreased in layer II/III in Nrg1-ICD injected samples (**Figure 34D**). For more information on how image analysis was performed, please refer to the corresponding section in Material and Methods (*Cortical profile and axonal preservation*).

To further elucidate whether this phenotype could be biased by viral infection, we analyzed the left motor cortex, corresponding to the injection site (**Figure 34A-B**). We failed to count individual infected neurons at this magnification to check if Nrg1-ICD presented more preference in some specific cortical layer. To try a different strategy, we used low exposure images to measure GFP intensity in the upper and lower half of the injection site, as showed in the cartoon of **Figure 34A**. This quantification showed that GFP intensity was greatly seen in upper layers in GFP group, while GFP intensity was homogeneously distributed along cortical layers in Nrg1-ICD ones (**Figure 34E**). At this point, it is important to remind that a mixture of Nrg1-ICD and GFP viruses was used for Nrg1-ICD samples to improve GFP signal along axonal projections, which add complexity to understand if Nrg1-ICD specifically infected lower cortical layers.

Considering this information, we tried to normalize the contralateral sprouting to the intensity measured in the injection site, finding out that the intensity of all the cortical layers was higher in Nrg1-ICD injected mice, compared to GFP samples (**Figure 34F**). Nonetheless, the data obtained from the analysis of intensity in the injection site did not necessarily correlate with the rationale of higher intensity means higher number of infected neurons, but it might be biased by intensity derived from neuronal dendrites and lateral sprouting.

Altogether, our data suggest that Nrg1-ICD expression increased GFP intensity in lower cortical layers, whereas reduced it in upper ones, speculating that it can be a potential molecular target to modulate contralateral cortico-cortical wiring in the physiological adult brain. However, it is relevant to consider the complexity of this analysis, due to different sources of variability, such as virus distribution along the injection site. Hence, future experiments are required to confirm the role of Nrg1 intracellular signaling in cortical remodeling in adult brain.

A

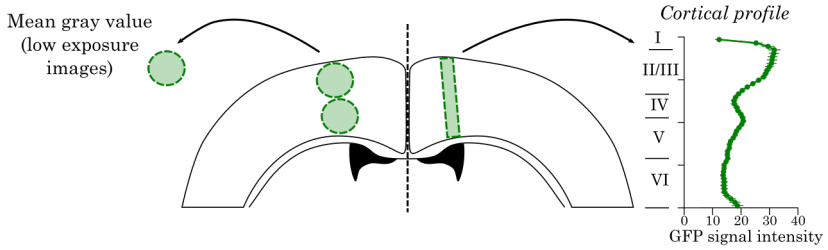

B *Young female mice*

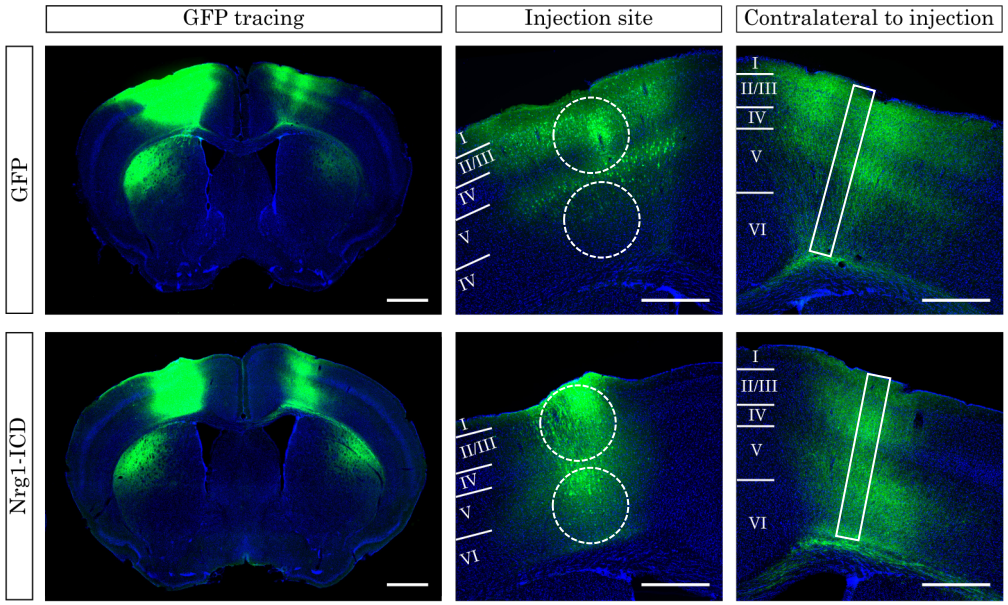

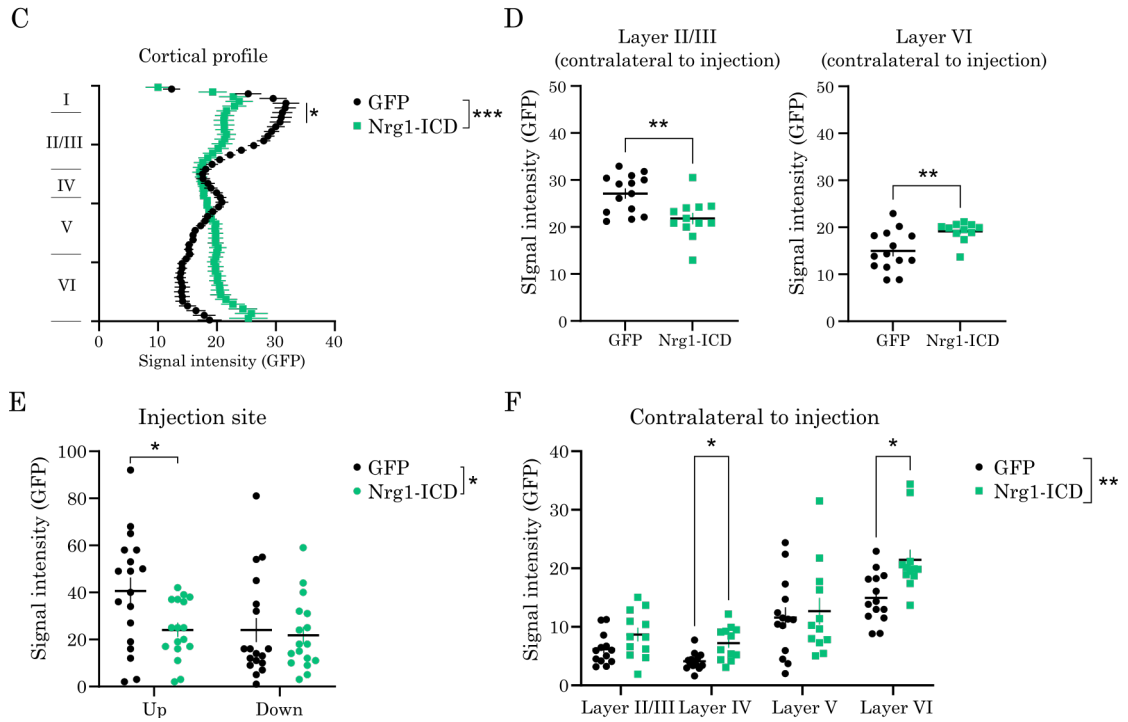

Figure 34. Nrg1-ICD expression could modulate cortical wiring pattern in young female mice (4 months) prior to injury induction. A) The cartoon illustrates the ROI selected to analyze GFP intensity in the injection site (left cortex, circles) and in the contralateral sprouting (right cortex, rectangle). B) Representative images of not injured samples. In detail, the middle column shows the injection site area, while in the right column the contralateral to injection cortex is shown to visualize cortical projection distribution along the cortical layers. Scale bar: 1mm, boxed area 500µm. C) The graph presents the normalized GFP intensity of the contralateral sprouting analyzed in the right cortex as shown in the cartoon (A) for GFP and Nrg1-ICD not injured samples. N= 14 (GFP) 13 (Nrg1-ICD) slices. Statistical analysis: two-way ANOVA with repeated measurements and Sídák's multiple comparison test. D) The graphs show normalized GFP intensity in the Layer II/III (left) and Layer V (right) in not injured samples. Statistical analysis: Unpaired t-test. E) The graph shows GFP intensity analyzed in the selected circles of the injection site as shown in the cartoon. F) The graph presents GFP intensity of the different cortical layers, relative to the injection site GFP intensity. Statistical analysis: two-way ANOVA with repeated measurements and Sídák's multiple comparison test.

Nrg1-ICD expression increased axonal sprouting in lower layers upon CCD.

Regarding the challenging result interpretation in the scenario of not injured samples, we evaluated whether Nrg1-ICD expression affected axonal sprouting upon CCD. According to what we showed above, we used Nrg1-ICD not injured samples as the basal state, which is ideal control under the rationale that Nrg1-ICD expression may remodel cortical profile.

As previously explained, we measured GFP intensity in the right motor cortex of comparable slices, selecting ROI in the ipsilesional area of injured samples. In the case of not injured brains, we selected homotopic regions in the right motor cortex, contralateral to the injection site (**Figure 35A**).

As seen in the analysis performed in GFP groups, the data showed a different cortical projection pattern upon injury compared to control conditions (**Figure 35B-C**). Specifically, we detected an increase in layer VI intensity, while a decrease in layer II/III intensity after CCD induction (**Figure 35D**).

Regarding these data, the results suggested similar conclusions in both GFP and Nrg1-ICD injured samples. To explore whether Nrg1-ICD expression produces any specific alteration in cortical sprouting within layers, we compared the fold change in GFP intensity of GFP and Nrg1-ICD injured groups, normalized to its respective not injured group. The data showed just a significant decrease in GFP intensity in layer VI in Nrg1-ICD injured samples, compared to GFP injured brains (**Figure 35E**).

Overall, these results suggest that a process of cortical remodeling is caused upon CCD, regardless Nrg1-ICD expression. Considering the intricacy of the analysis and, hence, in understanding this biological question, future experiments are required to better comprehend the role of Nrg1 intracellular signaling in cortical remodeling after cortical damage.

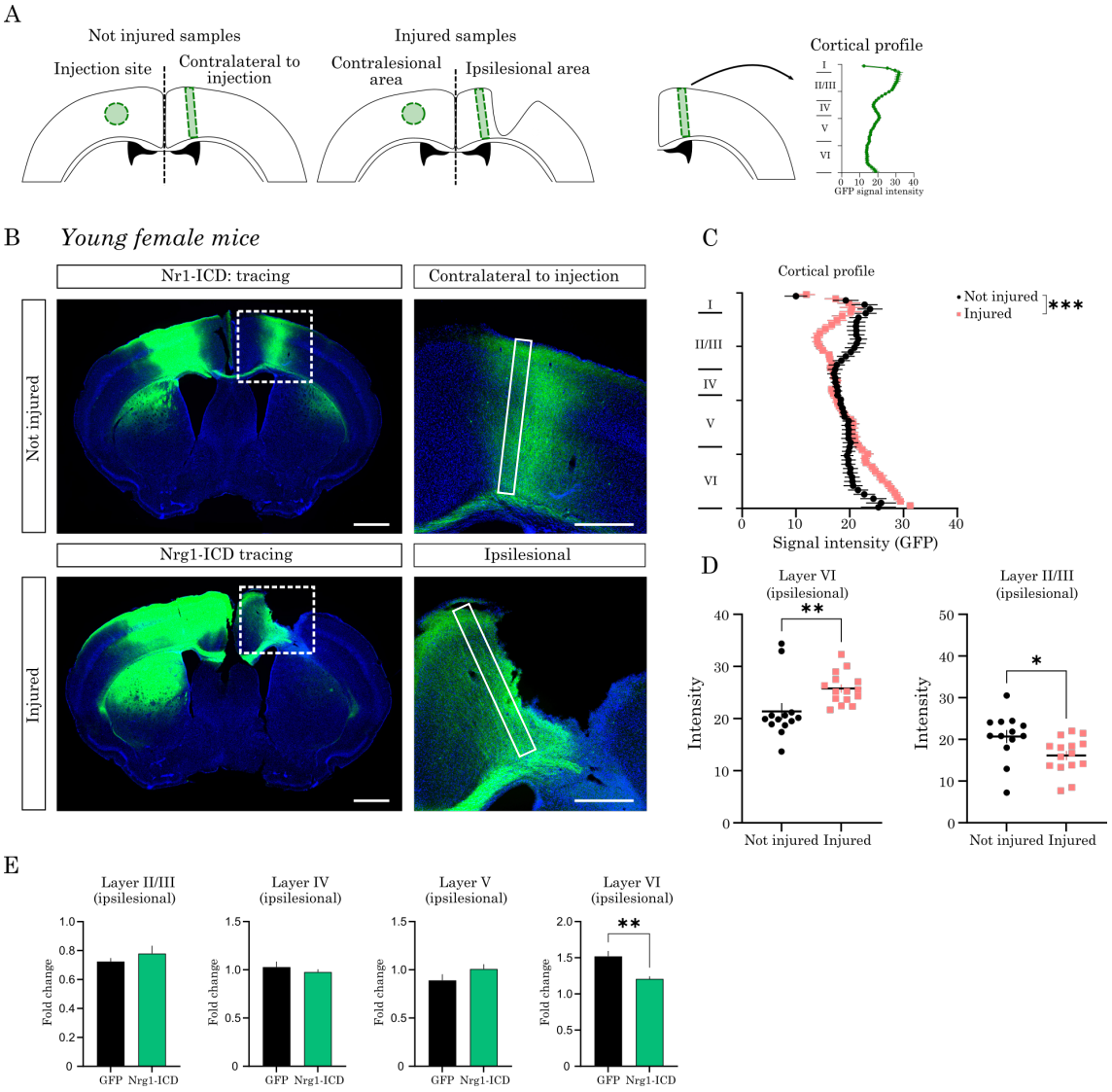

Figure 35. Nrg1-ICD expression increased cortical wiring in lower cortical layers in young female mice upon injury. A) The cartoon represent the ROI selected to analyze contralateral sprouting in both not injured and injured samples. B) Representative images of not injured and injured samples, expressing Nrg1-ICD. Magnified pictures of the boxed area are shown in the right. Scale bar: 1mm, boxed area 500µm. C) Graph represents the distribution of normalized GFP intensity along the cortex for not injured (labeled in black) and injured (labeled in red) samples. N = 13 (not injured) and 15 (injured) slices. Statistical analysis: two-way ANOVA with repeated measurements and Sídák's multiple comparison test. D) The graphs show the normalized GFP intensity values in Layer VI (left) and Layer II/III (right) of not injured (black) and injured (red) samples. Statistical analysis: Unpaired t-test. E) The graphs show the comparison of GFP intensity in layer II/III, IV, V and VI between GFP (black) and Nrg1-ICD (green) injured groups. The fold change is calculated by normalizing the data to each respective not injured group. N = 17 (GFP) and 15 (Nrg1-ICD). Statistical analysis: Unpaired t-test.

DISCUSSION

Brain damage induces axonal sprouting and the formation of novel neuronal circuitry patterns within PL areas. However, this process is limited in the CNS, especially in adult population, leading to permanent disabilities. Hence, understanding the molecular, cellular, and structural mechanisms underlying axonal sprouting and circuit remodeling is a pivotal step to ultimately promote functional recovery upon injury. Our results suggested that Nrg1 acute deletion prior to injury induction altered contralateral cortical wiring and restricted axonal preservation in both young and aged population. Hence, these data provide evidence that point out the relevance of Nrg1 signaling as a promising molecular target to ensure cortical wiring and axonal preservation upon cortical damage.

Herein, we target contralateral projections through the CC as an ideal experimental paradigm to study axonal sprouting upon injury. In this regard, the CC is the major mammalian commissural tract, connecting both hemispheres (De León Reyes et al., 2020; Fame et al., 2011). Furthermore, labeling callosal connections allows to separate the soma from the axonal projection in the same coronal section. Of note, this strategy has been used by several groups to understand the development of cortical connectivity (Courchet et al., 2013; Courchet et al., 2018; Mukai et al., 2015; Suárez et al., 2014). Recently, using *in vivo* imaging and retrograde trace labeling, it has been described that contralesional callosal neurons suffered a process of dendritic spine remodeling following cortical damage (Chovsepian et al., 2023; Empl et al., 2022). However, to the best of our knowledge, there is a lack of studies understanding the remodeling process of contralateral projections within cortical layers in the ipsilesional cortex.

Remarkably, we provided here a refined tool to deeply analyze contralateral cortical wiring by targeting a selective number of cortico-cortical projecting neurons, which gives a cell-autonomous readout. Furthermore, this experimental scenario overcomes the limitations observed in other histologic approaches that use neurofilament proteins as a generic marker of axons, but do not completely recapitulate cortical wiring processes (Carmichael et al., 2017).

Using this methodology, we examined whether contralateral projection distribution along cortical layers is altered upon CCD. Our results showed that GFP intensity along the cortical layers is modified following focal cortical injury. Interestingly, a decrease in GFP intensity is detected in layer II/III of injured samples, mainly targeted by callosal projections. Regarding this observation, we can speculate that layer II/III could be more vulnerable upon focal injury. Indeed, this explanation correlates to previous data describing that callosal neurons present a specific vulnerability in early stages following injury, showing a significant loss in dendritic spine density (Empl et al., 2022). Conversely, an increase in GFP intensity was observed in layer VI upon injury. Different anatomical and functional studies described that this cortical layer controls

the flow of information of cortical networks by targeting local cortical layers, thalamic and other cortical structures (Briggs, 2010). Regarding these data, we can speculate that a reinforce of lower cortical layers could be a compensatory response to the susceptibility shown in upper layers. However, we cannot assume a cortical circuitry shift upon CCD by histological characterization just one week after the damage. Therefore, future experiments at different time-points are required to better comprehend how cortical circuits are remodeled after cortical damage, complemented with functional approaches and synaptic markers characterization. Altogether, we provided a useful tool to analyze cortical circuit shaping after injury, which permits to investigate certain gene-of interest, such as Nrg1, as performed in this thesis.

The neuroprotective role of Nrg1 signaling upon brain damage has been mainly assessed using classical histological approaches to determine injury volume, neuronal survival, or glial/immune response after the administration of Nrg1 soluble form (Gu et al., 2017; Guan et al., 2015; Iaci et al., 2016; Xu et al., 2005; Zhang et al., 2018). However, considering that Nrg1 effect is only mediated by the activation of the ErbB4 receptor may conform a caveat in the literature, regarding that 1) ErbB4 is mainly expressed in PV^+ interneurons, represeting a small fraction of the total number of neurons and other cell types throughout the cortex and 2) Nrg1 entails a complex signaling process, where the activation of its intracellular pathway promotes neuronal survival upon stroke (Fazzari et al., 2010; Navarro-González et al., 2019). Additionally, most studies so far focused on the early neuroprotective response after damage, whereas how Nrg1 signaling contributes to axonal regeneration following damage remains poorly unaddressed.

To this aim, we developed a tamoxifen-inducible transgenic mouse model to acutely delete Nrg1 expression prior to cortical injury, disrupting all the variety of Nrg1 isoforms. Noteworthy, this experimental paradigm conforms the first attempt in the literature to investigate Nrg1 signaling in cortical wiring upon brain damage, where animals present a normal cortical development. In this context, our data did not reveal significant differences between cortical profiles comparing WT and Nrg1 deficient mice. However, examining specifically within layers, $Nrg1^{-/-}$ aged mice showed a decrease in GFP intensity in layer IV, whereas in $Nrg1^{-/-}$ younger mice we detected a trend toward decreased GFP intensity in layer V.

Additionally, we also quantified GFP intensity in the contralesional cortex to examine whether Nrg1 deletion can modulate structural changes in other connected brain areas. Interestingly, we observed that GFP intensity was reduced in upper layers of $Nrg1^{-/-}$ injured samples, offering novel insights of Nrg1 effect in the remodeling processes of contralesional cortex upon injury. In this sense, future analysis in higher magnification confocal images or using two-photon *in vivo* imaging could help to better understand whether these structural changes can be due to a decrease in neuronal survival or disruption in dendritic arborization after injury.

Although future studies are required to deeply ascertain the effect of Nrg1 signaling in modulating cortical circuitry upon damage, these data show that Nrg1 can be a potential factor in the process of cortical remodeling. Furthermore, considering that the cortical layers project to different brain regions and spinal cord, it would be also interesting to explore whether Nrg1 signaling modulates structural changes in different cortical and subcortical regions upon CCD.

To further study the relevance of Nrg1 signaling in axonal preservation upon injury, we adjusted the protocol of analysis, using horizontal ROIs to quantify GFP intensity within layer II/III, IV and V. This strategy allows us to investigate axonal integrity in PL areas in each specific cortical layer. Our data shows that $Nrg1^{-/-}$ animals presented a restricted axonal preservation within layer II/III, IV and V of the ipsilesional cortex in both young and aged mice. This piece of evidence correlates with recent data in which the administration of Nrg1 soluble isoform reduces SMI-32 expression upon cortical phototrombosis, used as a classical histologic marker of axonal degeneration (Cui et al., 2023). Hence, our data suggests that Nrg1 signaling is a potential neuromodulatory factor that may prevent from axonal degeneration upon cortical damage, necessary even in young adulthood.

To further elucidate the role of Nrg1 signaling in contralateral cortical wiring upon damage, we used viral vector under Synapsin promoter to specifically label and express Nrg1-ICD in a selective number of targeted cortico-cortical neurons. Interestingly, we observed that the cortical profile of Nrg1-ICD treated animals was already sculpt prior to injury, suggesting for the first time that Nrg1-ICD expression might promote changes in cortical rewiring in the adult brain.

Coincidentally, we also observed that GFP intensity pattern was homogeneously distributed through the different cortical layers in the injection site of Nrg1-ICD samples, whereas in the GFP group was highly found in upper cortical layers. On one hand, we can speculate that Nrg1-ICD could preferably infected neuronal cells of different cortical layers, such as layer V. On the other hand, the stimulation of Nrg1 intracellular signaling promotes dendrite maturation in postnatal developmental stages (Chen et al., 2010; Fazzari, Snellinx, Sabanov, et al., 2014). Regarding this fact, discrepancy in GFP intensity pattern can be not only due to differences in number or localization of targeted neurons, but also to changes in dendritic spine formations after Nrg1-ICD expression. Therefore, future analysis using higher magnification confocal images are required to understand the impact of Nrg1 intracellular signaling in neuronal number and distribution in adult cortex, as well as the maturation of dendritic arborization.

In the context of brain damage, our data showed that Nrg1-ICD expression also altered cortical profile in injured samples compared to not injured ones. Analyzing GFP intensity within layers, we observed an increase in layer VI while a decrease in layer II/III, likely to the results obtained comparing GFP groups. However, considering the possible influence of Nrg1-ICD in cortical

rewiring remodeling in physiological conditions, understanding the role of Nrg1 intracellular pathway in cortical sprouting upon brain damage entails a non-trivial interpretation in this model. To better unravel the importance of this signaling, it would be necessary to perform a different experimental scenario using lentiviral vectors, which induce gene expression more rapidly compared to adenoassociated virus (Zheng et al., 2018), or a viral construct whose expression can be conditionally inducible using tamoxifen to promote Nrg1-ICD expression after injury (Kelmenson, 2011).

Axonal regeneration is a complex scenario in which a combination of intrinsic and extrinsic events is involved in a multifactorial mode (Hilton & Bradke, 2017). During developmental stages, different signaling pathways are activated to promote axonal growth and elongation, regulating cytoskeletal dynamics, which are silenced in adulthood to avoid abnormal circuit connectivity (Curcio & Bradke, 2018). Hence, finding novel molecular targets that enhance these molecular programs can potentiated axonal regeneration. In this context, Nrg1 signaling has been described as a regulator of different signaling pathways that contribute to regeneration, such as PI3K/Akt/mTOR or RhoA/Cofilin in different *in vitro* and *in vivo* models of CNS and PNS injury (Guo et al., 2010; Hao et al., 2020; Mancuso et al., 2016; Mòdol-Caballero et al., 2018). However, the diverse types of Nrg1 isoforms and signaling pathways can produce different effects in physiological and injured states (Kataria et al., 2019). Therefore, future studies are required to entirely recapitulate the molecular and biochemical mechanisms underlying the effect of Nrg1 signaling upon regeneration.

Furthermore, several groups have described the relevance of Nrg1 signaling in the process of remyelination, which conforms an important regenerative event to enhance functional recovery. In this sense, it has been reported that the administration of Nrg1 promoted oligodendrocyte proliferation and myelin regeneration via the activation of PI3K/Akt pathway (Cui et al., 2023). However, this study evaluates Nrg1 exogenous effect via ErbB receptors, underestimating the impact of different Nrg1 isoforms. For example, Nrg1 type III is mainly retained in cell membrane, regulating myelination in a juxtracrine manner (Bartus et al., 2016; Birchmeier & Bennett, 2016). Of note, Nrg1 type III represent the most abundant isoform in adult brain (Liu et al., 2011). Hence, it would be interesting to investigate the biology of oligodendrocyte and remyelination process in our Nrg1 transgenic mice upon CCD, as well as specifically expressing Nrg1-ICD to evaluate whether the activation of its intracellular signaling can modulate concrete gene expression programs to enhance cortical regeneration.

Although our results provide intriguing information about the role of Nrg1 signaling in axonal sprouting after focal cortical injury, our study has several limitations. Our analysis is mainly focused on the histological characterization of contralateral wiring detected one week after injury. This limits our scientific question to axonal preservation rather than regeneration or

cortical plasticity, considering that molecular and cellular changes that promote cortical plasticity after injury occur in a time-dependent manner (Joy & Carmichael, 2021). Furthermore, some methods available in the literature used anterograde tracers injected after injury, such as BDA, to assess axonal sprouting after stroke, which may involve the cortical rewiring process of already established connections and the formation of new cortical projections from connected brain areas (Dancause et al., 2005; Joy et al., 2019; Overman et al., 2012). Conversely, we traced cortico-cortical projections using viral vectors 1 month prior to injury induction to ensure an adequate infection and expression rate. Despite the broad anteroposterior and lateromedial diffusion of viral vectors, it is worth mentioning that this experimental scenario may not fully recapitulate the strict process of axonal sprouting, defined as the compensatory growth of new connections from not injured axons of adjacent and distant connected brain regions. In this sense, our data may mainly reflect lateral sprouting and axonal displacement of already targeted contralateral projections.

Nevertheless, our model provides novel insights to study axonal regeneration and cortical rewiring after injury, which may help to fully understand the rewiring process of cortical circuits to PL areas and other connected regions of the brain. Hence, future experiments at different time-point and combining tracing techniques after injury will be required to better elucidate the role of Nrg1 signaling in cortical plasticity upon cortical damage, including complementary analysis of synaptic marker characterization, dendritic spine density remodeling and ultimately, two-photon *in vivo* imaging or electrophysiological functional approaches.

Overall, our data shed light on the effect of Nrg1 signaling as a potential regulator of contralateral cortical wiring and axonal preservation after cortical damage. We hope that the *in vivo* model developed here can provide a powerful experimental paradigm to elucidate the molecular and cellular basis of Nrg1 signaling in cortical regeneration after brain injury.

GENERAL DISCUSSION

Nrg1/ErbB signaling has been identified not only as a risk factor in psychiatric disorders, but also as a potential modulator in the context of CNS injury and repair (Kataria et al., 2019). In this scenario, several studies reported that Nrg1 promotes functional recovery upon ischemic stroke by preventing neuronal death and reducing neuroinflammatory responses. However, little is known about the effect of Nrg1 signaling in cortical regeneration upon brain damage. In this PhD project, we developed novel *in vitro* and *in vivo* models to better investigate the role of Nrg1 signaling, and specifically the activation of its intracellular pathway, in axonal sprouting and neuroprotection after cortical damage. Our results support the relevance of Nrg1 signaling, and specifically its intracellular pathway, as a promising molecular target after cortical damage.

In the current literature, most of the methodologies administered the recombinant soluble form of Nrg-1β in *in vitro* and *in vivo* injury models to investigate the effect of Nrg1 exogenous via activation of ErbB receptors (Cui et al., 2023; Gu et al., 2017; Guan et al., 2015; Guo et al., 2006; Iaci et al., 2016; Li et al., 2007; Noll et al., 2019; Shyu et al., 2004; Xu et al., 2004). However, Nrg1 protein embraces a complex biology, based on different isoforms that can produce diverse function in the nervous system. Furthermore, the effect of Nrg1 can be mediated by different signaling pathways, such as the translocation of its intracellular domain, which regulates gene expression (Bao et al., 2003; Mei & Nave, 2014; Mei & Xiong, 2008). Additionally, injury induction is usually provoked by the MCAO model which requires non-trivial surgical procedures that generate massive injuries, affecting cortical and subcortical areas. In this experimental paradigm, the analysis is mainly focused on functional motor characterization, quantification of injury volume by TTC staining and traditional histological and molecular approaches to study inflammatory response and biochemical mechanisms in peri-infarct tissue. However, the study of specific molecular and cellular events underlying cortical recovery and repair is difficult to address when brain tissue is considerably damaged. Even though this experimental set up implements significant results, novel models are required to unravel the molecular mechanisms underlying the intricacy of Nrg1 signaling in CNS repair.

In this context, we developed valuable genetic neuromodulatory models to specifically target Nrg1 signaling using *in vitro* and *in vivo* approaches. First, we used electroporation techniques to perform a sparse labeling of cortical cultures (Rodríguez-Prieto et al., 2021), applied to an affordable, user-friendly, and reproducible *in vitro* model of axonal injury. This strategy allows us to carry out GOF and LOF studies to examine Nrg1 signaling in axonal sprouting with a cell-autonomous resolution. Our results suggest that Nrg1, and concretely the activation of its intracellular signaling, promotes axonal outgrowth upon injury *in vitro*.

Moving forward to *in vivo* approaches, we first designed an innovative *in vivo* model of brain damage, combining tracing of cortico-cortical projection and a focal and reproducible cortical injury (named CCD). In this experimental scenario, we carried out an extensive behavioral characterization to offer sensible task to detect motor impairment in focal injuries. We also created a semi-automated 3D brain reconstruction from floating sections, which permits to combine different immunolabelings to study cellular and subcellular events upon injury. As a biological outcome, we analyzed the integrity of PNNs in the PL area, observing an abrupt disruption that correlates with microglia/macrophage activation. Overall, this model provides an effective methodological strategy to unveil the molecular and cellular interactions contributing to cortical regeneration after brain damage (González-Manteiga et al., 2022).

To better understand cortical rewiring in the brain damage scenario, we targeted contralateral cortico-cortical projections across the CC in WT young mice. As expected, we observed that the cortical profile was altered in injured animals, suggesting that contralateral projections to the ipsilesional cortex are affected by CCD. Interestingly, we detected that GFP intensity was notably reduced in cortical layer II/III, which is mainly targeted by callosal neurons, in concordance with previous data suggesting a particular vulnerability of callosal neurons to cortical injury (Chovsepian et al., 2023; Empl et al., 2022).

Next, we applied the CCD model to a tamoxifen-inducible transgenic mouse to induce acute ubiquitous Nrg1 deletion prior to cortical damage, allowing an extensive functional motor characterization and histological analysis in which we especially evaluate the impact of Nrg1 ablation in contralateral sprouting upon cortical damage. Interestingly, we observed for the first time that Nrg1 deficiency reduced axonal preservation within cortical layers upon focal cortical damage, and a functional motor impairment. Of note, this phenotype was seen in young (3-4 months) and aged (9-12 months) female mice, highlighting the relevance of Nrg1 signaling since early adulthood for neuroprotection upon brain damage.

We previously reported that Nrg1 intracellular signaling promotes neuronal survival upon hemorrhagic stroke (Navarro-González et al., 2019). To delve deeper into the effect of Nrg1, we further analyzed whether the activation of its intracellular pathways contributes to neuroinflammatory response and axonal sprouting upon CCD. To achieve this goal, we selectively targeted contralateral cortico-cortical neuronal projections in which we expressed Nrg1-ICD to facilitate axonal sprouting analysis, giving a cell-autonomous resolution. Surprisingly, we observed a trend towards decreased Iba1 staining in Nrg1-ICD-treated animals, suggesting that Nrg1 signaling can regulate the inflammatory response not only mediated by ErbB4 activation as usually described, but also by modulating a specific neuronal gene expression program.

Furthermore, we also observed that Nrg1 intracellular signaling can potentially modulate contralateral sprouting prior to injury induction in adult brain, which complicates data interpretation in the context of brain damage. However, we noted that future experiments are required to better elucidate whether Nrg1 intracellular signaling can enhance axonal regeneration upon injury using a different experimental strategy to express Nrg1-ICD after injury.

Noteworthy, most of the studies have focused on the PL area, where several molecular and cellular changes occur upon brain damage. However, our data and others provide further insights into the remodeling processes that take place in other connected brain regions after injury (Empl et al., 2022; Jones et al., 1996; Murphy & Corbett, 2009; Takatsuru et al., 2009). In our experimental scenario, we investigate the implication of contralateral cortico-cortical projections in the ipsilesional cortex, but also evaluated whether a remodeling process account in the contralesional cortex and how Nrg1 signaling contributes to it. Interestingly, we investigated PNN integrity after injury, detecting a decrease in the number and intensity of WFA^+ cells in aged Nrg1 deficient injured mice. Although PNNs are associated with reopening plasticity period, their role in the brain damage scenario is controversial and remains poorly understood (Bozzelli et al., 2018; Wang & Fawcett, 2012a; Wen et al., 2018). However, this preliminary data suggests that PNNs remodeling is not restricted to PL regions, but also to interconnected brain areas. Accordingly, we observed a different pattern of GFP intensity in the contralesional cortex in both young and aged $Nrg1^{-/-}$ injured mice. Nevertheless, future experiments including an extensive analysis of subcellular parameters, such as synaptic markers and dendritic arborization, are required to better understand whether these cellular and structural changes contribute to cortical remodeling upon damage.

In conclusion, in this PhD dissertation we have shown that the development of novel preclinical models of focal cortical damage plays a pivotal role in studying the structural, cellular, and molecular changes in the subacute phase after damage to promote cortical regeneration and thus functional recovery. Subsequently, this experimental scenario can help to identify new molecular targets that boost neuroprotection and axonal sprouting, such as Nrg1 signaling, which is proposed here as a promising therapeutic target in the context of cortical damage.

FUTURE PERSPECTIVES

Brain injury is a complex disorder that particularly affects the elderly population. Despite the rapid evolution of biomedical advances increasing life expectancy, we are facing an era of an aging population in which this kind of disorders become a socioeconomic burden. Major efforts have been developed to better understand the molecular and cellular pathways underpinning brain damage, declining the mortality rate. However, it is still the leading cause of long-term disabilities, and there is not an effective treatment available yet.

There are several reasons why the translation of basic research findings to the human clinics has failed. Most of the studies have been focused on neuroprotection immediately after the damage, offering a limited window of response. However, it has been reported that there is a remodeling process in the PL region and other connected brain regions that enhance axonal sprouting, remyelination and circuit rewiring in the months following injury. Thus, it is necessary to take a step back to elucidate in depth these cellular and structural modifications upon damage, which remains poorly understood in CNS repair. To this aim, the development of novel *in vivo* preclinical models, such as the CCD model described here, plays a critical role in the brain damage scenario, providing an intriguing methodology to better study these long-term outcomes that ultimately can enhance functional recovery. Remarkably, to better recapitulate the heterogeneity of such a complex disorder, it is noteworthy to investigate not only in male adult animals, but also using both female and aged individuals to better characterize sex- and age-dependent mechanisms upon brain damage.

This PhD dissertation offers compelling data that shed light in the role of Nrg1 in brain damage scenario. However, it also raises intriguing and thought-provoking questions which would be exciting to address in the future.

In terms of neuroinflammation upon damage, our data suggest that Nrg1 intracellular signaling can be a potential regulator of the microglia/macrophage response, and not only via ErbB receptor activation. However, we shortly investigated this response by offering a volumetric quantification using Iba1 staining. Hence, future experiments looking into different cellular and subcellular responses will be required to confirm this mechanism. For instance, it would be feasible to obtain higher magnification confocal images in our experimental paradigm to better quantify 1) microglial morphology, which is highly correlated with its functionality and 2) microglial colocalization with axonal terminals to verify whether this inflammatory response is limited but sufficient to promote cellular debris clearance to provide a favorable environment for axonal sprouting and plasticity.

Moreover, we have already described that Nrg1-ICD can modulate gene expression. Thus, the next question will be to better characterize the specific genetic program modulated *in vivo* after brain damage and whether it promotes an anti-inflammatory response. In this sense, recent biotechnological advances have developed novel adenoassociated vectors capable of crossing the BBB, providing an intriguing strategy that may inspired future CNS gene therapy applications. In preclinical models, compared to stereotactic injection which selectively targets a limited number of neurons, this experimental strategy provides a high transduction efficiency by a simple intravenous injection (Huang et al., 2019; Mathiesen et al., 2020). To specifically study neuronal populations, this viral vector can be designed under Synapsin promoter and sorting of labeled neurons can offer sufficient biological material for *in vivo* genetic characterization using microarrays and quantitative real-time PCR validation. Complementary to the study of the neuronal population, we can also particularly investigate how Nrg1-ICD can directly modulate the immune response, by sorting $Iba1^{+}$ cells from the PL area and check whether their genetic profile is modified towards an anti-inflammatory profile, associated with a regenerative state.

Another challenge in the field of brain damage is to better elucidate the role of Nrg1 signaling in the context of cortical regeneration and synaptic plasticity. We have shown that Nrg1 deletion reduces axonal preservation upon cortical damage. However, do these data correlate with neuronal dysfunction and aberrant cortical rewiring? We already checked that Nrg1 deficient mice exhibited a reduced functional motor recovery. Nevertheless, to strengthen our scientific claim in the context of regeneration and plasticity, different experiments should be carried out.

Maintaining an adequate excitatory and inhibitory (E/I) balance is critical for proper cortical function. After brain damage, GABAergic transmission is increased to prevent neuronal loss, but, if this inhibitory state is prolonged, contributes to functional impairment (Clarkson et al., 2010). However, exacerbation of neuronal excitability can also be detrimental to cortical recovery, which can lead to epilepsy in the patients (Gazaryan et al., 2019). Hence, another challenge in the field is to provide novel molecular targets that restore a functional E/I balance. Notably, Nrg1 plays an essential role in cortical circuit development, reported in different transgenic Nrg1 mouse lines. Therefore, understanding whether Nrg1 signaling modulates neuronal activity and synaptic neurotransmission is a promising open framework.

In this context, our CCD model can also be exploited to evaluate electrophysiological properties of the affected neurons by selectively labeling neuronal populations in which the soma is easily identifiable for whole-cell patch registration at a single-cell level. Additionally, using higher resolution confocal images in the injection site, it will be possible to analyze dendritic spine density, where a remodeling process has been identified after damage. Remarkably, both electrophysiological and spine characterization can be assessed by whole-cell patch clamp and

in vivo two-photon imaging respectively, offering a dynamic perspective of cortical circuitry restoration at different time points.

Cortical circuitry is not only by neuronal intrinsic electrical properties, but also by neurotransmission. To answer this question, combining different synaptic markers and specific neuronal populations immunolabeling to quantify $GAD65^+$ inhibitory buttons on pyramidal neurons or the density of Vglut1 excitatory terminals on PV^+ cells can provide novel insights in the role of Nrg1 signaling in synaptic plasticity upon brain damage in both ipsi- and contralesional cortex.

Finally, another challenge worth exploring is whether Nrg1 signaling regulates cortical regeneration after cortical damage. To analyze axonal regeneration after damage, combining anterograde tracers in the contralesional cortex with retrograde tracers in the PL region can be a useful tool. However, it could be technically challenging, considering the disruption of the BBB which may complicate correct compound uptake and lead to misinterpretation of data.

Interestingly, axonal sprouting is not only identified in the PL area, but also in other connected brain regions. Accordingly, our data showed a different cortical profile upon injury, as we observed increased GFP intensity in lower cortical layers, which generally project to other cortical and subcortical areas and to the spinal cord via the corticospinal tract. Hence, it would be interesting to investigate whether Nrg1 signaling can compensate for cortical injury by promoting circuitry restoration cortical in other CNS areas. To answer this question, a fancy experimental approach will be to perform monosynaptic circuit tracing using modified rabies virus injected into the contralesional cortex, as previously used in a recent publication to elucidate how callosal neurons modulate their input circuitry after TBI (Empl et al., 2022). Furthermore, this approach can be combined with viral vectors to specifically express or delete Nrg1 expression in a selective number of neurons immediately after the injury.

In conclusion, novel steps into in the brain damage scenario will evolve towards the field of neuronal regeneration and plasticity, which will have a huge impact in the coming years thanks to the innovative advances of biotechnological tools. We hope that the data presented in this dissertation will provide compelling evidence and inspire future research to unravel the potential role of Nrg1 signaling in cortical regeneration and rewiring after brain injury.

CONCLUSIONS

The objectives addressed during the development of this PhD project highlight the relevance in developing novel *in vitro* and *in vivo* injury models to investigate Nrg1 signaling upon brain damage, suggesting as an interesting neuroprotective factor. The main conclusions of this thesis are written below:

1- We developed a novel *in vitro* model of axonal injury with minimal technical requirements that is affordable, reproducible, and provides a cell-autonomous readout to quantify axonal outgrowth. In this model, we investigated the role of Nrg1 signaling in gain- and loss-of function approaches, suggesting that Nrg1, and specifically the activation of its intracellular pathway, promotes axonal outgrowth following axonal injury *in vitro*.

2- We established a novel *in vivo* model for multiplexed analysis to study cortical damage, combining a focal mechanical lesion and a precise tracing of contralateral callosal projections using viral vectors. Additionally, we developed a flexible and semi-automated workflow to perform volumetric measurements and cellular resolution studies of the cortical tissue in multiple series, investigating PNNs integrity in the PL area. We performed an exhaustive behavioral characterization of the motor impairment provoked by CCD.

3- Nrg1 deficient mice showed a subtle motor impairment response and an increase in Iba1 staining, indicating an inflammatory response. Mechanistically, we observed that the expression of Nrg1-ICD reduced neuroinflammation, suggesting that Nrg1 intracellular signaling can partly mediate the neuroinflammatory response.

4- Nrg1 deficient aged mice presented lower number of PNNs in the contralesional cortex, suggesting that Nrg1 signaling may be involved in the remodeling process of cortical connected areas.

5- Tracing cortico-cortical projections through the corpus callosum, we demonstrated that contralateral cortical wiring is modified upon CCD, observing an increase in GFP intensity in the lower layers of injured samples, compared to not injured condition.

6- We evaluated the role of Nrg1 signaling in cortical wiring following cortical damage using a refined conditional transgenic mouse line to induce an acute deletion of Nrg1 expression prior to CCD. In this experimental paradigm, we discovered that the absence of Nrg1 altered contralateral cortical wiring and reduced axonal preservation upon injury in young and aged female mice.

Supplementary material S1: Composition of the different media used for cortical neuronal cultures.

PLATING MEDIUM		
MEM	42,5	ml
10% Horse serum or FBS	5	ml
30% glucose (0,6% final concentration)	1	ml
PS (penicillin, 10000 U/ml; streptomycin, 10mg/ml)	0,5	ml
ELECTROPORATION MEDIUM		
Opti-MEM		
NEURONAL MEDIUM		
Neurobasal medium	48,5	ml
B-27	1	ml
Glutamax 200mM	0,125	ml
PS (penicillin, 1000 U/ml; streptomycin, 10 mg/ml)	0,5	ml

Supplementary material S2: Antibody information.

PRIMARY			**SECONDARY**		
Name	*Dilution*	*Reference*	*Name*	*Dilution*	*Reference*
Anti-GFP	1:500 (*in vitro*), 1:1000 (*in vivo*)	GFP-1010, Ave Labs	Anti-chicken 488	1:500	A-11039, Thermofisher, Waltham, MA, USA
Anti-RFP	1:1000	600-401-379, Rockland antibodies	Anti-Rabbit 555	1:500	A31572, Life Technologies, Carlsbad, CA, USA
Anti-Iba1	1:500	234004, Synaptic systems	Anti-Guinea Pig 647	1:500	A21450, Invitrogen
Anti-Parvalbumin	1:250	195002, Synaptic systems	Anti-Rabbit 555	1:500	A31572, Life Technologies, Carlsbad, CA, USA
Anti-WFA biotinylated	1:1000	L1516-2MG, Sigma Aldrich, St. Louis, MI, USA	Streptavidin CyTM5	1:500	PA45001, GE Healthcare, Chicago, IL, USA
			Streptavidin A555	1:500	S21381, Thermofisher
			Anti-Mouse 555	1:500	A-21137, Thermofisher

Supplementary material S3: Python code for sorting the image stacks.

Requirements:

This automatic process was written in the Python language. For code execution, we used a Python installation in version >3.9 and we installed the tifffile and skimage libraries that are not included in the default installation. To simplify this task, Anaconda v2021.11 software was installed, facilitating the execution environment in the current operating systems (Window, Linux and MacOS).

When executing the code from the terminal, it is executed with the following arguments:

+ python3 ordered_stack.py DIRECTORY_OF_MOUSES

This argument must be the folder where the mouse folders with the tif files of the region of interest are stored. This would be an example of the structure:

```
Project
├── Mouse_384
│   ├── AGM52_384_DAPI_mask.tif
│   ├── AGM52_384_DAPI_stack.tif
│   ├── AGM52_384_GFAP_stack.tif
│   ├── AGM52_384_GFP_stack.tif
│   └── AGM52_384_Iba1_stack.tif
├── Mouse_389
│   ├── AGM52_389_DAPI_mask.tif
│   ├── AGM52_389_DAPI_stack.tif
│   ├── AGM52_389_GFAP_stack.tif
│   ├── AGM52_389_GFP_stack.tif
│   └── AGM52_389_Iba1_stack.tif
├── Mouse_393
┆   ┆
┆
```

Remarkably, the nomenclature of the files must have a specific format for a correct functioning. A scheme would be "subject_id_type_orig-or-mask.tif" where:

- subject_id: is our subject identifier.
- type: is the type of file we have (DAPI, IGG, GFP and Iba1 channels). For code sake, all 4 files must be present.

- orig-or-mask: Indicates if it is the original image stack or a mask. In this case, we will only have a mask for the DAPI version.

Script:

```
import sys
import numpy as np
import cv2
import tifffile
import os
from skimage import io
from skimage import morphology as morph
from pathlib import Path
# It goes through all the folder of the mice. NOTE: “glob” parameter distinguishes between upper- and lower-case letters
for subject_path in sorted(Path(sys.argv[1]).glob("*Mouse*")):
    print(f"processing mouse {subject_path.name}")
    # Create a forder where png results will be stored
    png_results = subject_path.joinpath("png_results")
    os.makedirs(str(png_results), exist_ok=True)
# For each mouse folder, it lists the directory. The code saves all objects in the folder, regardless of whether it is a folder or an image
    stacks = list(subject_path.iterdir())
# It sees if there is a file in the stack that says "mask"
    if any(["mask.tif" in str(file_) for file_ in stacks]):
# Save the path of each image
        dapi_path = [file_ for file_ in stacks if "DAPI_stack.tif" in str(file_)][-1]
        mask_path = [file_ for file_ in stacks if "DAPI_mask.tif" in str(file_)][-1]
        red_path = [file_ for file_ in stacks if "GFAP_stack.tif" in str(file_)][-1]
        green_path = [file_ for file_ in stacks if "GFP_stack.tif" in str(file_)][-1]
        farred_path = [file_ for file_ in stacks if "Iba1_stack.tif" in str(file_)][-1]
 # Image upload
        dapi = np.array(io.imread(str(dapi_path)))
        mask = np.array(io.imread(str(mask_path)))
```

```
        red = np.array(io.imread(str(red_path)))

        green = np.array(io.imread(str(green_path)))

        farred = np.array(io.imread(str(farred_path)))

 # It creates a list with the size of the number of slices of the mask, save the area it takes up

        feret_area_list = np.zeros(mask.shape[0])

 # It scrolls through each slice of the mask stack

        for image_ind in range(mask.shape[0]):

# It saves a png file with the original mask

            cv2.imwrite(

                str(png_results.joinpath(f"{dapi_path.stem}_normal_mask_{image_ind}.png")), mask[image_ind]

            )

# Within the stack, it removes noise (e.g., speckles around the stack, background removal, debris around the slice)

            area_open = morph.area_opening(mask[image_ind], area_threshold=40000)

 # It saves a png with the mask processed with "area_opening"

            cv2.imwrite(

str(png_results.joinpath(f"{dapi_path.stem}_remove_small_objects_{image_ind}.png")), area_open

            )

# It eliminates vertexes of the brain, outline the contours of the brain

            kernel = cv2.getStructuringElement(cv2.MORPH_ELLIPSE, (7, 7))

            area_open = cv2.erode(area_open, kernel, iterations=5)

            # save a png with the mask processed with "erode"

            cv2.imwrite(str(png_results.joinpath(f"{dapi_path.stem}_E_{image_ind}.png")), area_open)

 # It rebuilds what has been eroded. NOTE: x2 is done so that the separate slices at the beginning are better sorted. If this does not work, you can use x3

            area_open = cv2.dilate(area_open, kernel, iterations=5)

            # save a png with the mask processed with "dilate"

            cv2.imwrite(str(png_results.joinpath(f"{dapi_path.stem}_ED_{image_ind}.png")), area_open)

            area_open = cv2.dilate(area_open, kernel, iterations=5)
```

```
# It saves a png with the mask processed with "dilate"
        cv2.imwrite(str(png_results.joinpath(f"{dapi_path.stem}_EDD_{image_ind}.png")),
area_open)
        # Finds the contours of the mask to be able to apply the convexHULL
        contours, hier = cv2.findContours(area_open, cv2.RETR_EXTERNAL,
cv2.CHAIN_APPROX_SIMPLE)
# It transforms the mask from grayscale to colour in order to display the result of
convexHULL
        color_img = cv2.cvtColor(area_open, cv2.COLOR_BGR2RGB)
# For each contour found in the image. Note: there should be only 1, but it may be the case
that the sample is split
        for contour_ind in range(len(contours)):
            # convex HULL: creates an outline of the object by skipping the convex parts
            hull = cv2.convexHull(contours[contour_ind], returnPoints=True)
            # Calculate the area
            area = cv2.contourArea(hull)
            # Save area
            feret_area_list[image_ind] += area
            color_img = cv2.addWeighted(
                color_img, 1., cv2.drawContours(color_img, [hull], 0, (100,240, 230), 7), 1., 0
            )
# It saves a png with the contour calculated with "convexHull" and the mask
        cv2.imwrite(str(png_results.joinpath(f"{dapi_path.stem}_hull_{image_ind}.png")),
color_img)
# It rearranges the cuts according to the calculated area
    dapi_ord = dapi[np.argsort(feret_area_list), ...]
    mask_ord = mask[np.argsort(feret_area_list), ...]
    red_ord = red[np.argsort(feret_area_list), ...]
    green_ord = green[np.argsort(feret_area_list), ...]
    farred_ord = farred[np.argsort(feret_area_list), ...]
# It saves the results in new tif files
    tifffile.imwrite(
        dapi_path.parent.joinpath(dapi_path.stem + "_ord" + ".tif"),
```

```
    dapi_ord,
    imagej=True
)
tifffile.imwrite(
    mask_path.parent.joinpath(mask_path.name + "_ord" + ".tif"),
    mask_ord,
    imagej=True
)
tifffile.imwrite(
    red_path.parent.joinpath(red_path.name + "_ord" + ".tif"),
    red_ord,
    imagej=True
)
# tifffile.imwrite(
#     green_path.parent.joinpath(green_path.name + "_ord" + ".tif"),
#     green_ord,
#     imagej=True
# )
tifffile.imwrite(
    farred_path.parent.joinpath(farred_path.name + "_ord" + ".tif"),
    farred_ord,
    imagej=True
)
```

Supplementary Material S4: Fiji code for stack alignment.

The following examples of IJ1 macros were written for stacks of 6 and 10 slices. If you work with smaller or bigger stacks, please customize the number of iterations according to the number of slices in the stack.

Script:

Example 1: stack with 6 slices

```
# Rename and split loop

sk=getTitle()

run("Stack to Images");

run("Images to Stack", "name= title=[]");

run("Stack to Images");

# Select and ROI. Stack with 6 slices.

# NOTE: please, customize this part depending on the number of slices in the stack.

selectWindow("-0001");

roiManager("Select", 0);

selectWindow("-0002");

roiManager("Select", 1);

selectWindow("-0003");

roiManager("Select", 2);

selectWindow("-0004");

roiManager("Select", 3);

selectWindow("-0005");

roiManager("Select", 4);

selectWindow("-0006");

roiManager("Select", 5);
```

```
# Align save to target, defined as "trg". NOTE: xxxx is the selected target. NOTE2: please, customize this part depending on the number of slices in the stack. An example is offered below for a stack of 6 samples.
trg= getString ("Target image, xxxx", 0003);
st1= "source=-0001 target=-"+trg+" rotate";
run("Align Image by line ROI", st1);
st2= "source=-0002 target=-"+trg+" rotate";
run("Align Image by line ROI", st2);
st3= "source=-0003 target=-"+trg+" rotate";
run("Align Image by line ROI", st3);
st4= "source=-0004 target=-"+trg+" rotate";
run("Align Image by line ROI", st4);
st5= "source=-0005 target=-"+trg+" rotate";
run("Align Image by line ROI", st5);
st6= "source=-0006 target=-"+trg+" rotate";
run("Align Image by line ROI", st6);
run("Images to Stack", "name=SkA title=aligned");
run("8-bit");
```

Example 2: stack with 10 slices

```
# Rename and split loop
sk=getTitle()
run("Stack to Images");
run("Images to Stack", "name= title=[]");
run("Stack to Images");
# Select and ROI. Stack with 6 slices.
# NOTE: please, customize this part depending on the number of slices in the stack.
selectWindow("-0001");
```

```
roiManager("Select", 0);
selectWindow("-0002");
roiManager("Select", 1);
selectWindow("-0003");
roiManager("Select", 2);
selectWindow("-0004");
roiManager("Select", 3);
selectWindow("-0005");
roiManager("Select", 4);
selectWindow("-0006");
roiManager("Select", 5);
selectWindow("-0007");
roiManager("Select", 6);
selectWindow("-0008");
roiManager("Select", 7);
selectWindow("-0009");
roiManager("Select", 8);
selectWindow("-0010");
roiManager("Select", 9);
```

 # Align save to target, defined as "trg". NOTE: xxx is the selected target. Stack with 10 slices.

 # NOTE: please, customize this part depending on the number of slices in the stack.

```
trg= getString ("Target image, xxxx", 0003);
st1= "source=-0001 target=-"+trg+" rotate";
run("Align Image by line ROI", st1);
st2= "source=-0002 target=-"+trg+" rotate";
```

```
run("Align Image by line ROI", st2);

st3= "source=-0003 target=-"+trg+" rotate";

run("Align Image by line ROI", st3);

st4= "source=-0004 target=-"+trg+" rotate";

run("Align Image by line ROI", st4);

st5= "source=-0005 target=-"+trg+" rotate";

run("Align Image by line ROI", st5);

st6= "source=-0006 target=-"+trg+" rotate";

run("Align Image by line ROI", st6);

st7= "source=-0007 target=-"+trg+" rotate";

run("Align Image by line ROI", st7);

st8= "source=-0008 target=-"+trg+" rotate";

run("Align Image by line ROI", st8);

st9= "source=-0009 target=-"+trg+" rotate";

run("Align Image by line ROI", st9);

st10= "source=-0010 target=-"+trg+" rotate";

run("Align Image by line ROI", st10);

run("Images to Stack", "name=SkA title=aligned");

run("8-bit");
```

REFERENCES

Abu-Rub, M., McMahon, S., Zeugolis, D. I., Windebank, A., & Pandit, A. (2010). Spinal cord injury in vitro: Modelling axon growth inhibition. In Drug Discovery Today (Vol. 15, Issues 11–12, pp. 436–443). https://doi.org/10.1016/j.drudis.2010.03.008

Agirman, G., Broix, L., & Nguyen, L. (2017). Cerebral cortex development: an outside-in perspective. In FEBS Letters (Vol. 591, Issue 24, pp. 3978–3992). Wiley Blackwell. https://doi.org/10.1002/1873-3468.12924

Al-Ali, H., Beckerman, S. R., Bixby, J. L., & Lemmon, V. P. (2017). In vitro models of axon regeneration. Experimental Neurology, 287(Pt 3), 423–434. https://doi.org/10.1016/j.expneurol.2016.01.020

Alia, C., Spalletti, C., Lai, S., Panarese, A., Micera, S., & Caleo, M. (2016). Reducing GABA A-mediated inhibition improves forelimb motor function after focal cortical stroke in mice. Scientific Reports, 6(October), 1–15. https://doi.org/10.1038/srep37823

Alizadeh, A., Dyck, S. M., Kataria, H., Shahriary, G. M., Nguyen, D. H., Santhosh, K. T., & Karimi-Abdolrezaee, S. (2017). Neuregulin-1 positively modulates glial response and improves neurological recovery following traumatic spinal cord injury. GLIA, 65(7), 1152–1175. https://doi.org/10.1002/glia.23150

Anrather, J., & Iadecola, C. (2016). Inflammation and Stroke: An Overview. Neurotherapeutics, 13(4), 661–670. https://doi.org/10.1007/s13311-016-0483-x

Anton, E. S., Marchionni, M. A., Lee, K. F., & Rakic, P. (1997). Role of GGF/neuregulin signaling in interactions between migrating neurons and radial glia in the developing cerebral cortex. Development, 124(18), 3501–3510.

Bao, J., Lin, H., Ouyang, Y., Lei, D., Osman, A., Kim, T. W., Mei, L., Dai, P., Ohlemiller, K. K., & Ambron, R. T. (2004). Activity-dependent transcription regulation of PSD-95 by neuregulin-1 and Eos. Nature Neuroscience, 7(11), 1250–1258. https://doi.org/10.1038/nn1342

Bao, J., Wolpowitz, D., Role, L. W., & Talmage, D. A. (2003). Back signaling by the Nrg-1 intracellular domain. Journal of Cell Biology, 161(6), 1133–1141. https://doi.org/10.1083/jcb.200212085

Bärmann, J., Walter, H. L., Pikhovych, A., Endepols, H., Fink, G. R., Rueger, M. A., & Schroeter, M. (2021). An analysis of the CatWalk XT and a composite score to assess neurofunctional deficits after photothrombosis in mice. Neuroscience Letters, 751. https://doi.org/10.1016/j.neulet.2021.135811

Barratt, H. E., Lanman, T. A., & Carmichael, S. T. (2014). Mouse intracerebral hemorrhage models produce different degrees of initial and delayed damage, axonal sprouting, and recovery. Journal of Cerebral Blood Flow and Metabolism, 34(9), 1463–1471. https://doi.org/10.1038/jcbfm.2014.107

Barros, C. S., Calabrese, B., Chamero, P., Roberts, A. J., Korzus, E., Lloyd, K., Stowers, L., Mayford, M., Halpain, S., & Müller, U. (2009). Impaired maturation of dendritic spines without disorganization of cortical cell layers in mice lacking NRG1/ErbB signaling in the

central nervous system. Proceedings of the National Academy of Sciences of the United States of America, 106(11), 4507–4512. https://doi.org/10.1073/pnas.0900355106

Bartolini, G., Sánchez-Alcañiz, J. A., Osório, C., Valiente, M., García-Frigola, C., & Marín, O. (2017). Neuregulin 3 Mediates Cortical Plate Invasion and Laminar Allocation of GABAergic Interneurons. Cell Reports, 18(5), 1157–1170. https://doi.org/10.1016/j.celrep.2016.12.089

Bartus, K., Galino, J., James, N. D., Hernandez-Miranda, L. R., Dawes, J. M., Fricker, F. R., Garratt, A. N., McMahon, S. B., Ramer, M. S., Birchmeier, C., Bennett, D. L. H., & Bradbury, E. J. (2016). Neuregulin-1 controls an endogenous repair mechanism after spinal cord injury. Brain, 139(5), 1394–1416. https://doi.org/10.1093/brain/aww039

Bellon, A. (2007). New genes associated with schizophrenia in neurite formation: A review of cell culture experiments. Molecular Psychiatry, 12(7), 620–629. https://doi.org/10.1038/sj.mp.4001985

Benowitz, L. I., & Carmichael, S. T. (2010). Promoting axonal rewiring to improve outcome after stroke. In Neurobiology of Disease (Vol. 37, Issue 2, pp. 259–266). https://doi.org/10.1016/j.nbd.2009.11.009

Birchmeier, C. (2009). ErbB receptors and the development of the nervous system. In Experimental Cell Research (Vol. 315, Issue 4, pp. 611–618). Academic Press Inc. https://doi.org/10.1016/j.yexcr.2008.10.035

Birchmeier, C., & Bennett, D. L. H. (2016). Neuregulin/ErbB Signaling in Developmental Myelin Formation and Nerve Repair. In Current Topics in Developmental Biology (Vol. 116, pp. 45–64). Academic Press Inc. https://doi.org/10.1016/bs.ctdb.2015.11.009

Bozzelli, L. P., Alaiyed, S., Kim, E., Villapol, S., & Conant, K. (2018). Proteolytic Remodeling of Perineuronal Nets: Effects on Synaptic Plasticity and Neuronal Population Dynamics. In Neural Plasticity (Vol. 2018). Hindawi Limited. https://doi.org/10.1155/2018/5735789

Briggs, F. (2010). Organizing principles of cortical layer 6. Frontiers in Neural Circuits, 4(FEB). https://doi.org/10.3389/neuro.04.003.2010

BrosiusLutz, A., & Barres, B. A. (2014). Contrasting the Glial Response to Axon Injury in the Central and Peripheral Nervous Systems. In Developmental Cell (Vol. 28, Issue 1, pp. 7–17). https://doi.org/10.1016/j.devcel.2013.12.002

Brown, C. E., Aminoltejari, K., Erb, H., Winship, I. R., & Murphy, T. H. (2009). In vivo voltage-sensitive dye imaging in adult mice reveals that somatosensory maps lost to stroke are replaced over weeks by new structural and functional circuits with prolonged modes of activation within both the peri-infarct zone and distant sites. Journal of Neuroscience, 29(6), 1719–1734. https://doi.org/10.1523/JNEUROSCI.4249-08.2009

Bublil, E. M., & Yarden, Y. (2007). The EGF receptor family: spearheading a merger of signaling and therapeutics. In Current Opinion in Cell Biology (Vol. 19, Issue 2, pp. 124–134). https://doi.org/10.1016/j.ceb.2007.02.008

Buffo, A., Rite, I., Tripathi, P., Lepier, A., Colak, D., Horn, A.-P., Mori, T., & Götz, M. (2008). Origin and progeny of reactive gliosis: A source of multipotent cells in the injured brain.

Proceedings of the National Academy of Sciences of the United States of America, 105(9), 3581–3586. https://doi.org/10.1073/pnas.0709002105

Buonanno, A. (2010). The neuregulin signaling pathway and schizophrenia: From genes to synapses and neural circuits. In Brain Research Bulletin (Vol. 83, Issues 3–4, pp. 122–131). https://doi.org/10.1016/j.brainresbull.2010.07.012

Campenot, R. B. (1977). Local control of neurite development by nerve growth factor (chemotaxis/culture methods/retrograde transport/sympathetic ganglia). In Cell Biology (Vol. 74, Issue 10).

Canazza, A., Minati, L., Boffano, C., Parati, E., & Binks, S. (2014). Experimental models of brain ischemia: A review of techniques, magnetic resonance imaging, and investigational cell-based therapies. Frontiers in Neurology, 5 FEB(February), 1–15. https://doi.org/10.3389/fneur.2014.00019

Caprio, F. Z., & Sorond, F. A. (2019). Cerebrovascular Disease: Primary and Secondary Stroke Prevention. In Medical Clinics of North America (Vol. 103, Issue 2, pp. 295–308). W.B. Saunders. https://doi.org/10.1016/j.mcna.2018.10.001

Caracciolo, L., Marosi, M., Mazzitelli, J., Latifi, S., Sano, Y., Galvan, L., Kawaguchi, R., Holley, S., Levine, M. S., Coppola, G., Portera-Cailliau, C., Silva, A. J., & Carmichael, S. T. (2018). CREB controls cortical circuit plasticity and functional recovery after stroke. Nature Communications, 9(1). https://doi.org/10.1038/s41467-018-04445-9

Carmichael, S. T. (2016a). Emergent properties of neural repair: Elemental biology to therapeutic concepts. Annals of Neurology, 79(6), 895–906. https://doi.org/10.1002/ana.24653

Carmichael, S. T. (2016b). The 3 Rs of Stroke Biology: Radial, Relayed, and Regenerative. In Neurotherapeutics (Vol. 13, Issue 2, pp. 348–359). Springer New York LLC. https://doi.org/10.1007/s13311-015-0408-0

Carmichael, S. T., Archibeque, I., Luke, L., Nolan, T., Momiy, J., & Li, S. (2005). Growth-associated gene expression after stroke: Evidence for a growth-promoting region in peri-infarct cortex. Experimental Neurology, 193(2), 291–311. https://doi.org/10.1016/j.expneurol.2005.01.004

Carmichael, S. T., Kathirvelu, B., Schweppe, C. A., & Nie, E. H. (2017). Molecular, cellular and functional events in axonal sprouting after stroke. Experimental Neurology, 287, 384–394. https://doi.org/10.1016/j.expneurol.2016.02.007

Carmichael, S. T., & Oise Chesselet, M.-F. (2002). Synchronous Neuronal Activity Is a Signal for Axonal Sprouting after Cortical Lesions in the Adult.

Carmichael, S. T., Wei, L., Rovainen, C. M., & Woolsey, T. A. (2001). New patterns of intracortical projections after focal cortical stroke. Neurobiology of Disease, 8(5), 910–922. https://doi.org/10.1006/nbdi.2001.0425

Chauhan, A., Moser, H., & McCullough, L. D. (2017). Sex differences in ischaemic stroke: Potential cellular mechanisms. Clinical Science, 131(7), 533–552. https://doi.org/10.1042/CS20160841

Chen, Y., Hancock, M. L., Role, L. W., & Talmage, D. A. (2010). Intramembranous valine linked to schizophrenia is required for neuregulin 1 regulation of the morphological development

of cortical neurons. Journal of Neuroscience, 30(27), 9199–9208. https://doi.org/10.1523/JNEUROSCI.0605-10.2010

Chovsepian, A., Empl, L., & Bareyre, F. M. (2023). Plasticity of callosal neurons in the contralesional cortex following traumatic brain injury. Neural Regeneration Research, 18(6), 1257–1258. https://doi.org/10.4103/1673-5374.360167

Clarkson, A. N., Huang, B. S., MacIsaac, S. E., Mody, I., & Carmichael, S. T. (2010). Reducing excessive GABA-mediated tonic inhibition promotes functional recovery after stroke. Nature, 468(7321), 305–309. https://doi.org/10.1038/nature09511

Conde, V., & Siebner, H. R. (2020). Brain damage by trauma. In Handbook of Clinical Neurology (Vol. 168, pp. 39–49). Elsevier B.V. https://doi.org/10.1016/B978-0-444-63934-9.00005-6

Corfas, G., Roy, K., & Buxbaum, J. D. (2004). Neuregulin 1-erbB signaling and the molecular/cellular basis of schizophrenia. In Nature Neuroscience (Vol. 7, Issue 6, pp. 575–580). https://doi.org/10.1038/nn1258

Courchet, J., Lewis, T. L., Lee, S., Courchet, V., Liou, D. Y., Aizawa, S., & Polleux, F. (2013). XTerminal axon branching is regulated by the LKB1-NUAK1 kinase pathway via presynaptic mitochondrial capture. Cell, 153(7), 1510. https://doi.org/10.1016/j.cell.2013.05.021

Courchet, V., Roberts, A. J., Meyer-Dilhet, G., Del Carmine, P., Lewis, T. L., Polleux, F., & Courchet, J. (2018). Haploinsufficiency of autism spectrum disorder candidate gene NUAK1 impairs cortical development and behavior in mice. Nature Communications, 9(1). https://doi.org/10.1038/s41467-018-06584-5

Cui, M. Y., Fu, Y. Q., Li, Z. L., Zheng, Y., Yu, Y., Zhang, C., Zhang, Y. Q., Gao, B. R., Chen, W. Y., Lee, Y. L., Won, M. H., Liao, M., Jian, Y., & Chen, B. H. (2023). Neuregulin-1/PI3K signaling effects on oligodendrocyte proliferation, remyelination and behaviors deficit in a male mouse model of ischemic stroke. Experimental Neurology, 362. https://doi.org/10.1016/j.expneurol.2023.114323

Curcio, M., & Bradke, F. (2018). Axon Regeneration in the Central Nervous System: Facing the Challenges from the Inside. Annual Review of Cell and Developmental Biology, 34(July), 495–521. https://doi.org/10.1146/annurev-cellbio-100617-062508

Dana, H., Chen, T. W., Hu, A., Shields, B. C., Guo, C., Looger, L. L., Kim, D. S., & Svoboda, K. (2014). Thy1-GCaMP6 transgenic mice for neuronal population imaging in vivo. PLoS ONE, 9(9). https://doi.org/10.1371/journal.pone.0108697

Dancause, N., Barbay, S., Frost, S. B., Plautz, E. J., Chen, D., Zoubina, E. V., Stowe, A. M., & Nudo, R. J. (2005). Extensive cortical rewiring after brain injury. Journal of Neuroscience, 25(44), 10167–10179. https://doi.org/10.1523/JNEUROSCI.3256-05.2005

De León Reyes, N. S., Bragg-Gonzalo, L., & Nieto, M. (2020). Development and plasticity of the corpus callosum. Development (Cambridge, England), 147(18), 1–15. https://doi.org/10.1242/dev.189738

del Pino, I., García-Frigola, C., Dehorter, N., Brotons-Mas, J. R., Alvarez-Salvado, E., Martínez de Lagrán, M., Ciceri, G., Gabaldón, M. V., Moratal, D., Dierssen, M., Canals, S., Marín, O., & Rico, B. (2013). Erbb4 Deletion from Fast-Spiking Interneurons Causes Schizophrenia-

like Phenotypes. Neuron, 79(6), 1152–1168. https://doi.org/10.1016/j.neuron.2013.07.010

Deng, W., Luo, F., Li, B. ming, & Mei, L. (2019). NRG1–ErbB4 signaling promotes functional recovery in a murine model of traumatic brain injury via regulation of GABA release. Experimental Brain Research, 237(12), 3351–3362. https://doi.org/10.1007/s00221-019-05680-2

Devienne, G., Picaud, S., Cohen, I., Piquet, J., Tricoire, L., Testa, D., Di Nardo, A. A., Rossier, J., Cauli, B., & Lambolez, B. (2021). Regulation of perineuronal nets in the adult cortex by the activity of the cortical network. Journal of Neuroscience, 41(27), 5779–5790. https://doi.org/10.1523/JNEUROSCI.0434-21.2021

Ding, C. Y., Ding, Y. T., Ji, H., Wang, Y. Y., Zhang, X., & Yin, D.-M. (2023). Genetic labeling reveals spatial and cellular expression pattern of neuregulin 1 in mouse brain. Cell & Bioscience, 13(1), 79. https://doi.org/10.1186/s13578-023-01032-4

Ding, Z., Dai, C., Zhong, L., Liu, R., Gao, W., Zhang, H., & Yin, Z. (2021). Neuregulin-1 converts reactive astrocytes toward oligodendrocyte lineage cells via upregulating the PI3K-AKT-mTOR pathway to repair spinal cord injury. Biomedicine and Pharmacotherapy, 134. https://doi.org/10.1016/j.biopha.2020.111168

Dixon, K. J. (2017). Pathophysiology of Traumatic Brain Injury. In Physical Medicine and Rehabilitation Clinics of North America (Vol. 28, Issue 2, pp. 215–225). W.B. Saunders. https://doi.org/10.1016/j.pmr.2016.12.001

Domínguez, S., Rey, C. C., Therreau, L., Fanton, A., Massotte, D., Verret, L., Piskorowski, R. A., & Chevaleyre, V. (2019). Maturation of PNN and ErbB4 Signaling in Area CA2 during Adolescence Underlies the Emergence of PV Interneuron Plasticity and Social Memory. Cell Reports, 29(5), 1099-1112.e4. https://doi.org/10.1016/j.celrep.2019.09.044

Domínguez-García, S., Geribaldi-Doldán, N., Gómez-Oliva, R., Ruiz, F. A., Carrascal, L., Bolívar, J., Verástegui, C., Garcia-Alloza, M., Macías-Sánchez, A. J., Hernández-Galán, R., Nunez-Abades, P., & Castro, C. (2020). A novel PKC activating molecule promotes neuroblast differentiation and delivery of newborn neurons in brain injuries. Cell Death and Disease, 11(4). https://doi.org/10.1038/s41419-020-2453-9

Ekmark-Lewén, S., Flygt, J., Kiwanuka, O., Meyerson, B. J., Lewén, A., Hillered, L., & Marklund, N. (2013). Traumatic axonal injury in the mouse is accompanied by a dynamic inflammatory response, astroglial reactivity and complex behavioral changes. Journal of Neuroinflammation, 10, 1–19. https://doi.org/10.1186/1742-2094-10-44

Empl, L., Chovsepian, A., Chahin, M., Kan, W. Y. V., Fourneau, J., Van Steenbergen, V., Weidinger, S., Marcantoni, M., Ghanem, A., Bradley, P., Conzelmann, K. K., Cai, R., Ghasemigharagoz, A., Ertürk, A., Wagner, I., Kreutzfeldt, M., Merkler, D., Liebscher, S., & Bareyre, F. M. (2022). Selective plasticity of callosal neurons in the adult contralesional cortex following murine traumatic brain injury. Nature Communications, 13(1). https://doi.org/10.1038/s41467-022-29992-0

Esper, R. M., Pankonin, M. S., & Loeb, J. A. (2006). Neuregulins: Versatile growth and differentiation factors in nervous system development and human disease. https://doi.org/10.1016/j.brainresrev.200

Falls, D. L. (2003). Neuregulins: Functions, forms, and signaling strategies. In Experimental Cell Research (Vol. 284, Issue 1, pp. 14–30). Academic Press Inc. https://doi.org/10.1016/S0014-4827(02)00102-7

Fame, R. M., MacDonald, J. L., & Macklis, J. D. (2011). Development, specification, and diversity of callosal projection neurons. In Trends in Neurosciences (Vol. 34, Issue 1, pp. 41–50). https://doi.org/10.1016/j.tins.2010.10.002

Fani Maleki, A., & Rivest, S. (2019). Innate Immune Cells: Monocytes, Monocyte-Derived Macrophages and Microglia as Therapeutic Targets for Alzheimer's Disease and Multiple Sclerosis. Frontiers in Cellular Neuroscience, 13. https://doi.org/10.3389/fncel.2019.00355

Fawcett, J. W., Fyhn, M., Jendelova, P., Kwok, J. C. F., Ruzicka, J., & Sorg, B. A. (2022). The extracellular matrix and perineuronal nets in memory. In Molecular Psychiatry (Vol. 27, Issue 8, pp. 3192–3203). Springer Nature. https://doi.org/10.1038/s41380-022-01634-3

Fazzari, P., Paternain, A. V, Valiente, M., Pla, R., Luján, R., Lloyd, K., Lerma, J., Marín, O., & Rico, B. (2010). Control of cortical GABA circuitry development by Nrg1 and ErbB4 signalling. Nature, 464(April), 1376–1380. https://doi.org/10.1038/nature08928

Fazzari, P., Snellinx, A., Sabanov, V., Ahmed, T., Serneels, L., Gartner, A., Shariati, S. A. M., Balschun, D., & De Strooper, B. (2014). Cell autonomous regulation of hippocampal circuitry via Aph1b-γ-secretase/neuregulin 1 signalling. ELife, 3. https://doi.org/10.7554/elife.02196

Fenlon, L. R., & Richards, L. J. (2015). Contralateral targeting of the corpus callosum in normal and pathological brain function. In Trends in Neurosciences (Vol. 38, Issue 5, pp. 264–272). Elsevier Ltd. https://doi.org/10.1016/j.tins.2015.02.007

Ferguson, B. R., & Gao, W. J. (2018). Pv interneurons: critical regulators of E/I balance for prefrontal cortex-dependent behavior and psychiatric disorders. Frontiers in Neural Circuits, 12(May), 1–13. https://doi.org/10.3389/fncir.2018.00037

Fernandez, P.-A., Tang, D. G., Cheng, L., Prochiantz, A., Mudge, A. W., & Raff, M. C. (2000). Evidence that Axon-Derived Neuregulin Promotes Oligodendrocyte Survival in the Developing Rat Optic Nerve. Neuron, 28, 81–90.

Flames, N., Long, J. E., Garratt, A. N., Fischer, T. M., Gassmann, M., Birchmeier, C., Lai, C., Rubenstein, J. L. R., & Marín, O. (2004). Short- and long-range attraction of cortical GABAergic interneurons by neuregulin-1. Neuron, 44(2), 251–261. https://doi.org/10.1016/j.neuron.2004.09.028

Flores, A. I., Narayanan, S. P., Morse, E. N., Shick, H. E., Yin, X., Kidd, G., Avila, R. L., Kirschner, D. A., & Macklin, W. B. (2008). Constitutively active Akt induces enhanced myelination in the CNS. Journal of Neuroscience, 28(28), 7174–7183. https://doi.org/10.1523/JNEUROSCI.0150-08.2008

Fluri, F., Schuhmann, M. K., & Kleinschnitz, C. (2015). Animal models of ischemic stroke and their application in clinical research. Drug Design, Development and Therapy, 9, 3445–3454. https://doi.org/10.2147/DDDT.S56071

Fowke, T. M., Galinsky, R., Davidson, J. O., Wassink, G., Karunasinghe, R. N., Prasad, J. D., Bennet, L., Gunn, A. J., & Dean, J. M. (2018). Loss of interneurons and disruption of perineuronal nets in the cerebral cortex following hypoxia-ischaemia in near-term fetal sheep. Scientific Reports, 8(1). https://doi.org/10.1038/s41598-018-36083-y

Franceschi, C., Bonafè, M., Valensin, S., Olivieri, F., De Luca, M., Ottaviani, E., & De Benedictis, G. (2000). Inflamm-aging An Evolutionary Perspective on Immunosenescence. Ann N Y Acad Sci., 908, 244–254.

Fricker, F. R., Lago, N., Balarajah, S., Tsantoulas, C., Tanna, S., Zhu, N., Fageiry, S. K., Jenkins, M., Garratt, A. N., Birchmeier, C., & Bennett, D. L. H. (2011). Axonally derived neuregulin-1 is required for remyelination and regeneration after nerve injury in adulthood. Journal of Neuroscience, 31(9), 3225–3233. https://doi.org/10.1523/JNEUROSCI.2568-10.2011

Galgano, M., Toshkezi, G., Qiu, X., Russell, T., Chin, L., & Zhao, L. R. (2017). Traumatic brain injury: Current treatment strategies and future endeavors. Cell Transplantation, 26(7), 1118–1130. https://doi.org/10.1177/0963689717714102

Gazaryan, L. M., Selyanina, N. V., Karakulova, Y. V., & Sosnin, D. Y. (2019). The Level of Neuregulin-1 after Traumatic Brain Injury and Formation of Post-Traumatic Epilepsy. Bulletin of Experimental Biology and Medicine, 167(2), 207–209. https://doi.org/10.1007/s10517-019-04492-2

Gerecke, K. M., Wyss, J. M., & Carroll, S. L. (2004). Neuregulin-1β induces neurite extension and arborization in cultured hippocampal neurons. Molecular and Cellular Neuroscience, 27(4), 379–393. https://doi.org/10.1016/j.mcn.2004.08.001

Gong, Y., Hart, E., Shchurin, A., & Hoover-Plow, J. (2008). Inflammatory macrophage migration requires MMP-9 activation by plasminogen in mice. The Journal of Clinical Investigation, 118(9), 3012–3024. https://doi.org/10.1172/JCI32750

González-Manteiga, A., Navarro-González, C., Sebestyén, V. E., Saborit-Torres, J. M., Talhada, D., Vayá, M. de la I., Ruscher, K., & Fazzari, P. (2022). A Novel In Vivo Model for Multiplexed Analysis of Callosal Connections upon Cortical Damage. International Journal of Molecular Sciences, 23(15). https://doi.org/10.3390/ijms23158224

Gouvêa-Junqueira, D., Falvella, A. C. B., Antunes, A. S. L. M., Seabra, G., Brandão-Teles, C., Martins-de-Souza, D., & Crunfli, F. (2020). Novel Treatment Strategies Targeting Myelin and Oligodendrocyte Dysfunction in Schizophrenia. In Frontiers in Psychiatry (Vol. 11). Frontiers Media S.A. https://doi.org/10.3389/fpsyt.2020.00379

Gu, N., Ge, K., Hao, C., Ji, Y., Li, H., & Guo, Y. (2017). Neuregulin1β Effects on Brain Tissue via ERK5-Dependent MAPK Pathway in a Rat Model of Cerebral Ischemia–Reperfusion Injury. Journal of Molecular Neuroscience, 61(4), 607–616. https://doi.org/10.1007/s12031-017-0902-4

Guan, Y.-F. F., Wu, C.-Y. Y., Fang, Y.-Y. Y., Zeng, Y.-N. N., Luo, Z.-Y. Y., Li, S.-J. J., Li, X.-W. W., Zhu, X.-H. H., Mei, L., & Gao, T.-M. M. (2015). Neuregulin 1 protects against ischemic brain injury via ErbB4 receptors by increasing GABAergic transmission. Neuroscience, 307, 151–159. https://doi.org/10.1016/j.neuroscience.2015.08.047

Guo, W. P., Fu, X. G., Jiang, S. M., & Wu, J. Z. (2010). Neuregulin-1 regulates the expression of Akt, Bcl-2, and bad signaling after focal cerebral ischemia in rats. Biochemistry and Cell Biology, 88(4), 649–654. https://doi.org/10.1139/O09-189

Guo, W. P., Wang, J., Li, R. X., & Peng, Y. W. (2006). Neuroprotective effects of neuregulin-1 in rat models of focal cerebral ischemia. Brain Research, 1087(1), 180–185. https://doi.org/10.1016/j.brainres.2006.03.007

Häggman Henrikson, J., Pombo Antunes, A. R., Wieloch, T., & Ruscher, K. (2020). Enhanced functional recovery by levodopa is associated with decreased levels of synaptogyrin following stroke in aged mice. Brain Research Bulletin, 155, 61–66. https://doi.org/10.1016/j.brainresbull.2019.11.019

Haley, M. S., & Maffei, A. (2018). Versatility and Flexibility of Cortical Circuits. In Neuroscientist (Vol. 24, Issue 5, pp. 456–470). SAGE Publications Inc. https://doi.org/10.1177/1073858417733720

Hancock, M. L., Nowakowski, D. W., Role, L. W., Talmage, D. A., & Flanagan, J. G. (2011). Type III neuregulin 1 regulates pathfinding of sensory axons in the developing spinal cord and periphery. Development, 138(22), 4887–4898. https://doi.org/10.1242/dev.072306

Hao, Q., Zhang, Y., Li, X., Liang, L., Shi, H., Cui, Z., & Yang, W. (2020). Upregulated neuregulin-1 protects against optic nerve injury by regulating the RhoA/cofilin/F-actin axis. Life Sciences, 264. https://doi.org/10.1016/j.lfs.2020.118283

Heegaard, W., & Biros, M. (2007). Traumatic Brain Injury. In Emergency Medicine Clinics of North America (Vol. 25, Issue 3, pp. 655–678). W.B. Saunders. https://doi.org/10.1016/j.emc.2007.07.001

Hilton, B. J., & Bradke, F. (2017). Can injured adult CNS axons regenerate by recapitulating development? Development (Cambridge), 144(19), 3417–3429. https://doi.org/10.1242/dev.148312

Holloway, P. M., & Gavins, F. N. E. (2016). Modeling Ischemic Stroke In Vitro: The Status Quo and Future Perspectives. Physiology and Behavior, 47(2), 561–569. https://doi.org/10.1016/j.physbeh.2017.03.040

Hoshino, S., Kobayashi, S., & Nakazawa, S. (1996). Prolonged and extensive IgG immunoreactivity after severe fluid-percussion injury in rat brain. Brain Research, 711(1–2), 73–83. https://doi.org/10.1016/0006-8993(95)01329-6

Hsieh, T. H., Cheong Lee, H. H., Hameed, M. Q., Pascual-Leone, A., Hensch, T. K., & Rotenberg, A. (2017). Trajectory of parvalbumin cell impairment and loss of cortical inhibition in traumatic brain injury. Cerebral Cortex, 27(12), 5509–5524. https://doi.org/10.1093/cercor/bhw318

Huang, N., & Sheng, Z. H. (2022). Microfluidic devices as model platforms of CNS injury-ischemia to study axonal regeneration by regulating mitochondrial transport and bioenergetic metabolism. Cell Regeneration, 11(1). https://doi.org/10.1186/s13619-022-00138-3

Huang, Q., Chan, K. Y., Tobey, I. G., Chan, Y. A., Poterba, T., Boutros, C. L., Balazs, A. B., Daneman, R., Bloom, J. M., Seed, C., & Deverman, B. E. (2019). Delivering genes across

the blood-brain barrier: LY6A, a novel cellular receptor for AAV-PHP.B capsids. PLoS ONE, 14(11), 1–17. https://doi.org/10.1371/journal.pone.0225206

Huebner, E. A., Kim, B. G., Duffy, P. J., Brown, R. H., & Strittmatter, S. M. (2011). A multi-domain fragment of Nogo-A protein is a potent inhibitor of cortical axon regeneration via Nogo receptor. Journal of Biological Chemistry, 286(20), 18026–18036. https://doi.org/10.1074/jbc.M110.208108

Iaci, J. F., Parry, T. J., Huang, Z., Pavlopoulos, E., Finklestein, S. P., Ren, J., & Caggiano, A. (2016). An optimized dosing regimen of cimaglermin (neuregulin 1β3, glial growth factor 2) enhances molecular markers of neuroplasticity and functional recovery after permanent ischemic stroke in rats. Journal of Neuroscience Research, 94(3), 253–265. https://doi.org/10.1002/jnr.23699

Jamjoom, A. A. B., Rhodes, J., Andrews, P. J. D., & Grant, S. G. N. (2021). The synapse in traumatic brain injury. In Brain (Vol. 144, Issue 1, pp. 18–31). Oxford University Press. https://doi.org/10.1093/brain/awaa321

Jones, T. A., Kleim, J. A., & Greenough, W. T. (1996). Synaptogenesis and dendritic growth in the cortex opposite unilateral sensorimotor cortex damage in adult rats: a quantitative electron microscopic examination 1. In Brain Research (Vol. 733). ELSEVIER.

Jonkman, J. E. N., Cathcart, J. A., Xu, F., Bartolini, M. E., Amon, J. E., Stevens, K. M., & Colarusso, P. (2014). An introduction to the wound healing assay using live-cell microscopy. In Cell Adhesion and Migration (Vol. 8, Issue 5, pp. 440–451). Landes Bioscience. https://doi.org/10.4161/cam.36224

Joung, I., Yoo, M., Woo, J. H., Chang, C. Y., Heo, H., & Kwon, Y. K. (2010). Secretion of EGF-like domain of heregulinβ promotes axonal growth and functional recovery of injured sciatic nerve. Molecules and Cells, 30(5), 477–484. https://doi.org/10.1007/s10059-010-0137-5

Joy, M. T., Ben Assayag, E., Shabashov-Stone, D., Liraz-Zaltsman, S., Mazzitelli, J., Arenas, M., Abduljawad, N., Kliper, E., Korczyn, A. D., Thareja, N. S., Kesner, E. L., Zhou, M., Huang, S., Silva, T. K., Katz, N., Bornstein, N. M., Silva, A. J., Shohami, E., & Carmichael, S. T. (2019). CCR5 Is a Therapeutic Target for Recovery after Stroke and Traumatic Brain Injury. Cell, 176(5), 1143-1157.e13. https://doi.org/10.1016/j.cell.2019.01.044

Joy, M. T., & Carmichael, S. T. (2021). Encouraging an excitable brain state: mechanisms of brain repair in stroke. Nature Reviews Neuroscience, 22(1), 38–53. https://doi.org/10.1038/s41583-020-00396-7

Karve, I. P., Taylor, J. M., & Crack, P. J. (2016). The contribution of astrocytes and microglia to traumatic brain injury. British Journal of Pharmacology, 173(4), 692–702. https://doi.org/10.1111/bph.13125

Kataria, H., Alizadeh, A., & Karimi-Abdolrezaee, S. (2019). Neuregulin-1/ErbB network: An emerging modulator of nervous system injury and repair. Progress in Neurobiology, June, 101643. https://doi.org/10.1016/j.pneurobio.2019.101643

Katarzyna Greda, A., & Nowicka, D. (2021). Hyaluronidase inhibition accelerates functional recovery from stroke in the mouse brain. Journal of Neurochemistry, 157(3), 781–801. https://doi.org/10.1111/jnc.15279

Kelmenson, P. (2011). CRE LOX BREEDING FOR BEGINNERS, PART 1. The Jackson Laboratory.

Kim, S. Y., & Nair, M. G. (2019). Macrophages in wound healing: activation and plasticity. Immunology and Cell Biology, 97(3), 258–267. https://doi.org/10.1111/imcb.12236

Kim, S. Y., Senatorov, V. V., Morrissey, C. S., Lippmann, K., Vazquez, O., Milikovsky, D. Z., Gu, F., Parada, I., Prince, D. A., Becker, A. J., Heinemann, U., Friedman, A., & Kaufer, D. (2017). TGFβ signaling is associated with changes in inflammatory gene expression and perineuronal net degradation around inhibitory neurons following various neurological insults. Scientific Reports, 7(1), 1–14. https://doi.org/10.1038/s41598-017-07394-3

Kim, Y. T., Karthikeyan, K., Chirvi, S., & Davé, D. P. (2009). Neuro-optical microfluidic platform to study injury and regeneration of single axons. Lab on a Chip, 9(17), 2576–2581. https://doi.org/10.1039/b903720a

Kugler, C., Thielscher, C., Tambe, B. A., Schwarz, M. K., Halle, A., Bradke, F., & Petzold, G. C. (2020). Epothilones Improve Axonal Growth and Motor Outcomes after Stroke in the Adult Mammalian CNS. Cell Reports Medicine, 1(9). https://doi.org/10.1016/j.xcrm.2020.100159

Kumaria, A. (2017). In Vitro Models as a Platform to Investigate Traumatic Brain Injury. ATLA, 45, 201–211.

Lai, T. W., Zhang, S., & Wang, Y. T. (2014). Excitotoxicity and stroke: Identifying novel targets for neuroprotection. In Progress in Neurobiology (Vol. 115, Issue C, pp. 157–188). Elsevier Ltd. https://doi.org/10.1016/j.pneurobio.2013.11.006

Latifi, S., Mitchell, S., Habibey, R., Hosseini, F., Donzis, E., Estrada-Sanchez, A. M., Rezaei Nejad, H., Levine, M., Golshani, P., & Thomas Carmichael, S. (2020). Neuronal network topology indicates distinct recovery processes after stroke. Cerebral Cortex, 30(12), 6363–6375. https://doi.org/10.1093/cercor/bhaa191

Lemke, G. (2006). Neuregulin-1 and Myelination. Sci. STKE, pe11. www.stke.org/cgi/content/full/sigtrans;2006/325/pe11

Li, Q., Cao, Y., Dang, C., Han, B., Han, R., Ma, H., Hao, J., & Wang, L. (2020). Inhibition of double-strand DNA-sensing cGAS ameliorates brain injury after ischemic stroke. EMBO Molecular Medicine, 12(4), 1–18. https://doi.org/10.15252/emmm.201911002

Li, R., Li, D. hui, Zhang, H. yu, Wang, J., Li, X. kun, & Xiao, J. (2020). Growth factors-based therapeutic strategies and their underlying signaling mechanisms for peripheral nerve regeneration. Acta Pharmacologica Sinica, November 2019, 1–12. https://doi.org/10.1038/s41401-019-0338-1

Li, S., Nie, E. H., Yin, Y., Benowitz, L. I., Tung, S., Vinters, H. V., Bahjat, F. R., Stenzel-Poore, M. P., Kawaguchi, R., Coppola, G., & Carmichael, S. T. (2015). GDF10 is a signal for axonal sprouting and functional recovery after stroke. Nature Neuroscience, 18(12), 1737–1745. https://doi.org/10.1038/nn.4146

Li, S., Overman, J. J., Katsman, D., Kozlov, S. V., Donnelly, C. J., Twiss, J. L., Giger, R. J., Coppola, G., Geschwind, D. H., & Carmichael, S. T. (2010). An age-related sprouting

transcriptome provides molecular control of axonal sprouting after stroke. Nature Neuroscience, 13(12), 1496–1506. https://doi.org/10.1038/nn.2674

Li, Y., Xu, Z., Ford, G. D., Croslan, D. R., Cairobe, T., Li, Z., & Ford, B. D. (2007). Neuroprotection by Neuregulin-1 in a Rat Model of Permanent Focal Cerebral Ischemia. Brain Research, 1184, 277–283.

Lim, L., Mi, D., Llorca, A., & Marín, O. (2018). Development and Functional Diversification of Cortical Interneurons. Neuron, 100(2), 294–313. https://doi.org/10.1016/j.neuron.2018.10.009

Lindau, N. T., Bänninger, B. J., Gullo, M., Good, N. A., Bachmann, L. C., Starkey, M. L., & Schwab, M. E. (2014). Rewiring of the corticospinal tract in the adult rat after unilateral stroke and anti-Nogo-A therapy. Brain, 137(3), 739–756. https://doi.org/10.1093/brain/awt336

Liu, K., Tedeschi, A., Park, K. K., & He, Z. (2011). Neuronal intrinsic mechanisms of axon regeneration. Annual Review of Neuroscience, 34, 131–152. https://doi.org/10.1146/annurev-neuro-061010-113723

Liu, X., Bates, R., Yin, D. M., Shen, C., Wang, F., Su, N., Kirov, S. A., Luo, Y., Wang, J. Z., Xiong, W. C., & Mei, L. (2011). Specific regulation of NRG1 isoform expression by neuronal activity. Journal of Neuroscience, 31(23), 8491–8501. https://doi.org/10.1523/JNEUROSCI.5317-10.2011

López-Bendito, G., Cautinat, A., Sánchez, J. A., Bielle, F., Flames, N., Garratt, A. N., Talmage, D. A., Role, L. W., Charnay, P., Marín, O., & Garel, S. (2006). Tangential Neuronal Migration Controls Axon Guidance: A Role for Neuregulin-1 in Thalamocortical Axon Navigation. Cell, 125(1), 127–142. https://doi.org/10.1038/jid.2014.371

Lu, Y., Sun, X. D., Hou, F. Q., Bi, L. L., Yin, D. M., Liu, F., Chen, Y. J., Bean, J. C., Jiao, H. F., Liu, X., Li, B. M., Xiong, W. C., Gao, T. M., & Mei, L. (2014). Maintenance of GABAergic activity by neuregulin 1-ErbB4 in amygdala for fear memory. Neuron, 84(4), 835–846. https://doi.org/10.1016/j.neuron.2014.09.029

Lysko, D. E., & Talbot, W. S. (2022). Unmyelinated sensory neurons use Neuregulin signals to promote myelination of interneurons in the CNS. Cell Reports, 41(7). https://doi.org/10.1016/j.celrep.2022.111669

Ma, V. Y., Chan, L., & Carruthers, K. J. (2014). Incidence, prevalence, costs, and impact on disability of common conditions requiring rehabilitation in the United States: Stroke, spinal cord injury, traumatic brain injury, multiple sclerosis, osteoarthritis, rheumatoid arthritis, limb loss, and back pa. In Archives of Physical Medicine and Rehabilitation (Vol. 95, Issue 5, p. 986). W.B. Saunders. https://doi.org/10.1016/j.apmr.2013.10.032

Ma, X., Aravind, A., Pfister, B. J., Chandra, N., & Haorah, J. (2019). Animal Models of Traumatic Brain Injury and Assessment of Injury Severity. In Molecular Neurobiology (Vol. 56, Issue 8, pp. 5332–5345). Humana Press Inc. https://doi.org/10.1007/s12035-018-1454-5

Ma, Y., Fan, P., Zhao, R., Zhang, Y., Wang, X., & Cui, W. (2022). Neuregulin-1 regulates the conversion of M1/M2 microglia phenotype via ErbB4-dependent inhibition of the NF-κB pathway. Molecular Biology Reports, 49, 3975–3986.

Madinier, A., Quattromani, M. J., Sjölund, C., Ruscher, K., & Wieloch, T. (2014). Enriched housing enhances recovery of limb placement ability and reduces aggrecan-containing perineuronal nets in the rat somatosensory cortex after experimental stroke. PLoS ONE, 9(3). https://doi.org/10.1371/journal.pone.0093121

Mancuso, R., Martínez-Muriana, A., Leiva, T., Gregorio, D., Ariza, L., Morell, M., Esteban-Pérez, J., García-Redondo, A., Calvo, A. C., Atencia-Cibreiro, G., Corfas, G., Osta, R., Bosch, A., & Navarro, X. (2016). Neuregulin-1 promotes functional improvement by enhancing collateral sprouting in SOD1G93A ALS mice and after partial muscle denervation. Neurobiology of Disease, 95, 168–178. https://doi.org/10.1016/j.nbd.2016.07.023

Mathiesen, S. N., Lock, J. L., Schoderboeck, L., Abraham, W. C., & Hughes, S. M. (2020). CNS Transduction Benefits of AAV-PHP.eB over AAV9 Are Dependent on Administration Route and Mouse Strain. Molecular Therapy - Methods and Clinical Development, 19, 447–458. https://doi.org/10.1016/j.omtm.2020.10.011

Mattugini, N., Bocchi, R., Scheuss, V., Russo, G. L., Torper, O., Lao, C. L., & Götz, M. (2019). Inducing Different Neuronal Subtypes from Astrocytes in the Injured Mouse Cerebral Cortex. Neuron, 103(6), 1086-1095.e5. https://doi.org/10.1016/j.neuron.2019.08.009

McBride, D. W., & Zhang, J. H. (2017). Precision Stroke Animal Models: the Permanent MCAO Model Should Be the Primary Model, Not Transient MCAO. Translational Stroke Research, 176(5), 139–148. https://doi.org/10.1007/s12975-017-0554-2

Mei, L., & Nave, K. A. (2014). Neuregulin-ERBB signaling in the nervous system and neuropsychiatric diseases. Neuron, 83(1), 27–49. https://doi.org/10.1016/j.neuron.2014.06.007

Mei, L., & Xiong, W. C. (2008). Neuregulin 1 in neural development, synaptic plasticity and schizophrenia. Nature Reviews Neuroscience, 9(6), 437–452. https://doi.org/10.1038/nrn2392

Mergenthaler, P., & Meisel, A. (2012). Do stroke models model stroke? DMM Disease Models and Mechanisms, 5(6), 718–725. https://doi.org/10.1242/dmm.010033

Meyer, D., & Birchmeier, C. (1995). Multiple essential functions of neuregulin in development. Nature, 378, 386–390.

Michalettos, G., Walter, H. L., Antunes, A. R. P., Wieloch, T., Talhada, D., & Ruscher, K. (2021). Effect of Anti-inflammatory Treatment with AMD3100 and CX3CR1 Deficiency on GABAA Receptor Subunit and Expression of Glutamate Decarboxylase Isoforms After Stroke. Molecular Neurobiology, 58(11), 5876–5889. https://doi.org/10.1007/s12035-021-02510-x

Michinaga, S., & Koyama, Y. (2021). Pathophysiological responses and roles of astrocytes in traumatic brain injury. In International Journal of Molecular Sciences (Vol. 22, Issue 12). MDPI. https://doi.org/10.3390/ijms22126418

Mòdol-Caballero, G., Santos, D., Navarro, X., & Herrando-Grabulosa, M. (2018). Neuregulin 1 reduces motoneuron cell death and promotes neurite growth in an in vitro model of motoneuron degeneration. Frontiers in Cellular Neuroscience, 11. https://doi.org/10.3389/fncel.2017.00431

Moskowitz, M. A., Lo, E. H., & Iadecola, C. (2010). The science of stroke: Mechanisms in search of treatments. Neuron, 67(2), 181–198. https://doi.org/10.1016/j.neuron.2010.07.002

Mukai, J., Tamura, M., Fénelon, K., Rosen, A. M., Spellman, T. J., Kang, R., MacDermott, A. B., Karayiorgou, M., Gordon, J. A., & Gogos, J. A. (2015). Molecular Substrates of Altered Axonal Growth and Brain Connectivity in a Mouse Model of Schizophrenia. Neuron, 86(3), 680–695. https://doi.org/10.1016/j.neuron.2015.04.003

Murphy, S. J., Mccullough, L. D., & Smith, J. M. (2004). Stroke in the Female: Role of Biological Sex and Estrogen. ILAR, 45(2), 147–159. http://www.nhlbi.nih.gov/about/framingham/index.

Murphy, T. H., & Corbett, D. (2009). Plasticity during stroke recovery: From synapse to behaviour. Nature Reviews Neuroscience, 10(12), 861–872. https://doi.org/10.1038/nrn2735

Murray, P. J., & Wynn, T. A. (2011). Protective and pathogenic functions of macrophage subsets. Nature Reviews Immunology, 11(11), 723–737. https://doi.org/10.1038/nri3073

Najem, D., Rennie, K., Ribecco-Lutkiewicz, M., Ly, D., Haukenfrers, J., Liu, Q., Nzau, M., Fraser, D. D., & Bani-Yaghoub, M. (2018). Traumatic Brain Injury: Classification, Models and Markers. Biochem. Cell Biol, 4, 391–406. www.nrcresearchpress.com

Navarro-Gonzalez, C., Carceller, H., Benito Vicente, M., Serra, I., Navarrete, M., Domínguez-Canterla, Y., Rodríguez-Prieto, Á., González-Manteiga, A., & Fazzari, P. (2021). Nrg1 haploinsufficiency alters inhibitory cortical circuits. Neurobiology of Disease, 157. https://doi.org/10.1016/j.nbd.2021.105442

Navarro-González, C., Huerga-Gómez, A., & Fazzari, P. (2019). Nrg1 Intracellular Signaling Is Neuroprotective upon Stroke. Oxidative Medicine and Cellular Longevity, 2019, 1–15. https://doi.org/10.1155/2019/3930186

Nichols, J., Bjorklund, G. R., Newbern, J., & Anderson, T. (2018). Parvalbumin fast-spiking interneurons are selectively altered by paediatric traumatic brain injury. Journal of Physiology, 596(7), 1277–1293. https://doi.org/10.1113/JP275393

Nogami, M., Takatsu, A., Endo, N., & Ishiyama, I. (1999). IgG immunohistochemistry for the assessment of brain injuries in forensic autopsies. Legal Medicine, 1(2), 76–79. https://doi.org/10.1016/S1344-6223(99)80016-9

Noll, J. M., Li, Y., Distel, T. J., Ford, G. D., & Ford, B. D. (2019). Neuroprotection by Exogenous and Endogenous Neuregulin-1 in Mouse Models of Focal Ischemic Stroke. Journal of Molecular Neuroscience, 69(2), 333–342. https://doi.org/10.1007/s12031-019-01362-4

Nudo, R. J. (2013). Recovery after brain injury: Mechanisms and principles. Frontiers in Human Neuroscience, 7(DEC), 1–14. https://doi.org/10.3389/fnhum.2013.00887

Olaya, J. C., Heusner, C. L., Matsumoto, M., Sinclair, D., Kondo, M. A., Karl, T., & Shannon Weickert, C. (2018). Overexpression of Neuregulin 1 Type III Confers Hippocampal mRNA Alterations and Schizophrenia-Like Behaviors in Mice. Schizophrenia Bulletin, 44(4), 865–875. https://doi.org/10.1093/schbul/sbx122

Ortega, M. C., Bribián, A., Peregrín, S., Gil, M. T., Marín, O., & de Castro, F. (2012). Neuregulin-1/ErbB4 signaling controls the migration of oligodendrocyte precursor cells during

development. Experimental Neurology, 235(2), 610–620. https://doi.org/10.1016/j.expneurol.2012.03.015

Overman, J. J., Clarkson, A. N., Wanner, I. B., Overman, W. T., Eckstein, I., Maguire, J. L., Dinov, I. D., Toga, A. W., & Carmichael, S. T. (2012). A role for ephrin-A5 in axonal sprouting, recovery, and activity-dependent plasticity after stroke. Proceedings of the National Academy of Sciences of the United States of America, 109(33), 1–10. https://doi.org/10.1073/pnas.1204386109

Ozen, I., Ruscher, K., Nilsson, R., Flygt, J., Clausen, F., & Marklund, N. (2020). Interleukin-1 beta neutralization attenuates traumatic brain injury-induced microglia activation and neuronal changes in the globus pallidus. International Journal of Molecular Sciences, 21(2). https://doi.org/10.3390/ijms21020387

Parker, M. W., Chen, Y., Hallenbeck, J. M., & Ford, B. D. (2002). Neuregulin expression after focal stroke in the rat. Neuroscience Letters, 334(3), 169–172. https://doi.org/10.1016/S0304-3940(02)01126-6

Pearson, C. S., Mencio, C. P., Barber, A. C., Martin, K. R., & Geller, H. M. (2018). Identification of a critical sulfation in chondroitin that inhibits axonal regeneration. ELife, 7(e37139). https://doi.org/10.7554/eLife.37139.001

Quattromani, M. J., Pruvost, M., Guerreiro, C., Backlund, F., Englund, E., Aspberg, A., Jaworski, T., Hakon, J., Ruscher, K., Kaczmarek, L., Vivien, D., & Wieloch, T. (2018). Extracellular Matrix Modulation Is Driven by Experience-Dependent Plasticity During Stroke Recovery. Molecular Neurobiology, 55(3), 2196–2213. https://doi.org/10.1007/s12035-017-0461-2

Rahman-Enyart, A., Lai, C., & Prieto, A. L. (2020). Neuregulins 1, 2, and 3 Promote Early Neurite Outgrowth in ErbB4-Expressing Cortical GABAergic Interneurons. Molecular Neurobiology, 57(8), 3568–3588. https://doi.org/10.1007/s12035-020-01966-7

Ransohoff, R. M. (2016). A polarizing question: do M1 and M2 microglia exist? Nature Neuroscience, 19(8), 987–991. https://doi.org/10.1038/nn.4338

Rey, C. C., Robert, V., Bouisset, G., Loisy, M., Lopez, S., Cattaud, V., Lejards, C., Piskorowski, R. A., Rampon, C., Chevaleyre, V., & Verret, L. (2022). Altered inhibitory function in hippocampal CA2 contributes in social memory deficits in Alzheimer's mouse model. IScience, 25(3). https://doi.org/10.1016/j.isci.2022.103895

Rico, B., & Marín, O. (2011). Neuregulin signaling, cortical circuitry development and schizophrenia. Current Opinion in Genetics and Development, 21(3), 262–270. https://doi.org/10.1016/j.gde.2010.12.010

Rieff, H. I., Raetzman, L. T., Sapp, D. W., Yeh, H. H., Siegel, R. E., & Corfas, G. (1999). Neuregulin Induces GABA A Receptor Subunit Expression and Neurite Outgrowth in Cerebellar Granule Cells.

Rodríguez-Prieto, Á., González-Manteiga, A., Domínguez-Canterla, Y., Navarro-González, C., & Fazzari, P. (2021). A Scalable Method to Study Neuronal Survival in Primary Neuronal Culture with Single-cell and Real-Time Resolution. Journal of Visualized Experiments, 2021(173). https://doi.org/10.3791/62759

Roy, K., Murtie, J. C., El-Khodor, B. F., Edgar, N., Pablo Sardi, S., Hooks, B. M., Benoit-Marand, M., Chen, C., Moore, H., Brunner, D., & Corfas, G. (2007). Loss of erbB signaling in oligodendrocytes alters myelin and dopaminergic function, a potential mechanism for neuropsychiatric disorders. PNAS, 104(19), 8131–8136. www.pnas.org/cgi/content/full/

Roy-O'Reilly, M., & McCullough, L. D. (2018). Age and sex are critical factors in ischemic stroke pathology. In Endocrinology (Vol. 159, Issue 8, pp. 3120–3131). Oxford University Press. https://doi.org/10.1210/en.2018-00465

Ryu, S., Lee, J. M., Bae, C. A., Moon, C. E., & Cho, K. O. (2019). Therapeutic efficacy of neuregulin 1-expressing human adipose-derived mesenchymal stem cells for ischemic stroke. PLoS ONE, 14(9). https://doi.org/10.1371/journal.pone.0222587

Salvador, E., Burek, M., & Förster, C. Y. (2018). An in vitro model of traumatic brain injury. In Methods in Molecular Biology (Vol. 1717, pp. 219–227). Humana Press Inc. https://doi.org/10.1007/978-1-4939-7526-6_17

Sammali, E., Alia, C., Vegliante, G., Colombo, V., Giordano, N., Pischiutta, F., Boncoraglio, G. B., Barilani, M., Lazzari, L., Caleo, M., De Simoni, M. G., Gaipa, G., Citerio, G., & Zanier, E. R. (2017). Intravenous infusion of human bone marrow mesenchymal stromal cells promotes functional recovery and neuroplasticity after ischemic stroke in mice. Scientific Reports, 7(1), 1–13. https://doi.org/10.1038/s41598-017-07274-w

Sawada, M., & Sawamoto, K. (2013). Mechanisms of neurogenesis in the normal and injured adult brain. In Keio Journal of Medicine (Vol. 62, Issue 1, pp. 13–28). https://doi.org/10.2302/kjm.2012-0005-RE

Sekine, Y., Lin-Moore, A., Chenette, D. M., Wang, X., Jiang, Z., Cafferty, W. B., Hammarlund, M., & Strittmatter, S. M. (2018). Functional Genome-wide Screen Identifies Pathways Restricting Central Nervous System Axonal Regeneration. Cell Reports, 23(2), 415–428. https://doi.org/10.1016/j.celrep.2018.03.058

Seo, W. M., Yoon, J., Lee, J. H., Lee, Y., Lee, H., Geum, D., Sun, W., & Song, M. R. (2022). Modeling axonal regeneration by changing cytoskeletal dynamics in stem cell-derived motor nerve organoids. Scientific Reports, 12(1). https://doi.org/10.1038/s41598-022-05645-6

Shahriary, G. M., Kataria, H., & Karimi-Abdolrezaee, S. (2019). Neuregulin-1 fosters supportive interactions between microglia and neural stem/progenitor cells. Stem Cells International, 2019. https://doi.org/10.1155/2019/8397158

Shyu, W. C., Lin, S. Z., Chiang, M. F., Yang, H. I., Thajeb, P., & Li, H. (2004). Neuregulin-1 reduces ischemia-induced brain damage in rats. Neurobiology of Aging, 25(7), 935–944. https://doi.org/10.1016/j.neurobiolaging.2003.10.012

Simmons, L. J., Surles-Zeigler, M. C., Li, Y., Ford, G. D., Newman, G. D., & Ford, B. D. (2016). Regulation of inflammatory responses by neuregulin-1 in brain ischemia and microglial cells in vitro involves the NF-kappa B pathway. Journal of Neuroinflammation, 13(1). https://doi.org/10.1186/s12974-016-0703-7

Snell, R. (2007). Neuroanatomía clínica (6a). Panamericana.

Sociedad Española de Neurología. (2019). El atlas del ictus en España.

Sommer, C. J. (2017). Ischemic stroke: experimental models and reality. Acta Neuropathologica, 133(2), 245–261. https://doi.org/10.1007/s00401-017-1667-0

Song, J. H., Choi, W., Song, Y. H., Kim, J. H., Jeong, D., Lee, S. H., & Paik, S. B. (2020). Precise Mapping of Single Neurons by Calibrated 3D Reconstruction of Brain Slices Reveals Topographic Projection in Mouse Visual Cortex. Cell Reports, 31(8). https://doi.org/10.1016/j.celrep.2020.107682

Stefansson, H., Sigurdsson, E., Steinthorsdottir, V., Bjornsdottir, S., Sigmundsson, T., Ghosh, S., Brynjolfsson, J., Gunnarsdottir, S., Ivarsson, O., Chou, T. T., Hjaltason, O., Birgisdottir, B., Jonsson, H., Gudnadottir, V. G., Gudmundsdottir, E., Bjornsson, A., Ingvarsson, B., Ingason, A., Sigfusson, S., … Stefansson, K. (2002). Neuregulin 1 and Susceptibility to Schizophrenia. American Journal of Human Genetics, 71(4), 877–892. https://doi.org/10.1086/342734

Suárez, R., Fenlon, L. R., Marek, R., Avitan, L., Sah, P., Goodhill, G. J., & Richards, L. J. (2014). Balanced interhemispheric cortical activity is required for correct targeting of the corpus callosum. Neuron, 82(6), 1289–1298. https://doi.org/10.1016/j.neuron.2014.04.040

Surles-Zeigler, M. C., Li, Y., Distel, T. J., Omotayo, H., Ge, S., & Ford, B. D. (2019). Transcriptomic analysis of neuregulin-1 regulated genes following ischemic stroke by computational identification of promoter binding sites: A role for the ETS-1 transcription factor. PLoS ONE, 13(6). https://doi.org/10.1371/journal.pone.0197092

Takatsuru, Y., Fukumoto, D., Yoshitomo, M., Nemoto, T., Tsukada, H., & Nabekura, J. (2009). Neuronal circuit remodeling in the contralateral cortical hemisphere during functional recovery from cerebral infarction. Journal of Neuroscience, 29(32), 10081–10086. https://doi.org/10.1523/JNEUROSCI.1638-09.2009

Talhada, D., Feiteiro, J., Costa, A. R., Talhada, T., Cairraõ, E., Wieloch, T., Englund, E., Santos, C. R., Goncąlves, I., & Ruscher, K. (2019). Triiodothyronine modulates neuronal plasticity mechanisms to enhance functional outcome after stroke. Acta Neuropathologica Communications, 7(1), 1–17. https://doi.org/10.1186/s40478-019-0866-4

Tan, Z., Robinson, H. L., Yin, D. M., Liu, Y., Liu, F., Wang, H., Lin, T. W., Xing, G., Gan, L., Xiong, W. C., & Mei, L. (2018). Dynamic ErbB4 Activity in Hippocampal-Prefrontal Synchrony and Top-Down Attention in Rodents. Neuron, 98(2), 380-393.e4. https://doi.org/10.1016/j.neuron.2018.03.018

Tao, Y., Dai, P., Liu, Y., Marchetto, S., Xiong, W. C., Borg, J. P., & Mei, L. (2009). Erbin regulates NRG1 signaling and myelination. Proceedings of the National Academy of Sciences of the United States of America, 106(23), 9477–9482. https://doi.org/10.1073/pnas.0901844106

Tasca, C. I., Dal-Cim, T., & Cimarosti, H. (2014). In Vitro Oxygen-Glucose Deprivation to Study Ischemic Cell Death. In Neuronal Cell Death: Methods and Protocols (Vol. 1254, pp. 197–210). Springer. https://doi.org/10.1007/978-1-4939-2152-2

Taveggia, C., Thaker, P., Petrylak, A., Caporaso, G. L., Toews, A., Falls, D. L., Einheber, S., & Salzer, J. L. (2008). Type III neuregulin-1 promotes oligodendrocyte myelination. GLIA, 56(3), 284–293. https://doi.org/10.1002/glia.20612

Taylor, A. M., Blurton-Jones, M., Rhee, S. W., Cribbs, D. H., Cotman, C. W., & Jeon, N. L. (2005). A microfluidic culture platform for CNS axonal injury, regeneration and transport. Nature Methods, 2(8), 599–605. https://doi.org/10.1038/nmeth777

Taylor, R. A., & Sansing, L. H. (2013). Microglial responses after ischemic stroke and intracerebral hemorrhage. Clinical and Developmental Immunology, 2013. https://doi.org/10.1155/2013/746068

Thapa, K., Khan, H., Singh, T. G., & Kaur, A. (2021). Traumatic Brain Injury: Mechanistic Insight on Pathophysiology and Potential Therapeutic Targets. In Journal of Molecular Neuroscience (Vol. 71, Issue 9, pp. 1725–1742). Humana Press Inc. https://doi.org/10.1007/s12031-021-01841-7

Tokita, Y., Keino, H., Matsui, F., Aono, S., Ishiguro, H., Higashiyama, S., & Oohira, A. (2001). Regulation of Neuregulin Expression in the Injured Rat Brain and Cultured Astrocytes.

Tuszynski, M. H., & Steward, O. (2012). Concepts and Methods for the Study of Axonal Regeneration in the CNS. In Neuron (Vol. 74, Issue 5, pp. 777–791). https://doi.org/10.1016/j.neuron.2012.05.006

Ueno, H., Fujii, K., Takao, K., Suemitsu, S., Murakami, S., Kitamura, N., Wani, K., Matsumoto, Y., Okamoto, M., & Ishihara, T. (2019). Alteration of parvalbumin expression and perineuronal nets formation in the cerebral cortex of aged mice. Molecular and Cellular Neuroscience, 95, 31–42. https://doi.org/10.1016/j.mcn.2018.12.008

Unda, B. K., Kwan, V., & Singh, K. K. (2016). Neuregulin-1 Regulates Cortical Inhibitory Neuron Dendrite and Synapse Growth through DISC1. Neural Plasticity, 2016, 1–15. https://doi.org/10.1155/2016/7694385

Uzdensky, A. B. (2018). Photothrombotic Stroke as a Model of Ischemic Stroke. Translational Stroke Research, 9(5), 437–451. https://doi.org/10.1007/s12975-017-0593-8

Varier, P., Raju, G., Madhusudanan, P., Jerard, C., & Shankarappa, S. A. (2022). A Brief Review of In Vitro Models for Injury and Regeneration in the Peripheral Nervous System. In International Journal of Molecular Sciences (Vol. 23, Issue 2). MDPI. https://doi.org/10.3390/ijms23020816

Walter, H. L., van der Maten, G., Antunes, R. R., Wieloch, T., & Ruscher, K. (2015). Treatment with AMD3100 attenuates the microglial response and improves outcome after experimental stroke. Journal of Neuroinflammation, 12(1). https://doi.org/10.1186/s12974-014-0232-1

Walter, J., Kovalenko, O., Younsi, A., Grutza, M., Unterberg, A., & Zweckberger, K. (2020). The CatWalk XT® is a valid tool for objective assessment of motor function in the acute phase after controlled cortical impact in mice. Behavioural Brain Research, 392(December 2019), 112680. https://doi.org/10.1016/j.bbr.2020.112680

Wang, D., & Fawcett, J. (2012). The perineuronal net and the control of cns plasticity. Cell and Tissue Research, 349(1), 147–160. https://doi.org/10.1007/s00441-012-1375-y

Watson, B. D., Dalton Dietrich, W., Busto, R., Wachtel, M. S., & Ginsberg, M. D. (1985). Induction of Reproducible Brain Idarction by Photochemically Initiated Thrombosis. Annals of Neurology, 17(5), 497–504.

Wen, T. H., Binder, D. K., Ethell, I. M., & Razak, K. A. (2018). The Perineuronal 'Safety' Net? Perineuronal Net Abnormalities in Neurological Disorders. In Frontiers in Molecular Neuroscience (Vol. 11). Frontiers Media S.A. https://doi.org/10.3389/fnmol.2018.00270

Willem, M. (2016). Proteolytic processing of Neuregulin-1. Brain Research Bulletin, 126, 178–182. https://doi.org/10.1016/j.brainresbull.2016.07.003

Witcher, K. G., Bray, C. E., Chunchai, T., Zhao, F., O'Neil, S. M., Gordillo, A. J., Campbell, W. A., McKim, D. B., Liu, X., Dziabis, J. E., Quan, N., Eiferman, D. S., Fischer, A. J., Kokiko-Cochran, O. N., Askwith, C., & Godbout, J. P. (2021). Traumatic brain injury causes chronic cortical inflammation and neuronal dysfunction mediated by Microglia. Journal of Neuroscience, 41(7), 1597–1616. https://doi.org/10.1523/JNEUROSCI.2469-20.2020

Wu, H., Zheng, J., Xu, S., Fang, Y., Wu, Y., Zeng, J., Shao, A., Shi, L., Lu, J., Mei, S., Wang, X., Guo, X., Wang, Y., Zhao, Z., & Zhang, J. (2021). Mer regulates microglial/macrophage M1/M2 polarization and alleviates neuroinflammation following traumatic brain injury. Journal of Neuroinflammation, 18(1), 1–20. https://doi.org/10.1186/s12974-020-02041-7

Wu, L., Walas, S. J., Leung, W., Lo, E. H., & Lok, J. (2015). Neuregulin-1 and neurovascular protection. Brain Neurotrauma: Molecular, Neuropsychological, and Rehabilitation Aspects, 561–568. https://doi.org/10.1201/b18126

Wu, W., Nguyen, T., Ordaz, J. D., Zhang, Y., Liu, N.-K., Hu, X., Liu, Y., Ping, X., Han, Q., Wu, X., Qu, W., Gao, S., Shields, C. B., Jin, X., & Xu, X.-M. (2022). Transhemispheric cortex remodeling promotes forelimb recovery after spinal cord injury. https://doi.org/10.1172/jci

Xiong, Y., Mahmood, A., & Chopp, M. (2013). Animal models of traumatic brain injury. Nature Reviews Neuroscience, 14(2), 128–142. https://doi.org/10.1038/nrn3407

Xiong, Y., Zhang, Y., Mahmood, A., & Chopp, M. (2015). Investigational agents for treatment of traumatic brain injury. In Expert Opinion on Investigational Drugs (Vol. 24, Issue 6, pp. 743–760). Informa Healthcare. https://doi.org/10.1517/13543784.2015.1021919

Xu, Z., & Ford, B. D. (2005). Upregulation of erbB receptors in rat brain after middle cerebral arterial occlusion. Neuroscience Letters, 375(3), 181–186. https://doi.org/10.1016/j.neulet.2004.11.039

Xu, Z., Ford, G. D., Croslan, D. J. R., Jiang, J., Gates, A., Allen, R., & Ford, B. D. (2005). Neuroprotection by neuregulin-1 following focal stroke is associated with the attenuation of ischemia-induced pro-inflammatory and stress gene expression. Neurobiology of Disease, 19(3), 461–470. https://doi.org/10.1016/j.nbd.2005.01.027

Xu, Z., Jiang, J., Ford, G., & Ford, B. D. (2004). Neuregulin-1 is neuroprotective and attenuates inflammatory responses induced by ischemic stroke. Biochemical and Biophysical Research Communications, 322(2), 440–446. https://doi.org/10.1016/j.bbrc.2004.07.149

Yan, F., Tan, X., Wan, W., Dixon, B. J., Fan, R., Enkhjargal, B., Li, Q., Zhang, J. J. H., Chen, G., & Zhang, J. J. H. (2017). ErbB4 protects against neuronal apoptosis via activation of YAP/PIK3CB signaling pathway in a rat model of subarachnoid hemorrhage. Experimental Neurology, 297, 92–100. https://doi.org/10.1016/j.expneurol.2017.07.014

Yan, T., Chopp, M., & Chen, J. (2015). Experimental animal models and inflammatory cellular changes in cerebral ischemic and hemorrhagic stroke. In Neuroscience Bulletin (Vol. 31, Issue 6, pp. 717–734). Science Press. https://doi.org/10.1007/s12264-015-1567-z

Yang, X., Arber, S., William, C., Li, L., Tanabe, Y., Jessell, T. M., Birchmeier, C., & Burden, S. J. (2001). Patterning of Muscle Acetylcholine Receptor Gene Expression in the Absence of Motor Innervation. Neuron, 30, 399–410.

Yilmaz, E. N., Bay, S., Ozturk, G., & Ucisik, M. H. (2020). Neuroprotective effects of curcumin-loaded emulsomes in a laser axotomy-induced cns injury model. International Journal of Nanomedicine, 15, 9211–9229. https://doi.org/10.2147/IJN.S272931

Yin, D., Chen, Y., Lu, Y., Bean, J. C., Shen, C., Liu, X., Smith, C., Xiong, W., & Mei, L. (2013). Reversal of behavioral deficits and synaptic dysfunction in mice overexpressing neuregulin 1. Neuron, 78(4), 644–657. https://doi.org/10.1016/j.neuron.2013.03.028.Reversal

Yin, D. M., Sun, X. D., Bean, J. C., Lin, T. W., Sathyamurthy, A., Xiong, W. C., Gao, T. M., Chen, Y. J., & Mei, L. (2013). Regulation of spine formation by ErbB4 in PV-positive interneurons. Journal of Neuroscience, 33(49), 19295–19303. https://doi.org/10.1523/JNEUROSCI.2090-13.2013

Zeiler, S. R., Gibson, E. M., Hoesch, R. E., Li, M. Y., Worley, P. F., O'Brien, R. J., & Krakauer, J. W. (2013). Medial premotor cortex shows a reduction in inhibitory markers and mediates recovery in a mouse model of focal stroke. Stroke, 44(2), 483–489. https://doi.org/10.1161/STROKEAHA.112.676940

Zhang, B., Zhang, H. X., Shi, S. T., Bai, Y. L., Zhe, X., Zhang, S. J., & Li, Y. J. (2019). Interleukin-11 treatment protected against cerebral ischemia/reperfusion injury. Biomedicine and Pharmacotherapy, 115(March 2019), 108816. https://doi.org/10.1016/j.biopha.2019.108816

Zhang, N., Lin, J., Chin, J. S., Zhang, K., & Chew, S. Y. (2020). A laser microdissection-based axotomy model incorporating the use of biomimicking fiber scaffolds reveals that microRNAs promote axon regeneration over long injury distances. Biomaterials Science, 8(22), 6286–6300. https://doi.org/10.1039/d0bm01380c

Zhang, Q., Esrafilzadeh, D., Crook, J. M., Kapsa, R., Stewart, E. M., Tomaskovic-Crook, E., Wallace, G. G., & Huang, X. F. (2017). Electrical stimulation using conductive polymer polypyrrole counters reduced neurite outgrowth of primary prefrontal cortical neurons from NRG1-KO and DISC1-LI mice. Scientific Reports, 7. https://doi.org/10.1038/srep42525

Zhang, Q., Yu, Y., & Huang, X. F. (2016). Olanzapine Prevents the PCP-induced Reduction in the Neurite Outgrowth of Prefrontal Cortical Neurons via NRG1. Scientific Reports, 6. https://doi.org/10.1038/srep19581

Zhang, R., Liu, C., Ji, Y., Teng, L., & Guo, Y. (2018). Neuregulin-1β Plays a Neuroprotective Role by Inhibiting the Cdk5 Signaling Pathway after Cerebral Ischemia-Reperfusion Injury in Rats. Journal of Molecular Neuroscience, 66(2), 261–272. https://doi.org/10.1007/s12031-018-1166-3

Zhang, X., Li, Y., Xu, H., & Zhang, Y. W. (2014). The γ-secretase complex: From structure to function. In Frontiers in Cellular Neuroscience (Vol. 8, Issue DEC). Frontiers Media S.A. https://doi.org/10.3389/fncel.2014.00427

Zhao, L. R., & Willing, A. (2018). Enhancing endogenous capacity to repair a stroke-damaged brain: An evolving field for stroke research. Progress in Neurobiology, 163–164, 5–26. https://doi.org/10.1016/j.pneurobio.2018.01.004

Zhao, R. R., Andrews, M. R., Wang, D., Warren, P., Gullo, M., Schnell, L., Schwab, M. E., & Fawcett, J. W. (2013). Combination treatment with anti-Nogo-A and chondroitinase ABC is more effective than single treatments at enhancing functional recovery after spinal cord injury. European Journal of Neuroscience, 38(6), 2946–2961. https://doi.org/10.1111/ejn.12276

Zheng, C. X., Wang, S. M., Bai, Y. H., Luo, T. T., Wang, J. Q., Dai, C. Q., Guo, B. L., Luo, S. C., Wang, D. H., Yang, Y. L., & Wang, Y. Y. (2018). Lentiviral Vectors and Adeno-Associated Virus Vectors: Useful Tools for Gene Transfer in Pain Research. In Anatomical Record (Vol. 301, Issue 5, pp. 825–836). Blackwell Publishing Inc. https://doi.org/10.1002/ar.23723